Design, construction and modelling of embroidered sensors made from graphene and metal coated yarn

A thesis submitted to the University of Manchester for the degree of Doctor of Philosophy

In the faculty of Science and Engineering
2019

Sirui Tan
School of Natural Science

Table of Contents

List of Figures

List of Tables

List of Acronyms

AA	Ascorbic Acid
BCG	Ballistocardiograph
BCB	Benzo Cyclobutene
CAD	Computer-Aided Design
CBRN	Chemical, Biological, Radiological or Nuclear
CNT	Carbon Nanotube
ECG	Electrocardiography
EEG	Electroencephalography
EMG	Electromyography
FAST	Fabric Assurance by Simple Testing
GO	Graphene Oxide
GWFS	Graphene Woven Fabrics
ICP	Intrinsically Conductive Polymers
MCEY	Metal Composite Embroidery Yarn
PCM	Polydimethylsiloxane
PDMS	Phase Change Material
PET	Polyethylene Terephthalate
PSE	Polyether Sulfone
PSF	Polysulfone
PSS	Polystyrene Sulfonate
PVA	Polyvinyl Alcohol
PZT	Lead Zirconate Titanate
RFID	Radio Frequency Identification
rGO	Reduced Graphene Oxide

RH	Relatively Humidity
SEM	Scanning Electron Microscopy
SFIT	Smart Fabric and Interactive Textiles
SH	Sodium Hydrosulphite
SWNT	Single Walled Carbon Nanotube
TFP	Tailored Fibre Placement
TPM	Twist Per Meter
TSF	Temperature sensing fabric

Abstract

Being the closest layer to our body, clothing provides an ideal platform for integrating sensors and actuators to monitor physiological signals. There is a large demand for developing reliable wearable sensors in biological sensing areas, such as wound moisture monitoring, human motion detections or long-term body temperature measuring. This research work has been carried out in order to manufacture reliable, flexible and comfortable embroidery sensors for pressure, temperature, moisture sensing and heating. Much work has been carried out in order to design and manufacture wearable sensors by knitting, weaving or printing. However, little work was found in literature on embroidery technique as the fabrication process. Recent work based on embroidery techniques are almost in wireless embroidered antenna areas.

In this thesis, the feasibility of using embroidery techniques to produce flexible, reliable and functional wearable sensors have been examined. The wearable sensors were embroidered by using the electro-conductive sewing yarns; graphene, carbon and silver coated sewing yarns were investigated in this research. Embroidered piezoresistive, moisture, temperature sensors and heating elements were designed, manufactured and evaluated. During the embroidery process, the stitch density and stitch size was found to have an influence on both mechanical properties and electrical properties of the sensors. Hence, in this research, the relationship between stitch density and stitch size and sensor sensitivity was investigated. The results in this thesis can be used to inform and provide guidelines for developing embroidered wearable sensors.

In this research, the embroidered sensors were analysed for sensitivity, high response speed, good long-term stability and repeatability in pressure, temperature and moisture sensing. Especially, the graphene yarns used in this research exhibited high sensitivity to pressure and moisture, the thermal electrical property of graphene material was found significant as well.

Declaration

I declare that no portion of the work referred to this thesis has been submitted in support of an application for another degree or qualification of this or any other university or other institute of learning.
23 September 2019

Copyright statement

i. The author of this thesis (including any appendices and/or schedules to this thesis) owns certain copyright or related rights in it (the "Copyright") and s/he has given The University of Manchester certain rights to use such Copyright, including for administrative purposes.

ii. Copies of this thesis, either in full or in extracts and whether in hard or electronic copy, may be made only in accordance with the Copyright, Designs and Patents Act 1988 (as amended) and regulations issued under it or, where appropriate, in accordance with licensing agreements which the University has from time to time. This page must form part of any such copies made.

iii. The ownership of certain Copyright, patents, designs, trademarks and other intellectual property (the "Intellectual Property") and any reproductions of copyright works in the thesis, for example graphs and tables "Reproductions"), which may be described in this thesis, may not be owned by the author and may be owned by third parties. Such Intellectual Property and Reproductions cannot and must not be made available for use without the prior written permission of the owner(s) of the relevant Intellectual Property and/or Reproductions.

iv. Further information on the conditions under which disclosure, publication and commercialisation of this thesis, the Copyright and any Intellectual Property and/or Reproductions described in it may take place is available in the University IP Policy (see http://documents.manchester.ac.uk/DocuInfo.aspx?DocID=2442 0), in any relevant Thesis restriction declarations deposited in the University Library, The University Library's regulations (see http://www.library.manchester.ac.uk/about/regulations/) and in The University's policy on Presentation of Theses

Acknowledgement

First of all, I would like to give my sincere and deepest gratitude to my supervisor, Dr Anura Fernando, a respectable, responsible and resourceful person, for spending his valuable time guidance and effort in supporting and helping me with great patience. Without his enlightening instruction, impressive kindness and patience, I could not have completed my PhD. His keen and vigorous academic observation enlightens me not only in this PhD but also in my future study.

I would also like to express my great appreciation to my co-supervisor Dr Nazmul Karim for sharing his knowledge of graphene and providing advices and sufficient graphene materials for my experiments. I am thankful to Dr Yuhua Wang for giving me training and advices on use of laboratory equipment, experimental setups. Additionally, And I would like to take this opportunity to thank all my friends who were with me during my studies at the University of Manchester as well.

Last but not least, l would like to thank my family members for supporting, understanding and encouragements during my PhD progress. Especially, I am thankful to my loving wife and daughter who gave me endless motivation to finish the research work.

Chapter 1 – Introduction

1.1 Background to textile sensors

Clothing, which provides a special environment to make the wearer feel comfortable when worn close to the body [1] is used very widely at all times. Since it is the body's closest layer, textiles act as an actuator and sensor integrating platform to check the physiological signals of the body (**Figure 1-1**). The textile sensors which are used to realise this end, are known as Electronic Textiles (e-textiles), which essentially are fabrics that are made using conductive yarn or fibres. These textile sensors have both physical properties such as good flexibility and the required sensory properties. More importantly, the mechanical performance of the textile sensors cannot be matched using existing mechanical and other solid-state sensors. Castano et al. [2]described e-textiles as the latest silicon seals which have drawn much attention because of their portability and soft computing capabilities. Although smart textiles are still in their development phase and cannot replace the conventional devices, at the current time, they are gradually catching up to the solid-state sensing and actuating devices in the industry and in the wearable electronics market.

Figure 1-1. Textile sensors on garments **[1]**

Also displaying the properties of flexible textiles, smart textiles have electromechanical fibre structures capable of responding to the environment's stimuli. Intelligence that can be created in e-textiles can be categorised into the following groups; active smart, passive smart and very smart [3]. According to definitions in the literature, passive smart sensing devices senses just the environment while active smart sensing devices react to the environment besides sensing it. With regard to smart materials, they are able to adapt their behaviour to the environmental conditions. Some physiological data from the body of humans can be calculated by the ability to sense by intelligent textiles, for example, pressure [4], body temperature [5] and the heartbeat rate [6], [7].

Basic electro-textile sensor structures can be produced using various traditional textile manufacturing methods, for example; weaving, embroidery, knitting, nonwovens and stitching [8]. The electro-textile sensors may be manufactured using many electrically conductive coated materials and conductive yarns available in the form of metal yarn, spun yarn and metal-coated yarn that can be utilised to provide suitable electrical sensor or actuator elements [8]. Also, these electro-conductive yarn may either be used as transmission lines and combine the sensor with the textile, provided the textile sensor is easy to use and comfortable to wear [9].

Textile sensors are generally made of conductive yarns/fabrics by using various methods to form different structures to meet the performance requirements and applications. Different conductive materials have specific conductivity and physical properties such as flexibility, ductility, strength and resistance. All of these characteristics of conductive materials will affect the final design and performance of the sensor. Fabric manufacturing methods (knitting, weaving and embroidering), the structure of the fabric (warp knitted, weft knitted, woven, sewn and braided structures), and the type of the sensor (pressure, humidity, flexure and temperature sensors) have a significant influence on the stability, service life, final performance and application.

Embroidery provides many advantages over other textile wearable sensor manufacturing processes such as weaving, knitting, nonwoven and printing in most aspects since it is not impeded by fabric or garment manufacturing technology and concerns of accurate positioning or geometrical accuracy. A computer-aided design (CAD) software that is used to create the embroidery designs allows the embroidery process to achieve a precision stitch pattern and circuit geometries. Also, yarns with different mechanical and electrical properties can be controlled and embroidered on single or multiple layers of substrate fabrics, and it can be employed on different types of textile and apparel products in one step. Although inkjet printing technique also allows CAD software to design and manufacture the circuit precisely, the poor washability, mechanical characteristics, life span and the high cost of the printer causes the printing technologies to be less preferable when manufacturing hardy wearable sensing products. In order to manage the vastness of wearable sensor manufacturing and extent of work involved, in this research, the work is mainly focused on electro-textile sensors and actuators such as embroidered piezoresistive, humidity/moisture and temperature sensors and embroidered heating elements (which are the most fundamental and standard sensors for any wearable sensing garment), and their design, manufacture and verification.

1.2 Problem definition

Electro-textile sensor manufacturing through the use of knitting, weaving, nonwoven methods of manufacture and printing poses a high level of restriction based on technology capital costs, skill levels of usage and flexibility in sensor integration. In order to overcome these hurdles, current research proposes embroidery as a more flexible, easier accurate and precise technology that can work with most advanced electroconductive materials and still produce flexible, accurate washable and long-lasting wearable sensors.

Currently research carried out to integrate graphene into wearable sensing through embroidery techniques is limited. Therefore, the current research aims to address this knowledge gap by using graphene coated yarns to create various wearable sensors and actuators. **Figure 1-2** is the uncoated yarn and graphene coated yarn.

Figure 1-2. (left) Uncoated yarn, (right) graphene coated yarn [10]

Although electrotextiles is a relatively new area, within a short period of time, it has become a very popular field of study the world over. One of the drawbacks these materials face is that unlike conventional materials used in the construction of sensors, the environmental properties around the manufacturing area of e-textiles can be easily influenced by the electro-textile material properties themselves, such as temperature, humidity. In constructing these sensors and actuators, one of the problems that scientists still find elusive is poor reliability due to the yarn meshing methods. Apart from that, the measuring accuracy of textile sensors, especially for fast and small movement, is also a weak point [11]. The strength, flexibility and stability of the fabrics, the conductivity of the conductive material and the structure of the whole sensor are the main factors that influence the measuring accuracy.

1.3 Aim and objectives

As discussed previously, there is an urgent need for developing flexible textile sensor

technologies using suitable electroconductive materials for accurate pressure, humidity/moisture and temperature detection. The main aim of this research is to investigate the design & manufacture of reliable, comfortable and flexible piezoresistive, humidity/moisture and temperature sensors using a current advanced 2D material, namely graphene and compare its performance with similar sensors manufactured through embroidery using metallic coated electroconductive yarns.

The objectives of this research are:

1. to select and investigate suitable materials for the construction of embroidered electro-textiles and their procurement. The selected electroconductive materials should have the required flexibility and conductivity;
2. to design and construct embroidered sensors and actuators for capturing pressure, temperature, humidity/moisture and heating. The embroidery parameters should be optimised to meet the final applications;
3. to investigate and characterise the performance of these sensors and actuators for acquiring the anticipated pressure, humidity/moisture, temperature and heating levels; and
4. to model and optimise the sensors and actuators for optimum performance and signal-to-noise ratio.

1.4 The scope of the research

In trying to construct better wearable sensors, in order to manage the amount of work undertaken and to match the research to a three-year PhD project, it is envisaged that specific sensor types would need to be addressed and they should be improved by accounting for their individual manufacturing and integration problems. In this case for the PhD project, the work is planned to address mainly three types of sensors; namely

embroidered piezoresistive sensors, embroidered temperature sensors and embroidered humidity/moisture sensors.

The piezoresistive wearable textile sensors that are currently available for bio-sensing have their main drawbacks due to the usage of improper electroconductive materials, non-uniformity of their design, construction & integration, their degradation due to oxidisation and unreliability due to all the above reasons. In addition, the resistance of the material is unstable due to change in temperature, washing and dust. These weaknesses can be corrected by choosing proper electroconductive materials. In the design of sensors and sensor networks, different shapes, densities, sizes and orientations of the electroconductive yarns and their contribution to the drapability, signal integrity, the level of contact the sensor will have with the body and their thermal performance need to be taken into account. For specific types of electrotextile sensors and actuators, in order to meet different application requirements, all these aspects should be considered.

As for electrotextile wearable humidity sensors, they have a large range of applications in the fields of sports, healthcare, first responders garments (CBRN garments) and in military smart garments due to their ability to monitor human sweat or urine[12]. Human sweat rate can be measured during exercise to monitor the body hydration status and the quantity of water needed to be replenished to the patient's body while bleeding rate too can be monitored to understand the severity of a wound and when to replace the binder; also a humidity sensors (especially in wireless mode) can be used to check whether the diapers used in care homes or disabled people's homes in order to monitor needs for changing [12-13]. Due to the increase in ageing population experienced in the countries, there are more concerns with regard to the elderly people's continence problems. As the continence of the elders continues to trouble the old people, nocturnal enuresis will also affect the children[15]. This will

then lead to a decrease in quality of life due to developmental and behavioural problems precipitated in wide ranges. Humidity sensors made as rigid sensors on large area flexible substrate[15-16], or directly printed onto the surface of the substrate by screen printing [18] are common these years. However, the disadvantage of these moisture sensors is lower flexibility, lower comfort, poor wash-ability and usually only one-point measurement. To control these drawbacks, a humidity sensor embroidered with conductive sewing yarn is more appropriate.

Rigid solid state or printed sensors that show stable and accurate performance are the main types of temperature sensors that are mainly used in current wearable sensing garments. However, the main disadvantage of rigid and printed sensors that are used currently are their poor flexibility, the discomfort resulting from the rigidity and their poor washability [19]. To solve these problems, textile temperature sensors were developed and were mainly used in the last five years. Polanský et al [20] found that compared to other types of textile temperature sensors, embroidered temperature sensors can achieve measurements with larger area, and the embroidered sensors do not need additional encapsulation when used with proper material, which will lead to a quick response to sudden temperature changes. Besides, the large measuring area, the embroidered sensors can be comfortably combined with current cloth or other textile manufacturing process. In addition, the use of embroidery techniques for constructing wearable textile sensors brings all the advantages embroidery process experiences over other textile sensor manufacturing processes; quick and simple senor integration, CAD operated geometrically precise and neat sensor construction and location, construction of multi material sensors through the use of multi head textile sensor embroidery.

1.5 Thesis layout

This thesis is presented in seven chapters and the summary of the thesis layout is as follows.

The first chapter introduces the general background of electrotextiles and the requirement for such sensors created through embroidery. The chapter also contains the problem definition for this work and a summary of the research approach.

Chapter 2 presents a detailed literature review, in which the detailed information on materials available for constructing wearable textile sensors, manufacturing methods, sensor technologies and sensor networks, available analytical models available to describe their performance, measurement methodologies suitable for sensor signal capture, noise level measurement and the evaluation of their response speeds, in addition to the background on which these specific advanced technologies exist.

Chapter 3 gives information about the methodology for this research work. The working principle of the piezoresistive sensor, humidity sensor and temperature sensors were explained in it. Also, the conductive sewing materials, substrate fabrics, the backing materials, and the test equipment were introduced. Additionally, the working principle of the data acquisition technology and its setup are included in this chapter.

Chapter 4 describes the first publication prepared for this alternative thesis submission, which is, “Highly Sensitive and Ultra-flexible Graphene-Based Embroidered Piezo-resistive Wearable Sensor for Bio-Signal Detection Application”. It included the design and construction process of the piezoresistive sensors, the test method, process and results, conclusion and the discussion.

Chapter 5 presents the second paper, “Investigation of graphene based embroidered

moisture sensors". The design and manufacturing process of the moisture sensors were explained in detail in this chapter. It also contains the experiment method, process and results of the moisture sensor. The data analysis, conclusion and discussion were also included.

Chapter 6 presents the third publication, "Investigation of a graphene based flexible embroidered temperature sensor". It consists of the design and manufacture of the sensor, the experimental work carried out for the development and the evaluation of the sensor and the discussion and conclusion on its performance.

Chapter 7 is an overall discussion and conclusion chapter. The summary of the experiments, whether the results are satisfactory, evaluation of the research and the initial findings are given in this chapter. It also presents, potential applications and future work that can be carried out in order to enhance the proposed sensor technologies.

1.6 Summary

Research of publications has revealed that there is a gap in the technology of accurate development of flexible and reliable textile sensors through embroidery methods that can be used on garments for human movement, bio-signal, humidity and temperature sensing. Various electroconductive sewing yarns have been investigated to create the flexible embroidered sensors and actuators. In this research, the silver coated sewing yarns and non-metallic materials like graphene and carbon were selected to produce the sensors. The conductive sewing yarns are integrated with the substrate fabric by using standard embroidery techniques. The research limits the method of manufacture to embroidery and the type of sensors/actuators designed and constructed to Embroidered piezoresistive sensors, embroidered humidity/moisture sensors and embroidered

temperature/heating sensors/actuators. Most basic parameters in embroidery, that is the stitch size and stitch density of the sensor structure are adjusted to meet all the requirement. Embroidered sensors are characterised under quasi-static and dynamic situations to evaluate their performance. The response speed of the humidity and temperature sensors are investigated as well. The mathematical models of the electro/thermo/mechanical performance of the embroidered sensors with different stitch size and stitch density are calculated. The mathematic models provide characteristics and predictions of the performance of the embroidered sensors with different embroidery parameters over variable pressure levels.

This chapter is mainly about the research background, the problem definition and the aims and objectives for this research. The research investigates the usage of embroidery as a textile sensor manufacturing technology together with its ability to process advanced electroconductive materials such as electroconductive yarn, filaments and conductive inks. Especially the research evaluates Graphene coated cotton yarn as a sewing yarn to evaluate the effect of graphene in these specific sensor technologies when integrated using embroidery methods. Therefore, the research will look at various sensor construction parameters and electroconductive material parameters to arrive at the optimum electroconductive yarns for the use in embroidery machines. In order to be critical of the work carried out, in addition, the research will look at the limits of reliability the sensors are associated with.

Chapter 2 – Literature view

2.1 Background

Integration of precision and robust sensor and actuator technology in textiles is an emerging issue that has attracted intensive research as the expert seeks to develop e-textiles. The use of e-textiles has been proven beneficial in various industries such as automobiles, medical, tissue engineering among others. The electrotextiles are a viable technology used to detect bio sensory information of the wearer as well as other environmental signals around the wearer, such as the condition of the atmosphere, gestures from environmental movements, temperature, and humidity among others. Many of these electrotextiles are sensing elements incorporated in the textiles in order to perform specific functions. This chapter gives a review of various literatures and a comprehensive analysis of electrotextiles covering a wide range of topics from development, current progress, advantages and disadvantages, areas of further research and incorporation in the industry. The review has established that major breakthroughs have been made in different fields and electrotextiles will be in the market in the near future if few shortcomings are addressed.

The development of new functional materials that has the ability to detect and react to external stimuli also known as the smart material has attracted great interest in the recent past. Smart fabrics have been developed to be incorporated in the technological world in different fields such as medical and tissue engineering among others. According to Castano et al. [2] smart fabric sensors are imbued with sensing properties that are sensitive to chemical and physical stimuli. The greatest challenge in the development of smart materials is the incorporation of materials with desirable properties while at the same time preserving properties of both components, for example the attachment of piezoelectric transducers or LED that is the light emitting

diodes directly in the fabric and also the optical fibres. The construction of fabric sensors which should be non-toxic, washable and defiant to surface shear have also posed a great challenge. Alternative routes have been sought by various researchers and this literature presents an analysis of these studies while giving the main outcomes of the studies.

According to Van Langenhove et al. [3] smart textiles were initially defined in Japan in 1989 as the initial textile material made from intelligent materials and was marked as silk yarn. Smart textile has amplified interest in the Western world whose criteria is designed to meet the transforming world of technology. Intelligent textiles actually are textiles that have the active ability to detect, react and adapt to environmental stimuli such as electrical, chemical, thermal, magnetic or other origin. The smart textiles are designed to fit with electronics creating two categories; the first-generation and the second generation of intelligent clothes. In the first generation the electronic components and they were wiring required to be carefully removed from the coat before washing. Alternatively, in the subsequent generation these components are changed into full textile materials which has the ability to perform combined roles.

Castano et al. [2] thought that fabric sensors can be modified into different categories of transducers such as sensors and actuators. Smart fabric sensors at an intrinsic level consist of active fibres while at the extrinsic level they consist of discrete electronic components. It is discussed that geometry and mechanical requirements are dependent strongly on the application purpose of the fabric sensor. Elasticity, temperature and humidity are dependent on sensitivity. The lack of standards, cost, low reliability and lack of large quantity of available components are the main challenges of the development of wearable sensing technologies. Other shortcomings that require address are the fabric sensors which pose no health risks, washable and resistant to surface shear.

The challenges for those researchers who desired to develop the electrotextiles, the electrotextiles need to meet some requirements. According to Cherenack et al.[21], a number of these requirements are discussed below, for instance due to the exposure to a mechanically demanding environment over extended time, continuously or daily the circuits need to be extremely rugged. Another one of the challenges is that the presence of circuits on smart textiles should not interfere with its washability and comfort. The required specifications for commercial smart textiles are often not met because they may be conflicting and rigid. However, more recent electrotextile developments have managed to gradually address many of these challenges such as washability and wear resistance and thereby the electrotextiles can be integrated into garments.

Lymberis et al. [22] presented an ongoing major research and development activities and identified various gaps and challenges that are likely to face smart fabrics in future. According to their research, Smart fabric and interactive textiles (SFIT) is an area that is not only promising but also has great industrial and socioeconomic potential combining advanced material processing, microelectronics, sensors, telecommunication, complex material processing, nanotechnologies, informatics, medicine and biochemistry. The micro system is expected to have a great contribution to the innovation of smart textile through functionality and integration including redesigning of various components to increase their compatibility with the textile, development of new SFIT integrating textile materials and identification of production technology that is appropriate. In order to achieve this, they opined that low cost of production, management of power to ensure cost effectiveness and optimization of processes is necessary. They pointed specific outstanding issues such as packaging or cabling, lack of specifically designed fibres for e-textile, lack of connectors that connect textiles to electronics, inadequate personnel with interdisciplinary background, and lack of personnel with the ability to manage productive sectors that are multidisciplinary in

nature.

Van Langenhove [3] explored the precise meaning of electrotextiles and analysed various possibilities and the circumstances of affairs and need for future research in electrotextiles in their paper. They noted that the introduction of electrotextiles necessitates the need to take textile industry to a high technological level. They stated the need to incorporate technological domains such as biotechnology, computer science, polymer chemistry, microelectronics, and material science in textile industry which will bring a distinct view of textile possibilities from different angles. They pointed out that the real challenge is in developing a mechanical actuator that is strong and act as an artificial muscle.

On the other hand, Van Pieterson et al. [21] evaluated the challenges and opportunities in electrotextiles and also discussed the basics of electrotextiles such as textile interconnect lines and textile fabrication methods, components of output devices and textile sensors and integration of the various components into the textile architectures. They observed that the focus of commercial smart textiles is changing and in the near future it will focus on heating, sensing and lighting applications. According to Kirstein, T. et al. [23], the electrotextiles will also be used in automobiles driven by the most recent preface of electric cars. Nonetheless, there are couple of issues that will require address to ensure smart transition to industrial applications from research laboratories. The existing barriers include lack of regulations, standardisation, collaboration among partners in the value chain, and coordination [24].

2.2 Electrotextile sensors

According to Pacelli et al. [25] response linearity is one of the main components required in the development of strain gauge sensors. A linear relationship between resistance change and applied strain is required to make it possible to identify the value of resistance with the variable that is measured. The results indicate that intelligent bio cloths are ready for the market as it meets market needs that is defined by industrial feasibility and lastly, it meets the needs of the user in terms of comfort.

According to Meyer et al. [26], the textile pressure sensors have the capacity to measure the pressure of the human body. Several textile sensors were developed covering different capabilities such as flexibility, soft sensors with a high local resolution such as motion detection, pressure –soreness prevention.

Meyer [4] in another study presented another sensor for textile pressure that can also be integrated in clothing. In his study, Meyer used the sensing principle of a variable capacitor. The sensor was modelled using algorithms to reduce the sources of error to below 5 percent. The study indicated that the sensor is useful in supervising the distribution of pressure in a compression stocking and also measuring the activities of the muscle.

Yao et al. [27] argued that sensors that are highly sensitive, cost effective and highly flexible are exceedingly enviable in the prospective generation of devices that are foldable and portable. They recommended sensors that are highly incorporated into the synthetic skin to replicate the location and strength of the pressure that is forced on the skin surface. According to Taelman et al. [28] the piezo resistive sensors that introduce the imposed pressure have been widely used due to the fact that they facilitate easy signal collection, cost effective and include feasible preparation.

In another study, Paradiso et al. [29] presented a system suitable for monitoring health of an individual, named WEALTHY. The system is based on an interface of wearable textiles which is executed by amalgamating electrodes, links in fabric forms and integrating sensors. The system is also based on a modern communication system and an advanced techniques of signal processing. The study aimed at showing the feasibility of the system and its capability in acquiring biomedical signals simultaneously. The capability of this system was also compared to a standard monitoring system. The results of the study indicated that the information obtained using this system was also comparable with the information obtained in the average sensors. The system is also premeditated to scrutinize persons suffering from diseases such as cardiovascular especially at some point in the treatment phase. Besides, the system aids the skilled workers who are subject to psychological and physical stress as well as professional health risks.

Ferreras et al. [30], in their paper also reported that there is increasing interest in the topic of integrating the smart materials into interfaces that are human wearable. In their paper, they report that wearable electronics could offer tailored comfort, security and healthcare. The article pointed out that the focal confront experienced in electronic textiles is incorporating the textile materials with the desired functionality. The article however mentioned that it has been possible to achieve the smart textiles through attaching the electronic components or devices such as piezoelectric transducers and optical fibres on clothes directly. It is observed that, due to the distinct nature of the components, the approach can result to worsening of the automatic properties of the textile.

In conclusion, this chapter has presented an in-depth review of the current state of e-textile technologies and the field of wearable sensors. Despite the benefits attributed to

smart materials, there are couple of issues that will need to be addressed to ensure smart transition to industrial applications from research laboratories.

2.3 Materials

Conductive materials are among the most important factors which influence a sensor's behaviour; different conductive materials have different conductivity and physical properties such as flexibility, ductility and strength. Due to the different variations, conductive materials can be used for many different applications.

According to Domvoglou et al.'s article, conductive yarns can be classfied into these categories:

I. carbon black filled fibres or carbon fibres;

II. conductive substances coated textiles;

III. introducing metal into the textile structures, such as stainless steel, fibres or nickel wires;

IV. incorporating ICP (Intrinsically conductive polymers) effectively into the textile structure to modify the polymer structure [31].

2.3.1 Metallic materials

Metallic materials include metal, metal coated (**Figure 2-1**) and metal wrapped material. Metallic materials are usually washable and resistant to attack from insects. Additionally, metal fibres have a relatively lower resistance and excellent thermal resistance. However, some of them like nickels might cause skin allergies, and oxidisation and corrosion of metallic material have huge influence on the conductivity of metallic materials, especially silver.

Figure 2-1. Metallic coated sewing yarns (TIBTECH, Silverpam 250) [32]

Linz et al. conducted an experiment that was based on the silver-coated polyamide (Statex 117/17, Shiledex) with a relatively high resistance (500 Ω/m). In their opinion, conductive yarns used for an embroidered sensor must be sewable and conductive on the outside so that only metal coated filaments can meet both the requirements [33].

Roh, J. used metal composite embroidery yarn (MCEY) which can develop robust and reliable fabric touch sensing surfaces for wearable e-textiles. In e-textiles, this technique can be applied to automated production, thus avoiding the need for hand craft production. The two different MCEY used in this project were made by wrapping and twisting superfine metal yarns (silver plated copper filament, diameter of 0.04mm) over polyester filaments [34].

Zhang. et al, used silver coated p-phenylene-2,6-benzobisoxazolen fibres (D.C. resistance is 0.008Ω/cm, diameter is 15μm). Due to its specific structure, this fibre has great mechanical strength and flexibility [35].

A multifilament yarn coated with silver was used by Mayer et al. It has a resistance of 120 Ω/m and the resistance only increased a few percent after being washed several times [36]. Guido et al used silver-coated yarn as well. 0.81 ohms/cm silver-coated

nylon yarn from Lame Lifesaver, which consists of 98% polyester and 2% Lycra, was used in his experiment [37]. Kannaian et al. also used silver-coated yarn in their project. They reported that silver-coated yarns are highly conductive, more flexible, soft and pliable [38].

A knitted strain sensor created by Zhang et al. used stainless steel yarns and carbon yarns. In their paper, they found the contacting resistance to be the most important aspect in the sensing mechanism [39]–[43]. Yang et al. also used stainless steel to construct their knitted strain sensors; stainless yarn, being a metallic yarn, shows an intrinsically conductive property and the resistance of the yarn for each unit length is even and independent of tensile deformation [44].

Holg used constantan resistive wires and copper wires in his experiments. He believed a typical diameter of sewn yarns is from 40 μm to100μm and the diameter of the conductive yarn should be chosen respective to the sensor dimensions and final application [45]. Kim et al. thought copper to be the most widely used electrical conductor; however, like most metals, it has three main disadvantages: flexibility, fabrication and price. And they thought using electroconductive yarn instead of metal wires could be the solution to these problems [46].

2.3.2 Carbon materials

In the earth's crust, carbon is one of the most abundant elements. Carbon fibre is a conductive material with good and stable mechanical and electrical properties. Carbon materials (**Figure 2-2**) used recently are carbon-coated material, carbon fibre-twisted yarn and carbon nanotube. Compared to metallic materials, carbon materials usually demonstrate a high level of corrosion resistance, durability and no oxidization. Besides these advantages, carbon materials are also lightweight, and have high tensile strength and good electrical conductivity; but when carbon materials are exposed to high impact,

they are liable to break. Also, the cost of using carbon materials is relatively higher.

Figure 2-2. Non-metallic coated sewing yarns (TIBTECH, Carbon Tenax) [32]

Mattmann et al. used carbon particles to make conductive yarns which demonstrate a high level of accuracy. They focused on the influences of temperature and humidity on resistance. However, the sensor only showed a reaction to resistance humidity but not to temperature [47].

Capineri et al. [48]noted that piezoresistive materials such as polypyrrole or carbon are attractive and used for pressure sensors. The textile piezoresistive sensor was built with a pressure sensitive layer between two conductive fabric layers. Due to the electrical properties of carbon, they developed a sensor with very low temperature coefficient of resistivity. However, because the sensors consisted of three layers, they proved insufficiently flexible.

Guo, X. et al. [49] printed carbon black composite dielectric on a flexible textile substrate which shows high flexibility, which is comfortable to wear and achieved high sensitivity of 0.02536%/KPa. Additionally, the response speed of the sensor is relatively fast at the range of 0-700 KPa.

Yamada et al.[50] preferred carbon as well; a thin film of carbon nanotube was

manufactured by them. The carbon nanotube thin film presents a large measuring range up to 280%, and it achieves a relatively faster response speed, lower creep and higher durability.

Han et al. [51] also employed a single-wall carbon nanotube; they coated the carbon nanotube on a cotton yarn. The CNT-cotton yarn sensors displayed a high uniformity, good mechanical properties and repeatability. They believed that these CNT-cotton yarn sensors can be widely used due to their low cost.

Yamada and Han, Devaux et al. [52]used carbon nanotube as well. They melted spinning carbon nanotube with polylactide to fabricate conductive multifilament yarns for humidity detection. This spinning multifilament yarn shows high sensitivity to the changes in humidity and repeatability.

Foroughi et al. used Spandex and carbon nanotube composites yarns to manufacture a three-dimensional textile using an interlock circular knitting machine. This knitted structure is highly actuatable, stretchable and electrically conductive. During tensile tests, this knitted carbon nanotube sensor presented linearity and lower hysteresis in the strain ranges from 0% to 80% [53].

2.3.3 Graphene materials

Carbon has many allotropes, and each of them shows different properties that can meet different requirements. Graphene is one of these allotropes and shows an excellent conductivity and mechanical properties. It is the thinnest and strongest material with both heat and electrical conductivity. Graphene is a one atom thin sheet of carbon atoms; it is a flat monolayer of carbon atoms in a 2D honeycomb structure. It was described as the ‘new wonder material’ due to its conductivity and mechanical properties. An

individual carbon atom has four outer shell electrons, however in graphene, each carbon atom is connected to three atoms, and there is one atom in third dimension freely which is available for electronic conduction. The electronic movement of graphene is very high even at room temperature, leading to high conductivity [54]. However, it is susceptible to oxidative environments and the cost of graphene is higher than that of other materials. Graphene is applied due to its excellent mechanical, electrical, thermal, transport, thermoelectric and gas-barrier properties.

Due to the strong cohesive force between the graphene sheets in the graphite, the graphene production process is difficult. However, graphene oxide (GO) can be produced by graphite on oxidation; the hydrophilic functional groups can increase the intercalation of water molecules into the graphite; hence the GO sheet can be easily separated from the graphite. After the GO sheet is produced, the sodium borohydride or hydrazine hydrate can be used to produce reduced graphene oxide (rGO) which is conductive. Additionally, other methods like chemical conversion, chemical vapor deposition, unzipping of carbon nanotubes, discharge and self-assembling of surfactants can be used for graphene production [55].

Generally, the graphene materials used in textile areas are graphene-coated or printed yarns or fabrics (**Figure 2-3**).

Figure 2-3. Graphene-coated yarns **[10]**

Trung et al.[56] used single reduction graphene oxide fibre to manufacture the temperature sensors. It shows good recovery time, fast response time and high responsivity following changes in temperature. However, the sensitivity of rGO fibre-based temperature sensors is not satisfied.

Wang et al. [57]adhered the graphene woven fabrics (GWFs) on composite film and polymer to form a flexible strain sensor. The graphene strain sensor exhibits relatively good sensitivity, good repeatability, super resistance to oxidization and easy fabrication. They believed the GWF-based piezoresistive sensors have a great amount of applications due to their high sensitivity.

Yun et al. [58]presented flexible and durable graphene yarns and fabrics wrapped with RGO. BSA proteins were used as the adhesives for increasing the absorption of GO onto yarns and fabrics. By using this method, they manufactured rGO materials based on nylon, cotton, nonwoven and polyester. The rGO materials demonstrated conductivity and repeatability during the cyclic tests.

Boland et al. [59]soaked the rubber band in an NMP: water: graphene mixture after the rubber was treated in toluene for 3.5 h to produce a graphene- rubber composite for body motion detection. The graphene-rubber composite exhibits high sensitivity, and is high stretchable (more than 800%) with the gauge factor up to 35.

Yapici et al. [60]dip coated a nylon fabric by using the rGO to produce a conductive textile electrode for bio signal detection. The rGO-coated nylon fabric provides flexibility, comfort and durability for wearable sensor applications, and washes well. Although the rGO electrodes can capture clear and accurate ECG signals with only two electrodes, the contact impedance of the rGO electrode is higher than that of the silver

electrode.

Yang et al. [61]developed a graphene woven strain sensor for human motion detection. This graphene woven strain sensor shows a linear relationship between strain and resistance. Additionally, the graphene woven strain sensor presents good long-term stability, great comfort, and high sensitivity.

Cheng et al. [62]developed a low-cost and scalable fabrication method for graphene composite fibre by dip coating. The graphene was coated on a highly elastic polyester winded polyurethane yarn. This composite fibre exhibits good sensitivity to tensile strain and has a large working range. In addition, the composite fibre also shows excellent bending and torsion sensitivity.

Yun et al. [63]used reduced graphene oxides to demonstrate a bendable and washable wearable gas sensor. The fabric gas sensor was made from a cotton wrapped rGO yarn and polyester wrapped rGO. The gas sensor presents good chemical durability to several detergent washing tests and good mechanical durability to 1000 bending tests.

2.4 Fabrication

2.4.1 Coating

Metallic materials can be coated on the polymer or the natural non-conductive yarns to achieve conductivity. Such yarns can be produced by chemical processes like electroplating as the primary method. After the procedure, the entire textile is covered with conducive layers. Other methods that can enable the production of an ex-textile include sputtering, conducive polymer coating and chemical vapor deposition [64].
In order to achieve conductive coating, metal textiles that have high conductivity like silver and copper are used in plating into natural fabrics [65]. Non-metal conductive

materials can also be used as coating layers. For example, a single walled carbon nanotube (SWCNT) can be used as an aqueous solution alongside electroconductive ink. Without losing their flexibility, polyester and cotton materials can absorb the SWCNT ink and are then coated with conducive layers. The conductivity of the materials increased with repeated absorption of the ink [66].

It is advantageous to use conductive layer coating materials because they are flexible, easy to cut and can be sewn to desired designs. They also provide spaces for curving and fitting electronic devices on different positions of the human body making the materials desirable in areas of electromagnetic shielding. However, coated materials usually demonstrate poor wash ability, the encapsulation process needs to be employed to protect the conductive ink from water.

Yao et al, [27] designed a fractured microstructure device to augment the sensitivity of the piezo resistive sensors. A conductive graphene sponge was made by dip-coating as shown in **Figure 2-4**. The PU sponge was dip coated by using the GO solution to form a thin layer of graphene oxide, and then the centrifugation process was used to wash the unwanted graphene oxide solution. After the sponge was dried, it was dipped into the hydrogen iodide solution to reduce the GO. After the coating process, the RGO sponge was softened by hydrothermal treatment. Their study indicated that the graphene sponge can perceive a force as low as 9 pa and provide a sharp output signal at a pressure of 45 Pa. In addition, the coating process is low-cost and easily scalable.

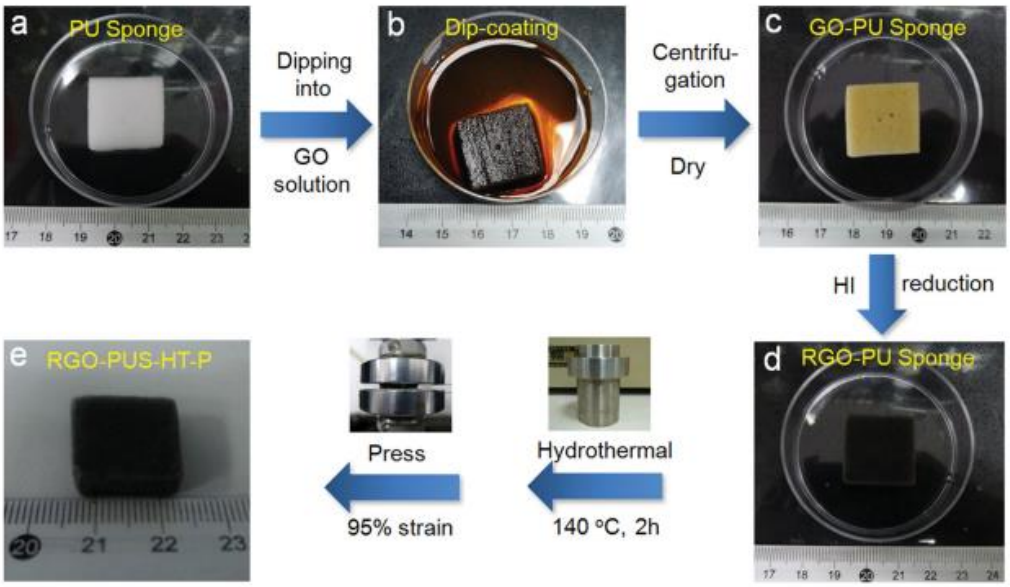

Figure 2-4. The fabrication process of the graphene-wrapped sponge **[26]**

Cheng et al.[62] also used dip-coating to produce their graphene sensor; **Figure 2-5** shows the dip-coating process of their sensor. Before the dip-coating process, Cheng et al. used air plasma treatment in order to etch the sample, which can greatly improve the hydrophilicity of the sample.

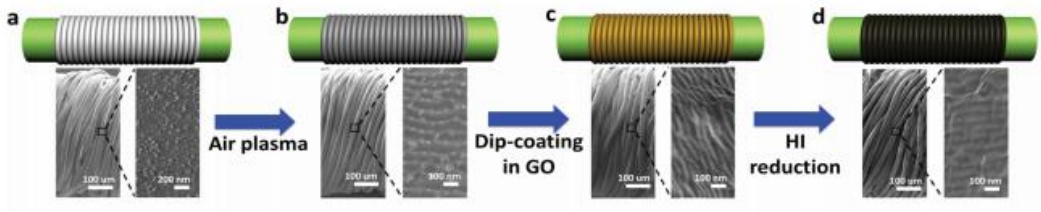

Figure 2-5. The dip-coating process of the graphene-based fibre **[60]**

Zhang et al. [67] used another coating process which consists of several rollers, a coating bath and an oven for drying (**Figure 2-6**). The polyurethane/ carbon nanotube solution was poured into the coating bath. The yarn was driven by the three rollers and coated on the second roller; the roller carried the ink to the coating bath and dyed the yarn. Between the second roller and third roller, a heating oven was used to dry the coated yarn to fix the ink on the yarn.

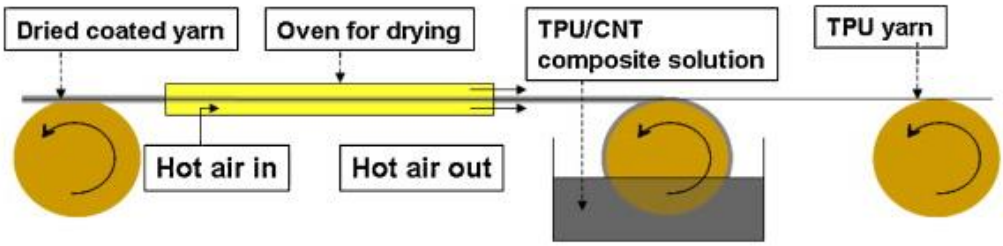

Figure 2-6. Roller-coating process **[65]**

2.4.2 Printing

Printing is an important sensor manufacturing process; the conductive ink was printed on the substrate fabric in certain patterns to form a conductive circuit for different applications. There are two main printing methods used nowadays: inkjet printing and screen printing. Both of these methods are based on conductive ink which contains certain concentrates of conductive particles such as silver, carbon or graphene [68]. To meet the different demands of inkjet printing and screen printing, the inks should realise varies requirements. During the printing process, the conductive ink can be accurately printed on the substrate fabric, even if the pattern is small and complex in size.

The pattern of the screen printing is decided by the stencil screen, and the conductive ink is printed on the substrate fabric using the stencil (**Figure 2-7**). The ink is spread by using the squeegee; the squeegee is moved across the screen to fill the stencil with the ink. This whole process is controlled by hand which means it is a non-controllable process. The force of the hand decides the thickness and evenness of the printed pattern. Compared to inkjet printing, screen printing needs more ink for the same size of pattern. However, any type of ink can be used for screen printing.

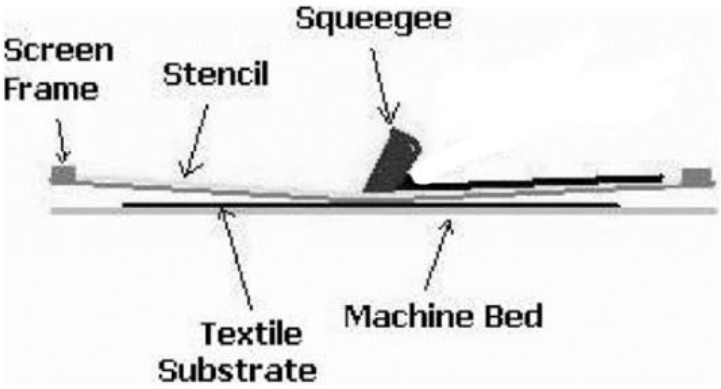

Figure 2-7. Principle of screen printing **[66]**

Inkjet printing is based on a computerised printer; the printed pattern can be designed on the computer by a CAD software. The thickness and evenness of the printed pattern are controlled by the printer. However, the ink used for inkjet printing should have lower particle aggregation due to the size of the nozzle, and it should be resistant to oxidation. In addition, the conductive ink should have suitable viscosity and surface tension to be printed on the substrate fabric; ink with relatively lower viscosity or higher surface tension may be jetted with limited performance [69].

Cao et al.[70] used carbon nanotubes and screen printing to produce a washable electronic textile which can measure touch and gesture. This screen-printed carbon nanotubes sensor exhibits not only excellent flexibility and stability, but it also has high conductivity and air permeability.

Pacelli et al. [25] developed their sensors by screen printing as well. The conductive elastomer ink was printed on the substrate fabric to produce a textile piezoresistive sensor for movement and posture detection. It shows a large range of linear relationship between strain and resistance.

However, Lee et al. [71] preferred inkjet printing, Ag ink was printed on the polyimide

and then metallized at 250 ℃ for 30 min. The metallized silver-printed pattern presents very low resistance. (6 μΩ /cm). Additionally, they believed that inkjet printing shows high productivity and is an environmentally friendly method which can also minimize material loss.

Valeton et al. [72] used a silver-containing metallo-organic ink to inkjet print on the polyethylene terephthalate (PET) substrate. The conductivity of the printed sensor is 10% of bulk silver which is higher than the other non-metallic sensors. However, the printed sample has a lower working range (only 2% strain).

The main disadvantage of the printing process is its poor wash ability; usually a non-conductive layer should be printed to cover the printed conductive circuit which will increase the cost and manufacture time. Additionally, the cost of inkjet printing is relatively higher than that of other fabrication processes, and the screen printing process is a uncontrollable and time-consuming process since a new stencil screen needs to be manufactured every time the design changes.

2.4.3 Weaving

Weaving is a fabrication method which can produce fabric by interlacing two sets of yarns (weft and warp yarns) at right angles. Woven sensing fabric is generally made by weft inserting the electronic conductive yarns (i.e. the filling yarns) and the weft yarns are non-conductive yarns[73]. Plain weaves, atlas weaves and twill weaves are the most common and simple woven patterns to manufacture woven sensing fabric. Different woven structures will have a huge influence on the final performance of the sensing fabric, especially its mechanical properties.

2.4.3.1 Plain weaving

Plain weave is the simplest and tightest weave pattern among all of the structures of woven fabric; the weft yarn passes through the warp yarn alternatively in this structure (**Figure 2-8**). The plain weave has the maximum number of binding points which can strengthen the structure and make the fabric robust and tight. It also has more snag resistance; however, plain-woven structures generally wrinkle more and have a lower tear strength.

2.4.3.2 Atlas weaving

Atlas weaving is also known as satin weaving (**Figure 2-8**) which is produced by four or more weft yarns floating over a warp yarn or four warp yarns floating over a weft yarn. An atlas woven fabric structure is relatively looser than a plain woven structure due to these floating yarns [74]. The structure is suitable for inserting electroconductive yarns into the structure to produce sensing fabric; however, it is not dimensionally stable. The interlace points within the atlas woven structure are covered by warp and weft yarns which allow the atlas fabric to achieve a smooth surface. However, this structure has lower durability compared to a plain-woven structure since the floats snag easily.

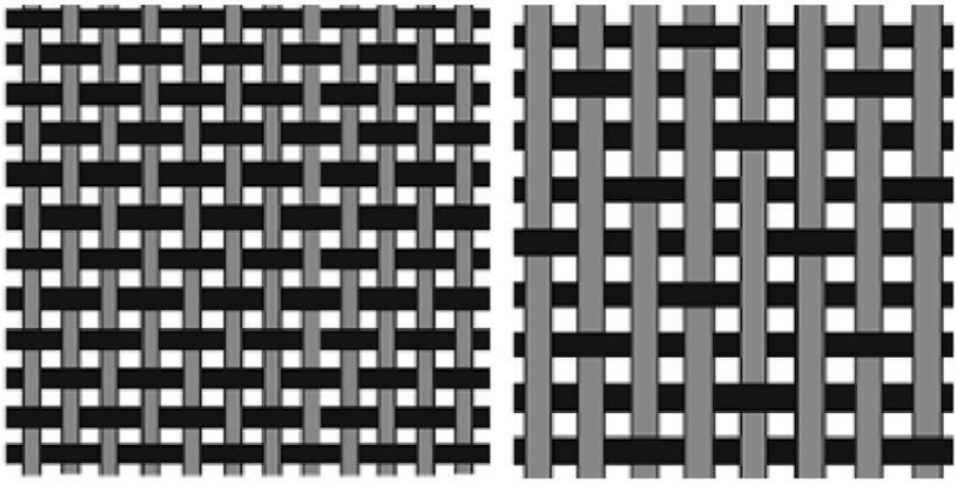

Figure 2-8. (left) plain weaving structure, (right) satin weaving structure **[74]**

2.4.3.3 Twill weaving

Twill weaving (**Figure 2-9**) is the third fundamental weaving structure. This structure is repeated in that the weft yarn passes through one or more warp yarns, and then under two or more warp yarns. Twill woven fabric is strong and durable; it has more wrinkle resistance and is more resistant to soiling than plain fabric, but the cost of the fabrics is relatively higher when compared to that of the other two woven structures.

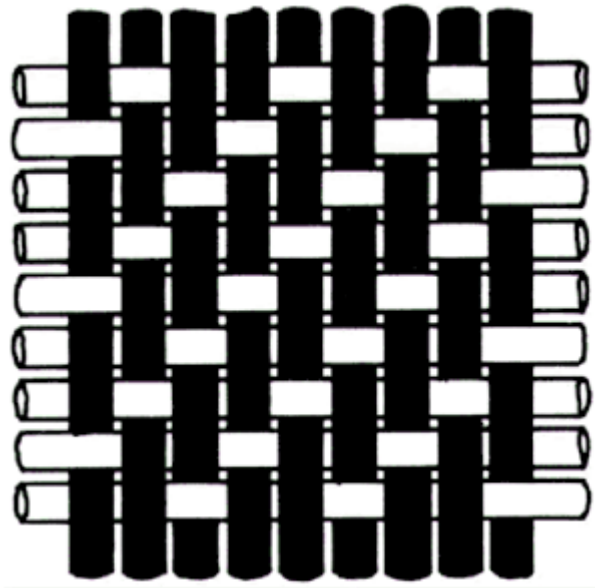

Figure 2-9. Twill weaving structure **[73]**

Enokibori et al. [75], also proposed a pressure sensor that is based on a novel e-textile (**Figure 2.10**). The authors argued that fabric is a universal material that we use in our lives and is widely used in different items, such as clothing, sheets and seats. If these objects can have sensor functions, they can easily help humans without having to change their lifestyles much. The proposed sensor is highly durable and suitable for mass production. It is also woven and its material is made of common fibres that use cheap and special material such as optical fibre. The structure of the textile supports the mechanism of the sensor.

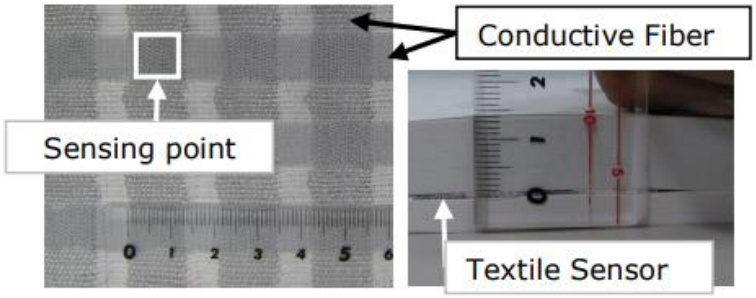

Figure 2-10. E-textile pressure sensor **[73]**

Rothmaier et al. [76] developed a pressure sensitive textile sensor by integrating thermoplastic silicone fibres into atlas and plain-woven fabric. Compared to plain woven structure, only a few yarns rise from the bottom to the top; hence, there is less resistance change caused by micro bends when the yarn moves from the bottom to the top (**Figure 2-11**). The sensors exhibit good sensitivity in the ranges of 0- 30N.

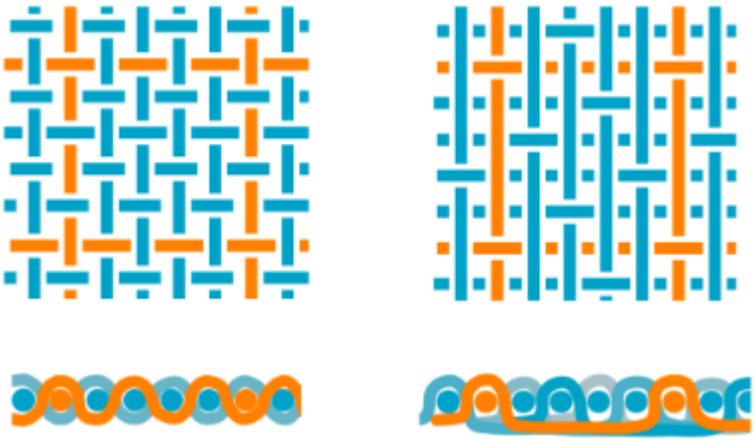

Figure 2-11. Plain and atlas weave pattern **[74]**

Although the weaving technique is low cost and fast and the woven fabric has high elastic recovery, the flexibility and lower tear strength are issues that need to be addressed.

2.4.4 Knitting

Knitting technology is the fabrication process of combining the loops of yarns to create the fabric. Two sets of yarns are feed into the needle bed and interlaced with each other

in the knitting machine. Unlike the weaving process, the yarns are always straight; the yarn in the knitted fabric follows a meandering path. The warp yarn follows the lengthways on the fabric, and the weft goes across from side to side [77]. To produce wearable sensing fabric, the sensing fabric should have specific shape to suit a specific part of the human body [78]. Hence, the knitting technique is a suitable fabrication process to manufacture a wearable sensor that fits the body closely, and it can also provide a comfortable and flexible environment for the wearer.

2.4.4.1 Flatbed knitting

The needle arrangement in the flat bed knitting machine can be adjusted manually to meet different requirements. With the help of a flat-bed knitting machine, some complex structures like double jerseys, jacquards and intarsias can be accurately produced. However, when compared to the circular knitting machine, the speed of a flat-bed knitting machine is relatively slower [79]. **Figure 2-12** shows the manufacturing process of a flat-bed knitting machine; the conductive yarn is inserted into the machine and interlaced with the non-conductive yarns to form the knitting loops.

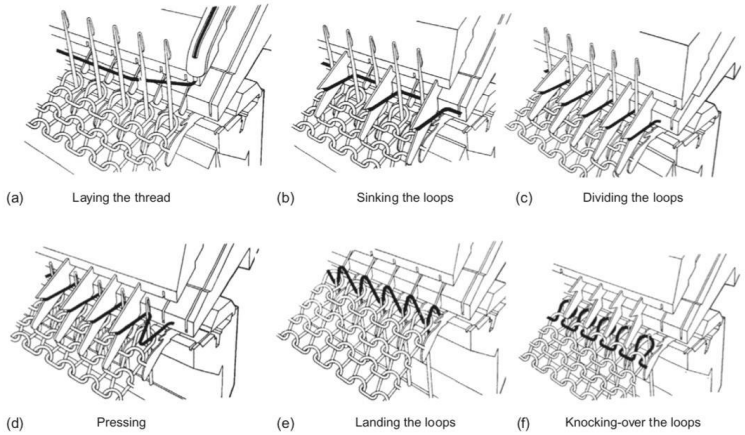

Figure 2-12. The manufacturing process of flat-bed knitting machine **[77]**

2.4.4.2 Circular knitting

Circular knitting (**Figure 2-13**) is a seamless technique which can produce stretchable,

comfortable and flexible fabrics. It is the most productive method in the knitting industry. Paradiso et al. [29] found that one of the variation between circular knitting and flatbed knitting is that circular knitting can only produce intarsia and double knitting structures separately while those structures are able to be manufactured together in the flat-bed knitting machine. The main advantage of circular knitting is its seamless technique which can fabricate elastic and comfortable fabrics at a lower cost.

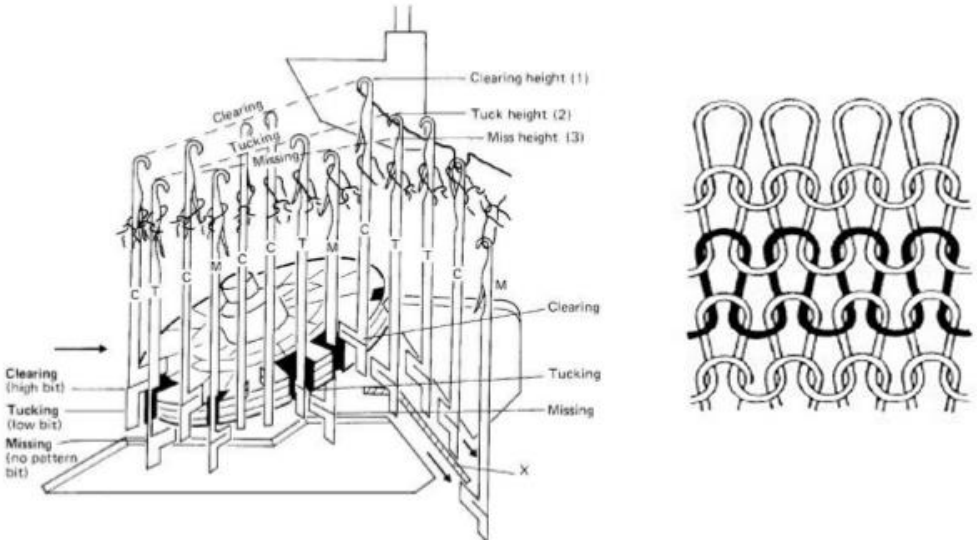

Figure 2-13. Circular knitting process **[28]**

According to Li et al. [80], the manufactured knitted pressure sensors (**Figure 2-14**) can evaluate peripheral stress of up to 283kPa and an electric transmission of 9.8k., They also noted that pressure sensors have excellent transmission and the fabric pressure sensor that is 3D can be as high as 50.31kPa. This means that the 3D fabric pressure sensor is superior to pressure sensors which are textile-based. The electrical resistance of manufactured sensors changes when the pressure decreases due to the twisting of fibres in the space layer and to more conductive connections.

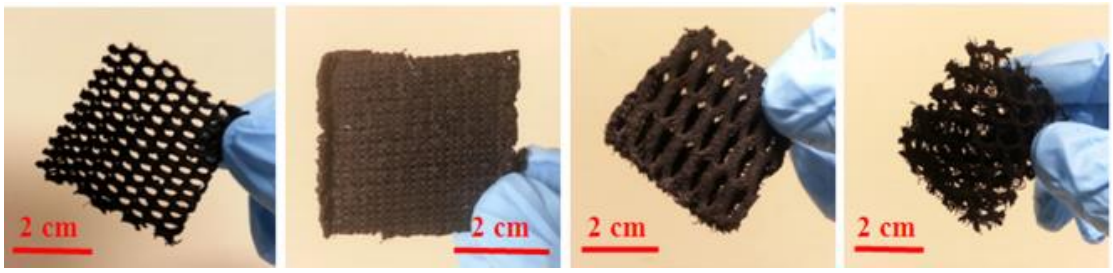

Figure 2-14.Four types of warp-knitted spacer fabric **[78]**

Pacelli et al. [79] (**Figure 2-15**), while evaluating the "sensing fabrics for monitoring physiological and biochemical variables: E-textile solutions", observed variations in electrical resistance due to mechanical deformation. A strong relationship between change in strain amplitude and resistance was established. They also observed that the application of trapezoidal wave as mechanical input increased the value of electric resistance and later decreased to a steady state value. These systems are advantageous because there is a possible of wearing them for a long time devoid of discomfort.

Figure 2-15. (Left) Flat knitted fabric electrodes, (Right) Seamless knitted fabric electrodes **[77]**

Compared to woven fabrics, knitted fabrics achieve a relatively higher tear strength, permeability and high elasticity. However, the thickness and bending modulus of the knitted fabric are relatively higher and the dimensional stability lower than the woven fabric.

2.4.5 Embroidery

The embroidery technique is an important fabrication method to produce smart wearable sensor, which attached the conductive sewing yarns to substrate fabrics to form the sensor structure. This technique is important in the production of fabrics which are conductive and can also apply yarn materials or monofilaments to specific substrates of a given geometry [81]. According to Stoppa [68], the researchers from MIT are regarded as developers in discovering the patterns of embroidery that can be interconnected with component pads or introduced to electric circuits.

A review of technical embroidery for smart textiles was conducted by Mecnika et al. [82] in which they basically classified technical applications of embroidery into medicine, engineering and smart textiles which are the three main application fields. The embroidered reinforcement structure is applied in automotive engineering, construction and aerospace engineering. Such composite reinforcements have various properties developed by the TFP technique due to the critical influence that fibre orientation has on the stress in the components. Embroidery is a new technology in tissue engineering and medical textile production. Nonetheless, it is successfully being utilized in the creation of three-dimensional structures for the purposes of tissue engineering and in wound dressing [83]. Lastly, embroidery is widely used in smart textiles as it is a great asset in the flexible and wearable development of electronics. It is often known as e-broidery due to its application in conductive materials. The standard embroidery and TFP techniques are mostly applied in developing textile structures that are interactive.

As pointed out by Mecnika et al [82], embroidery is advantageous because only one process of manufacturing will be employed when combining the supporting electronics with the conducive tracks in essential and complex geometry. On the other hand, electronic devices are conveniently created by embroidery due to both electronic devices and conductive paths sharing the same manufacturing process. In fact, among all the fabrication methods, this is the most unique productivity performance. Embroidery technologies exhibit an excellent efficiency when using multi-head embroidery machine[74]. Embroidery technique as the decoration process, it has a lower production cost and can also achieve functional and aesthetic in the same time [84].

According to past literature, there are three embroidery methods: standard embroidery, chain stitch embroidery and TFP [73].

2.4.5.1 Chain-stitch embroidery.

In the creation of textile-based sensors, chain-stitch embroidery is considered to be an important component. Similar to the crochet in geometry, the chain-stitch guarantees accuracy and when applied to the construction of the moss and kettle's embroidery, it is of significant benefit. However special attention should be given when selecting the end use of a machine because it is different from the ordinary embroidery machine.

Due to the uniqueness of the embroidery machines from a mechanical perspective, the same production techniques are applied. For example, in moss embroidery, single systems are used, making them core during the development of three-dimensional structures and the creation of electrode elements. The three-dimensional electrodes are important because they can flexibly adapt to body geometries and they feel comfortable upon contact with the skin. However, should a single yarn system break, the entire system will fall apart.

Figure 2-16 is a moss embroidery textile electrode. This electrode can be used as a sensor electrode for body signal monitoring, for example electroencephalography (EEG) or electromyography (EMG), electrocardiography (ECG).

Figure 2-16. Textile electrode obtained by moss embroidery **[79]**

2.4.5.2 Tailor Fibre placement (TFP)

The major difference between fibre replacements that are tailored and the other

approaches of embroidery is that, the former is defined by a three-yarn system. Therefore, the TFP allows precise penetration of base fabrics as well as a continuous installation of conductive textile materials. Because of its highly controlled property of geometry, the method can be used in ideal materials as a requirement for fit customization loading. The lower and upper yarns can be used to fix conductive fibres into base materials as shown in the working principle in **Figure 2-17**.

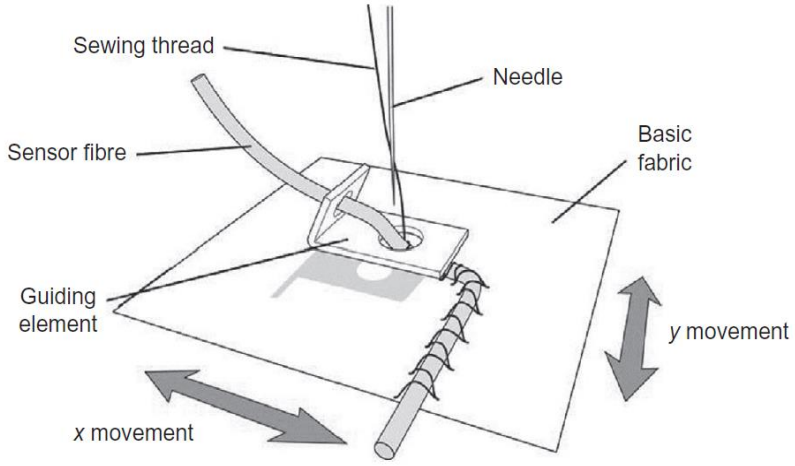

Figure 2-17. Basic principle driving tailored fibre placement (TFP) technologies **[71]**

The Tailored Fibre Placement techniques when compared with other materials of embroidery, are more independent of material selection. Although some materials cannot be embroidered on textiles, they can be directly placed on the fabric. Thus, this method creates a geometry of multiple sensors with stable fixation while undergoing textile embroidering as shown in **Figure 2-18.**

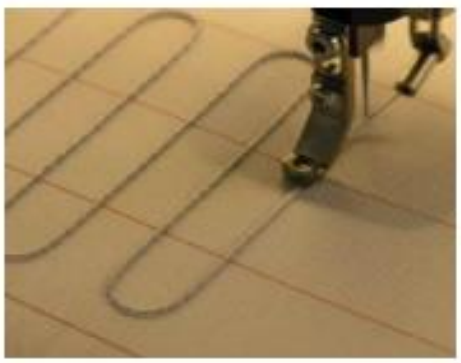

Figure 2-18. TFP embroidered stainless steel fibre for heating textiles **[71]**

2.4.5.3 Standard embroidery

Standard embroidery, also known as the Sozni stitch, uses the double lock stitch. This process consist of two sets of yarns: the upper and lower bobbin yarn. The upper yarns are kept on a tube shape bobbin and is fed through the needle while the lower yarns are kept on a smaller bobbin under the sewing panel. During the embroidery period, the substrate materials are held together by an embroidery frame with a backing material. The movement of the frame is controlled by the computerised embroidery machine. In order to create a desired patter, the movements are from the y and x directions, where the bobbin yarn is carried by the needle and penetrates the materials and by using a rotating gripper, the textiles interlace with the upper yarn.

The double lock stitches are used to create conductive pads since the lower and upper yarns provide accommodation for electric devices. Because the fabrics from standard embroidery are conductive when the lower and upper yarns are conductive, the conductive filaments are only contained in the upper material and if proper tension is used, they can be electrically half insulated.

In fact, standard embroidery can be used to utilize both the multi-head and single head machines of embroidery. When the electric parts are embroidered with a multi-head machine and the right pattern is produced in one step, this method can be time saving and accurate in the production of smart sensors.

Unlike the other methods of manufacturing textile sensors, in the process of embroidery, yarns experience various levels of tensile; they are affected by several factors such as dynamic load, bending, friction, and abrasion [85], [86] During embroidery, the lower yarn is usually thinner than the upper one, since the filling quality of the embroidered element is very important [85], [86]. Various stitch directions and different stitch

densities are used to fill the embroidery area; the lower yarn loop is not be visible from the front side, since the upper yarn loop becomes bigger than the lower one in the vent of cross-over of yarns[85]–[87].

Jucienė, M. et al [86] found that, because of the influence of mechanical forces at work during the process of embroidery, the embroidery systems are defective and, as a result their physical properties will change, meaning that the size of the embroidered sample does not match the actual size of the designed digital image. They believed that to prevent this effect, the physical and mechanical properties of fabrics and yarns shall be determined and to obtain an embroidery sample with a more accurate size, the direction and the properties of the materials are important [85].

Jucienė, M. et al found that the filling compression along the stitches (**Figure 2-19a**), quality of filling, such as an uneven edge, visible spaces between stitches, (**Figure 2-19b**) and the fabric yarn slippage at the edges of the embroidered element (**Figure 2-19c**) are the main and most common embroidery defects. Also, they discovered that the embroidered pattern area decreases compared to the digital area, and using polyester embroidered yarns can achieve a greater decrease value [86].

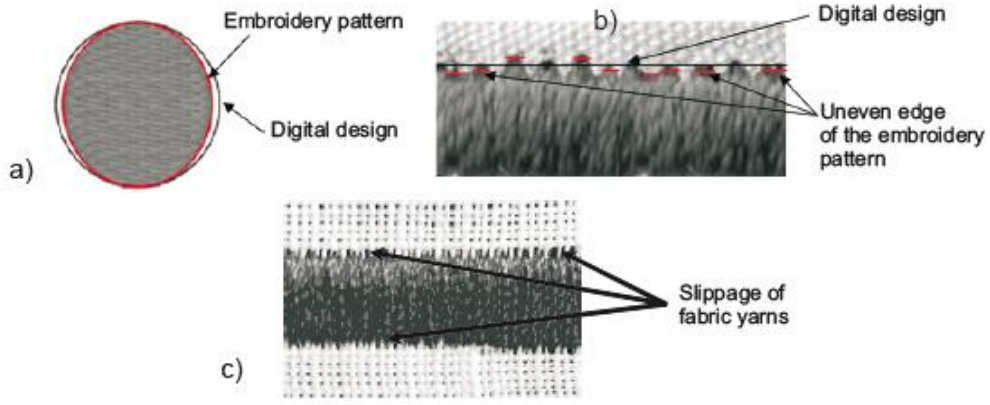

Figure 2-19. a) Filling compression along the stitches, b) Uneven edge of the embroidered pattern, c) Slippage of fabric yarns **[84]**

Figure 2-20 illustrates a system that consists of material, upper embroidered yarn, as

well as lower embroidered yarn. A required tension balance of embroidery yarns within a stitch (when a lower yarn occupies 1/3 to 2/3) eliminates the probability of the lower yarn being seen on the front side of the embroidery area [82] .

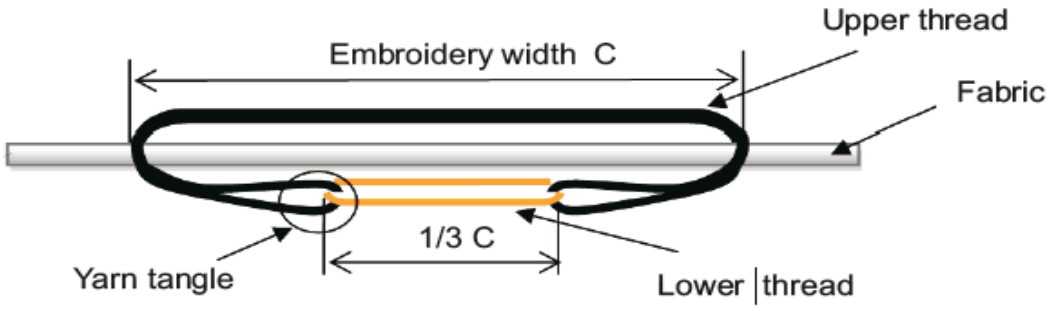

***Figure 2-20. Embroidery system of a single stitch* [82]**

Tsolis, A. et al determined that the electric field strength and textiles macro-fibres structure can be changed by using different embroidery patterns and stitch densities during the embroidery process. The central wave frequency of 100MHZ is reduced in the circuit due to the irregularly shaped embroidered sample [88].

2.4.5.4 Embroidered substrate fabric

Since they are placed close to the skin, smart textiles that are wearable have basic standards when being constructed. This makes the selection of suitable base structure materials an essential for both optimization of the skin contact comfort ability and subsequent fabrication circuits. During the selection of wearable textiles, tubular, depth, whole garment structures and spacer fabrics should be considered [89]. The woven fabrics are less stretchable compared to knitted fabrics. Woven structures are manufactured by interlacing warp and weft yarn, some woven structures mentioned in Chapter 2.4.3, structures like atlas woven structures are suitable for embroidered substrate fabric. Nonwoven fabric is a common embroidered substrate fabric material as well. It is generally made by different bonding techniques like entangled from fluid jet or adhesive bonding [90]. Fibres or filaments are melted by these bonding techniques

to form a new structure with higher strength.

Akerfeldt et al. chose a plain warp-knitted substrate (density is 220g/ m^2) which has approximately 32 wales and courses per centimetre in both directions. This substrate was chosen for its good elasticity and stability in all directions [91].

Roh et al. [92]used conductive-polymer-infused, nonwoven fabrics (Eeonyx) instead of conductor-loaded elastomeric materials (Zoflex) to minimise hysteresis and provide long-term stable uniform resistivity. They tried to use carbon-loaded paper which is inexpensive. However, it is not for complex Multitouch as it leads to high connection and integration costs.

Low loss and highly flexible polydimethylsiloxane (PDMS) were chosen by Zhang et al. due to its mechanical flexibility. What is more, its permittivity can be changed by dispersing ceramic powders into the PDMS matrix to adjust (its relative permittivity $\varepsilon r = 3.0$) [35], [93]

A more complex substrate was used by Linz et al. The flexible substrate they used consisted of a 50µm polyamide foil structured on both sides with 17µm copper; 5µm nickel; flash gold and 15µm solder resistor which shows a higher strength and good stability during embroidery and testing [33].

A type of Lycra (coolmax), often used for sports clothing, was chosen to be the substrate by Taelman et al. It has good stretch properties in both directions but the sensitivity to the electric charging is poor. Additionally, it has good heat regulating and moisture properties [28].

Apart from those substrates, Roh used a nonwoven cotton substrate [14] and Jayaraman

et al. used electro-optical fabric which is relatively expensive and might need printed circuit board electronics [94]–[96].

2.4.5.5. Embroidered sensor

Taelman et al. [28] used a ConTex project as depicted in **Figure 2-21** in their experiment; ConTex project can make it possible to monitor the physiological parameters of the body continuously and unobtrusively. However, the signal output of the ConTex project (a contactless sensor) is not very stable.

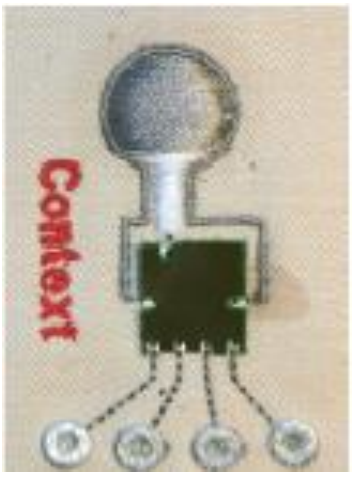

Figure 2-21. Embroidered contactless sensor **[27]**

According to Åkerfeldt et al. [97] the sources of energy were, however, available and would be generated from mechanical motions, body heat and radiation. They designed several embroidered sensors which were sewn on a glove to manufacture a textile sensing glove (**Figure 2-22**). The general idea is mainly to alter the disparity in temperature amid the environment and human body into an electric energy using thermo generators; this would be incorporated in clothing. Others observed that solar energy would be used to supply energy which would be stored in micro-batteries.

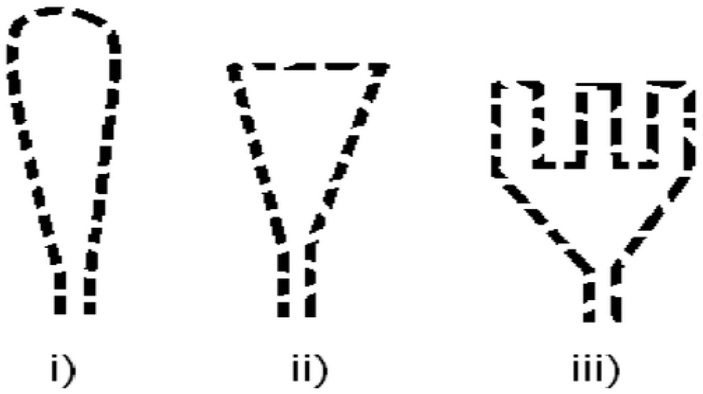

Figure 2-22. Different patterns of embroidered sensors designed by Åkerfeldt **[95]**

Zhang et al. [39] made a different pressure sensor using an embroidery machine as shown in **Figure 2-23** and **Figure 2-24**. The conductive continous filament yarns in the warp and weft directions are stitched by non-conductive yarns, and this structure can provide stable sensing points.

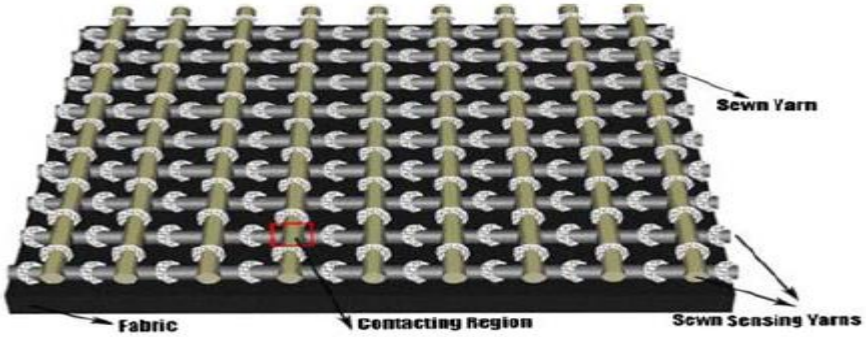

Figure 2-23. Embroidered pressure sensor **[37]**

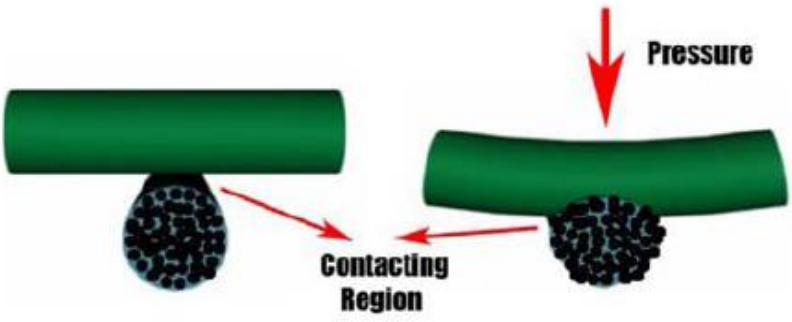

Figure 2-24. Yarn to yarn contacting region **[37]**

Moradi et al. [98] made two different patterns, pattern I was made by sewn horizontal lines and pattern II consisted of one horizontal line and zigzags sewn on it as seen in

Figure 2-25. They altered the density of Pattern I and Pattern II to build several different samples to investigate whether the density of each pattern has a significant influence on the final performance of the sensors.

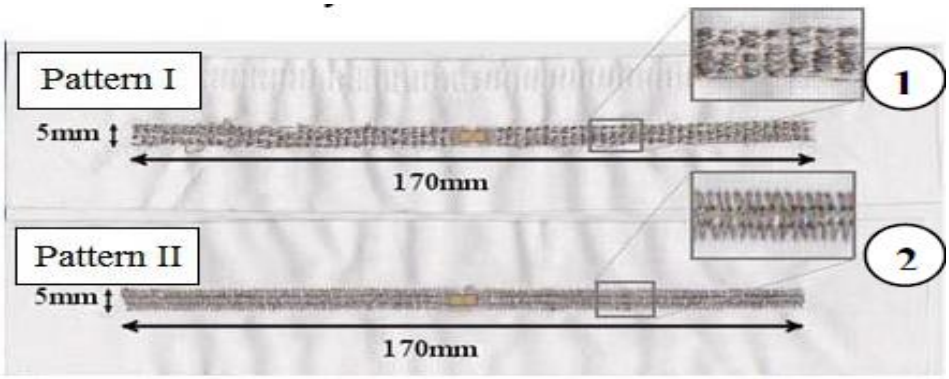

Figure 2-25. Zigzag patterns of stitching **[96]**

Zhang et al. [35] used a double stitching structure as illustrated in **Figure 2-26** to improve conductivity and it also allows the realisation of extremely thin slot and strip connections.

Figure 2-26. Double stitching structure **[33]**

Kallmayer et al. [99] used a horseshoe structure as shown in **Figure 2-27** which allows interruptions to be detected. By using multiple areas covered with this structure, a course localisation of penetration can be achieved.

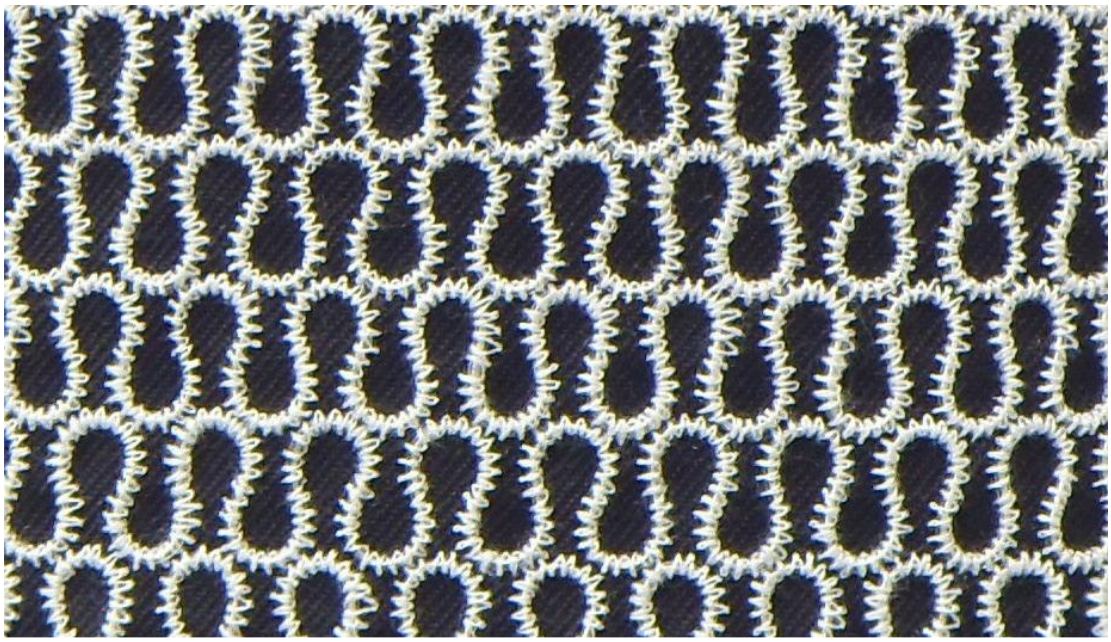

***Figure 2-27. Horseshoe structure* [97]**

This structure can be used in a pressure sensor as seen in **Figure 2-28**; it consists of two conductive layers and an insulating elastic foam layer. This sensor can monitor dynamic changes of pressure instead of making quantitative pressure measurements.

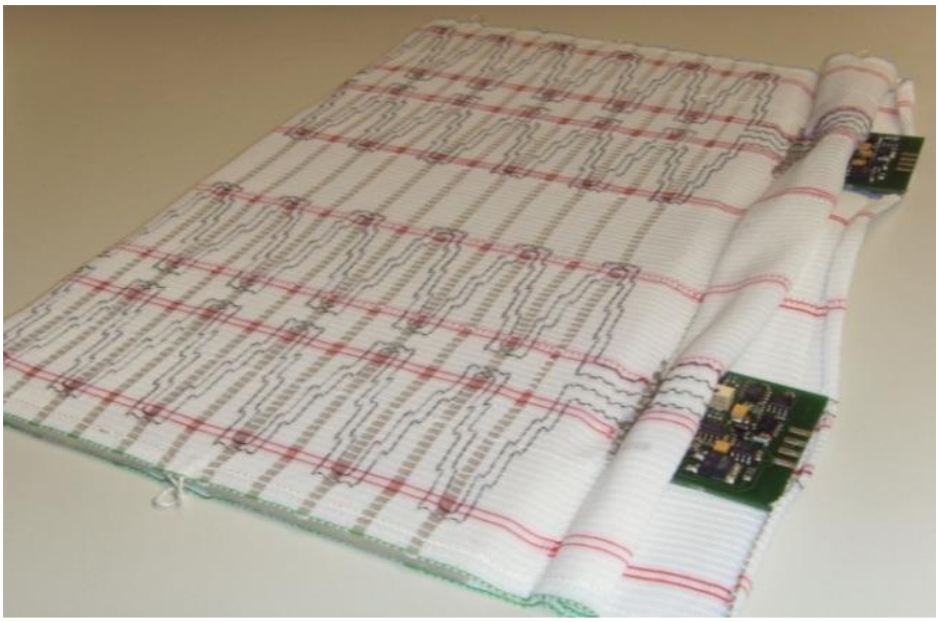

***Figure 2-28. Embroidered pressure sensor* [97]**

Byrne [100] used several different patterns in his research work for evaluation: A, B, C and D used the same pattern but different conductive yarns as can be seen in **Figure 2-29**. E and F used the same conductive yarn but E used a flat embroidery stitch while F

used an open chain stitch.

Figure 2-29. Various embroidered structures **[98]**

Hasani et al. [101] designed a strain radio frequency identification (RFID) –enabled sensor with the help of a dipole type antenna as pictured in **Figure 2-30**. This sensor combines both chipped and chipless RFID. They have proved in their publication that RFID-enabled strain sensors can be detected using chipless detection techniques as accurately as for the chipped technique [101]. Not only Hasani used RFID, Kim et al [102], Moradi et al [98] and Vena et al [101]used RFID sensing technology. They thought RFID could be a potential solution to the maintenance of the battery of remote sensors. A passive RFID sensor can obtain energy from the electromagnetic field, which means the operation of the sensor does not need any battery.

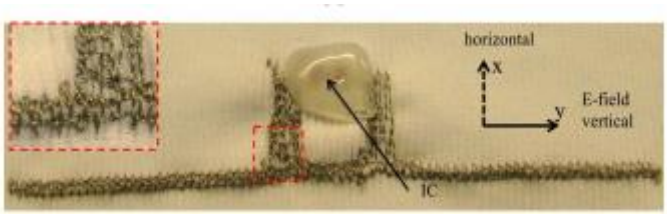

Figure 2-30. Embroidered antenna **[99]**

Dunne et al. [37], [103]used a simple cover stitch structure to build the stretch sensor shown in **Figure 2.31**, of which the top yarn is a conductive yarn and the under yarn is

cotton/poly yarn. This sensor presents an approximately linear response in the elastic region and this is highly correlated with elongation.

Figure 2-31. Embroidered strain sensor **[101]**

Kim et al. carried out a series of tests to show the relationship between the conductivity of embroidered sensors and the sewing repetition number, stitch gap and sewing thickness as illustrated in **Figure 2-32**. It can be seen from the graph that the sensor with lower thickness and stitch gap and a higher repetition number has better conductivity [102].

type	spec	C	type	spec	C
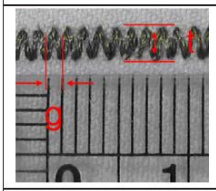	t:2mm g:1mm i:1	$2e^2$	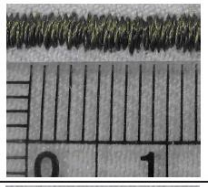	t:2mm g:0.5mm i:1	$4e^2$
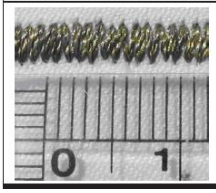	t:3mm g:1mm i:1	$3e^2$	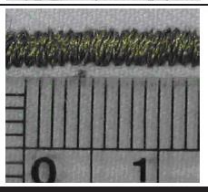	t:2mm g:0.5mm i :2	$2e^3$

Figure 2-32. Parameters for each embroidered zigzag sample **[100]**

Pola et al .[104]compared different types of textile electrodes (**Figure 2-33**) and searched for good measurement positions. The properties of the first four structurally different electrodes were compared in the first part. One of the electrodes was handmade with fabric embroidered with conductive yarn and the others were manufactured in the industry. The test focused on examining the extent to which the

textile electrode can stay put in different positions during movements. The embroidered electrode produced the best results. This electrode was in touch with the skin. They discovered that a good position may not apply to all because of the variance in body shapes that people possess.

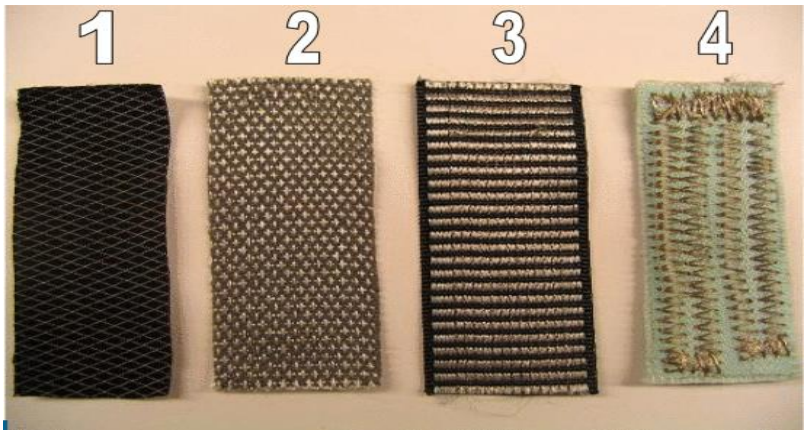

Figure 2-33. Textile electrode, 1) knitted, 2-3) woven, 4) embroidered **[102]**

Cho et al. [105] carried out research on the "performance evaluation of textile-based electrodes and motion sensors for smart clothing." They compared the new electrodes developed in the lab and the wave forms of the conventional AgCl electrode to scrutinize the ECG electrode usability. They established that the efficiency of the electrodes using metallic embellishing was high when its substrate was fabric mixed with the metal. The best conductivity in textile-based electrodes was obtained from Cu/Ni plated fabrics. The braided piezo-resistive fabric (**Figure 2-34**) showed better durability and more exact resistance changes. The posture and movement of the human body was detected from the relationship between the electrical resistance and the extension.

Figure 2-34. ECG shirt with embroidered ECG electrodes **[103]**

Roh [34], explored the textile touch sensing interaction design using a simple and uncomplicated technique of fabrication with a new metal composite embroidery (MCEYs) (**Figure 2-35**), aiming for a reliable and robust position and pressure sensors for wearable interfaces that are tangible. The study used a resistive method to enhance an accurate positional indicator in order to make the MCEY touch sensors. A simple embroidered potentiometer structure was tested as an input device. The study successfully used both the one- and two-point methods of sensing. The findings of the study were that the touch sensors indicated the likelihood of a flexible, frivolous, soft and a touchpad that was freely foldable as a common solution. The study also indicated that the smart textile field may be highly valued.

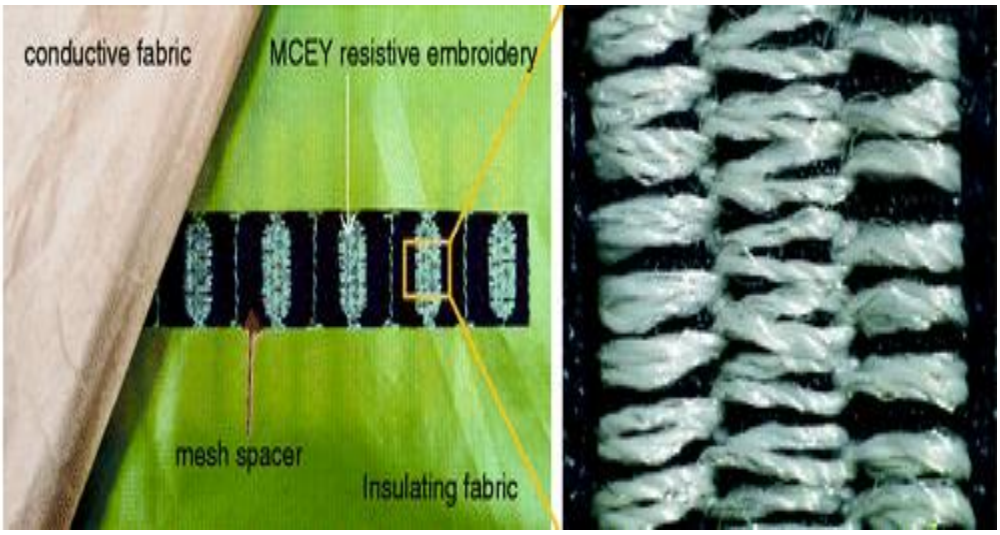

Figure 2-35. The MCEY embroidered potentiometer **[32]**

Trindade et al. [106]in their article presented the design, method of production, characterization and integration of textile sensors for the continuous monitoring of the respiration and cardiac vital signals. The article presents the EKG sensors which were of circular shape and a diameter of 25 mm and comprised of duo fabric layers. One of the fabric layers had a diameter of 16 mm and had an embroidery pattern (**Figure 2-36**). The layer was produced with yarns that were electrically conductive. The other fabric layer integrated a snap fastener. The study concluded that the embroidery method indicates a high degree of versatility to produce interconnects and textile sensors that are integrated in the clothing systems. The study also concluded that the method was considered suitable because it is based on digital systems and is therefore suitable for custom demand and large-scale production.

(a)

(b)

Figure 2-36. a) chest band with three electrodes interconnected, b) standard electrode and textile electrodes **[104]**

Gilliland et al. [107], in their study explored the use of textile Swatch book Interface in creating widgets similar to GUI that control mobile devices. As per the guidelines of creating an Embroidered Textile Interface (**Figure 2-37**), the research work used a

silver-coated yarn. The thinner conductive yarns had limited resistance per unit length compared to the thicker yarns. The brother domestic embroidery machines were preferred for this study as they use the same instructions and format as the large machines, yet they are inexpensive. The Brother Entrepreneur PR- 650 semi-professional machine was considered to be the best embroidering conductive yarn. The brother industrial machine is good for tension control as a predictable rate; however, the machine would not accept the needle. High tension from the machines and thin needle are some of the reasons that would make the needle break. The study introduced a number of widgets with textile interface and also showed a hybrid sensitive system that tolerates the interfaces capacitances charging system.

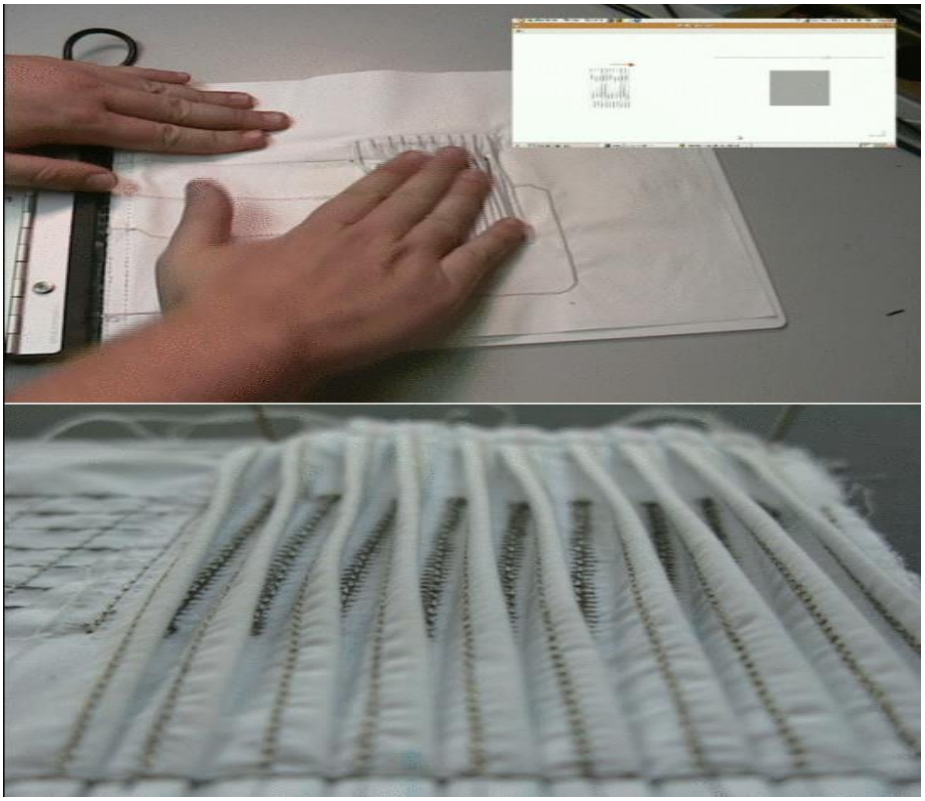

Figure 2-37. The interface swatch book and embroidered circuit **[105]**

Soukup et al. [19] pointed out that the existed moisture sensors demonstrate poor wash ability, have only one-point measurement and are low comfort. They designed and manufactured an embroidered structure with a 90 mm*90 mm sensing area (**Figure 2-38**). Stainless steel wires were used as the conductive yarns, and the sensors were tested

in a climatic chamber that is thermostatically controlled. The relative humidity was changed from 50 to 98%, and the test results were stable and repeatable.

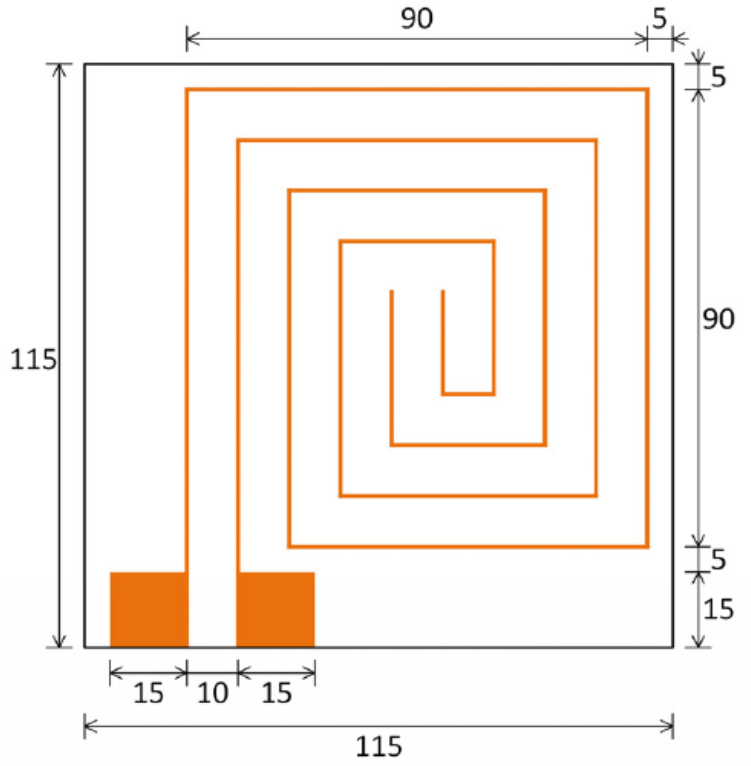

***Figure 2-38. Structure of embroidered moisture sensor* [18]**

Polansky et al. [20] designed a large area embroidered temperature sensor with hybrid resistive yarn (**Figure 2-39**). They pointed out that embroidered sensor with round corner can improve the mechanical resistance to the washing/drying process. The sensors were tested within an air oven, and the temperature was varied from 40 to 120℃. The embroidered sensor shows a faster response speed to a sudden temperature change than the others. Additionally, the temperature sensor presents a linear relationship between the resistance and the temperature. It also showed good long-term stability.

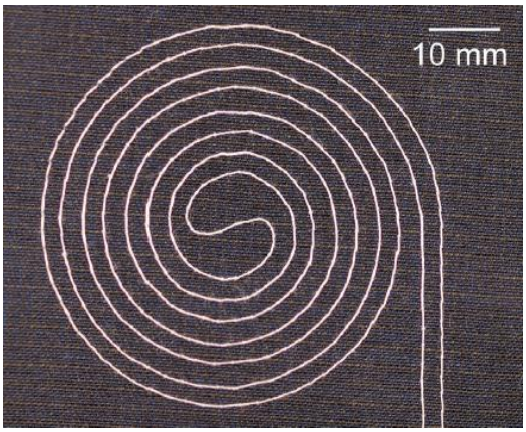

Figure 2-39. Structure of the embroidered temperature sensor **[19]**

Zhang, Wang and Volakis (2012) [93] also presented novel, body-worn, medical antennas and sensors based on e-fibres (**Figure 2-40**). In their research, a double layer fabcic was embroidered in order to improve surface conductivity and minimize yarn gaps and physical discontinuities. They established that the textile version of communication and lung sensors were equivalent to their metallic counterparts. In addition, textile sensors and antennas are durable and robust after repeated washing, flexing and drying. In order to avoid long time abrasion and corrosion, the future packaging process was in the process of development.

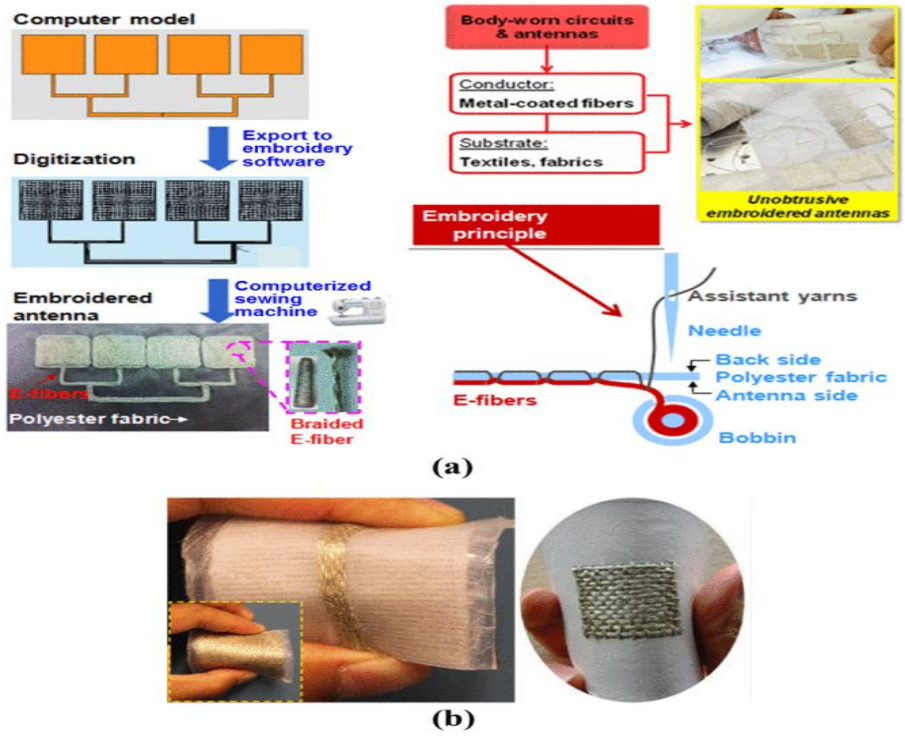

Figure 2-40. Fabrication process of the body-worn antennas and sensors **[91]**

2.4.6 Summary

Coating, printing, weaving, knitting and embroidery are the main electronic textiles manufacturing processes. However, they are not independent processes; these five manufacturing methods complement each other when produce textile sensors. For example, the mechanical properties of coated, printed and embroidered sensors are mainly based on substrate fabrics (knitted, nonwoven or woven fabrics), and the electrical properties of some woven, knitted and embroidered sensors generally depend on coated yarns.

Zhang Shiyu et al. [108]compared the five fabrication processes in their research. **Table 1** illustrates the summary of the properties of each fabrication process.

Table 1. Summary of the comparison of five fabrication processes **[106]**

	Weaving or knitting	**Printing**	**Coating or dying**	**Embroidery**
Ability of producing small pattern accurately	Medium	**Highest**	Low	Medium
Waste due to cutting	Yes	**No**	Yes	**No**
Initial investment	High	Highest	**Lowest**	Medium
Commercial materials available	**Yes**	Yes, but fewer	**Yes**	**Yes**
Whether the substrate fabric needed	**Yes**	No	No	No
Complexity of the fabrication process	**Easy**	Difficult	Medium	**Easy**

Aesthetic	**Yes**	**Yes**	No	**Yes**
Optimum applications	For customized Textile patterns	For small, complex patterns	For shielding, coarse patterns, large patterns	For small, complex patterns
Additional processes (cutting, sewing and hemming)	Yes	**No**	Yes	**No**
Reference	[109]–[116]	[117]–[125]	[110]–[116]	[131]–[143]

2.5 Electrical measurement of electrotextile sensors

Two main types of textile sensor were investigated and manufactured: capacitive and resistive type sensors. Electrical resistance is the easiest electrical parameter to measure with a highly accuracy over a wide range. Also, the capacitive sensor is relatively sensitive to the changes in the environment and it is more likely to be corroded [146]. In this research, all the sensors designed and manufactured are resistive sensors.

The common methods for measuring resistance are two-wire resistance measurement, four-wire resistance measurement and the Wheatstone bridge [147], [148].

The theory of two-wire resistance measurement is mainly based on Ohm's law (**Equation 1**); **Figure 2-41** is a basic circuit of two-wire resistance measurement. In **Figure 2-41**, V_m is the voltage measured by the meter and V_R is the voltage across resistor.

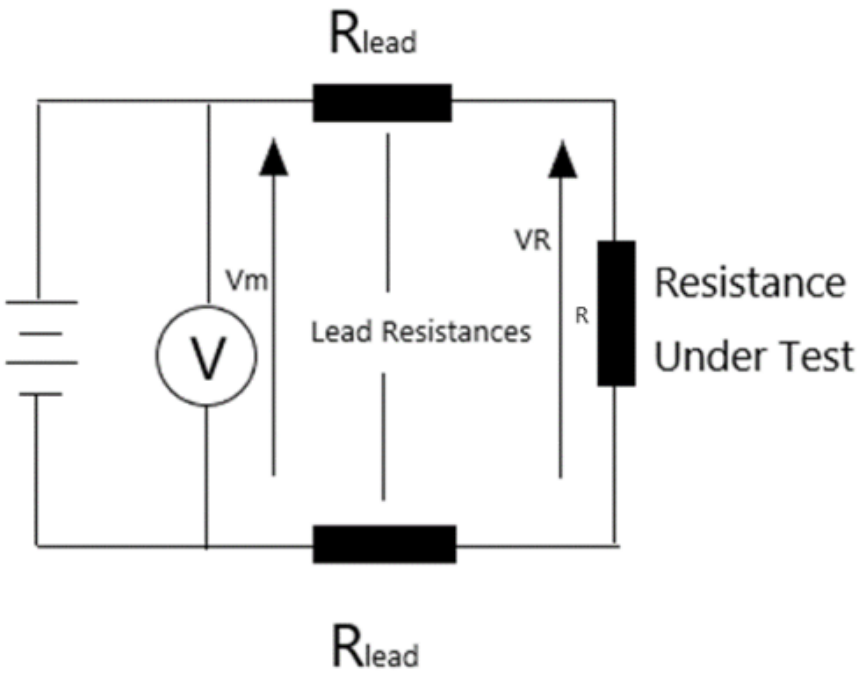

Figure 2-41. Two-wire resistance measurement

$$\frac{V_m}{I} = R + (2R_{lead}) \quad (2\text{-}1)$$

Where,

V_m is the voltage measured by the meter,

V_R is the voltage across the resistor,

R_{lead} is the resistance of the wire,

And R is the resistance under test

The main drawback of two-wire resistance measurement is its relatively lower accuracy, especially a low resistance measurement, since the resistance of the lead is added to the measurement. The current causes a small but not negligible voltage across the lead resistances; hence the measured voltage (V_m) is not the same as the voltage across the resistance under test (V_R). The actual resistance R should be less than the measurement.

Due to the limitation of the two-wire resistance measurement, four-wire resistance measurement (**Figure 2-42**) was developed and used. In this situation, the current passes through the resistance under test via one set of lead resistances, and the voltage

across the resistance under test through the other set of lead resistances. The current on the meter is negligible; hence the measured voltage (V_m) is the same as the voltage across the resistance under test (V_R). As a result, the four-wire method achieves a higher level of accuracy than the two-wire method. However, the accuracy of the four-wire method is still not enough, and both two-wire and four-wire methods might be influenced by the temperature.

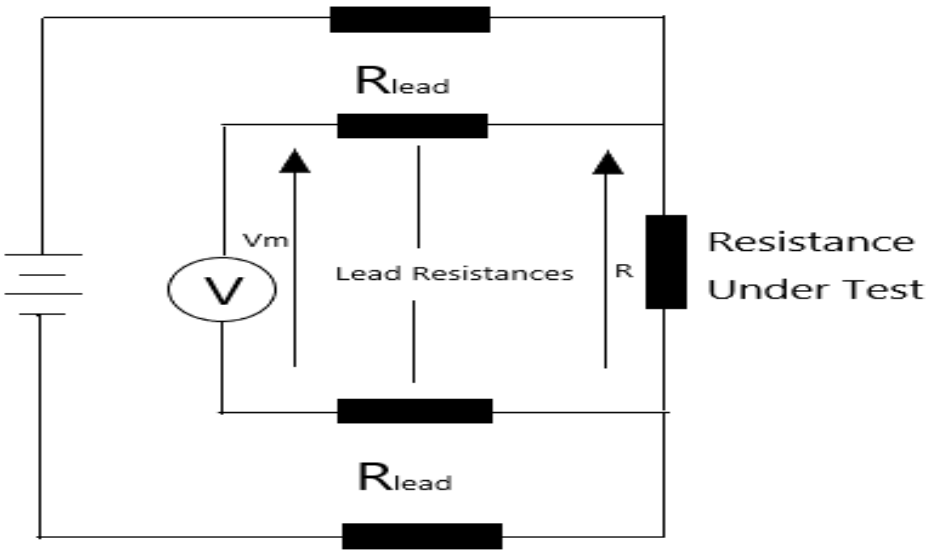

Figure 2-42. Four-wire resistance measurement

The Wheatstone bridge circuit contains two series-parallel arrangements of resistance connected between a voltage supply terminal. **Figure 2-43** shows the circuit diagram of a Wheatstone bridge. Wheatstone bridge is used to measure the unknown resistance by comparing it to a known value of resistances, and the bridge should be balanced before measurement.

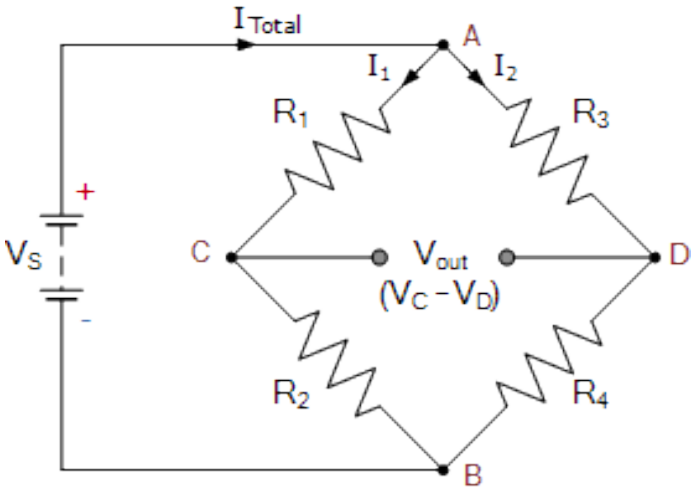

Figure 2-43. Wheatstone bridge

From the figure,

The voltage at C point $= V\frac{R_2}{R_1+R_2}$ (2-2)

The voltage at D point $= V\frac{R_4}{R_3+R_4}$ (2-3)

At balance : $V_C = V_D$ (2-4)

Hence, $\frac{R_2}{R_1+R_2} = \frac{R_4}{R_3+R_4}$ (2-5)

Hence, $\frac{R_1}{R_2} = \frac{R_3}{R_4}$ (2-6)

There are three types of Wheatstone bridge: full bridge, half bridge and quarter bridge. The full bridge circuit has four virable resistors, the half bridge circuit has two virable resistors and two fixed and equal resistors, and the quarter bridge has three fixed and equal resistors and only one virable resistor. As each type of Wheatstone bridge has different properties, they all have a different application. Usually, a full bridge circuit is used to measure more than one virable resistor, and the quarter bridge circuit is used to measure an unknown but constant resistor. As for the half bridge, it is used for high accuracy resistance measurement which changes over a relatively large range. Hence, the half bridge circuit is used for further resistance measurement.

2.5.1 Signal noise

There are generally two types of noise in wearable sensing garments: mechanical and electrical noise. The mechanical noise of the wearable sensors is an unavoidable problem, especially for cardiorespiratory sensors[149]. Mechanical noise can be divided into two categories: sensor intrinsic noise and motion induced noise. Sensor intrinsic noise, also known as system noise, has great influence on the wearable sensor measurement, such as the parasitic noise in capacitive sensors [150]–[152], and the temperature noise for piezoresistive sensors [153]–[155]. However, capacitive sensors present a weak resistivity to motion artefacts and noise [156]. The system noise can be measured by placing the sensor on a flat surface, and the resistance of the samples recorded for 15 minutes. The standard deviation of the changes in resistance is the system noise [157]. Motion induced noise occurs when measuring the respiration rate during body movement or measuring pressure during bending. These types of noise can be generally decreased by using a redundant sensor to pick out the real signal from the noise [158].

Electrical noise will affect the signal quality of the wearable sensing garment; the signal mainly includes the environment noise, body noise and skin-electrode interface noise[159], [160]. Body noise consists of muscle activity, skin potentials and cardiovascular activity. It can be reduced by using data processing techniques like a flitter. Environment noises usually come from electromagnetic interference from the electronics and moving electric charges near the testing environment. Skin-electrode interface noise is usually generated by the relative motion of electrodes on the skin; it can be decreased by using a robust mechanical layer of the sensor on the body.

2.6 Theory

2.6.1 The operation principle of embroidered piezoresistive sensor

Sensors based on the piezo-resistive effect trigger a response when the electrical resistance of a material changes in response to an applied strain. When the piezo-resistive effect is subjected to a strain stimulus, the resistance varies, and the sensor provides an electrical response. Piezo-resistive sensors are usually manufactured by one of two methods: one type is made from electroconductive yarns or fabrics; the other type is made using electroconductive ink. Alexander Bell's microphone using carbon rods under strain is a significant application of piezoresistive [92].

The pressure sensor is used primarily to measure the pressure of gases, liquids and textiles. It covers all the intelligent textiles. The force-sensitive piezo sensor is used to measure the activity of different muscles.

It is flexible and soft which implies that when the sensor is applied to clothing, it will not influence the comfort and flexibility of the textile [75]. Although sensors can have such properties, they also need to be produced at low cost in order not to overly affect the overall product cost [161]. Thus, when selecting the material, both the costs and the properties of the materials should be considered. **Figure 2-44** illustrates the normal structure of the pressure sensor. When pressure is applied to the sensor, the sensor structure is changed and this leads to changes in the sensor's resistance.

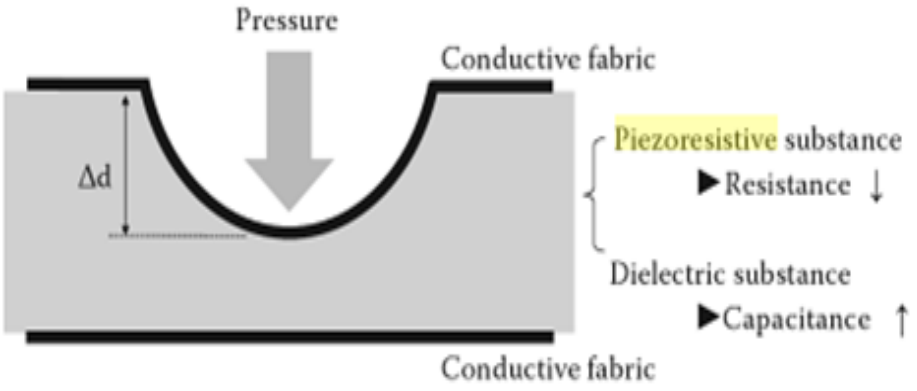

Figure 2-44. Pressure Sensor Structure [73]

With the increasing development of smart textiles, flexible strain sensors are now in high demand due to their wearable, extendable and excellent elastic properties to cover a 3D surface [162]. For example, wearable sensors can detect vital signals in real time of a wearer's health for medical applications [163]–[165].Textile strain sensors are widely used to monitor physiological or biomechanical properties of the human body, such as heart rate, body movements and motions of joints. In order to monitor these properties, the sensors should be flexible, comfortable, breathable and non-obtrusive for daily activities [162].

Embroidered sensors can be used to measure some physical-technical parameters such as capacity, pressure, strain, and temperature [45]. An advantage of the embroidered sensor is its cost effectiveness, especially when large area sensors are needed. The manufacturing process of embroidered sensors can be described as using fine metallic wires, conductive coated or other conductive yarns attached to the fabrics by stitching techniques to form designed electrical circuits or other designed shapes. The common diameter of the conductive yarn ranges from 40μm to 100μm, in order to manufacture neat and clean samples, the diameter of the sewing yarn should be low.

The operational principles of a piezo-resistance sensor are based on the piezo-resistance

effect which is a change in the resistance of a piezo-resistance material when mechanical strain or pressure is applied [91], [166]. According to the equation, $\rho_\sigma = (\partial_\rho/\rho)/ \varepsilon$, where ∂_ρ is change in resistivity, ρ is original resistivity and ε is strain. Thus, when pressure or strain is applied to the piezo-resistance sensor, the resistance is changed. And the equation can be transformed to $R=\rho*L/S$ where R is the resistance of the conductor, L is the length of the conductor and S is the area of the conductor. As for an embroidered sensor, L is the length of the conductive sewing yarn (stitch numbers), S is the distribution area of the conductive yarn (the density of the embroidered sensor). When pressure or strain is applied to the sensor, the sensor is deformed and the density of the sensor varies, leading to a change in the resistance of the sensor.

The measurement principle for a piezo-resistance sensor is commonly based on the Wheatstone bridge circuit. When the sensor resistance varies due to the piezo-resistance effect, the resistance can be calculated by comparing this voltage change to the reference voltage divider [167].

2.6.2 The operation principle of embroidered resistance type moisture sensor

As mentioned in Chapter 2, moisture sensors are usually resistance type or capacitance type. Since resistance is more easily measured than capacitance, and resistance type sensors are generally more stable than capacitance type sensors, capacitance type sensors are more likely influenced by humidity, temperature and other environmental parameters. A resistance type embroidered sensor usually consists of two separate electrodes and when water is present between the two electrodes, the open circuit is connected and becomes a closed circuit (**Figure 2-45**). The current can then be passed from one electrode to the other one and the changes in resistance can be measured by the equipment.

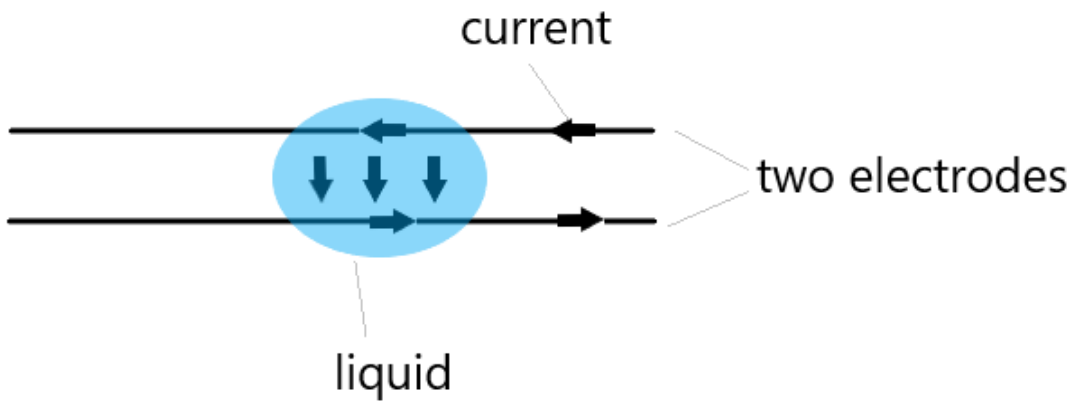

Figure 2-45. Operation of the textile moisture sensor

2.6.3 The operation principle of embroidered temperature sensor and heating element

The working principle of a temperature sensor is based on the resistance of the conductive yarn that varies due to changes in its temperature. Equation (2-7) below shows the relationship between the resistance of the conductive yarn:

$$R_{ref} = \frac{4l\rho_{ref}}{\pi d^2} \quad (2\text{-}7)$$

Where,

R_{ref} is the resistance of the conductive yarn at the reference temperature

ρ_{ref} is the resistivity of the conductive yarn at the reference temperature

l is the length of the conductive yarn

d is the diameter of the conductive yarn

The equation (8) below stated the relationship between temperature and the resistance of the conductors:

$$R = R_{ref}[1 + \alpha(T - T_{ref}) \quad (2\text{-}8)$$

Where,

R= conductor resistance at temperature "T"

R_{ref} = conductor resistance at reference temperature T_{ref}

α = Temperature coefficient of resistance for conductor material

When the temperature changes, the resistance of the sensor will react to the changes in temperature. Additionally, if the relationship of the resistance and the temperature is linear, then the temperature can be calculated by measuring the resistance of the sensor.

The operating principle of the heat patch is based on Joule's first law (equation 2-9), which is also known as resistive heating; this is the process by which the passage of an electric current through a conductor releases heat.

$$Q = I^2Rt = \frac{U^2}{R}t \quad (2\text{-}9)$$

Where,

Q = the amount of heat

I = the current through the conductor

R = the resistance of the conductor

U = the voltage measured across the conductor

t = the time

It can be seen from equation 2-9, with a constant power supplied, in order to get a higher Q, namely a higher heat output, the resistance of the conductor should be relatively lower. **Figure 2-46a and 2-46b** show a series circuit and a parallel circuit respectively. For N equal resistances in series, the total resistance of the circuit is NR, and for N equal resistances in parallel, the total resistance of the circuit is R/N. It can be clearly found that R/N is always lower than NR.

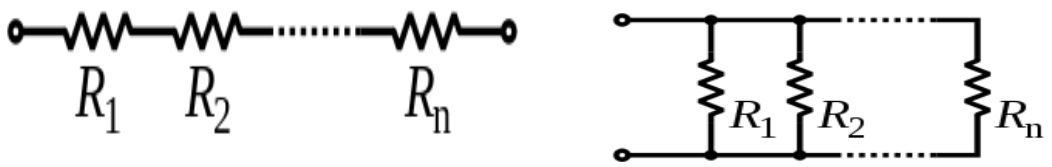

(a) **(b)**

Figure 2-46. a) Series circuit, b) Parallel circuit

2.7 Applications

2.7.1 Piezoresistive sensors

According to Wang et al. [168]elastic and supple pressure sensors (**Figure 2-47**) are critical components of wearable electronics that are useful and applied in our modern daily lives. According to their findings, the pressure sensors have the ability to measure pressure up to a maximum capacity of 2000kpa. This covers the whole range of the interaction between human and machine. The range was measured and the sensor sensitivity was determined quantitatively by the adjustment of the Young's modulus of the geometrical dimensions and the two conversional layers. The rise in young modulus of the support increased the range of the maximum pressure. The sensor cyclic compression was conducted on an Instron 5566 mechanical testing series machine in which the compressing speed was 40 mm/min and a compression displacement of 1.92 mm with a compression ratio of 40%.

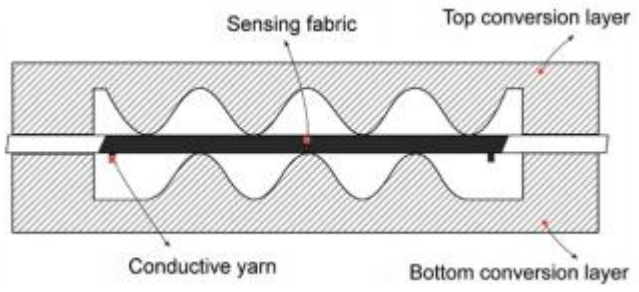

Figure 2-47. Structure of a typical pressure sensor **[159]**

Dunne et al. [103] carried out research on the "Initial development and testing of a novel foam-based pressure sensor for wearable sensing." They described the development of the foam sensor and prototype sensing garment bearing sensors (**Figure 2-48**) in various parts such as torso to determine the rate of breathing, neck movement, shoulder movement and the scapula pressure. They established that foam shows a conductance response that is linearly positive, relative to the increase in pressure. Tests on torsos indicated that it reacts in a measurable and predictable behaviour to neck movement, scapula pressure, shoulder movement, and breathing. The results revealed that there is great hope for the use of polypyrrole foam as a sensor for wearable, ubiquitous computing and medical applications.

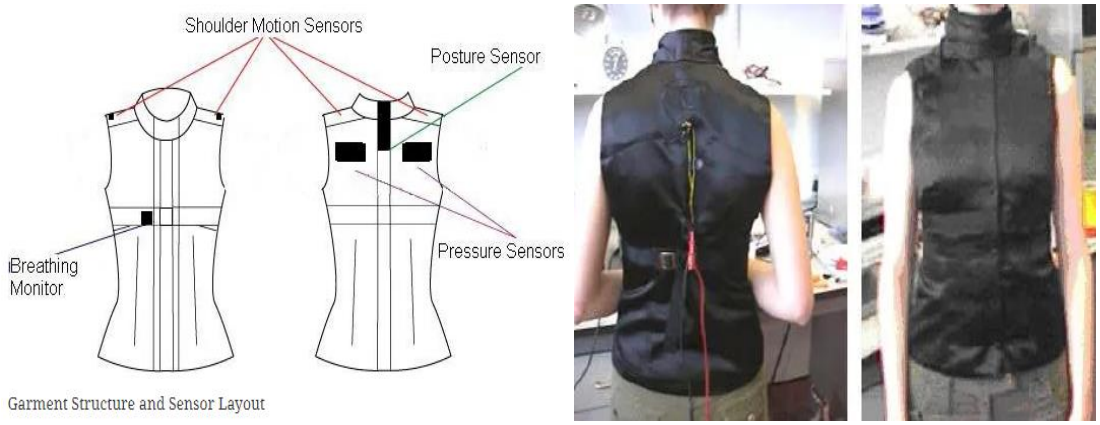

Figure 2-48. (Left) Garment structure, (Right) The photo type pressure torso garment **[101]**

Rundqvist [169], while analyzing the piezoelectric behaviour of "woven constructions based on poly (Vinylidene fluoride) bi-component fibres" (**Figure 2-49**), established that different conductive materials influence PVDF fibres in a myriad of ways which depend on the resistance of the material. His studies show that there was a possibility of integrating a piezoelectric bi-component fibre into a textile construction and conductive yarns could be used as outer electrodes to produce a fully textile piezoelectric sensor. He integrated various bi-components of PVDF fibres into different weave constructions such as twill weave and weft rib. The integration of different

conductive materials was done using a PVDF bi-component fibre which helped in the analysis of the behaviour of the PVDF material.

Figure 2-49. Woven fabric before and after being coated **[161]**

Meyer et al. [26] developed sensors for textiles with a standard error of below 4 percent and a special resolution of 20*20 mm (**Figure 2-50**). The sensors were inserted on the upper arm to determine forearm deflection between 0 and 135 degrees due to muscle bending. The study indicated that the sensors were able to detect the activities of the muscles. The study recommended that the sensors be applied to different movements as well as other muscles to confirm that the sensors can also be used for detection of muscle activities as well as motion tracking.

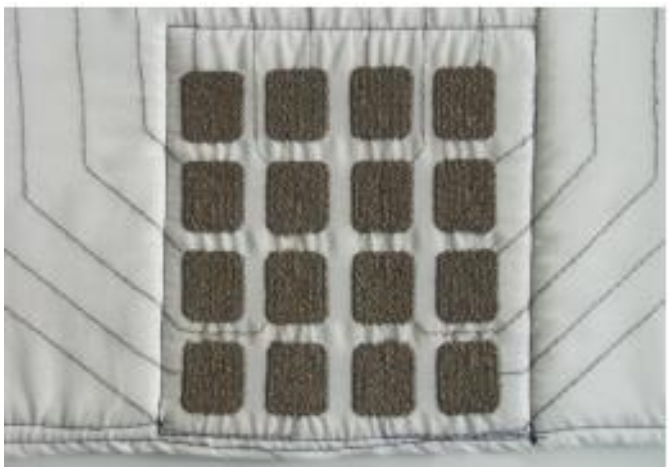

Figure 2-50. Textile pressure sensor matrix **[25]**

Hamdani et al. [170] also sought to "examine the application of the Piezo- Resistive Cardiorespiratory sensor system in an automobile safety belt." The study was based on

the fact that heart failure and respiratory conditions may be difficult to predict and can occur with little warning. The safety belt of a car is primarily designed to make the vehicle occupant safe in the event of an accident. This study developed a model safety belt (**Figure 2-51**) which is used to acquire heart and respiratory signals. The model protective belt was based on a nonwoven material constructed from copper ink to enable it to work on a piezo-resistive property. The Ballistocardiograph (BCG) signal can be measured due to the force exerted by the expansion of thorax/abdomen. The research work indicated that it is possible to achieve stable respiration signals due to the expanding nature of the abdomen. However, the study recommended that further research needs to be carried out in a way that improves sensor sensitivity in order to enhance its capacity to also sense the heart rate.

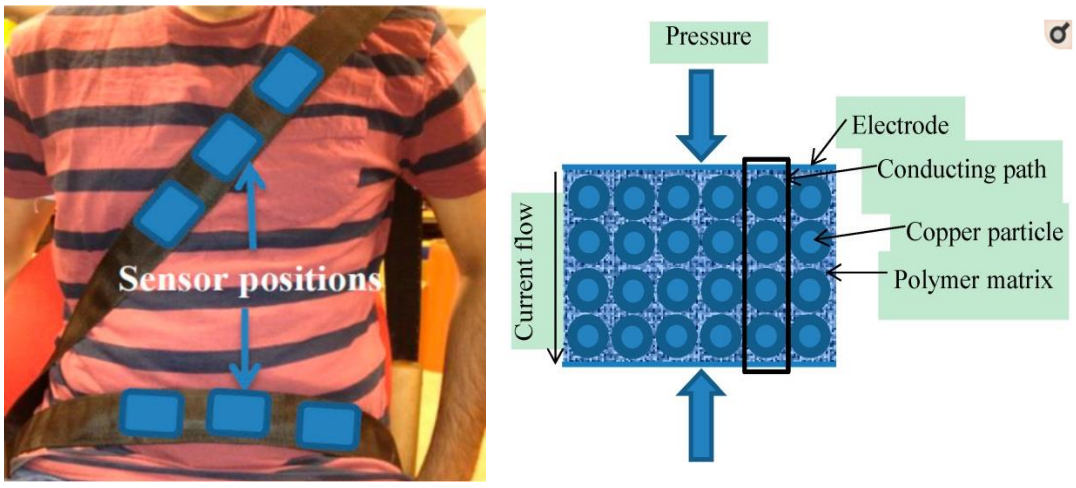

***Figure 2-51. Prototype safety belt and the schematic diagram of the piezoresistive sensor* [162]**

Gong et al.[171], in their study also presented a sensor that is exceedingly receptive to pressure with gold nanowires that are ultra-thin (**Figure 2-52**). The ultra-thin gold nanowires are perfunctorily flexible blocks with high potential for application in the future. The study reported a fabrication strategy that is cost effective and efficient in constructing a highly sensitive sensor for pressure by sandwiching a tissue paper that is impregnated with ultra-thin gold nanowire. The sensors can be run on a battery voltage of 1.5 V and have the capacity to detect pressing forces as low as 13 Pa. The sensors also consume less energy. In addition, the study also concluded that the sensors have

the capacity to resolve acoustic vibrations, torsional forces, bending and pressing forces. Due to its mechanical flexibility and sensing properties, the system enables the screening of heart beats as well as petite tremors from music.

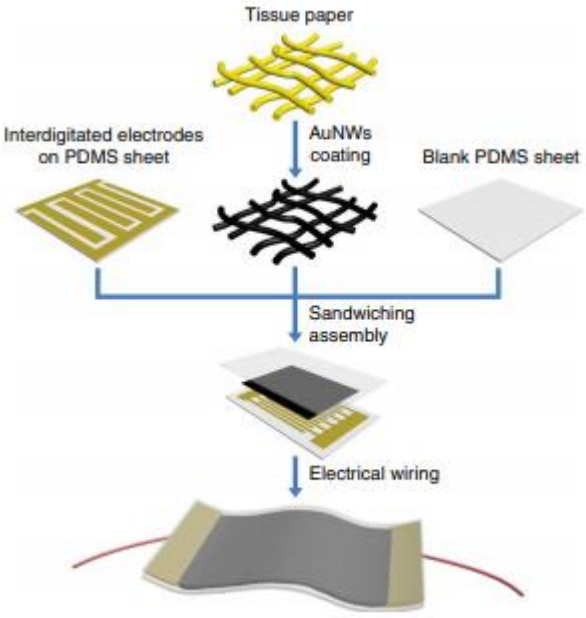

Figure 2-52. Fabrication process of the AuNW-coated tissue paper **[163]**

Huang et al.[172] presented smart textiles sensors which are fabric-based to scrutinize respiration, posture and gesture. In their study, most of their sensors that were fabric-based had a coating of either piezo resistive materials or conductive fibres that were directly knitted into fabrics. The study focused on the sensors that are yarn-based and fabricated using fibres that are piezo resistive, regular polyester and elastic fibres. The sensors were fabricated using both the double and single wrapping methods. The performance of the sensors was measured using the resistance changes under variable loadings. The conducting means of the electrical fabric and yarn are replicated by the use of the circuit network to examine major elements that contribute to the fabric sensor. The double wrapping yarn was considered a better sensing element due to its symmetric structure and its high ability to resist higher linearity and slippage. The study also investigated the effect of using the twist per meter (TPM). The findings indicated no considerable effects of using different TPM. It was concluded that the fibre-based antenna can trace the respiratory signals precisely.

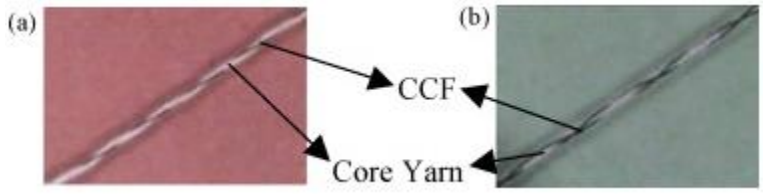

Figure 2-53. The yarn structure of yarn-based piezoresistive sensor **[164]**

According to Salibindla et al. [173], "pressure sensors are generally used in the body networks to measure the physical force that is exerted by the limbs." The article also gives examples of two main sensors: the piezoelectric sensors and the force sensitive resistors. The two sensors are based on a technology that embraces rigid semiconductors (**Figure 2-54**). For the sensors to accommodate human movements, the antennae must be made highly bendable. The other fabric layer contained a snap fastener. The study concluded that the embroidery method demonstrates a high degree of versatility to produce interconnects and textile sensors that are integrated in the clothing systems.

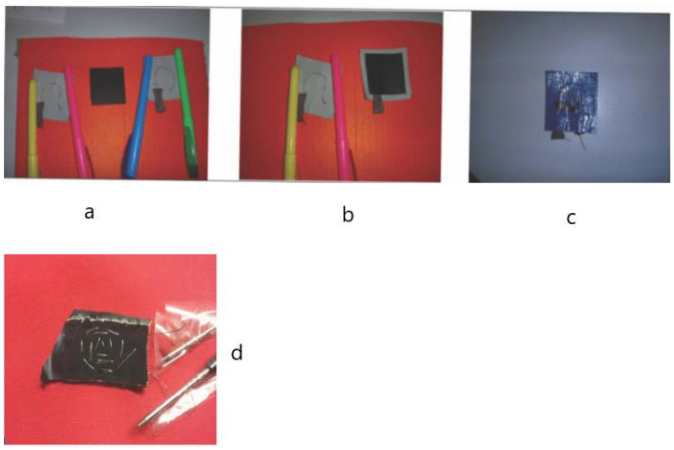

Figure 2-54. a-c) the fabrication process of the type 1 sensor, d) sensor type 2 **[165]**

The research therefore focused on designing stress sensors that are flexible, and focused particularly on the effect of thin film carbon and electrode composition. In the study, fourteen sensor designs with resistive layers of velostat as a piezo were built with electrode materials such as tin, copper and silver. The sensors were classified into different types, depending on the insulating material as well as the conducting material

used. The results of the tests indicated that the performance and reliability of the sensors were high and repeatable.

Goy et al.. [174] mentioned that pressor sensors are highly valuable transducers which are applicable to numerous medical applications. The authors argued that the lightweight pressure sensors have a poor capacity of gauging the pressure of contact amid two surfaces. The study involved fabricating different sensors using several types of wearable sensor for contact pressures. A sandwiched piezo-resistive film and different conductive textile materials were used (**Figure 2-55**). The aim of the study was to obtain their metrological properties and determine the physical characteristics that enhance their capability in measuring contact pressures. The study revealed that it is possible to attain sensors of contact pressures with reasonable sensitivity, assortment and repeatability via the process of fabrication.

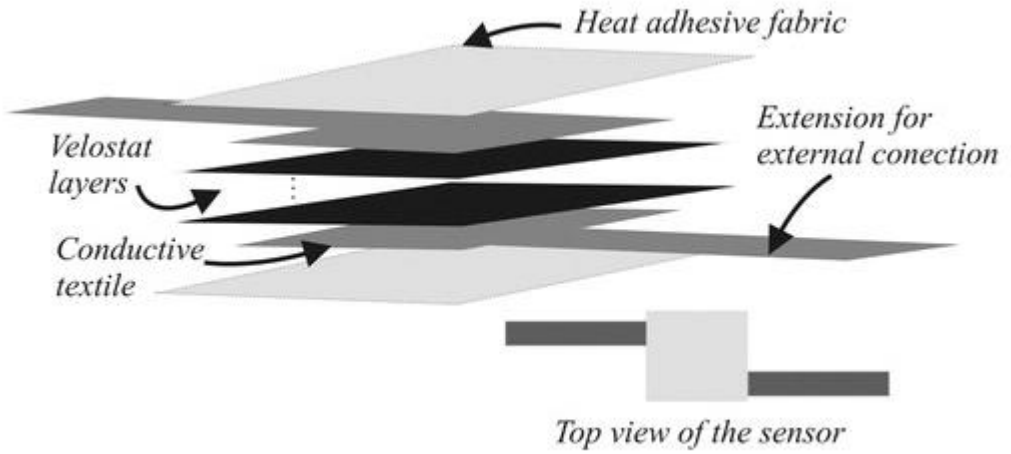

Figure 2-55. Contact pressure sensors structure **[166]**

Meyer et al. [36]also designed a sensor made of textile for quantifying the circulation of pressure around the human body. The conductive textiles were used to build sensors which were set on both sides of the spacer that is compressible and formed a capacitor that is variable. The use of the fabrics made the sensors more comfortable, washable, comfortable and unobtrusive. Preisach's model was used to model the sensor and reduce

the error of measurement to 5%. The models were used in reducing the hysteresis of the model. The study concluded that the textile sensor can be used for classifying sitting postures with accuracy.

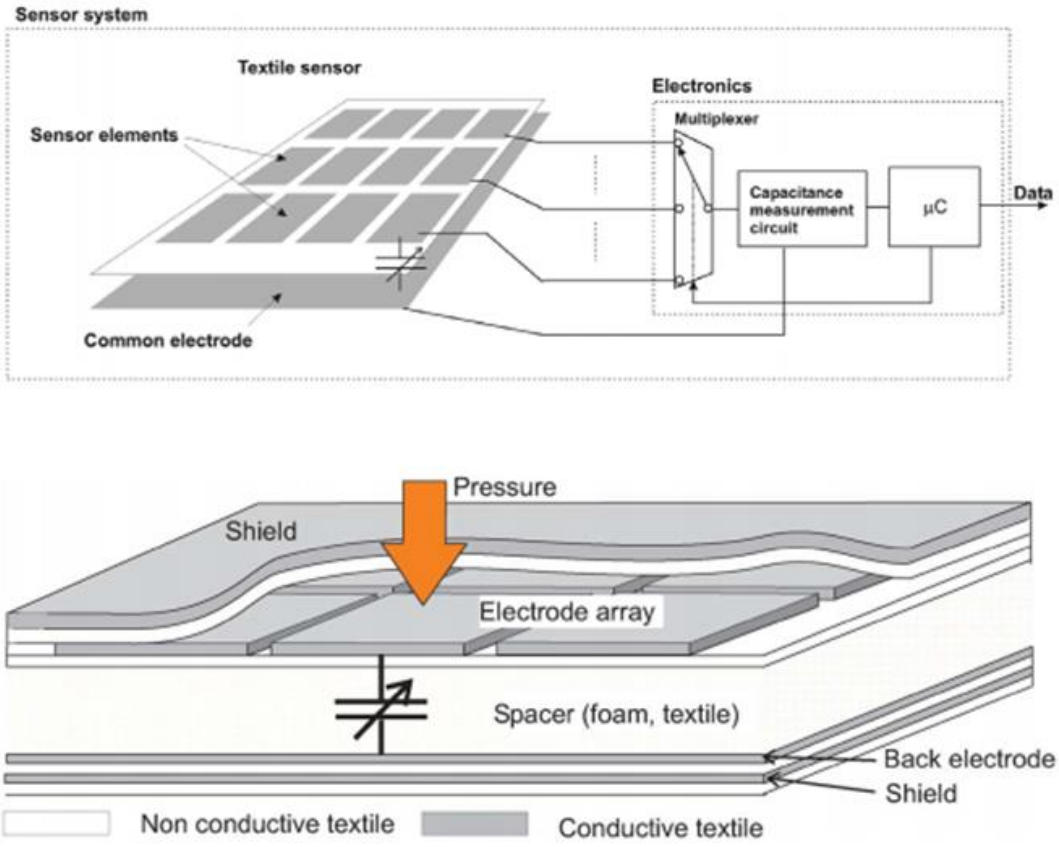

Figure 2-56. The structure of the sensor matrix **[34]**

Schwartz et al.[175]also argued that supple force sensors are part of the electronic skin that allows future robots and biomedical prostheses to naturally interact with the environment and humans. The article focused on flexible organic thin film transistors which are pressure-sensitive (**Figure 2-57**). The maximum sensitivity of the transistors was 8.4 kPa^{-1} with a low consumption of power. The study revealed that the features that were pyramid-shaped were more receptive to force than the line-shaped features. Further investigations also indicated that the device would even operate efficiently in the twisted state needed for bio-monitoring and for electronic skin applications. The device was also found to be suitable for long term diagnostics.

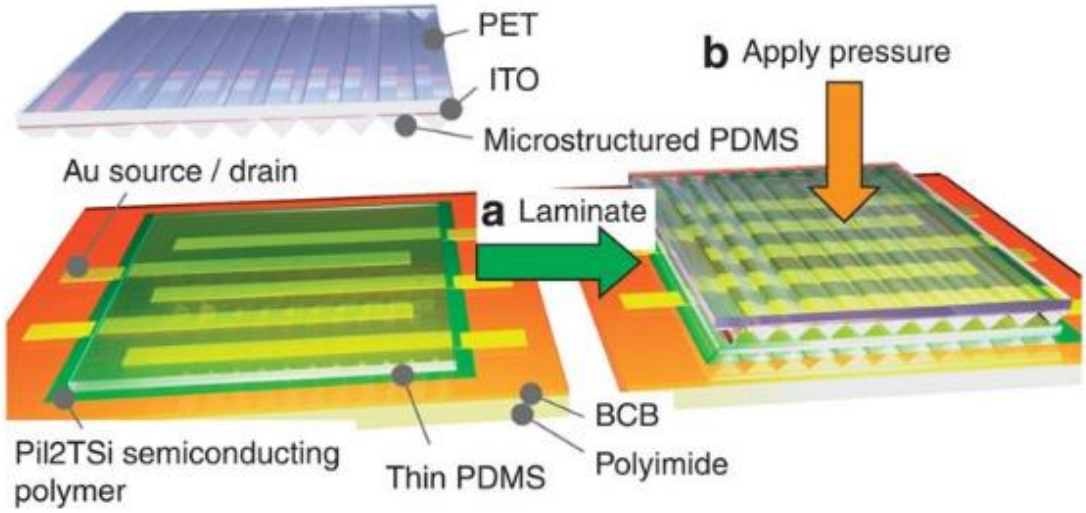

Figure 2-57. Schematic of the fabrication of the pressure sensitive transistor **[167]**

Baldoli et al. [176] argued that matrix textile sensors can also be used to measure the distribution of pressure on robotics, consumer and wearable electronics, automotive systems and also in the biomedical field (**Figure 2-58**). The study employed novel tests to consider sensitivity in terms of surface curvature, shear force and stretch. The results of the study indicated that the matrix textile sensors demonstrate a performance of high quality. However, the study noted a drawback of piezoresistive sensing elements and limited dynamic accuracy.

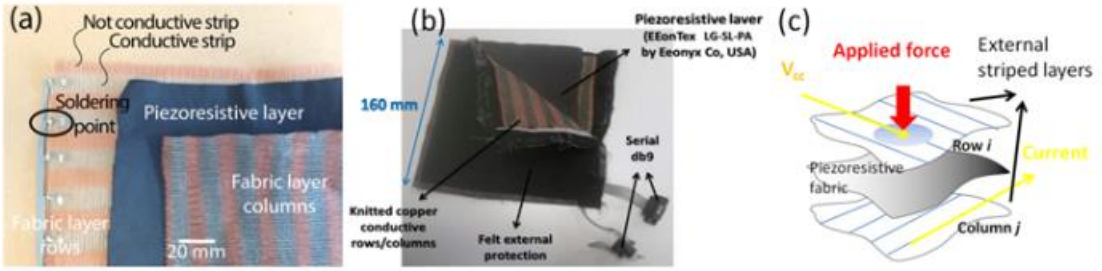

Figure 2-58. a) multilayer sensor matrix, b) complete sensor matrix, c) the sketch of the multilayer structure **[168]**

Zhang at al. [41] also presented a design that involves a fundamentally electrical conductive sensor that is based on textiles (**Figure 2-59**). The authors suggested that the structure of the textiles exhibits flexibility, breathability and deformable properties, making them wearable. The paper introduces a method of sensing experimentally and

theoretically to discover the strategy for obtaining a strain sensor from the textile. The conducting means of the electrical fabric and yarn are replicated by the use of the circuit network to examine major elements that contribute to the fabric sensor. The study revealed that the key factor that influences the mechanism of sensing is determined and created by the fabric structure. The structure can be created by two contacting yarns or fibres.

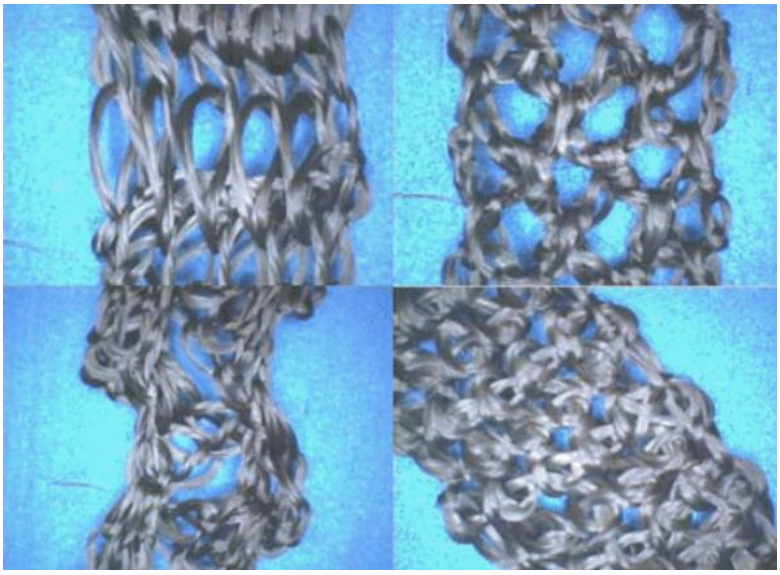

***Figure 2-59. Steel fibre crochet structure fabric sensors* [39]**

2.7.2 Moisture sensors

Moisture and humidity detection are core in the application of athletic, medical, home and industrial technologies. During food, wood, pharmaceutical and semiconductor production, it is important to monitor the levels of humidity. This implies that there are several applications of humidity level arrangements that have been used to control varying levels of water vapour [177], [178].

Humidity changes are detected using the textile moisture sensor, which has the working principle of resistance and capacitance and is responsible for responding to moisture variations accordingly. The first type of moisture detection sensor is the capacitive humidity sensor which works in keeping with changes in the dielectric constant. The

other moisture detection sensor is the resistive humidity textile sensor which responds to water vapour because of its conductivity variations [179]. Specific humidity expresses the speed of vapour, whereas relative humidity is the percentage of the vapour content in air under some specified temperatures compared to the vapour content in the air under measuring temperature.

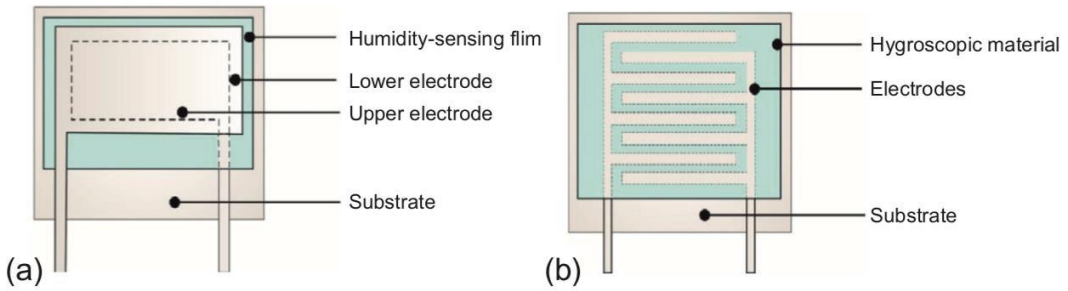

Figure 2-60. a) capacitance moisture sensor, b) resistance moisture sensor **[170]**

During the construction of capacitive humidity sensors like polysulfone (PSF), polyether sulfone (PSE) and divinyl siloxane benzo cyclobutene (BCB), polymers can be a great option. Nanofibres can be sensitized with the incorporated substrates or polymers [2]. Since Polypyrrole responds to humidity change more rapidly, it can be woven into materials too. Typically, textile-coated sensors are used to determine the variations of water vapour, depending on whether they are carbon-based or organic-based materials.

Since textiles have specific properties like transport and water absorption, they can be used as a sensor's optimization compound [74]. Generally, the selection of conductive sensors, in terms of tactile property and durability, may be affected by improved wearable experience.

2.6.2.1 Capacitive moisture sensor

Primarily, the capacitive humidity sensors are comprised of two electrodes with a dielectric placed between the electrodes. The RH values are therefore decided by the

capacitance change of the dielectric constant, also called the dielectric temperature. To guarantee the ability of water absorption, the dielectric material of the capacitive humidity sensor should be hygroscopic. To monitor the humidity signals, a conductive fluid should be employed to the sensor system's two electrodes, which will lead to the changes in the capacitance of the sensor. Capacitive moisture sensor generally has higher accuracy compared to resistive moisture sensor [180].

2.6.2.2 Resistive moisture sensor

Resistive moisture sensor is also widely used, it measures the change of humidity by monitoring the electric conductivity of the sensor. Generally, while the humidity increased, the resistance of the sensor is decreased, the changes in humidity to the electrical conductivity follows an inverse relationship. When compared to capacitive sensor, resistive moisture sensor is more suitable for measuring the humidity in relatively higher humidity environment, it can measure the environment humidity up to 90%. However, the performance of the resistive sensor in lower environment humidity (5% RH) is not satisfied [15].

Pereira et al. [181] designed and manufactured a multi-layer moisture sensor matrix (**Figure 2-61**). Two woven fabrics made of cotton and stainless-steel conductive yarns were used as the sensing layer of the moisture sensor, and the top, bottom and middle layers are cotton knitted fabrics used as the absorbing layers. NaCl solution was used to monitor human sweat. The moisture sensor the authors made demonstrates a good response to water and the materials they used are friendly to human skin.

Figure 2-61. Textile moisture sensor matrix **[173]**

Ataman et al. [182] developed a humidity and temperature sensor based on plastic foil. Several multilayers sensor structure (**Figure 2-62**) with 60 mm*2 mm were designed and manufactured; they were inserted into a woven structure to form the moisture sensor structure. The woven sensors demonstrated good sensing behaviour, are low-cost and reliable.

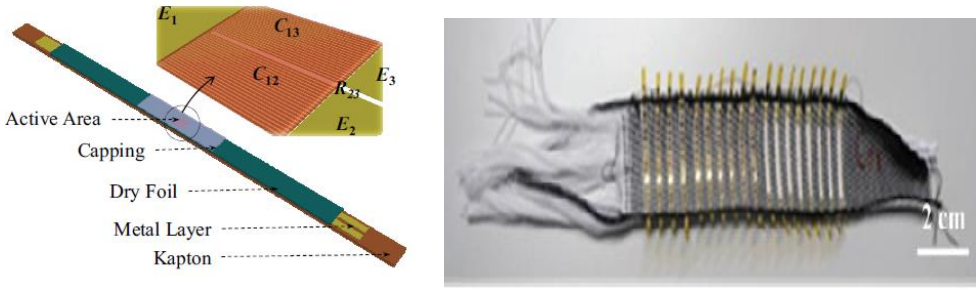

Figure 2-62. (Left) Multilayer sensor structure, (Right) images of the woven sensor **[174]**

Parkova et al. [180] investigated the substrate fabric for textile moisture sensors. A burette was used to apply distilled water on the fabric surface to measure the wettability and wet area for different fabrics (**Figure 2-63**). According to their results, polyester fabrics showed a relatively best wettability while cotton fabrics achieved a relatively larger wet area. They believed that the wettability of fabric has a huge influence on sensor signal detection. Additionally, they found cotton and polyester- blended fabric demonstrate the best performance with rather fast absorption speed and a wet area that

is quite large in size.

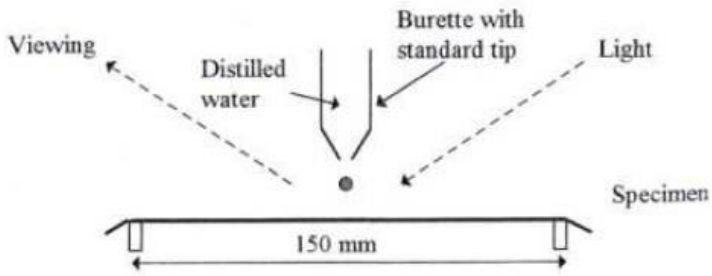

Figure 2-63. Fabric wettability test **[172]**

Mattana et al. [183]used two types of printed moisture capacitance and resistance sensor; the structure of the sensors can be seen in **Figure 2-64**, Both of them were tested within a climatic chamber, the relative humidity increased from 25 to 80% and the capacitance of the sensors were recorded. After the test, they found both of the moisture sensors can clearly measure changes in humidity; however, the response speed is long. Additionally, they pointed out that this situation can be addressed by changing a different measurement configuration.

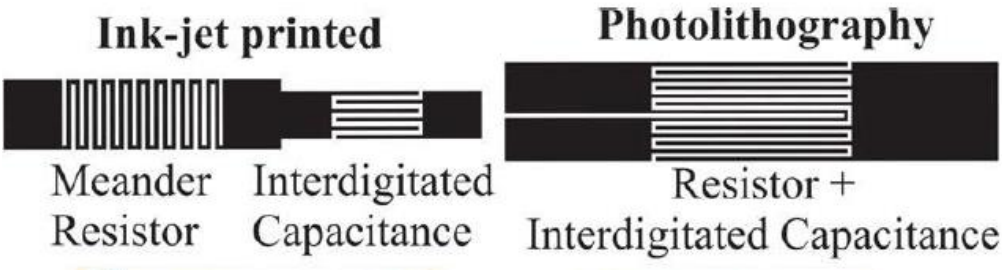

Figure 2-64. The structures of two types of moisture sensor **[175]**

Kinkeldei et al.[184] used the conductive polymer PEDOT:PSS film to construct their moisture sensor (**Figure 2-65**). The moisture sensor was tested in a climate chamber and the humidity was varied from 30 to 50% relative humidity. This moisture sensor achieved a linear distribution till 60% and started to saturate at a higher humidity.

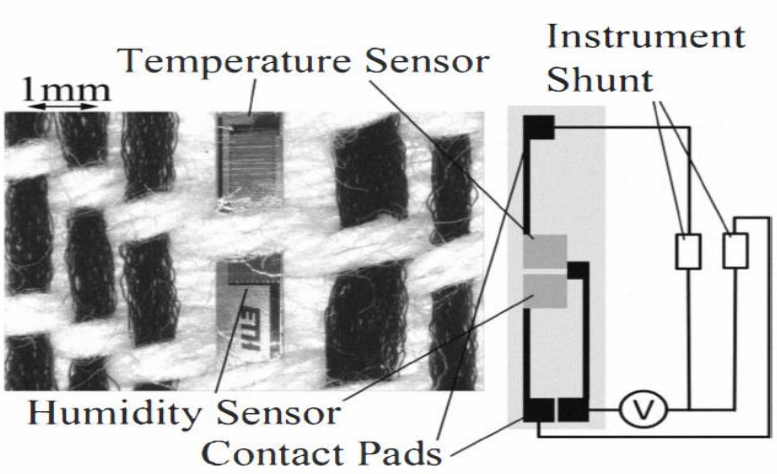

Figure 2-65. Structure of the PEDOT:PSS film moisture sensor **[176]**

Shuaib et al. [185] constructed an embroidered passive UHF RFID textile tag as a moisture sensor. They found that this textile tag is fully passive and can easily be integrated with materials that are fit for wearable applications. However, the moisture absorbing process should be improved to make the result more accurate.

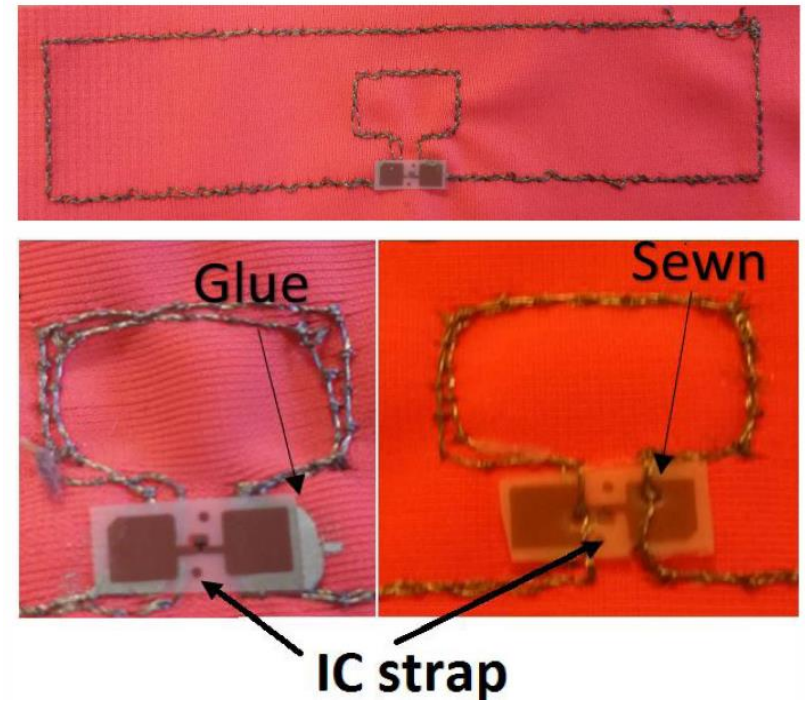

Figure 2-66. UHF RFID textile tag **[177]**

2.7.3 Temperature sensors & Heating elements

According to research, the main working principle of temperature sensor is the electrical resistance of conductive yarn that respond to the changes in temperature. Due to the properties of different conductive yarns for temperature sensing purpose, they can be divided into two groups: conductive materials with positive temperature coefficient of resistance (metallic materials or graphene) and semiconductor with negative temperature coefficient of resistance (carbon, germanium or silicon). The resistance of the conductive materials with positive temperature coefficient will increase due to temperature increased, while the resistance of semiconductors like carbon will decrease due to temperature increased.

The smart heating garment mainly consist of four categories: The Phase Change Material (PCM) heating garment, the chemical heating garment, the electrically heating garment and fluid flow heating garment [186]–[189]. The PCM heating garment and chemical heating garment have an unavoidable drawback which is the heating temperature cannot be controlled accurate, especially there is a risk of skin burnt by using the chemical heating elements. As for the fluid flow heating garment, due to the fluid tubes are inserted into the garment, the garment is not flexible and not comfortable to wear. Hence, the textile wearable heating garments are mainly electrically heating garments.

The working principle of electrically heating garments are mainly based on Joule's law, when the current goes through the circuit, it generates heat. It is relatively safer for the wearers, the power supplied is usually under 9 Volts. Additionally, if the flexible materials are used, the wearable heating garment can be flexible, comfortable and light weight to wear. The highest temperature of electrically heating garments can reach is generally around 40℃ which is also safe to the wearer [190].

To make a smart textile with both actuating and sensing functions, Roh et al. [191] developed a novel metal composite embroidery yarn for a temperature and heating purpose. Four different embroidered patterns were designed and manufactured by them (**Figure 2-67**). All four structures were supplied by a 7.4V power to test the heating performance of them. The temperature sensing behaviour was tested in a dynamic temperature control system, and the temperature varied from 20 to 40℃.

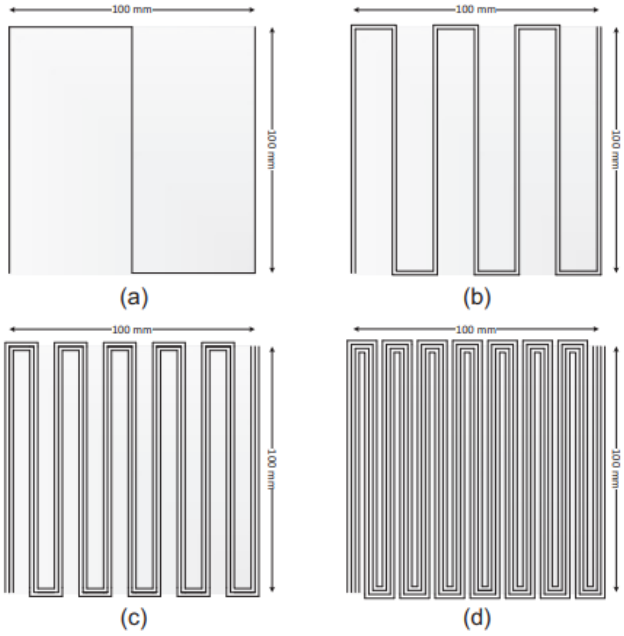

Figure 2-67. Heating element structure, a) Single conductive sewing line of 400 mm in length. b) Two parallel sewing lines of 800 mm in length. c) Three parallel sewing lines of 1200 mm in length. d) Four parallel sewing lines of 1600 mm in length. **[183]**

Schimmack et al. [192] developed a metal-polymer hybrid fibre for temperature monitor purpose (**Figure 2-68**). A constant input of 25V was supplied to the sensor, and the sensor demonstrates a relatively fast and accurate reaction to temperature changes, even at 2℃.

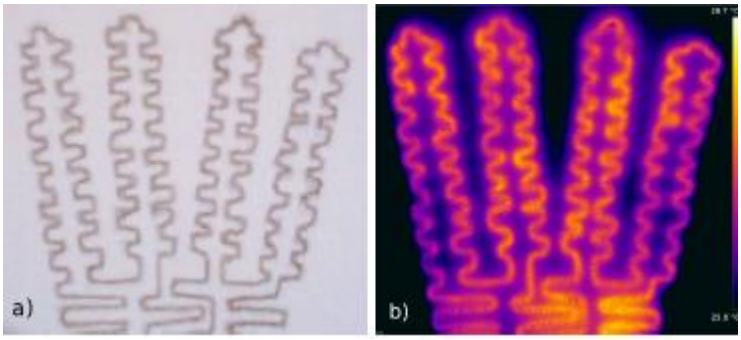

Figure 2-68. Metal-polymer hybrid-based heating element **[184]**

Li et al. [193] presented a whole fabric-based temperature sensor through the integration of a continuous metal fibre into a woven fabric. The sensor was put into a temperature controlled oil bath with temperatures ranging from 25 to 45℃. It showed a stable temperature sensitivity, high accuracy, good resolution fast response speed, and very low hysteresis in cyclic tests.

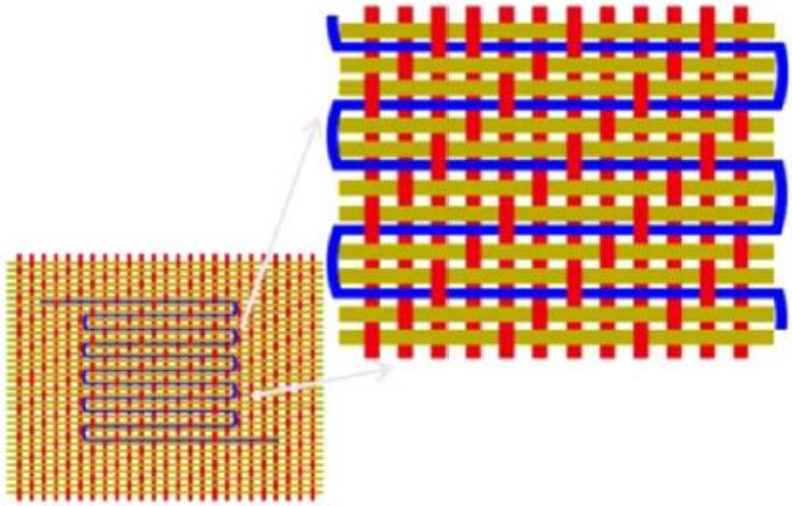

Figure 2-69. Full fabric-based temperature sensor **[185]**

Carbon nanotube and PVDF materials were used to manufacture a temperature sensor by Sibinski et al. [5](**Figure 2-70**). Copper, silver-plated and PVDF materials were selected first due to their high temperature resistance, and they were tested at the range of 100-850℃. PVDF was chosen due to its higher flexibility and lower mass factor with sufficient thermal resistance. The sensors were tested in a temperature range of 20 to 160℃. It shows a proper linearity and temperature coefficient within 30 to 45℃ which

is an extended temperature range for human skin temperature control.

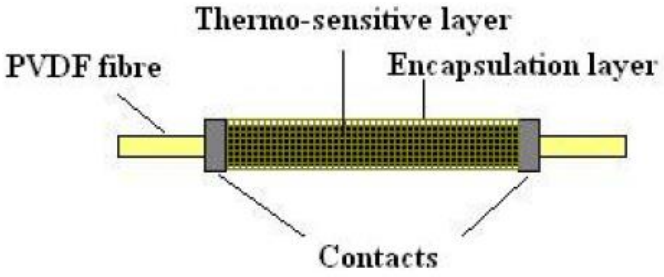

Figure 2-70. Thermistor structure **[5]**

Husain et al. [194] pointed out that the desirable properties of the sensing element of a TSF should consist of: nominal resistance, sensitivity, response time, self-heating, repeatability, mechanical properties, availability and reproducibility. A computerized flat-bed knitting machine was used to produce their temperature sensor (**Figure 2-71**). The samples were tested within a laboratory oven at the temperature points of 30℃ ,40℃ ,50℃ and 60℃. The resistance versus temperature curves present a linear relationship with a coefficient of determination in the range of 0.99 to 0.999.

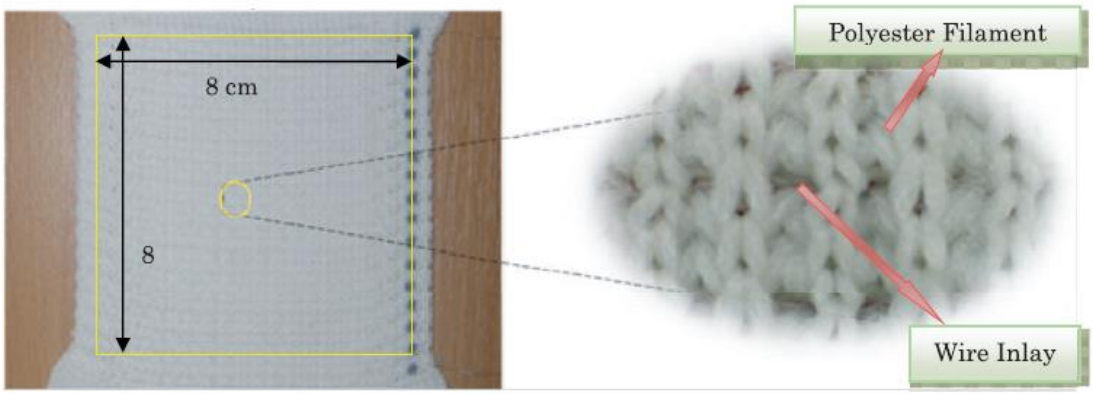

Figure 2-71. Flat-bed knitted temperature sensor **[186]**

Lee et al. [195] made a PEDOT: PSS-based temperature sensing yarn by dip dyeing 3 cm cotton yarns in PEDOT: PSS. The thermal electrical property was measured by calculating the resistance of the sensor as the temperature varied from -50 to 80 ℃. It demonstrates high flexibility, is a fast, low cost and simple fabrication process, and is small and light.

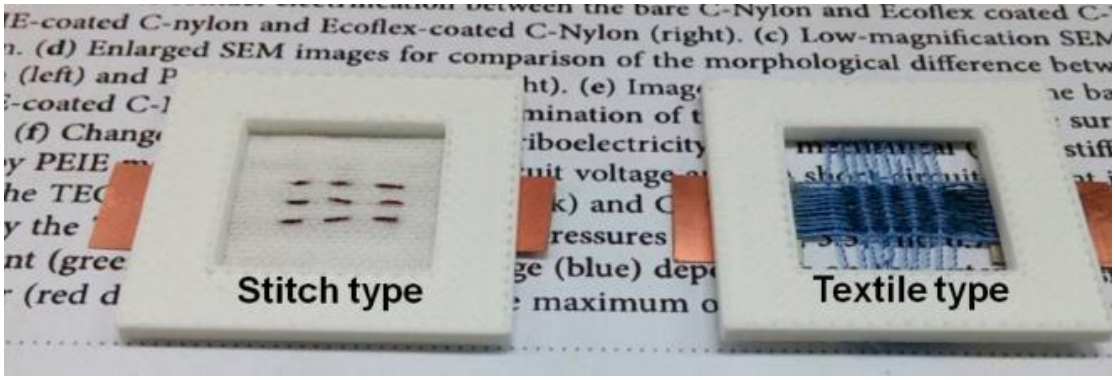

Figure 2-72. temperature sensing yarn-based sensors **[187]**

Bielska et al. [196] developed a thermo-sensitive material by using a substrate material – polyamide foil "KAPTON" which has high temperature and moisture resistance (**Figure 2-73**). Sensors were placed in a calorimeter covered by thermal insulation, and the resistance of the sensor was measured from 30 to 42 ℃. The temperature sensor shows high flexibility, and a good linear relationship between resistance and temperature and high thermal resistance change.

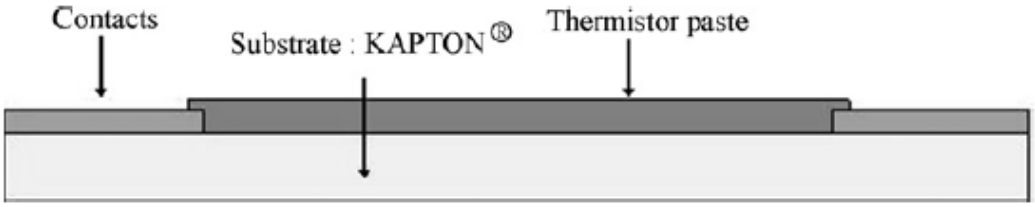

Figure 2-73. Sensor structure of the polymer temperature sensor **[194]**

Hannah et al. [197]developed a temperature sensor based on a ferroelectric capacitor, and commercially available ferroelectric lead zirconate titanate (PZT) was used. The PZT sensor capacitance was calculated at temperatures from 22 to 90 ℃. During the test, the capacitance of the sensor displayed a linear dependence on the temperature.

Hao et al. [198] designed a polypyrrole-coated knitted fabric for heating purposes, and the PPy filaments were prepared by polymerizing them on the cotton fibres (**Figure 2-74**). The cotton was treated first by chemicals to make it non-wettable. 3V, 6V, 7.5V and 9V voltage were supplied to the PPy-cotton and the static temperatures are 28, 56, 76 and 83℃ respectively.

Figure 2-74. PPy-Cotton heating element **[190]**

Talha et al.[199] used pyrrole reagent grade 98% to coat a nylon 6.6 knitted fabric and to manufacture an electrothermal fabric. Five different sizes of heating element were made, and 18V voltage was supplied to these heating elements. During the test, heating element with 5*1cm^2 can reach over 114 ℃ in less than 3 minutes.

A stainless-steel knitted structure was used by Fernando et al.[200] for heating purposes. In order to provide currents to each course of the knitted fabric, the silver- coated polymeric yarn was used to manufacture two bus bars for the knitted heating elements (**Figure 2-75**). The stainless-steel yarns and elastomeric yarns were used to make the knitted structure by using a computerized Shima Seiki knitting machine. The stainless knitted structure can produce a large amount of heat at a low voltage.

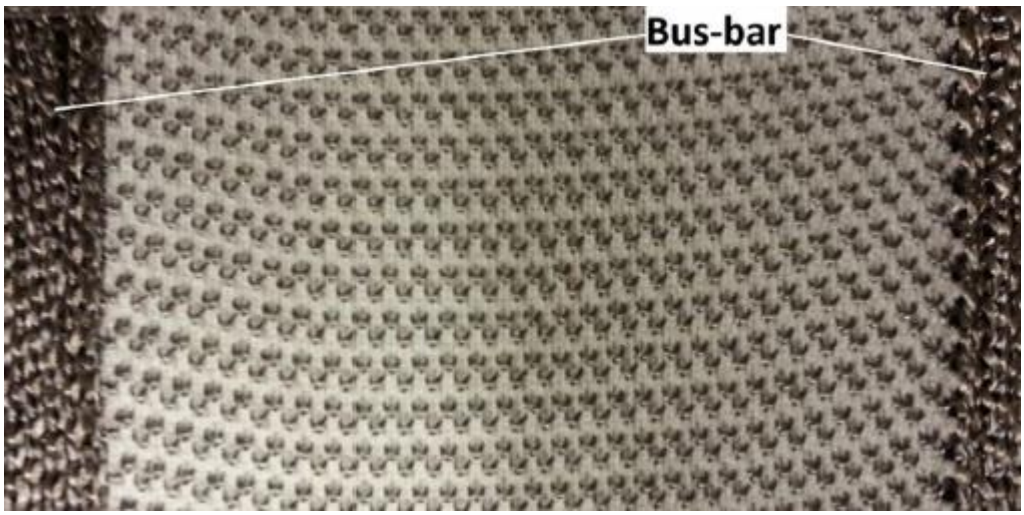

Figure 2-75. Stainless steel knitted fabric with silver bus bars **[192]**

Zhang et al. [201] made a low power consuming heating element by using PEDOT-

coated fibres (**Figure 2-76**). The PEDOT fibres were woven to a fabric and combined with cotton inner gloves and an outer protective casing to form a heating glove. The heating gloves consisted of three lightweight and breathable fabric layers and only needed a 3v battery; the temperature of the gloves then increases to a desirable warm temperature after 10-20s.

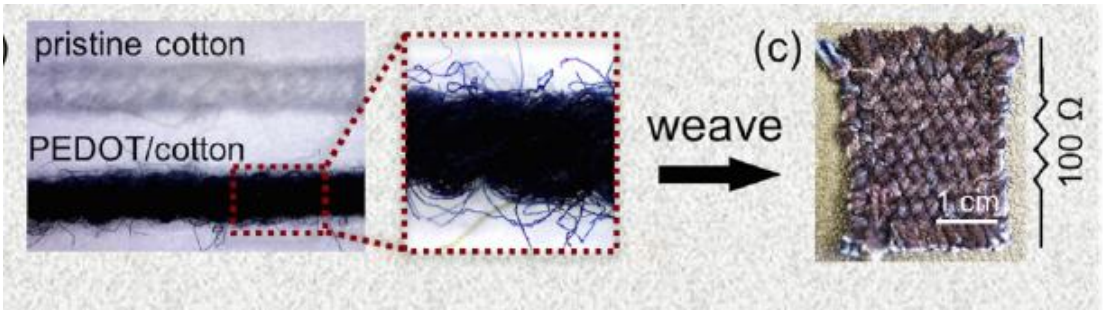

Figure 2-76. PEDOT fibre and PEDOT woven fabric **[193]**

2.8 References

[1] X. Tao, *Wearable electronics and photonics*. 2005.

[2] L. M. Castano and A. B. Flatau, "Smart fabric sensors and e-textile technologies: A review," *Smart Materials and Structures*, vol. 23, no. 5. 2014.

[3] L. Van Langenhove and C. Hertleer, "Smart clothing: A new life," *Int. J. Cloth. Sci. Technol.*, vol. 16, no. 1–2, pp. 63–72, 2004.

[4] J. Meyer, "Textile pressure sensor: Design, error modeling and evaluation," *Ph.D. Diss.*, pp. 1–120, 2008.

[5] M. Sibinski, M. Jakubowska, and M. Sloma, "Flexible temperature sensors on fibers," *Sensors*, vol. 10, no. 9, pp. 7934–7946, 2010.

[6] F. Chiarugi *et al.*, "Measurement of heart rate and respiratory rate using a textile-based wearable device in heart failure patients," in *Computers in Cardiology*, 2008, vol. 35, pp. 901–904.

[7] M. Peltokangas, J. Verho, and A. Vehkaoja, "Night-time EKG and HRV monitoring with bed sheet integrated textile electrodes," *IEEE Trans. Inf. Technol. Biomed.*, vol. 16, no. 5, pp. 935–942, 2012.

[8] O. Atalay and W. R. Kennon, "Knitted strain sensors: Impact of design parameters on sensing properties," *Sensors (Switzerland)*, vol. 14, no. 3, pp. 4712–4730, 2014.

[9] A. Bonfiglio and D. De Rossi, *Wearable monitoring systems*. 2011.

[10] S. Afroj *et al.*, "Engineering Graphene Flakes for Wearable Textile Sensors via Highly Scalable and Ultrafast Yarn Dyeing Technique," *ACS Nano*, vol. 13, no. 4, pp. 3847–3857, 2019.

[11] R. McLaren, F. Joseph, C. Baguley, and D. Taylor, "A review of e-textiles in neurological rehabilitation: How close are we?," *Journal of NeuroEngineering and Rehabilitation*, vol. 13, no. 1. 2016.

[12] P. Salvo, F. Di Francesco, D. Costanzo, C. Ferrari, M. G. Trivella, and D. De

Rossi, “A wearable sensor for measuring sweat rate,” *IEEE Sens. J.*, vol. 10, no. 10, pp. 1557–1558, 2010.

[13] V. Candas, J. P. Libert, G. Brandenberger, J. C. Sagot, C. Amoros, and J. M. Kahn, “Hydration during exercise - Effects on thermal and cardiovascular adjustments,” *Eur. J. Appl. Physiol. Occup. Physiol.*, vol. 55, no. 2, pp. 113–122, 1986.

[14] R. J. Maughan, S. M. Shirreffs, and J. B. Leiper, “Errors in the estimation of hydration status from changes in body mass,” *J. Sports Sci.*, vol. 25, no. 7, pp. 797–804, 2007.

[15] I. Parkova, A. Vališevskis, I. Ziemele, U. Briedis, and A. Vilumsone, “Improvements of Smart Garment Electronic Contact System,” *Adv. Sci. Technol.*, vol. 80, pp. 90–95, 2012.

[16] R. B. Katragadda and Y. Xu, “A novel intelligent textile technology based on silicon flexible skins,” in *Proceedings of the IEEE International Conference on Micro Electro Mechanical Systems (MEMS)*, 2007, pp. 301–304.

[17] G. López, V. Custodio, and J. I. Moreno, “LOBIN: E-textile and wireless-sensor-network-based platform for healthcare monitoring in future hospital environments,” *IEEE Trans. Inf. Technol. Biomed.*, vol. 14, no. 6, pp. 1446–1458, 2010.

[18] C. Kutzner, R. Lucklum, R. Torah, S. Beeby, and J. Tudor, “Novel screen printed humidity sensor on textiles for smart textile applications,” in *2013 Transducers and Eurosensors XXVII: The 17th International Conference on Solid-State Sensors, Actuators and Microsystems, TRANSDUCERS and EUROSENSORS 2013*, 2013, pp. 282–285.

[19] R. Soukup, A. Hamacek, L. Mracek, and J. Reboun, “Textile based temperature and humidity sensor elements for healthcare applications,” in *Proceedings of the 2014 37th International Spring Seminar on Electronics Technology, ISSE 2014*, 2014, pp. 407–411.

[20] R. Polanský *et al.*, “A novel large-area embroidered temperature sensor based on an innovative hybrid resistive thread,” *Sensors Actuators, A Phys.*, vol. 265, pp. 111–119, 2017.

[21] K. Cherenack and L. Van Pieterson, “Smart textiles: Challenges and opportunities,” *Journal of Applied Physics*, vol. 112, no. 9. 2012.

[22] A. Lymberis and R. Paradiso, “Smart fabrics and interactive textile enabling wearable personal applications: R&D state of the art and future challenges,” in *Proceedings of the 30th Annual International Conference of the IEEE Engineering in Medicine and Biology Society, EMBS’08 - “Personalized Healthcare through Technology,”* 2008, pp. 5270–5273.

[23] M. Sergio, N. Manaresi, M. Tartagni, R. Guerrieri, and R. Canegallo, “A Textile Based Capacitive Pressure Sensor,” in *Proceedings of IEEE Sensors*, 2002, vol. 1, no. 2, pp. 1625–1630.

[24] X. Lin and B. C. Seet, “A Linear Wide-Range Textile Pressure Sensor Integrally Embedded in Regular Fabric,” *IEEE Sens. J.*, vol. 15, no. 10, pp. 5384–5385, 2015.

[25] M. Pacelli, L. Caldani, and R. Paradiso, “Textile piezoresistive sensors for biomechanical variables monitoring,” in *Annual International Conference of the IEEE Engineering in Medicine and Biology - Proceedings*, 2006, pp. 5358–5361.

[26] J. Meyer, P. Lukowicz, and G. Tröster, “Textile pressure sensor for muscle activity and motion detection,” in *Proceedings - International Symposium on Wearable Computers, ISWC*, 2006, pp. 69–74.

[27] H. Bin Yao *et al.*, “A flexible and highly pressure-sensitive graphene-polyurethane sponge based on fractured microstructure design,” *Adv. Mater.*, vol. 25, no. 46, pp. 6692–6698, 2013.

[28] J. Taelman, T. Adriaensen, C. Van Der Horst, T. Linz, and A. Spaepen, “Textile integrated contactless EMG sensing for stress analysis,” in *Annual*

International Conference of the IEEE Engineering in Medicine and Biology - Proceedings, 2007, pp. 3966–3969.

[29] R. Paradiso, G. Loriga, and N. Taccini, "A wearable health care system based on knitted integrated sensors," *IEEE Trans. Inf. Technol. Biomed.*, vol. 9, no. 3, pp. 337–344, 2005.

[30] L. R. Ferreras *et al.*, "Highly piezoresistive textiles based on a soft conducting charge transfer salt," *J. Mater. Chem.*, vol. 21, no. 3, pp. 637–640, 2011.

[31] D. Domvoglou and S. Vassiliadis, *Electronics and Computing in Textiles*, no. February. London: Bookboon, 2012.

[32] "TibTech." [Online]. Available: http://smartshop.tibtech.com/. [Accessed: 22-Jun-2020].

[33] T. Linz, C. Kallmayer, R. Aschenbrenner, and H. Reichl, "Embroidering electrical interconnects with conductive yarn for the integration of flexible electronic modules into fabric," in *Proceedings - International Symposium on Wearable Computers, ISWC*, 2005, vol. 2005, pp. 86–89.

[34] J. S. Roh, "Textile touch sensors for wearable and ubiquitous interfaces," *Text. Res. J.*, vol. 84, no. 7, pp. 739–750, 2014.

[35] L. Zhang, Z. Wang, S. Salman, and J. L. Volakis, "Embroidered textiles for RF electronics and medical sensors," in *2012 IEEE International Conference on Wireless Information Technology and Systems, ICWITS 2012*, 2012.

[36] J. Meyer, B. Arnrich, J. Schumm, and G. Troster, "Design and modeling of a textile pressure sensor for sitting posture classification," *IEEE Sens. J.*, vol. 10, no. 8, pp. 1391–1398, 2010.

[37] G. Gioberto and L. Dunne, "Theory and characterization of a top-thread coverstitched stretch sensor," in *Conference Proceedings - IEEE International Conference on Systems, Man and Cybernetics*, 2012, pp. 3275–3280.

[38] T. Kannaian, R. Neelaveni, and G. Thilagavathi, "Design and development of embroidered textile electrodes for continuous measurement of

electrocardiogram signals," *J. Ind. Text.*, vol. 42, no. 3, pp. 303–318, 2013.

[39] H. Zhang and X. M. Tao, "A single-layer stitched electrotextile as flexible pressure mapping sensor," *J. Text. Inst.*, vol. 103, no. 11, pp. 1151–1159, 2012.

[40] H. Zhang, X. Tao, T. Yu, and S. Wang, "Conductive knitted fabric as large-strain gauge under high temperature," *Sensors Actuators, A Phys.*, vol. 126, no. 1, pp. 129–140, 2006.

[41] H. Zhang and X. Tao, "From wearable to aware: Intrinsically conductive electrotextiles for human strain/stress sensing," in *Proceedings - IEEE-EMBS International Conference on Biomedical and Health Informatics: Global Grand Challenge of Health Informatics, BHI 2012*, 2012, pp. 468–471.

[42] H. Zhang, X. Tao, T. Yu, S. Wang, and X. Cheng, "A novel sensate 'string' for large-strain measurement at high temperature," in *Measurement Science and Technology*, 2006, vol. 17, no. 2, pp. 450–458.

[43] H. Zhang, X. Tao, S. Wang, and T. yu, "Electro-Mechanical Properties of Knitted Fabric Made From Conductive Multi-Filament Yarn Under Unidirectional Extension," *Text. Res. J.*, vol. 75, no. 8, pp. 598–606, 2005.

[44] K. Yang, G. L. Song, L. Zhang, and L. W. Li, "Modelling the electrical property of 1×1 rib knitted fabrics made from conductive yarns," in *2009 2nd International Conference on Information and Computing Science, ICIC 2009*, 2009, vol. 4, pp. 382–385.

[45] H. Elsner, "Textile technological integration of sensor modules in lightweight composite structures and possible applications," *Newsl. ECAS*, pp. 8–10, 2010.

[46] Y. Kim, K. Lee, Y. Kim, and Y. Chung, "Wearable UHF RFID tag antenna design using flexible electro-thread and textile," in *IEEE Antennas and Propagation Society, AP-S International Symposium (Digest)*, 2007, pp. 5487–5490.

[47] C. Mattmann, F. Clemens, and G. Tröster, "Sensor for measuring strain in textile," *Sensors*, vol. 8, no. 6, pp. 3719–3732, 2008.

[48] L. Capineri, “Resistive sensors with smart textiles for wearable technology: From fabrication processes to integration with electronics,” in *Procedia Engineering*, 2014, vol. 87, pp. 724–727.

[49] X. Guo, Y. Huang, X. Cai, C. Liu, and P. Liu, “Capacitive wearable tactile sensor based on smart textile substrate with carbon black /silicone rubber composite dielectric,” *Meas. Sci. Technol.*, vol. 27, no. 4, 2016.

[50] T. Yamada *et al.*, “A stretchable carbon nanotube strain sensor for human-motion detection,” *Nat. Nanotechnol.*, vol. 6, no. 5, pp. 296–301, 2011.

[51] J. W. Han, B. Kim, J. Li, and M. Meyyappan, “A carbon nanotube based ammonia sensor on cotton textile,” *Appl. Phys. Lett.*, vol. 102, no. 19, 2013.

[52] E. Devaux, C. Aubry, C. Campagne, and M. Rochery, “PLA/carbon nanotubes multifilament yarns for relative humidity Textile sensor,” *J. Eng. Fiber. Fabr.*, vol. 6, no. 3, pp. 13–24, 2011.

[53] J. Foroughi *et al.*, “Knitted Carbon-Nanotube-Sheath/Spandex-Core Elastomeric Yarns for Artificial Muscles and Strain Sensing,” *ACS Nano*, vol. 10, no. 10, pp. 9129–9135, 2016.

[54] S. V. Morozov *et al.*, “Giant intrinsic carrier mobilities in graphene and its bilayer,” *Phys. Rev. Lett.*, vol. 100, no. 1, 2008.

[55] R. K. Layek and A. K. Nandi, “A review on synthesis and properties of polymer functionalized graphene,” *Polymer*, vol. 54, no. 19. pp. 5087–5103, 2013.

[56] T. Q. Trung, H. S. Le, T. M. L. Dang, S. Ju, S. Y. Park, and N. E. Lee, “Freestanding, Fiber-Based, Wearable Temperature Sensor with Tunable Thermal Index for Healthcare Monitoring,” *Adv. Healthc. Mater.*, vol. 7, no. 12, 2018.

[57] T. Yang *et al.*, “Torsion sensors of high sensitivity and wide dynamic range based on a graphene woven structure,” *Nanoscale*, vol. 6, no. 21, pp. 13053–13059, 2014.

[58] Y. J. Yun, W. G. Hong, N. J. Choi, B. H. Kim, Y. Jun, and H. K. Lee, "Ultrasensitive and highly selective graphene-based single yarn for use in wearable gas sensor," *Sci. Rep.*, vol. 5, 2015.

[59] C. S. Boland *et al.*, "Sensitive, high-strain, high-rate bodily motion sensors based on graphene-rubber composites," *ACS Nano*, vol. 8, no. 9, pp. 8819–8830, 2014.

[60] M. K. Yapici, T. Alkhidir, Y. A. Samad, and K. Liao, "Graphene-clad textile electrodes for electrocardiogram monitoring," *Sensors Actuators, B Chem.*, vol. 221, 2015.

[61] Z. Yang *et al.*, "Graphene Textile Strain Sensor with Negative Resistance Variation for Human Motion Detection," *ACS Nano*, vol. 12, no. 9, pp. 9134–9141, 2018.

[62] Y. Cheng, R. Wang, J. Sun, and L. Gao, "A Stretchable and Highly Sensitive Graphene-Based Fiber for Sensing Tensile Strain, Bending, and Torsion," *Adv. Mater.*, vol. 27, no. 45, pp. 7365–7371, 2015.

[63] Y. J. Yun, W. G. Hong, W. J. Kim, Y. Jun, and B. H. Kim, "A novel method for applying reduced graphene oxide directly to electronic textiles from yarns to fabrics," *Adv. Mater.*, vol. 25, no. 40, pp. 5701–5705, 2013.

[64] C. Gonçalves, A. F. da Silva, J. Gomes, and R. Simoes, "Wearable e-textile technologies: A review on sensors, actuators and control elements," *Inventions*, vol. 3, no. 1, 2018.

[65] S. Q. Jiang, E. Newton, C. W. M. Yuen, and C. W. Kan, "Chemical silver plating and its application to textile fabric design," *J. Appl. Polym. Sci.*, vol. 96, no. 3, pp. 919–926, 2005.

[66] X. Zhang, T. V. Sreekumar, T. Liu, and S. Kumar, "Properties and structure of nitric acid oxidized single wall carbon nanotube films," *J. Phys. Chem. B*, vol. 108, no. 42, pp. 16435–16440, 2004.

[67] R. Zhang *et al.*, "Carbon nanotube polymer coatings for textile yarns with good

strain sensing capability," *Sensors Actuators, A Phys.*, vol. 179, pp. 83–91, 2012.

[68] M. Stoppa and A. Chiolerio, "Wearable electronics and smart textiles: A critical review," *Sensors (Switzerland)*, vol. 14, no. 7. pp. 11957–11992, 2014.

[69] S. Stassi, V. Cauda, G. Canavese, and C. F. Pirri, "Flexible tactile sensing based on piezoresistive composites: A review," *Sensors (Switzerland)*, vol. 14, no. 3. pp. 5296–5332, 2014.

[70] R. Cao *et al.*, "Screen-Printed Washable Electronic Textiles as Self-Powered Touch/Gesture Tribo-Sensors for Intelligent Human-Machine Interaction," *ACS Nano*, vol. 12, no. 6, pp. 5190–5196, 2018.

[71] K. J. Lee, B. H. Jun, T. H. Kim, and J. Joung, "Direct synthesis and inkjetting of silver nanocrystals toward printed electronics," *Nanotechnology*, vol. 17, no. 9, pp. 2424–2428, 2006.

[72] J. J. P. Valeton *et al.*, "Room temperature preparation of conductive silver features using spin-coating and inkjet printing," *J. Mater. Chem.*, vol. 20, no. 3, pp. 543–546, 2010.

[73] V. Mecnika, K. Scheulen, C. F. Anderson, M. Hörr, and C. Breckenfelder, "Joining technologies for electronic textiles," in *Electronic Textiles: Smart Fabrics and Wearable Technology*, 2015, pp. 133–153.

[74] P. Bosowski, M. Hoerr, V. Mecnika, T. Gries, and S. Jockenhövel, "Design and manufacture of textile-based sensors," in *Electronic Textiles: Smart Fabrics and Wearable Technology*, 2015, pp. 75–107.

[75] Y. Enokibori, A. Suzuki, H. Mizuno, Y. Shimakami, and K. Mase, "E-textile pressure sensor based on conductive fiber and its structure," in *UbiComp 2013 Adjunct - Adjunct Publication of the 2013 ACM Conference on Ubiquitous Computing*, 2013, pp. 207–210.

[76] M. Rothmaier and F. Clemens, "Textile pressure sensor made of flexible plastic optical fibers," *EMPA Activities*, no. 2008–2009. p. 55, 2008.

[77] R. Paradiso and M. Pacelli, “Textile electrodes and integrated smart textile for reliable biomonitoring,” in *Proceedings of the Annual International Conference of the IEEE Engineering in Medicine and Biology Society, EMBS*, 2011, pp. 3274–3277.

[78] O. Chetelat *et al.*, “New biosensors and wearables for cardiorespiratory telemonitoring,” in *3rd IEEE EMBS International Conference on Biomedical and Health Informatics, BHI 2016*, 2016, pp. 481–484.

[79] M. Pacelli, G. Loriga, N. Taccini, and R. Paradiso, “Sensing fabrics for monitoring physiological and biomechanical variables: E-textile solutions,” in *Proceedings of the 3rd IEEE-EMBS International Summer School and Symposium on Medical Devices and Biosensors, ISSS-MDBS 2006*, 2006, pp. 1–4.

[80] J. Li and B. Xu, “Novel highly sensitive and wearable pressure sensors from conductive three-dimensional fabric structures,” *Smart Mater. Struct.*, vol. 24, no. 12, 2015.

[81] T. Gries and K. Klopp, “Methoden zur Verfahrensbewertung,” in *Füge- und Oberflächentechnologien für Textilien*, 2007, pp. 251–266.

[82] V. Mecnika, M. Hoerr, I. Krievins, S. Jockenhoevel, and T. Gries, “Technical Embroidery for Smart Textiles: Review,” *Mater. Sci. Text. Cloth. Technol.*, vol. 9, p. 56, 2015.

[83] D. B. Sitotaw and B. F. Adamu, “Tensile Properties of Single Jersey and 1×1 Rib Knitted Fabrics Made from 100% Cotton and Cotton/Lycra Yarns,” *J. Eng. (United Kingdom)*, vol. 2017, 2017.

[84] S. Zhang *et al.*, “Embroidered wearable antennas using conductive threads with different stitch spacings,” in *LAPC 2012 - 2012 Loughborough Antennas and Propagation Conference*, 2012.

[85] Ž. Juchnevičienė, M. Jucienė, and S. Radavičienė, “The research on the width of the closed-circuit square-shaped embroidery element,” *Medziagotyra*, vol.

23, no. 2, pp. 186–190, 2017.

[86] S. Radavičiene and M. Juciene, “Influence of embroidery threads on the accuracy of embroidery pattern dimensions,” *Fibres Text. East. Eur.*, vol. 92, no. 3, pp. 92–97, 2012.

[87] D. A. Chernenko, “Systematization of Design Parameters for Automated Embroidery and Modeling of Deformation System of ‘Fabric-Embroidery,’” 2006.

[88] A. Tsolis, W. G. Whittow, A. A. Alexandridis, and J. Y. C. Vardaxoglou, “Embroidery and related manufacturing techniques for wearable antennas: Challenges and opportunities,” *Electronics* , vol. 3, no. 2. pp. 314–338, 2014.

[89] J. McCann and D. Bryson, *Smart Clothes and Wearable Technology*. 2009.

[90] P. D. Dubrovski and P. F. Čebašek, “Analysis of the mechanical properties of woven and nonwoven fabrics as an integral part of compound fabrics,” *Fibres Text. East. Eur.*, vol. 13, no. 3, pp. 50–53, 2005.

[91] E. Reimer and L. Danisch, “Pressure sensor based on illumination of a deformable integrating cavity,” *US Pat. 5,917,180*, pp. 1–8, 1999.

[92] J. Roh *et al.*, “Robust and Reliable Fabric and Piezoresistive Multitouch Sensing Surfaces for Musical Controllers,” *Proc. Int. Conf. New Interfaces Music. Expr.*, no. June, pp. 393–398, 2011.

[93] L. Zhang, Z. Wang, and J. L. Volakis, “Textile antennas and sensors for body-worn applications,” *IEEE Antennas Wirel. Propag. Lett.*, vol. 11, pp. 1690–1693, 2012.

[94] S. Jayaraman, “Full fashioned weaving process for production of a woven garment with intelligence capability,” *U.S. Pat. No. 6 145 551*, p. 16, 2000.

[95] E. P. Scilingo, F. Lorussi, A. Mazzoldi, and D. De Rossi, “Strain-sensing fabrics for wearable kinaesthetic-like systems,” *IEEE Sens. J.*, vol. 3, no. 4, pp. 460–467, 2003.

[96] F. Lorussi, E. P. Scilingo, A. Tesconi, A. Tognetti, and D. De Rossi, “Wearable

sensing garment for posture detection, rehabilitation and tele-medicine," in *Proceedings of the IEEE/EMBS Region 8 International Conference on Information Technology Applications in Biomedicine, ITAB*, 2003, vol. 2003-Janua, pp. 287–290.

[97] M. Åkerfeldt, A. Lund, and P. Walkenström, "Textile sensing glove with piezoelectric PVDF fibers and printed electrodes of PEDOT: PSS," *Text. Res. J.*, vol. 85, no. 17, pp. 1789–1799, 2015.

[98] E. Moradi, K. Koski, L. Ukkonen, Y. Rahmat-Samii, T. Björninen, and L. Sydänheimo, "Embroidered RFID tags in body-centric communication," in *2013 International Workshop on Antenna Technology, iWAT 2013*, 2013, pp. 367–370.

[99] C. Kallmayer and E. Simon, "Large area sensor integration in textiles," in *International Multi-Conference on Systems, Signals and Devices, SSD 2012 - Summary Proceedings*, 2012.

[100] C. A. Byrne, "Design of an e-textile sleeve for tracking knee rehabilitation for older adults," 2013.

[101] M. Hasani, A. Vena, L. Sydanheimo, L. Ukkonen, and M. M. Tentzeris, "Implementation of a dual-interrogation-mode embroidered RFID-Enabled strain sensor," *IEEE Antennas Wirel. Propag. Lett.*, vol. 12, pp. 1272–1275, 2013.

[102] Y.-H. Kim and Y.-C. Chung, "UHF RFID Dipole Tag Antenna Design Using Flexible Electro-Thread," *J. Korean Inst. Electromagn. Eng. Sci.*, vol. 19, no. 1, pp. 1–6, 2008.

[103] L. E. Dunne, S. Brady, B. Smyth, and D. Diamond, "Initial development and testing of a novel foam-based pressure sensor for wearable sensing," *Journal of NeuroEngineering and Rehabilitation*, vol. 2. 2005.

[104] T. Pola and J. Vanhala, "Textile electrodes in ECG measurement," in *Proceedings of the 2007 International Conference on Intelligent Sensors,*

Sensor Networks and Information Processing, ISSNIP, 2007, pp. 635–639.

[105] G. Cho, K. Jeong, M. J. Paik, Y. Kwun, and M. Sung, "Performance evaluation of textile-based electrodes and motion sensors for smart clothing," *IEEE Sens. J.*, vol. 11, no. 12, pp. 3183–3193, 2011.

[106] I. G. Trindade, F. Martins, R. Miguel, and M. S. Silva, "Design and Integration of Wearable Devices in Textiles," 2014.

[107] S. Gilliland, N. Komor, T. Starner, and C. Zeagler, "The textile interface swatchbook: Creating graphical user interface-like widgets with conductive embroidery," in *Proceedings - International Symposium on Wearable Computers, ISWC*, 2010.

[108] S. Zhang, "Design advances of embroidered fabric antennas," Loughborough University, 2014.

[109] E. R. Post, M. Orth, R. R. Russo, and N. Gershenfeld, "E-broîdery: Design and fabrication of textile-based computing," *IBM Syst. J.*, 2000.

[110] D. Cottet, J. Grzyb, T. Kirstein, and G. Tröster, "Electrical Characterization of Textile Transmission Lines," *IEEE Trans. Adv. Packag.*, vol. 26, no. 2, pp. 182–190, 2003.

[111] I. Locher, M. Klemm, T. Kirstein, and G. Tröster, "Design and characterization of purely textile patch antennas," *IEEE Trans. Adv. Packag.*, vol. 29, no. 4, pp. 777–788, 2006.

[112] K. J. Noh, Y. K. Son, B. S. Kim, and I. Y. Cho, "Wearable network using Optical e-Textile Antenna for NLOS," in *Digest of Technical Papers - IEEE International Conference on Consumer Electronics*, 2012, pp. 556–557.

[113] S. Gimpel, U. Möhring, H. Müller, A. Neudeck, and W. Scheibner, "Textile-based electronic substrate technology," *J. Ind. Text.*, vol. 33, no. 3, pp. 179–189, 2004.

[114] P. Salonen and H. Hurme, "A novel fabric WLAN antenna for wearable applications," in *IEEE Antennas and Propagation Society, AP-S International*

Symposium (Digest), 2003, vol. 2, pp. 700–703.

[115] Y. Ouyang and W. J. Chappell, "High frequency properties of electro-textiles for wearable antenna applications," *IEEE Trans. Antennas Propag.*, vol. 56, no. 2, pp. 381–389, 2008.

[116] E. J. Power, "Knitting of electroconductive yarns," 2006, pp. 55–60.

[117] I. Locher and G. Tröster, "Screen-printed Textile Transmission Lines," *Text. Res. J.*, vol. 77, no. 11, pp. 837–842, 2007.

[118] Y. Kim, H. Kim, and H. J. Yoo, "Electrical characterization of screen-printed circuits on the fabric," *IEEE Trans. Adv. Packag.*, vol. 33, no. 1, pp. 196–205, 2010.

[119] A. Chauraya *et al.*, "Inkjet printed dipole antennas on textiles for wearable communications," *IET Microwaves, Antennas Propag.*, vol. 7, no. 9, pp. 760–767, 2013.

[120] M. M. Tentzeris *et al.*, "Inkjet-printed RFIDs for wireless sensing and anti-counterfeiting," in *Proceedings of 6th European Conference on Antennas and Propagation, EuCAP 2012*, 2012, pp. 3481–3482.

[121] Y. Li, R. Torah, S. Beeby, and J. Tudor, "Inkjet printed flexible antenna on textile for wearable applications," *Text. Inst. World Conf.*, 2012.

[122] A. Rida, L. Yang, R. Vyas, and M. M. Tentzeris, "Conductive inkjet-printed antennas on flexible low-cost paper-based substrates for RFID and WSN applications," *IEEE Antennas and Propagation Magazine*, vol. 51, no. 3. pp. 13–23, 2009.

[123] M. Mäntysalo and P. Mansikkamäki, "An inkjet-deposited antenna for 2.4 GHz applications," *AEU - Int. J. Electron. Commun.*, vol. 63, no. 1, pp. 31–35, 2009.

[124] Y. Li, R. Torah, S. Beeby, and J. Tudor, "An all-inkjet printed flexible capacitor on a textile using a new poly(4-vinylphenol) dielectric ink for wearable applications," in *Proceedings of IEEE Sensors*, 2012.

[125] S. Merilampi, T. Björninen, V. Haukka, P. Ruuskanen, L. Ukkonen, and L.

Sydänheimo, “Analysis of electrically conductive silver ink on stretchable substrates under tensile load,” *Microelectron. Reliab.*, vol. 50, no. 12, pp. 2001–2011, 2010.

[126] J. Lilja and P. Salonen, “Textile material characterization for softwear antennas,” in *Proceedings - IEEE Military Communications Conference MILCOM*, 2009.

[127] M. Klemm and G. Troester, “Textile UWB Antennas for Wireless Body Area Networks,” *IEEE Trans. Antennas Propag.*, vol. 54, no. 11, pp. 3192–3197, 2006.

[128] T. F. Kennedy, P. W. Fink, A. W. Chu, N. J. Champagne, G. Y. Lin, and M. A. Khayat, “Body-worn E-textile antennas: The good, the low-mass, and the conformal,” *IEEE Trans. Antennas Propag.*, vol. 57, no. 4 PART. 1, pp. 910–918, 2009.

[129] D. L. Paul, C. Jayatissa, G. S. Hilton, and C. J. Railton, “Conformability of a textile antenna for reception of digital television,” in *2010 Loughborough Antennas and Propagation Conference, LAPC 2010*, 2010, pp. 225–228.

[130] M. in het Panhuis, J. Wu, S. A. Ashraf, and G. G. Wallace, “Conducting textiles from single-walled carbon nanotubes,” *Synth. Met.*, vol. 157, no. 8–9, pp. 358–362, 2007.

[131] L. Hu *et al.*, “Stretchable, porous, and conductive energy textiles,” *Nano Lett.*, vol. 10, no. 2, pp. 708–714, 2010.

[132] Y. Bayram *et al.*, “E-textile conductors and polymer composites for conformal lightweight antennas,” *IEEE Trans. Antennas Propag.*, vol. 58, no. 8, pp. 2732–2736, 2010.

[133] L. Ukkonen, L. Sydänheimo, and Y. Rahmat-Samii, “Sewed textile RFID tag and sensor antennas for on-body use,” in *Proceedings of 6th European Conference on Antennas and Propagation, EuCAP 2012*, 2012, pp. 3450–3454.

[134] Z. Wang, L. Zhang, D. Psychoudakis, and J. L. Volakis, “GSM and Wi-Fi

textile antenna for high data rate communications," in *IEEE Antennas and Propagation Society, AP-S International Symposium (Digest)*, 2012.

[135] Y. Ouyang and W. Chappell, "Measurement of electrotextiles for high frequency applications," in *IEEE MTT-S International Microwave Symposium Digest*, 2005, vol. 2005, pp. 1679–1682.

[136] T. Acti *et al.*, "High performance flexible fabric electronics for megahertz frequency communications," in *LAPC 2011 - 2011 Loughborough Antennas and Propagation Conference*, 2011.

[137] E. Koski *et al.*, "Fabrication of embroidered UHF RFID tags," in *IEEE Antennas and Propagation Society, AP-S International Symposium (Digest)*, 2012.

[138] L. Zhang, Z. Wang, and J. L. Volakis, "Embroidered textile circuits for microwave devices," in *IEEE Antennas and Propagation Society, AP-S International Symposium (Digest)*, 2012.

[139] J. H. Choi, Y. Kim, K. Lee, and Y. Chung, "Various wearable embroidery RFID tag antenna using electro-thread," in *2008 IEEE International Symposium on Antennas and Propagation and USNC/URSI National Radio Science Meeting, APSURSI*, 2008.

[140] Z. Wang, L. Zhang, Y. Bayram, and J. L. Volakis, "Embroidered E-fiber-polymer composites for conformal and load bearing antennas," in *2010 IEEE International Symposium on Antennas and Propagation and CNC-USNC/URSI Radio Science Meeting - Leading the Wave, AP-S/URSI 2010*, 2010.

[141] T. Maleszka and P. Kabacik, "Bandwidth properties of embroidered loop antenna for wearable applications," in *European Microwave Week 2010, EuMW2010: Connecting the World, Conference Proceedings - European Wireless Technology Conference, EuWiT 2010*, 2010, pp. 89–92.

[142] Z. Wang, L. Zhang, Y. Bayram, and J. L. Volakis, "Multilayer printing of embroidered RF circuits on polymer composites," in *IEEE Antennas and*

Propagation Society, AP-S International Symposium (Digest), 2011, pp. 278–281.

[143] L. Zhang, Z. Wang, D. Psychoudakis, and J. L. Volakis, "E-fiber electronics for body-worn devices," in *Proceedings of 6th European Conference on Antennas and Propagation, EuCAP 2012*, 2012, pp. 760–761.

[144] Z. Wang, L. Zhang, Y. Bayram, and J. L. Volakis, "Embroidered conductive fibers on polymer composite for conformal antennas," *IEEE Trans. Antennas Propag.*, vol. 60, no. 9, pp. 4141–4147, 2012.

[145] J. L. Volakis, L. Zhang, Z. Wang, and Y. Bayram, "Embroidered flexible RF electronics," in *2012 IEEE International Workshop on Antenna Technology, iWAT 2012*, 2012, pp. 8–11.

[146] W. Y. Du, *Resistive, capacitive, inductive, and magnetic sensortechnologies*. 2014.

[147] J. Janesch, "Two-wire vs. four-wire resistance measurements: which configuration makes sense for your application?," *Keithley kiadványa*, no. May, pp. 2–4, 2013.

[148] K. Hoffmann, "Applying the wheatstone bridge circuit," *HBM S1569-1.1 en, HBM, Darmstadt, Ger.*, pp. 1–28, 2001.

[149] J. Heikenfeld *et al.*, "Wearable sensors: Modalities, challenges, and prospects," *Lab on a Chip*, vol. 18, no. 2. pp. 217–248, 2018.

[150] S. Yao and Y. Zhu, "Wearable multifunctional sensors using printed stretchable conductors made of silver nanowires," *Nanoscale*, vol. 6, no. 4, pp. 2345–2352, 2014.

[151] X. Zhao, Q. Hua, R. Yu, Y. Zhang, and C. Pan, "Flexible, Stretchable and Wearable Multifunctional Sensor Array as Artificial Electronic Skin for Static and Dynamic Strain Mapping," *Adv. Electron. Mater.*, vol. 1, no. 7, 2015.

[152] Z. Chen and R. C. Luo, "Design and implementation of capacitive proximity sensor using microelectromechanical systems technology," *IEEE Trans. Ind.*

Electron., vol. 45, no. 6, pp. 886–894, 1998.

[153] M. Amjadi, Y. J. Yoon, and I. Park, "Ultra-stretchable and skin-mountable strain sensors using carbon nanotubes-Ecoflex nanocomposites," *Nanotechnology*, vol. 26, no. 37, 2015.

[154] Y. Wang, A. X. Wang, Y. Wang, M. K. Chyu, and Q. M. Wang, "Fabrication and characterization of carbon nanotube-polyimide composite based high temperature flexible thin film piezoresistive strain sensor," *Sensors Actuators, A Phys.*, vol. 199, pp. 265–271, 2013.

[155] J. C. Suhling and R. C. Jaeger, "Silicon piezoresistive stress sensors and their application in electronic packaging," *IEEE Sens. J.*, vol. 1, no. 1, pp. 14–30, 2001.

[156] S. N. Nihtianov and G. C. M. Meijer, "Application challenges of capacitive sensors with floating targets," in *IEEE AFRICON Conference*, 2011.

[157] C. Zysset *et al.*, "Textile integrated sensors and actuators for near-infrared spectroscopy," *Opt. Express*, vol. 21, no. 3, p. 3213, 2013.

[158] I. D. Castro, R. Morariu, T. Torfs, C. Van Hoof, and R. Puers, "Robust wireless capacitive ECG system with adaptive signal quality and motion artifact reduction," in *2016 IEEE International Symposium on Medical Measurements and Applications, MeMeA 2016 - Proceedings*, 2016.

[159] S. Yao and Y. Zhu, "Nanomaterial-Enabled Dry Electrodes for Electrophysiological Sensing: A Review," *Jom*, vol. 68, no. 4. pp. 1145–1155, 2016.

[160] K. E. Mathewson, T. J. L. Harrison, and S. A. D. Kizuk, "High and dry? Comparing active dry EEG electrodes to active and passive wet electrodes," in *Psychophysiology*, 2017, vol. 54, no. 1, pp. 74–82.

[161] M. Sergio, N. Manaresi, M. Nicolini, D. Gennaretti, M. Tartagni, and R. Guerrieri, "A textile-based capacitive pressure sensor," *Sens. Lett.*, vol. 2, no. 2, pp. 153–160, 2004.

[162] H. Zhang, “Flexible textile-based strain sensor induced by contacts,” *Meas. Sci. Technol.*, vol. 26, no. 10, 2015.

[163] S. Brady, K. T. Lau, W. Megill, G. G. Wallace, and D. Diamond, “The development and characterisation of conducting polymeric-based sensing devices,” in *Synthetic Metals*, 2005, vol. 154, no. 1–3, pp. 25–28.

[164] Y. L. Yang, M. C. Chuang, S. L. Lou, and J. Wang, “Thick-film textile-based amperometric sensors and biosensors,” *Analyst*, vol. 135, no. 6, pp. 1230–1234, 2010.

[165] M. C. Chuang *et al.*, “Textile-based Electrochemical Sensing: Effect of Fabric Substrate and Detection of Nitroaromatic Explosives,” *Electroanalysis*, vol. 22, no. 21, pp. 2511–2518, 2010.

[166] P. Wellman, J. Son, and R. Howe, “System generating a pressure profile across a pressure sensitive membrane,” *U.S. Pat. No. 5 983 727*, 1999.

[167] S. Kon and R. Horowitz, “A High-Resolution MEMS Piezoelectric Strain Sensor for Structural Vibration Detection,” *IEEE Sens. J.*, vol. 8, no. 12, pp. 2027–2035, 2008.

[168] Y. Wang, T. Hua, B. Zhu, Q. Li, W. Yi, and X. Tao, “Novel fabric pressure sensors: Design, fabrication, and characterization,” *Smart Mater. Struct.*, vol. 20, no. 6, 2011.

[169] K. Rundqvist, “Piezoelectric behaviour of woven constructions based on poly(vinylidene fluoride) bicomponent fibres,” Swedish School of Textiles, 2013.

[170] S. T. A. Hamdani and A. Fernando, “The application of a piezo-resistive cardiorespiratory sensor system in an automobile safety belt,” *Sensors (Switzerland)*, vol. 15, no. 4, pp. 7742–7753, 2015.

[171] S. Gong *et al.*, “A wearable and highly sensitive pressure sensor with ultrathin gold nanowires,” *Nat. Commun.*, vol. 5, 2014.

[172] C. T. Huang, C. L. Shen, C. F. Tang, and S. H. Chang, “A wearable yarn-based

piezo-resistive sensor," *Sensors Actuators, A Phys.*, vol. 141, no. 2, pp. 396–403, 2008.

[173] S. Salibindla, B. Ripoche, D. T. H. Lai, and S. Maas, "Characterization of a new flexible pressure sensor for body sensor networks," in *Proceedings of the 2013 IEEE 8th International Conference on Intelligent Sensors, Sensor Networks and Information Processing: Sensing the Future, ISSNIP 2013*, 2013, vol. 1, pp. 27–31.

[174] C. B. Goy *et al.*, "Design, fabrication and metrological evaluation of wearable pressure sensors," *J. Med. Eng. Technol.*, vol. 39, no. 3, pp. 208–215, 2015.

[175] G. Schwartz *et al.*, "Flexible polymer transistors with high pressure sensitivity for application in electronic skin and health monitoring," *Nat. Commun.*, vol. 4, 2013.

[176] I. Baldoli, M. Maselli, F. Cecchi, and C. Laschi, "Development and characterization of a multilayer matrix textile sensor for interface pressure measurements," *Smart Mater. Struct.*, vol. 26, no. 10, 2017.

[177] Z. M. Rittersma, "Recent achievements in miniaturised humidity sensors - A review of transduction techniques," *Sensors and Actuators, A: Physical*, vol. 96, no. 2–3. pp. 196–210, 2002.

[178] K. Reijula, "Moisture-problem buildings with molds causing work-related diseases," *Adv. Appl. Microbiol.*, vol. 55, pp. 175–189, 2004.

[179] J. Avloni, R. Lau, M. Ouyang, L. Florio, A. R. Henn, and A. Sparavigna, "Polypyrrole-coated nonwovens for electromagnetic shielding," *J. Ind. Text.*, vol. 38, no. 1, pp. 55–68, 2008.

[180] I. Parkova, A. Valisevskis, and A. Vilumsone, "Test of Moisture Sensor Activation Speed," *Int. J. Electr. Comput. Electron. Commun. Eng.*, vol. 8, no. 4, pp. 656–660, 2014.

[181] T. Pereira, P. Silva, H. Carvalho, and M. Carvalho, "Textile moisture sensor matrix for monitoring of diSabled and bed-rest patients," in *EUROCON 2011* -

International Conference on Computer as a Tool - Joint with Conftele 2011, 2011.

[182] C. Atamana *et al.*, "Humidity and temperature sensors on plastic foil for textile integration," in *Procedia Engineering*, 2011, vol. 25, pp. 136–139.

[183] G. Mattana *et al.*, "Woven temperature and humidity sensors on flexible plastic substrates for e-textile applications," *IEEE Sens. J.*, vol. 13, no. 10, pp. 3901–3909, 2013.

[184] T. Kinkeldei, C. Zysset, K. H. Cherenack, and G. Troster, "A textile integrated sensor system for monitoring humidity and temperature," in *2011 16th International Solid-State Sensors, Actuators and Microsystems Conference, TRANSDUCERS'11*, 2011, pp. 1156–1159.

[185] D. Shuaib, L. Ukkonen, J. Virkki, and S. Merilampi, "The possibilities of embroidered passive UHF RFID textile tags as wearable moisture sensors," in *2017 IEEE 5th International Conference on Serious Games and Applications for Health, SeGAH 2017*, 2017.

[186] L. Marick, "Electrically heated wearing apparel," *unites states Pat. US2277772*, 1942.

[187] C. Y. L. Chan and D. R. Burton, "A low level supplementary heating system for free divers," *Ocean Eng.*, vol. 9, no. 4, pp. 331–346, 1982.

[188] E. H. Wissler, "Simulation of fluid-cooled or heated garments that allow man to function in hostile environments," *Chem. Eng. Sci.*, vol. 41, no. 6, pp. 1689–1698, 1986.

[189] H. Shim, E. A. Mccullough, and B. W. Jones, "Using Phase Change Materials in Clothing," *Text. Res. J.*, vol. 71, no. 6, pp. 495–502, 2001.

[190] D. G. Greenhalgh, M. B. Lawless, B. B. Chew, W. A. Crone, M. E. Fein, and T. L. Palmieri, "Temperature threshold for burn injury: An oximeter safety study," *J. Burn Care Rehabil.*, vol. 25, no. 5, pp. 411–415, 2004.

[191] J. S. Roh and S. Kim, "All-fabric intelligent temperature regulation system for

smart clothing applications," *J. Intell. Mater. Syst. Struct.*, vol. 27, no. 9, pp. 1165–1175, 2016.

[192] M. Schimmack, B. Haus, P. Leuffert, and P. Mercorelli, "An extended kalman filter for temperature monitoring of a metal-polymer hybrid fibre based heater structure," in *IEEE/ASME International Conference on Advanced Intelligent Mechatronics, AIM*, 2017, pp. 376–381.

[193] Q. Li *et al.*, "Full fabric sensing network with large deformation for continuous detection of skin temperature," *Smart Mater. Struct.*, vol. 27, no. 10, 2018.

[194] M. D. Husain, R. Kennon, and T. Dias, "Design and fabrication of Temperature Sensing Fabric," *J. Ind. Text.*, vol. 44, no. 3, pp. 398–417, 2014.

[195] J. W. Lee, D. C. Han, H. J. Shin, S. H. Yeom, B. K. Ju, and W. Lee, "PEDOT:PSS-based temperature-detection thread for wearable devices," *Sensors (Switzerland)*, vol. 18, no. 9, 2018.

[196] S. Bielska, M. Sibinski, and A. Lukasik, "Polymer temperature sensor for textronic applications," *Mater. Sci. Eng. B Solid-State Mater. Adv. Technol.*, vol. 165, no. 1–2, pp. 50–52, 2009.

[197] S. Hannah, H. Gleskova, S. Matuska, and R. Hudec, "Towards the development of a wearable temperature sensor based on a ferroelectric capacitor," in *12th International Conference ELEKTRO 2018, 2018 ELEKTRO Conference Proceedings*, 2018, pp. 1–4.

[198] D. Hao, B. Xu, and Z. Cai, "Polypyrrole coated knitted fabric for robust wearable sensor and heater," *J. Mater. Sci. Mater. Electron.*, vol. 29, no. 11, pp. 9218–9226, 2018.

[199] S. T. A. Hamdani, A. Fernando, M. D. Hussain, and P. Potluri, "Study of electro-thermal properties of pyrrole polymerised knitted fabrics," *J. Ind. Text.*, vol. 46, no. 3, pp. 771–786, 2016.

[200] S. T. A. Hamdani, A. Fernando, and M. Maqsood, "Thermo-mechanical behavior of stainless steel knitted structures," *Heat Mass Transf. und*

Stoffuebertragung, vol. 52, no. 9, pp. 1861–1870, 2016.

[201] L. Zhang, M. Baima, and T. L. Andrew, “Transforming Commercial Textiles and Threads into Sewable and Weavable Electric Heaters,” *ACS Appl. Mater. Interfaces*, vol. 9, no. 37, pp. 32299–32307, 2017.

Chapter 3 – Methodology

3.1 Material and sample preparation

3.1.1 Material

Embroidered sensors consist of conductive sewing yarn (lower yarn), nonconductive sewing yarn (upper yarn), substrate fabric and backing material. In this thesis, three different electroconductive sewing yarns were used to manufacture the piezoresistive sensor: silver coated sewing yarn, carbon fibre twisted yarn and graphene coated sewing yarn. A silver coated yarn is a standard yarn, and compared to the other conductive yarn, silver coated sewing yarn shows a higher conductivity. Generally, there are three types silver yarn used in sensor fabrication: twisted short fibre silver yarn, continuous silver yarn and elastomeric silver yarn.

First yarn is the elastomeric silver sewing yarn (Silverpam 250, Tibtech) that was used for the construction of embroidered sensors in this thesis. Silverpam 250 is a grafted antibacterial silver coated yarn with 198 ohms/m and 250dtex. However, the electrical resistance of the silver coated yarn is not stable since silver relatively easily gets oxidised in air. To investigate a yarn that has less tendancy to get oxidised in air, carbon (Carbon Tenax, Tibtech) and graphene (national graphene institute) were used. Carbon coated yarn is usually stable and relatively lower priced and graphene has opened up a wide range of flexible electronics applications due to its outstanding electrical, mechanical and other performance properties. Carbon Tenax is a twisted sewing yarn with a resistivity which reaches up to 218 ohms per meter and has a count of 0.14 grams per meter. It is a yarn with "Z" twist with a break elongation of 1.5%. Carbon fibre is a multifuctional material, with an unlimited range of applications, such as golf club shafts, car parts and aircraft wings. Given the large number of applications, carbon fibre has

become more and more important in our daily lives recently. Carbon Tenax is a high-tech material; it is extremely strong and durable. Graphene was used due to its advance properties and we would like to investigate how the graphene yarns cooperate with the pressure sensor. The nonconductive sewing yarn is a normal polyester sewing yarn (ISACORD 40).

There are two types of substrate fabric used in this thesis: non-elastic nonwoven fabric and elastic knitted fabric. In order to investigate the mechanical properties for only the embroidered structure, non-elastic nonwoven fabric was used for the fundamental experiments. For the later application, like bio-signal sensing, elastic knitted substrate was used to improve the elasticity of the sensor. The non-elastic nonwoven fabric was bought from Abakhan fabric store which is a cotton fabric with 0.4463mm thickness (warp 530/10cm, weft 270/10cm).

As for the backing material, normally three types are used: heat removal backing material, water soluble material and glue type backing material. Heat removal backing material needs to be removed by an iron which will have a huge influence on the resistance of the conductive yarn. Based on a simple test, the resistance of the silver embroidered sensor increases 10%-20% after iron treatment. Glue type backing material needs to use a glue to attach the nonwoven backing material to the substrate which is normally used for decorating embroidered products. It is hard to remove and generally cannot be removed clearly which means the residual nonwoven backing material will have an effect on the mechanical properties of the embroidered sensor. Hence, the water-soluble backing material (**Figure 3-1**) was selected for further experiments. The frame, which is used to fix the substrate fabric and backing material during this research is 100 mm*100 mm.

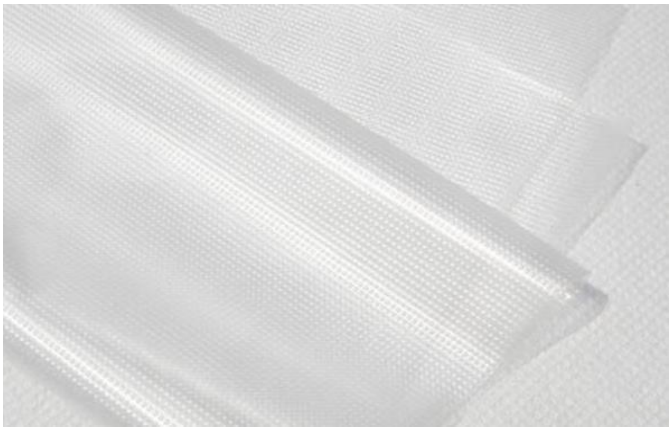

Figure 3-1. Water-soluble backing material

3.1.2 Sample Fabrication

To produce the embroidered sensor samples, sensors were designed by using the embroidery machine's (**Figure 3-2)** proprietory CAD design software (PE-DESIGN, **Figure 3-3**). Besides the area and shape of the sensors, the stitch density, stitch size and sewing yarn orientation can be adjusted by using the software. After the sensor structures were designed on the software, the design patterns were transferred to the computerised embroidery machine by a memory card. Substrate fabric was fixed by the frame with a backing material under the substrate material (**Figure 3-4**). The backing material was used to provide more strength to the substrate fabric; otherwise the substrate fabric might be influenced by the movement of the needle which might result in sample deformation. Then, the upper and bottom bobbins were installed accordingly, and the frame was fixed between the needle and the sewing panel. After the embroiderry machine yarn tension is determined, the designed embroidered pattern can be manufactured on the substrate fabric. Due to different stitch densities, stitch sizes and types of material, the yarn tension should be adjusted to a suitable value (Reason is given in Chapter 2, **Figure 2-19 and 20**).

Once the sensors are constructed, the substrate fabric is rinsed or soaked under warm water to remove the water-soluble backing material, and then the samples are dried

before being tested.

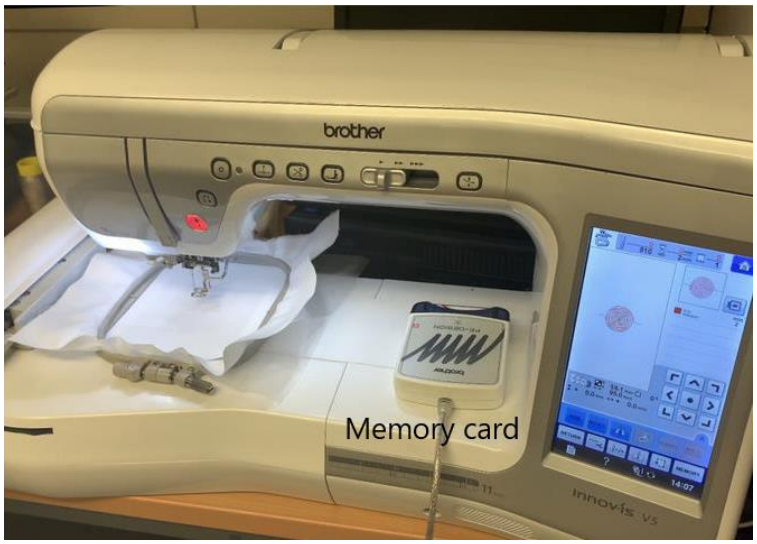

Figure 3-2. Embroidery machine (Brother IS-V5) and the memory card

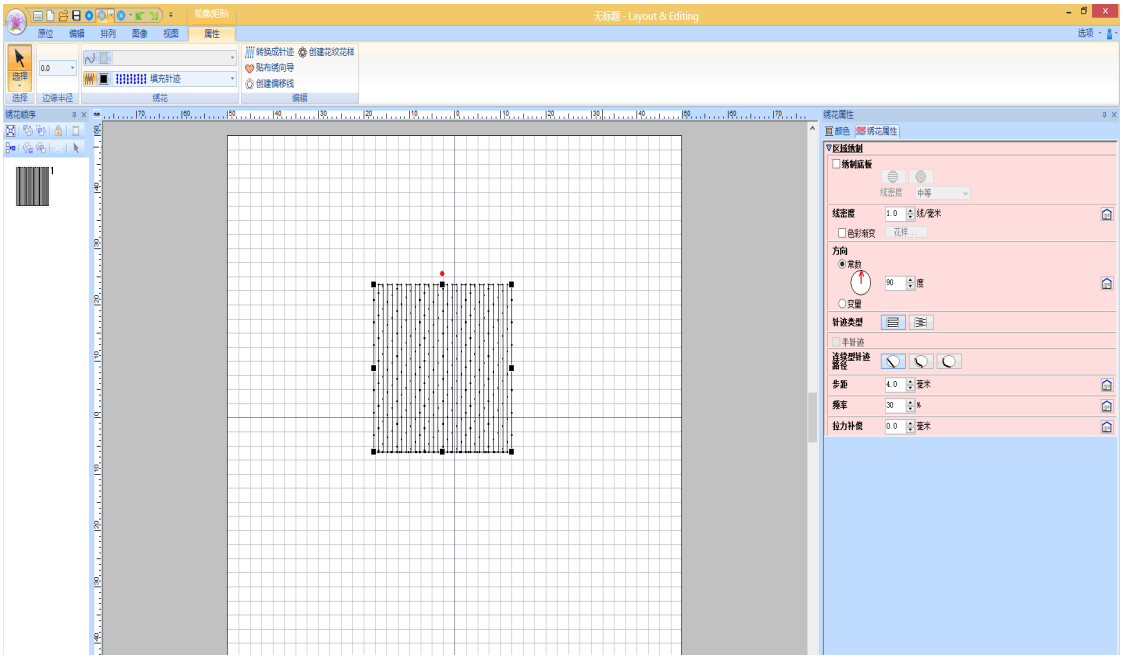

Figure 3-3. PE-Design software

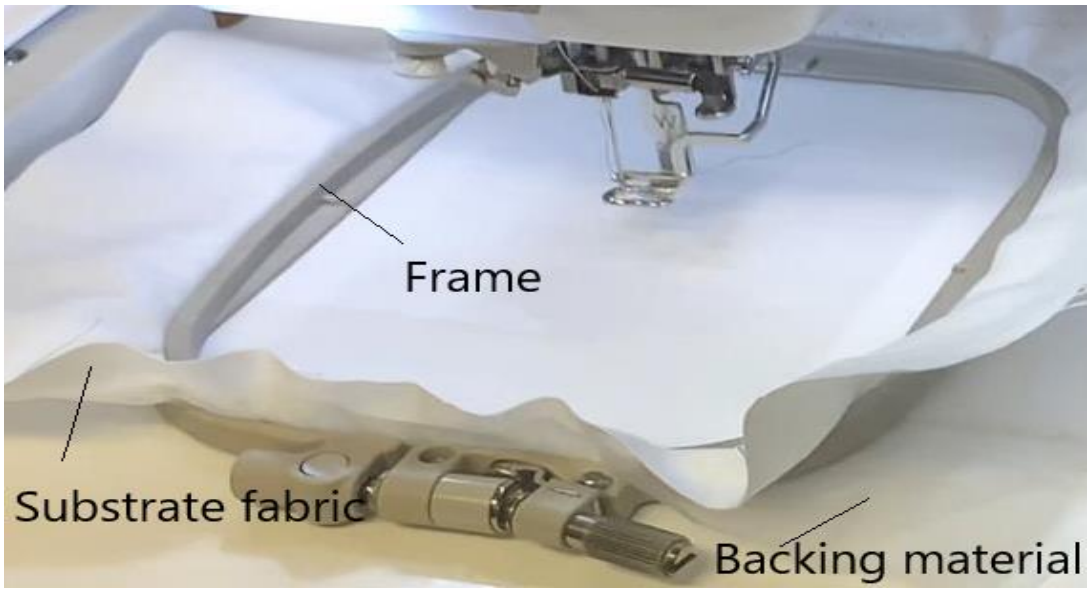

Figure 3-4. The backing material, substrate fabric and the frame

3.2 Test method

3.2.1 Mechanical test

The mechanical properties of the sensor samples and the substrate fabrics were tested under a computerised tensile testing machine (Zwick/Roell Z050, **Figure 3-5**). The test parameters were set by using the X-pert software which can change the type of test (compression or tensile, single or cyclic test), speed of the machine during the test and the maximum and minimum standard force/ nominal strain during the test. The machine mainly consists of a load cell, a movable stage and two grippers or two compression boards, depending on the type of the test (**Figure 3-6**). During the compression test, the samples were placed above a wooden cube to control the thrust surface. There are four different load cells: 20N, 100N,1000N and 10KN. The larger load cell has a larger working range while the smaller load cell can be accurate to more decimal places. For example, 20N load cell can be accurate to the 3rd decimal place (0.001), but the 10KN load cell can only be accurate to the first decimal place (0.1).

Figure 3-5. Zwick/Roell Z050 tensile tester

Figure 3-6. (Left) Machine during tensile test, A is the gripper. (Right) Machine during compression test, A is the compression board and B is the wooden cube

Hence, the smaller load cell can achieve more accurate results when the working range

(elastic limit) of the samples is smaller. Each sample's elastic limit should be tested and measured under a bigger load cell, and then the size of the load cell for further testing decided, depending on the elastic limit of the sample. All the grippers and compression boards were insulated for the testing of sensors and electroconductive materials.

3.2.2 Measurement of the resistance

As discussed in Chapter 2, half bridge resistance measurement was used for capturing the electrical resistance signals due to its relatively lower error. **Figure 3-7** is the typically Wheatstone half bridge circuit.

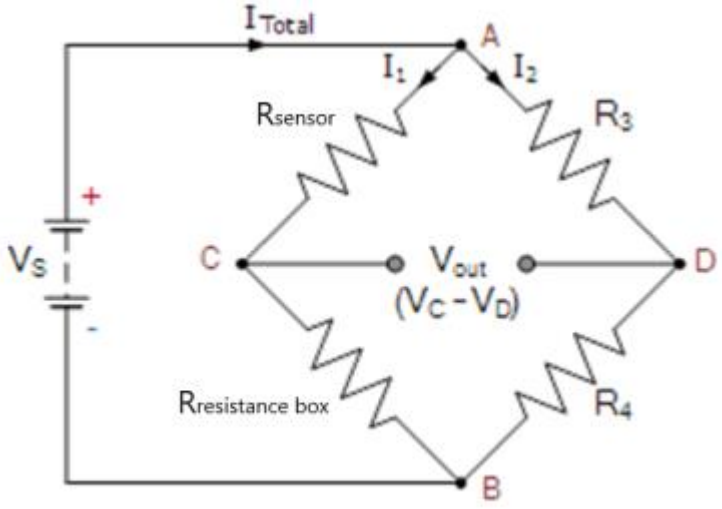

Figure 3-7. Wheatstone half bridge circuit

In **Figure 3-7**, R_3 and R_4 are fixed and equal resistors and the resistance box is used to balance the circuit.

Based on Equation 2-6 in Chapter 2, the relationship between R_{sensor} (R_s) and $R_{resistance\ box}$ (R_{rb}) is shown below:

$$\frac{R_S}{R_S+R_{rb}} = \frac{R_4}{R_3+R_4} = \frac{1}{2} \quad (3\text{-}1)$$

When the sensor is compressed or stretched, the resistance of sensor changed and the balanced of the circuit is broken. Therefor, the V_C is no longer equal to V_D.

$$V_{C\text{-}D}=V\frac{R_s}{R_s+R_{rb}} - V\frac{R_4}{R_3+R_4} \quad (3\text{-}2)$$

Combine equation 10 and 11,

$$\frac{V_{C-D}}{V} = \frac{R_S}{R_S+R_{rb}} - \frac{1}{2} \quad (3\text{-}3)$$

Hence,

$$R_s = R_{rb}\frac{(1-2\frac{V_{C-D}}{V})}{(1+2\frac{V_{C-D}}{V})} \quad (3\text{-}4)$$

In this research, the $\frac{V_{C-D}}{V}$ can be directly obtained by using the NI-9219 data acquisition card (**Figure 3-8a**). During the test, the resistance box (**Figure 3-8b**) was adjusted to balance the bridge before the measurement, and the data acquisition card measured and recorded the $\frac{V_{C-D}}{V}$ reading while the sensors were compressed or stretched. The resistance of the sensor can then be calculated by using Equation 3-4.

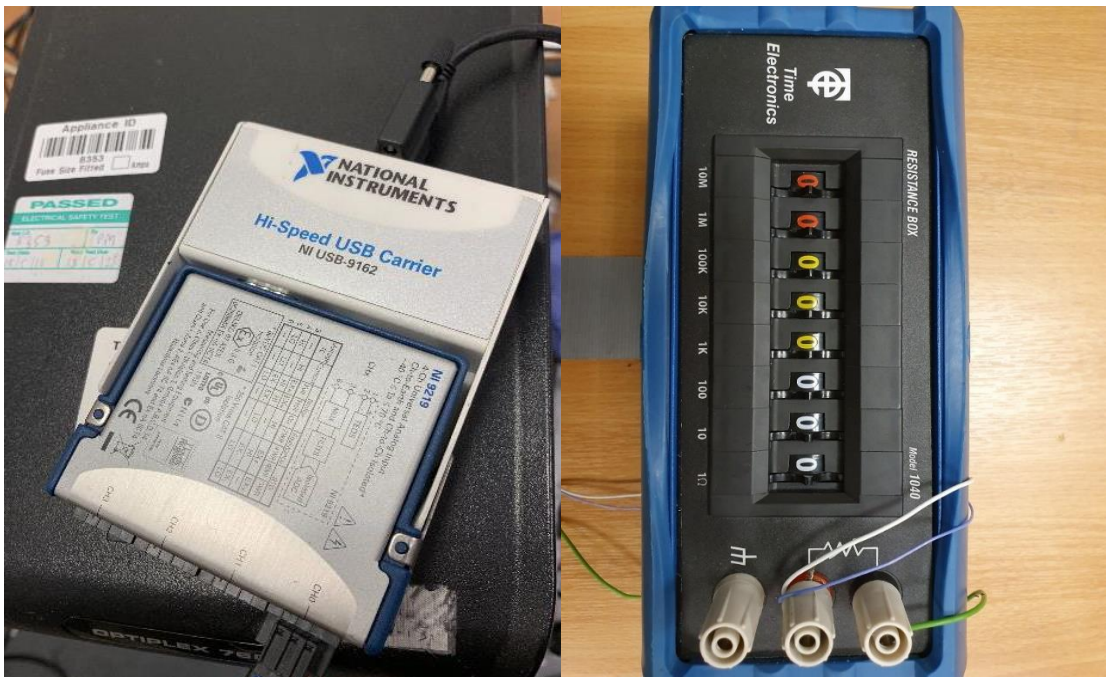

(a) **(b)**

Figure 3-8. a) National Instrument data acquisition card, b) Resistance box

3.2.3 Washability test

In order to define the life experience of a sensor, the wash test must be carried out.

Being a smart wearable sensor, the daily laundry is not avoidable, which means the sensor should have a good washability on both electrical and mechanical side. On a Roaches Washtec-P TOC 3002, laundry tests were carried out by using the standard EN ISO 105-C06:1997 A1M. The wash time was 45 minutes under 40°C.

For the wash test, 4 g of detergent was added into a sample per litre of deionized water. Additionally, 25 stainless steel balls were added to the bottle. To serve as a fixed weight to the sample, a rotating shaft is used and it will not sink into the water before the wash test is finished. The solution is then removed from the solution after the test, then rinsed and later dried.

Chapter 4 - Highly Sensitive and Ultra-flexible Graphene-Based Embroidered Piezo-resistive Wearable Sensors for Bio-Signal Detection

4.1 Introduction

Wearable sensing garments provide a comfortable and functional environment to the wearer which is not replaceable [1]. Integrating sensors or actuators into sensing garments to achieve a comfortable, flexible and reliable platform to monitor the body's physiological signals were widely investigated recently. Some physiological data from the human body, such as heart rate [2-3], body temperature [4] and pressure on the body [5] can be monitored and measured by using a wearable sensing garment as seen in **Figure 4-1**.

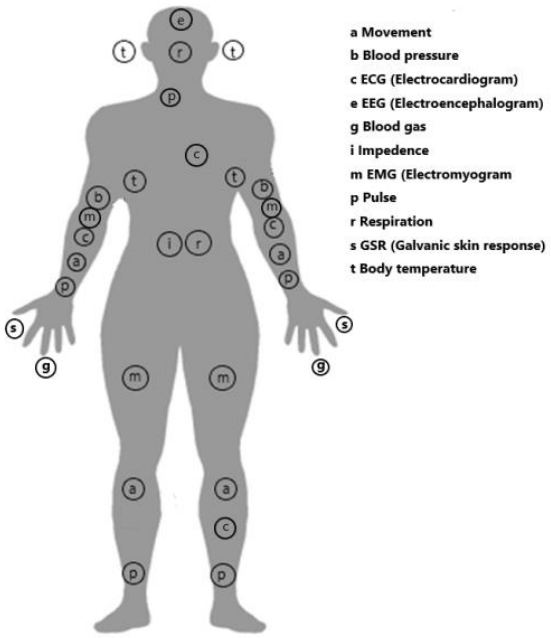

Figure 4-1. Bio-Signals can be measured on human body

The smart wearable sensing area is a fast-growing, promising and advanced research area due to their ability to make the life simple, healthier and comfortable. In order to combine the sensing behaviour and wearable garments, textile sensors were developed by using conductive yarn or fibres. Textile sensors, also known as e-textiles, have drawn much attention due to their soft computing capabilities and portability [6]. However, the poor washability, accuracy and ductility of the textile sensors have delayed the development phase of e-textiles. Nonetheless, there are a couple of issues that will require addressing to ensure transition to smart industrial applications from research laboratories. The existing barriers include lack of regulations, lack of standardisation, lack of collaboration among partners in the value chain, and lack of coordination [7].

Although electrotextiles are a relatively new area, within a short period of time, it has become a very popular field of study the world over. One of the drawbacks these materials face is that unlike conventional materials used in the construction of sensors, the properties of e-textiles can easily be influenced by many external factors such as movement, vibration, any mechanical deformation, temperature, humidity and other variables like perspiration when measured on human beings.

Generally, when a sensor is made, it is made to measure a particular physical variable. However, in a textile sensor created through a typical textile manufacturing method, the orientation of the fibres is such that in trying to measure a single physical parameter such as strain produces many other conditions such as bending/unbending, twisting/untwisting and compression. Therefore, an attempt to discover pure strain will result in measuring a combination of parameters, thereby introducing much noise in the collected data. Apart from that, the resolution of a signal acquired by a textile sensor is also a weak point. The piezo-resistive textile sensors that are currently available for bio-sensing have main drawbacks due to the usage of improper electroconductive materials, non-uniformity of their integration, their degradation due to oxidisation and due to the

unreliability of the whole sensor construction.

Basic electrotextile sensing structures can be created using several traditional manufacturing methods such as knitting, weaving, nonwovens, embroidery and printing [6]. There are many electrically conductive coated materials and conductive yarns available in the form of spun yarn, metal yarn and metal-coated yarn that can be utilised to create conductive elements [8]. In addition, these yarns play a role as transmission lines or sensing components in the sensors. Additionally, to combine the sensor with the textile, the textile sensor should be easy to use and comfortable to wear [9].

In this paper, we developed our piezoresistive sensors by using the standard embroidery technique which is one of the most efficient textile fabrication methods. In addition, the use of embroidery techniques for constructing wearable textile sensors brings all the advantages embroidery process experiences over other textile sensor manufacturing processes; quick and simple senor integration, CAD operated geometrically precision and neat sensor construction and accurate location and construction of multi-material sensors through the use of multi-head textile sensor embroidery.

Not like the other methods of manufacturing textile sensors, in the embroidery process, embroidery yarns are affected by several factors such as dynamic load, bending, friction, and abrasion [11,13]. During embroidery, the lower yarn is regularly thinner than the upper one since the filling quality of the embroidered element is very important [11,13]. Various stitch directions and different stitch densities are used to fill the embroidery area. The lower yarn loop shall not be visible from the top side, due to the upper yarn loop becomes bigger than the lower one in case of cross-over of yarns [11-13].

Graphene is one of the hottest research areas in chemical, physical and materials

research fields. It has excellent electrical, mechanical and thermo-electrical properties which makes it an optimum material for textile sensors. In this research, graphene coated electroconductive yarn was mainly investigated for piezoresistive sensor construction. Carbon and metallic coated yarn too were chosen to compare with the graphene coated yarn. The challenges in the use of currently available electroconductive metal coated fibre materials for constructing electrotextile sensors is the nature of materials and processors of application that could prove to be expensive, toxic and non-biodegradable, and sometimes not very stable. In this field, graphene has opened up a wide range of flexible electronics applications due to its outstanding electrical, mechanical, membrane and other performance properties. Up to now, graphene coated yarn has had relatively few investigations for being used to construct textile sensors and actuators.

4.2 Methodology

4.2.1 Materials

Embroidered sensors consist of conductive sewing yarn (lower yarn), nonconductive sewing yarn (upper yarn), substrate fabric and backing material. In order to investigate the capability of graphene yarn for being used to manufacture textile sensors, metallic coated yarn and non-metal carbon conductive yarn were chosen to be the control group experiments. The carbon and silver coated sewing yarns are commercially available sewing yarns from TIBTECH. Silver was selected due to its high conductivity, the silver sewing yarn used in this paper is the Silverpam 250 (TIBTECH) which is a grafted antibacterial silver coated yarn with 198 ohms/m. This silver yarn exhibits an elastic strain up to 10% which is an ideal material for sensor construction. However, the oxidisation is not avoidable even with an antibacterial layer. Carbon materials are usually stable and relatively lower cost. Carbon Tenax (TIBTECH) which is used in this research is a carbon fibre Z twisted sewing yarn with its resistivity reaches 218

ohms per meter. Although, the brittleness of carbon fibre is unavoidable, the high conductivity and excellent washability are much better than carbon coated materials. Carbon Tenax is a high-tech material; it shows a high strength and durability.

4.2.2 Device design and fabrication

To produce the embroidered piezoresistive sensor, the sensor was designed on PE-Design software. During the experiments carried out to determine the optimum stitch size and the stitch density for the sensor, stitch size was changed from 1 mm to 9 mm and the stitch density was changed from 0.5 to 1. The upper yarn is usually selected to be a nonconductive yarn to prevent the conductive particles from the friction between the upper yarn and the needle hole from being deposited on the fabric. After the design process, the substrate fabric and the backing material (which is used to increase the strength of the substrate fabric) were fixed by a frame, and once the frame has been placed under the needle, the embroidered piezoresistive sensor was manufactured by the machine.

4.2.3 Pressure sensing, Durability and Mechanical Force Differentiation

The embroidered piezoresistive sensor that was manufactured according to the description above was subjected to compressive cyclic tests starting from 0.1N to 2 N using a computerised Zwick/Roell tensile tester machine. The ramp and release rates were set at 3 mm/min. The electrical response was continuously monitored and recorded using a National Instrument-9219 data acquisition card. To test the long-duration stability of the sensor, the piezoresistive sensor was compressed and released for 100 cycles using the tensile tester machine.

4.2.4 Characterisation

The surface morphology of the three conductive sewing yarns was characterised by the scanning electron microscopy (Hitachi 3000). The Zwick/Roll computerised tensile testing machine was used to provide compression for the sensor and a National Instrument data acquisition card (NI-9219) was used to record the changes in resistance during the compression test. A Plux Bio-sensing system was used to measure the ECG and BCG signals from the human body.

4.2.5 Washing/Laundering Procedures

Wash ability test is necessary for the smart wearable sensors to test the sensor's mechanical and electrical performance after several times washed. In this paper, a Roaches Washtec-P TOC 3002 (Birstall, UK) was used for the washability test. The test was carried out according to EN ISO 105-C06:1997 A1M. The wash time was 45 minutes under 40°C.

4.3 Results and Discussion

The graphene coated cotton yarn was sourced from the National Graphene Institute, UK. In the construction of this yarn the inventors have used the Hummers method to oxidise the graphene, and ascorbic acid (AA) and sodium hydrosulphite (SH) have been used as the reducing agents [10]. The PSS/PVA had been used to functionalise the surface of rGO flakes to achieve a better dispersibility and prevent agglomeration [10].

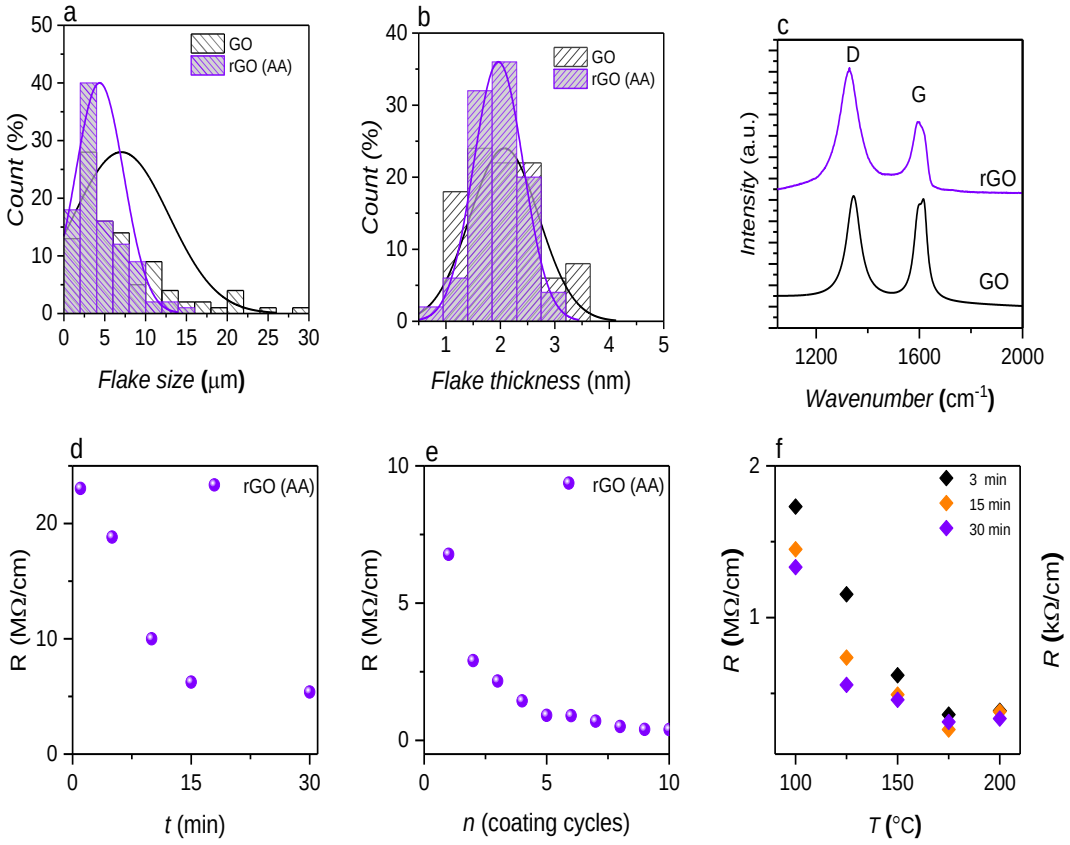

***Figure 4-2. (a) Flake size of rGO (AA) (b) Flake thickness of rGO (AA) (c) Raman spectra of GO and rGO. (d) Change of resistance of rGO yarn with coating time. (e) Number of coating cycles vs resistance of rGO coated dried yarn. (f) Change of resistance of rGO yarn with curing time and temperature* [10].**

Figure 4-2a shows the flake size distribution of the rGO, it can be seen that after the reduction with SH and AA, the flake size of the rGO is around 4.86 μm. **Figure 4-2b** is the flake thickness distribution of the rGO, it shows that after reduction, the flake thickness of the rGO is around 2.2 nm. **Figure 4-2c** is the Raman spectra of GO and rGO, The Raman spectra of GO and rGO shows characteristic peaks at ~ 1344.78 cm-1 and 1605.95 cm-1, corresponding to D and G bands [10]. **Figure 4-2d** illustrates that the resistance of rGO coated yarn decreases significantly with increasing coating time. As seen in **Figure 4-2e**, the resistance of the rGO coated yarn decreases rapidly up to 3

cycles, and after 3 cycles, the changes in resistance are very small. This might be caused by the cotton yarn absorbing enough graphene flakes during the first 3 cycles. **Figure 4-2f** exhibits the significant effect of curing time and temperature on the conductivity of the rGO coated yarn [10].

The fabrication of the embroidered sensor consists of design and embroidering processes. Once the sensor was designed, we can use the conductive yarns to manufacture the embroidered sensor. Three different conductive sewing yarns were used in this paper: Silver coated yarn (Silverpam, Tibtech), carbon Tenax (Tibtech) and graphene sewing yarn (National Graphene Institute, NGI). The SEM images of those three yarns are shown in **Figure 4-3**.

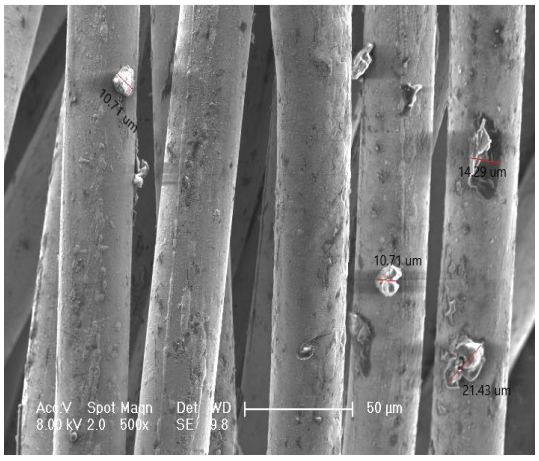

(a)

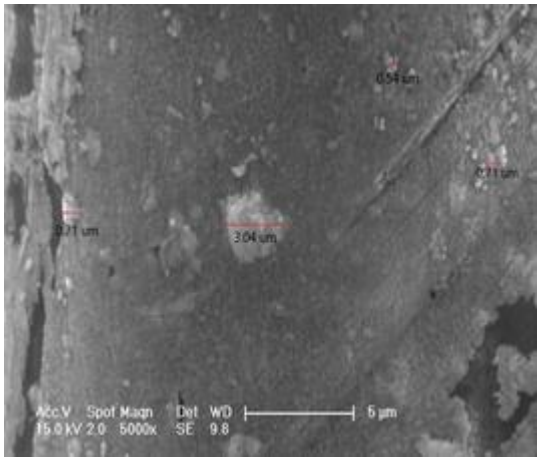

(b)

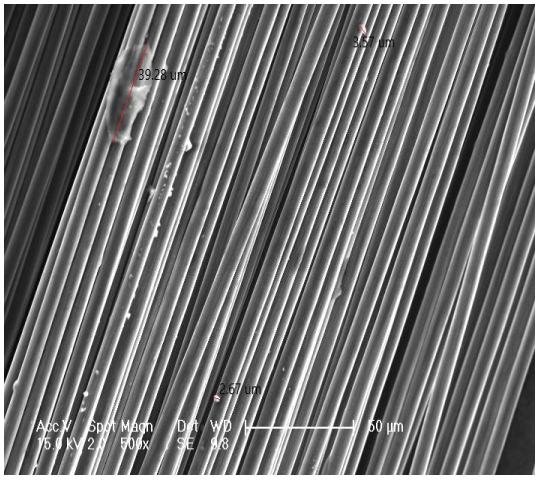

(c)

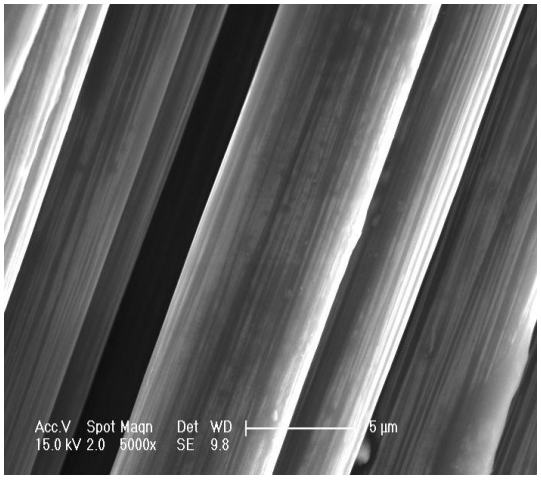

(d)

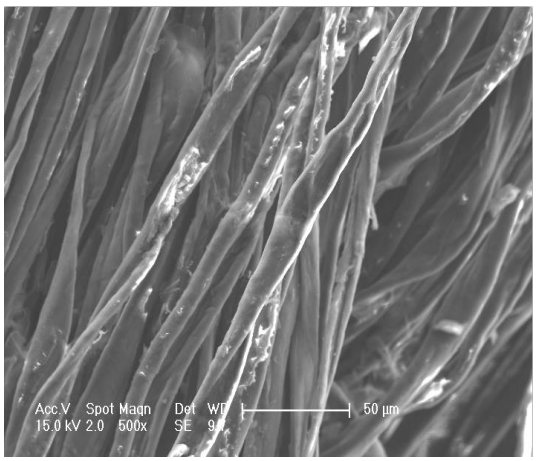

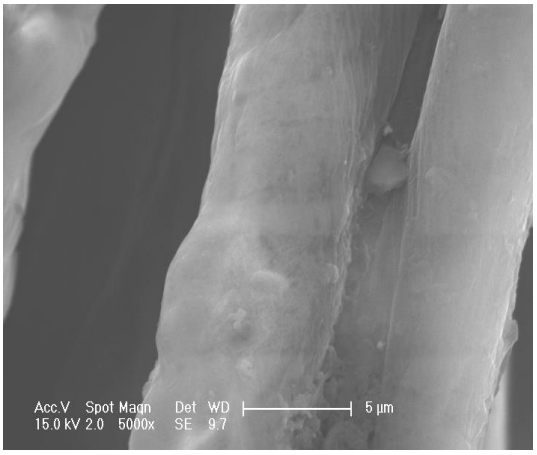

(e) **(f)**

Figure 4-3. Characteristics of the electroconductive sewing yarns. (a) SEM image of silver coated yarn at 500 times magnification. (b) SEM image of silver coated yarn at 5000 times magnification. (c) SEM image of carbon Tenax at 500 times magnification. (d) SEM image of carbon Tenax at 5000 times magnification. (e) SEM image of graphene yarn at 500 times magnification. (f) SEM image of graphene yarn at 5000 times magnification.

Figures 4-3a and **b** are the SEM images of silver coated yarn at different magnification. It can be seen that the silver particles are almost uniformly distributed on the surface. However, there are still some big particles which might lead to non-uniformity in electrical resistance. The silver coated yarn was cut into 10 samples of 10 mm to measure the electrical resistance, where the resistance of this silver yarn was found to be 0.198 ± 0.002 Ω / mm. **Figures 4-3c** and **d** are the SEM images of Carbon Tenax fibre and **Figures 4-3e** and **f** are the SEM images of graphene sewing yarn at different magnification. Compared to the graphene yarn, carbon represents much better uniformity and smoother surface due to it being a carbon fibre twisted yarn.

The investigation of the three electro-conductive sewing yarns shows positive resistance variations during tensile tests and negative resistance variations during compression tests. **Figure 4-4a** illustrates the mechanical properties of those three yarns

during tensile break test, **Figures 4-4b-d** represent the electrical properties of each yarn during the tensile test within the elastic limit. **Figures 4-5a to b** illustrate the compression test results of these three yarns up to the breakpoint and within the elastic limit respectively.

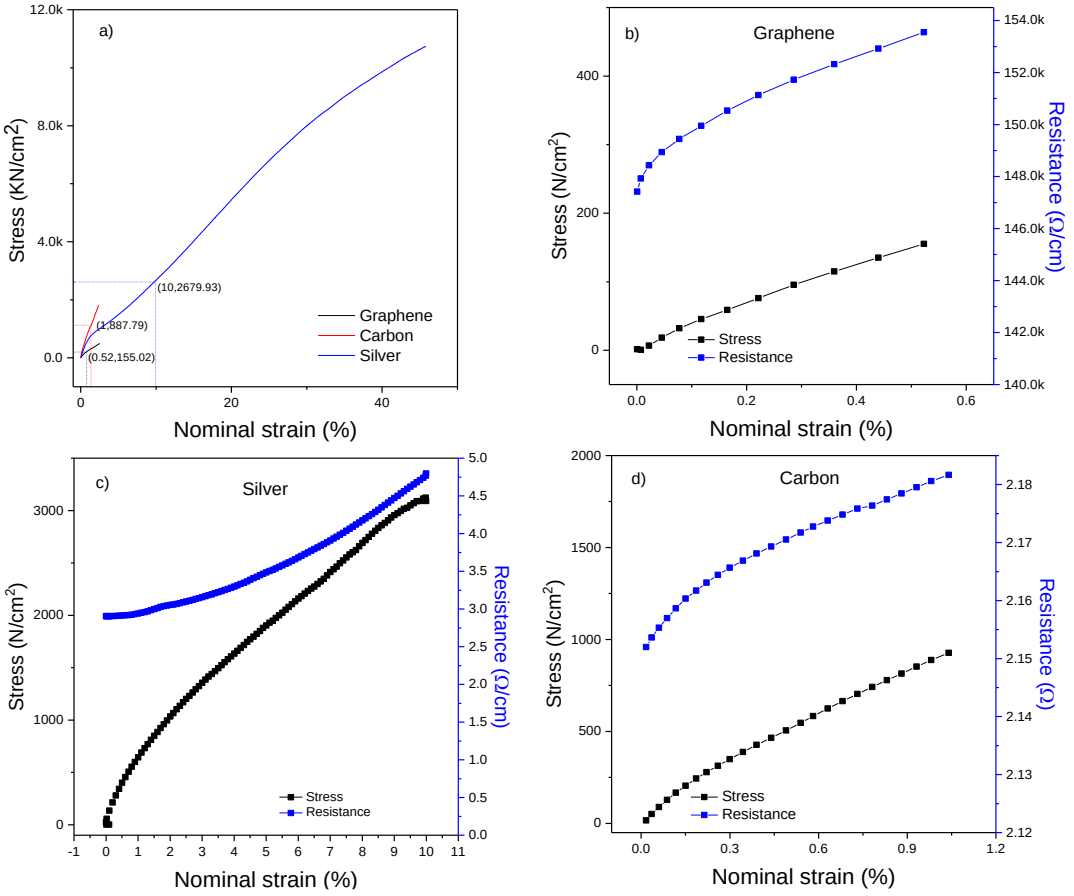

Figure 4-4. Tensile tests of silver, carbon and graphene sewing yarns. (a) Tensile break tests of silver, carbon and graphene sewing yarns. (b) Tensile test of graphene sewing yarn within elastic limit. (c) Tensile test of Carbon Tenax within elastic limit. (d) Tensile test of silver coated yarn within elastic limit.

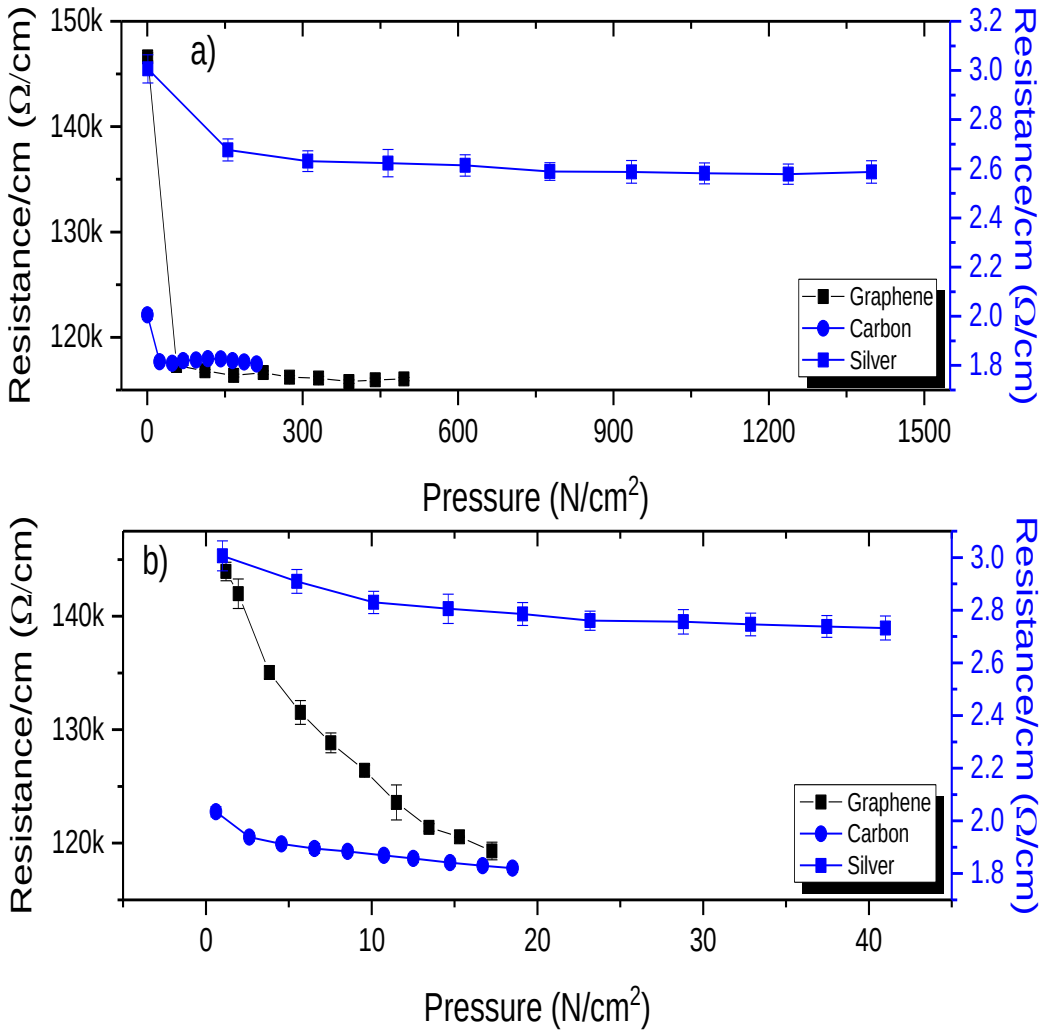

Figure 4-5. Yarn compression test results. (a) Compression test of silver, carbon and graphene yarns up to the break point. (b) Compression test of silver carbon and graphene yarns within the elastic limit.

Table 2. Mechanical properties for the conductive sewing yarns

	Young's modulus (pa)	Strength at break point (N)	Elastic limit (%)
Graphene	1692.31	2.8	0.52
Carbon	26800	52.4	1
Silver	190	7.6	10

It can be seen from **Figures 4-4a,** and **table 2** that silver coated sewing yarn shows the best elasticity among these three yarns. It can be stretched to 10% within the elastic limit, and the electrical resistance of silver coated yarn increased significantly during the tensile test. Carbon fibre shows the highest strength, but lowest elasticity. It would not break until the tensile force reached 52.4 N. The core of the carbon coated yarn is cotton, so the strength and the elastic limit are both relatively lower than the other two yarns. However, in **Figures 4-4b to d**, the electrical properties of these three yarns during tensile tests are shown. The graphene yarn shows a relatively linear relationship between the tensile force and the electrical resistance, which is an important feature for sensor performance. Also as seen in the **Figure 4-4 b,** the changes in the electrical resistance of graphene yarns were more significant.

As seen from **Figures 4-5a and b,** the graphene coated yarn shows a relatively better performance during the compression test, where the resistance is seen to decrease fast with a steep slope. The silver sewing yarn used in this paper is the finest yarn among these three yarns, however, in the case of the silver yarn, the electrical resistance only changed by 0.02 Ω /mm during the compression test from 0 to 40 Pa. Compared to silver coated yarns, the carbon fibre twisted yarn shows better results, an electrical resistance change of 0.02 Ω /mm during the compression test from 0 to 18.5 Pa.

After the yarn tests, in order to investigate the relationship between stitch size and the performance of the sensor, 5 samples were made with 2mm separation between adjacent lines but with different stitch sizes (1 mm, 3 mm, 5 mm, 7 mm and 9 mm) were made for each yarn material. These are numbered as 0.5-1, 0.5-3, 0.5-7 and 0.5-9. Also 5 samples with 1 mm separation between adjacent lines but different stitch size (1 mm, 3 mm, 5 mm, 7 mm and 9 mm) too was made for each sewing yarn. These were numbered 1-1, 1-3, 1-5, 1-7 and 1-9. The sensor size was set at 20 mm X 20 mm. **Figure 4-6a**

is the sketch of the embroidered sensor design and **Figure 4-6b** is the carbon embroidered sensor sample with 5 mm stitch size.

(a) **(b)**

Figure 4-6. Embroidered piezoresistive sensor sketch and sample. (a) Embroidered pattern sketch on design software. (b) Carbon embroidered sensor sample.

All the sensors were subjected to compressive cyclic tests starting from 0.1N to 2 N. A pre-load was applied to fix the sensor between compression board and a wooden cube which is the same size as the sensor and used to control the thrust face. Once the sensor was fixed, two crocodile clips were connected to the sensor for the data acquisition card to record the changes in electrical resistance. **Figures 4-7 to 4-9** show the compression test results for those embroidered piezoresistive sensors made of coated graphene, carbon and silver coated yarns respectively.

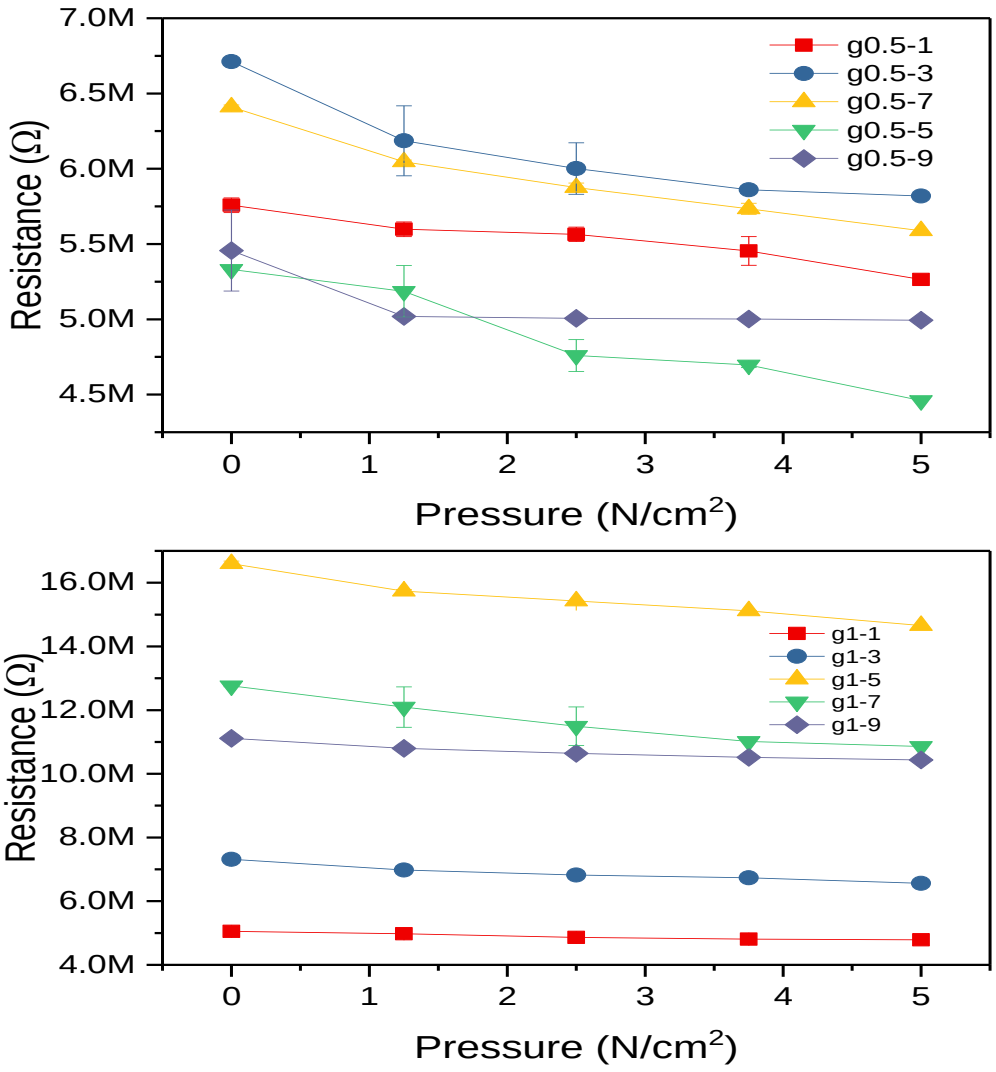

Figure 4-7. Compression test results of graphene piezoresistive sensor

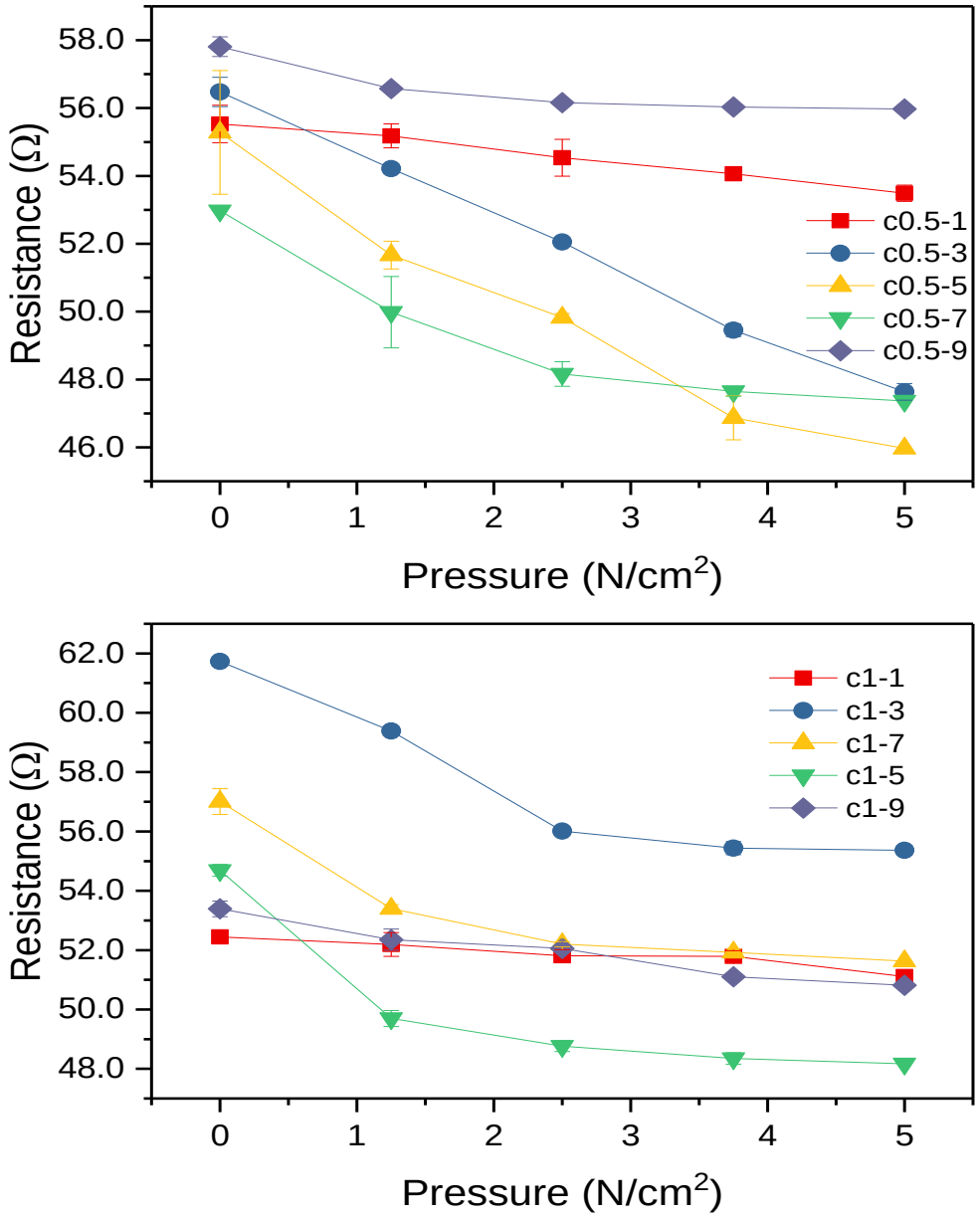

Figure 4-8. Compression test results of carbon piezoresistive sensor

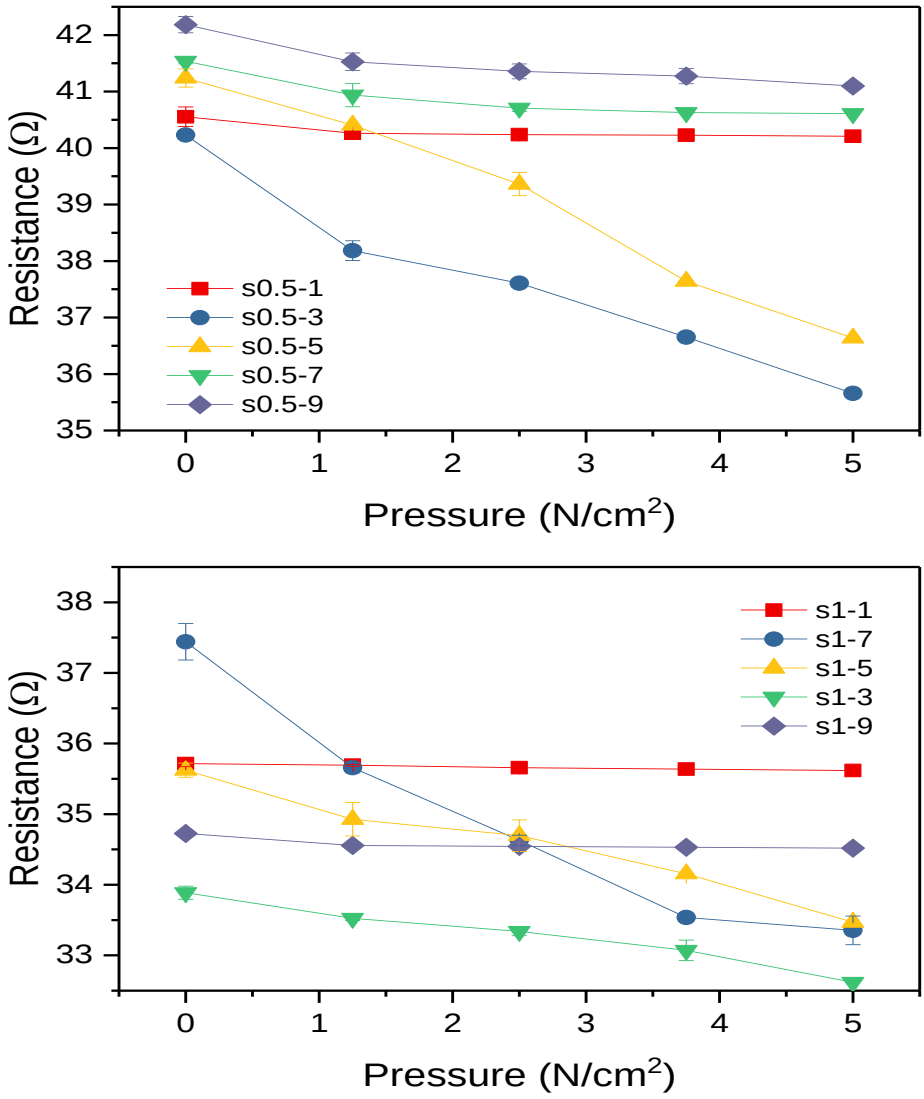

Figure 4-9. Compression test results of silver piezoresistive sensor

Figure 4-7 to 4-9 mainly illustrate the relationship between the yarn stitch size and sensor electrical resistance. These figures show that generally sensors with 5 mm stitch size show higher change in electrical resistance. When the stitch density increased from 0.5 to 1 sewing lines per mm, sensors with relatively higher stitch size shows higher change in electrical resistance, especially for those sensors made by relatively thicker sewing yarn (Carbon). **Figure 4-8** shows that carbon embroidered sensors with 5 mm stitch size show larger changes in the resistance in **Figure 4-8 top figure**, but carbon

embroidered sensor with 7 mm stitch size shows larger resistance changes in **Figure 4-8 bottom figure**. When the stitch density is increased, sensors become stiffer due to the increasing of the number of stitches within a unit area. When pressure was applied on the sensors, the deformation of the stiffer sensor is relatively lower than that of the more flexible sensor. Hence the changes in electrical resistance of the stiffer sensor is not as significant as that of the flexible sensor. However, increasing the stitch size and stitch density at the same time can be used to overcome this problem. This is explained by the fact that while the stitch density increased, sensor with higher stitch size shows higher change in electrical resistance.

Table 3. The sensitivity of the sensors with different parameters

$\frac{\Delta R}{R_0}$		Stitch size				
		1	3	5	7	9
Stitch density	silver 0.5	-0.547%	-8.881%	-11.586%	-2.306%	-2.141%
	silver 1	-0.188%	-3.375%	-6.042%	-10.917%	-0.605%
	carbon 0.5	-4.041%	-15.798%	-14.858%	-10.585%	-2.831%
	carbon 1	-2.766%	-10.357%	-11.926%	-9.916%	-4.829%
	graphene 0.5	-8.015%	-13.306%	-16.325%	-12.828%	-5.719%
	graphene 1	-4.580%	-10.102%	-11.687%	-15.059%	-6.103%

Table 3 is the calculated $\Delta R/R_0$ results from **Figure 4-7 to 4-9**, graphene sewing yarn, generally for 2 mm embroidery line separation and the sensors with 5 mm stitch size show higher relative change in electrical resistance (Higher $\Delta R/R_0$). Similarly, carbon sewing yarn, the embroidery lines with 2 mm line separation with 3 mm stitch size gives higher relative change in electrical resistance (Higher $\Delta R/R_0$). For silver sewing yarn 2 mm line separation with 5 mm stitch size gives the higher relative change in electrical resistance (Higher $\Delta R/R_0$). Therefore generally, it can be assumed that for

all three materials, 2 mm line separation and 5 mm stitch size for embroidered patches gives the highest relative change in electrical resistance.

Considering the results of the yarn compression cyclic tests and sensors compression cyclic tests, carbon and graphene yarn were used for further experiments. To investigate the influence of the design and shape of the sensor, five different designs were designed and manufactured (5mm stitch size and 2mm line separation) (**Figure 4-10**).

The size of sensor A to C is 20x20 mm and size of sensor D and E is 40x40 mm. Sensors A to C are single side electroconductive designs due to only the bottom sewing yarn being electroconductive while Sensor D and E are electroconductive in both sides. As indicated in **Figure 4-10** D and E, the black stitch lines in sensor D and E were embroidered first on the top of the substrate fabric, and then the fabric was turned over and the red stitch lines were embroidered on the reverse side of the substrate fabric. During the compression cycle, two electroconductive silver fabrics (20x20 mm) were placed on the two sides of sensor D and E to form a sandwich type of sensor.

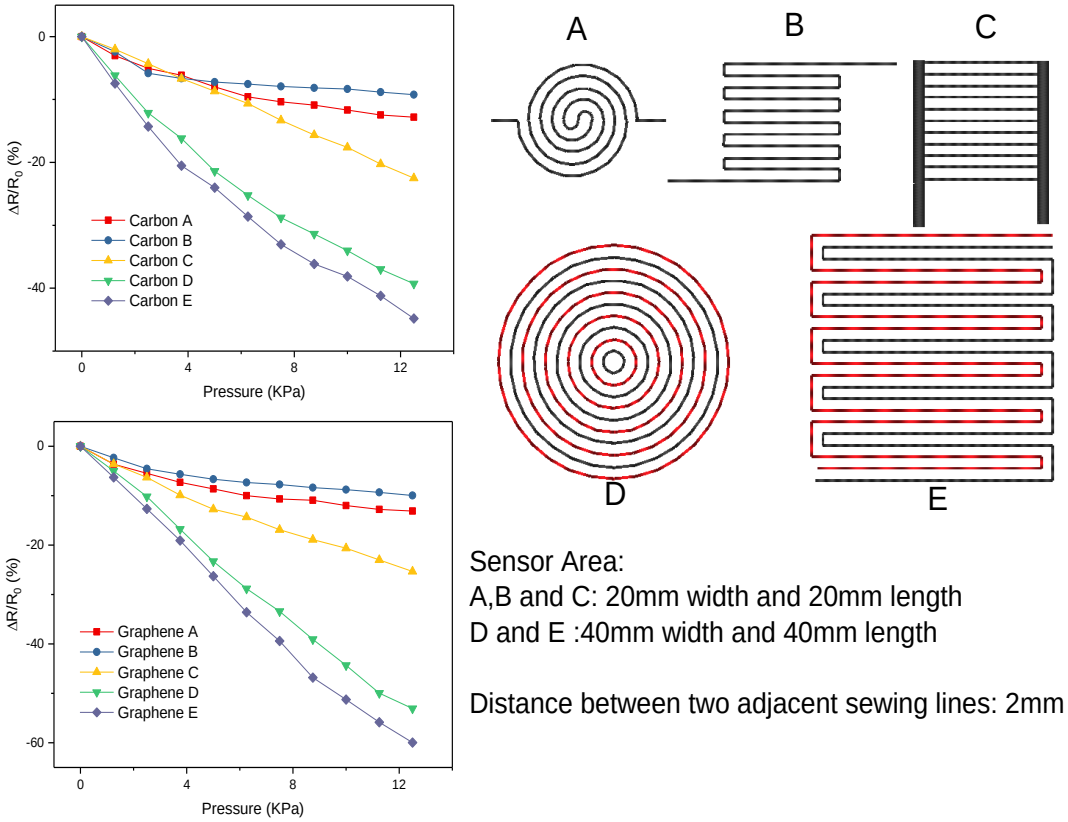

Figure 4-10.Compression cyclic test results of Sensor A-E.

It can be clearly seen that the sensors with D and E designs represent relatively better performance during the cyclic test. Sensor designs D and E provided a relatively higher electrical resistance and larger changes in electrical resistance during compression tests, especially for graphene embroidered sensors. Additionally, graphene sensors with E design shows a high relative change in electrical resistance; its resistance decreased approximately 60% from 0 to 12500 Pa, same as carbon sensor with E design of which resistance decreased 45% from 0 to 12500 Pa.

To compare the multiple layer designs D and E with embroidered multiple-layer patches (**Figure 4-11a-b**), a sensor fabric was embroidered with 3 stitches per mm and 5 mm stitch size.

(a) **(b)**

Figure 4-11. a) sketch of the design, b) prototype of the sensor

These sensor patches were produced with one, two, three and four embroidery layers. An insulation tape was used to fix the multiple layer embroidery sensor designs and also protect them. The sensors were tested on the tensile tester with the pressure varying from 0 to 12.5 KPa (at speed of 3 mm/min), **Figure 4-12** shows the compression test result. The results in **Figure 4-12** shows a linear relationship between the sensitivity and pressure for multilayer sensors. In plotting the sensitivity over time for the optimum sensor from **Figure 4-12**, it shows a flat response in the sensitivity of the sensor at the highest pressure for the sensor with two layers. The sensitivity of the sensor is a critical parameter to evaluate the performance of the sensor. By increasing the layers from 1 to 4, the sensitivity of the sensor shows an increase from 0.00278 Pa^{-1} (one layer) to 0.00505 Pa^{-1} (two layers), and then decrease to 0.00371 Pa^{-1} (three layers) and 0.00338 Pa^{-1} (four layers). It is obvious that sensors with two-layer embroidery sensor designs have relatively higher sensitivity and a linear relationship between 0 to 12500 Pa.

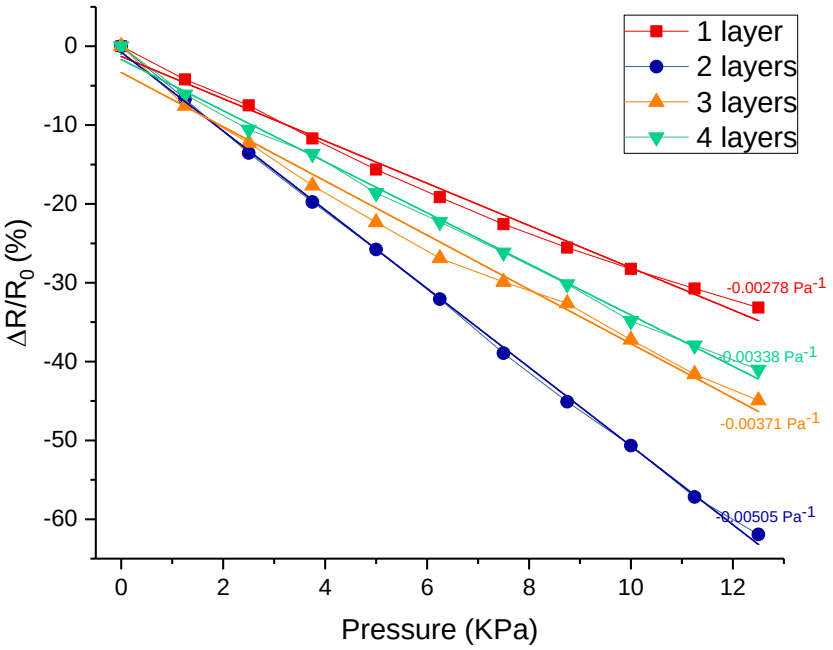

Figure 4-12. Compression test result of sensors with different layers

To test the durability and stability of the sensors, a 400 cycles cyclic test and a long-term stability test were carried out for the two layers sensor, where the results can be seen in **Figure 4-13**. During the cyclic compression test, the sensor was observed to show good stability and durability, where the resistance of the sensor did not change significantly after the test. Additionally, the sensor showed good retention and stability since there was no significant variation of the resistance while the applied pressure was stable at different values.

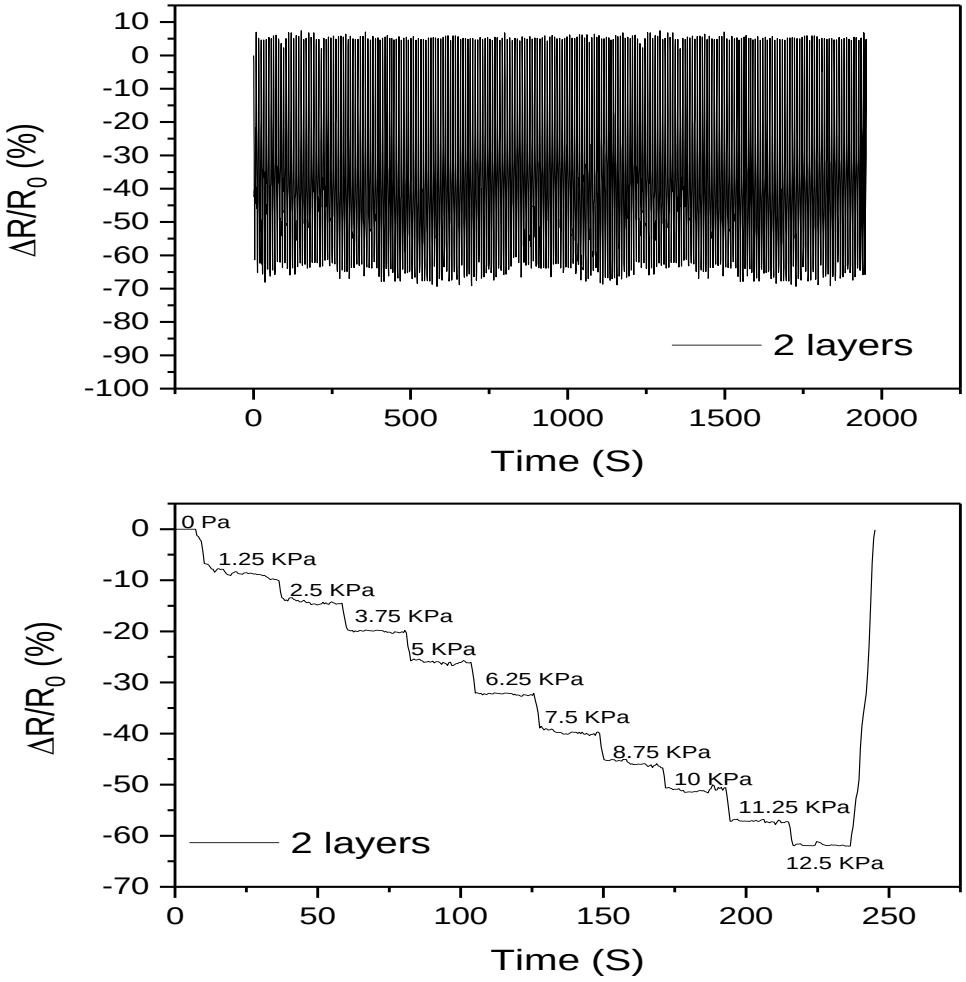

Figure 4-13. (upper)Cyclic test result of the 2 layers sensor, (Lower) long-term stability test result of the 2 layers sensor

To investigate the washability of the sensors, the washability test was employed on the sensor according to the standard BS EN ISO 105 C06 C1S where the samples were washed 5 and 10 times. After the sensors were washed and dried, a single compression test and a 5-cycle cyclic test were carried out on them. The result can be seen in **Figure 4-14**.

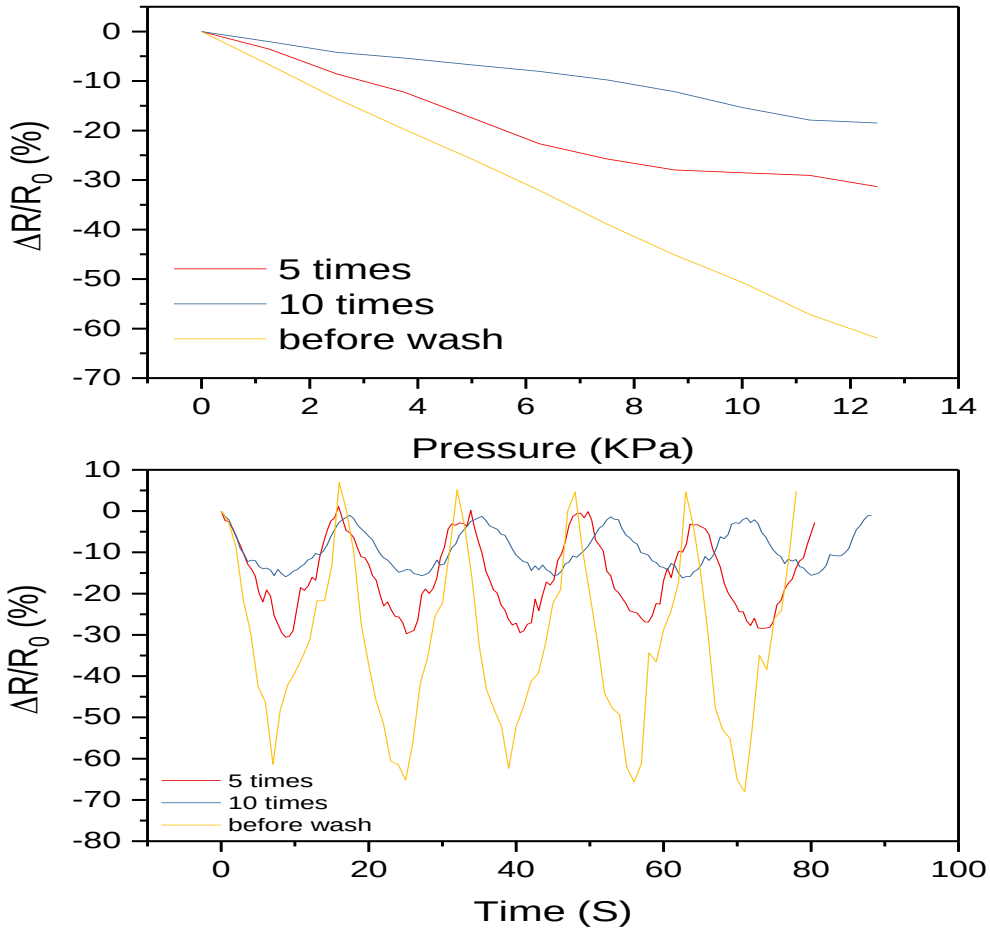

Figure 4-14. (upper) compression test of the 2 layers sensor before and after wash, (lower) cyclic test result of the 2 layers sensor before and after wash.

Comparing the samples after washing with unwashed samples, it is clear that the electrical resistance of the washed samples were relatively higher than the unwashed samples. The total electrical resistance increased by 17.6% after 5 times washing and 42.3 % after 10 times washing. The washing process has a significant influence on the signal output stability, sensitivity and conductivity of the sensor as well.

Figure 4-15 a-d are the test results of the two-layer sensors during a breathing test, finger touch test and a ball impact test.

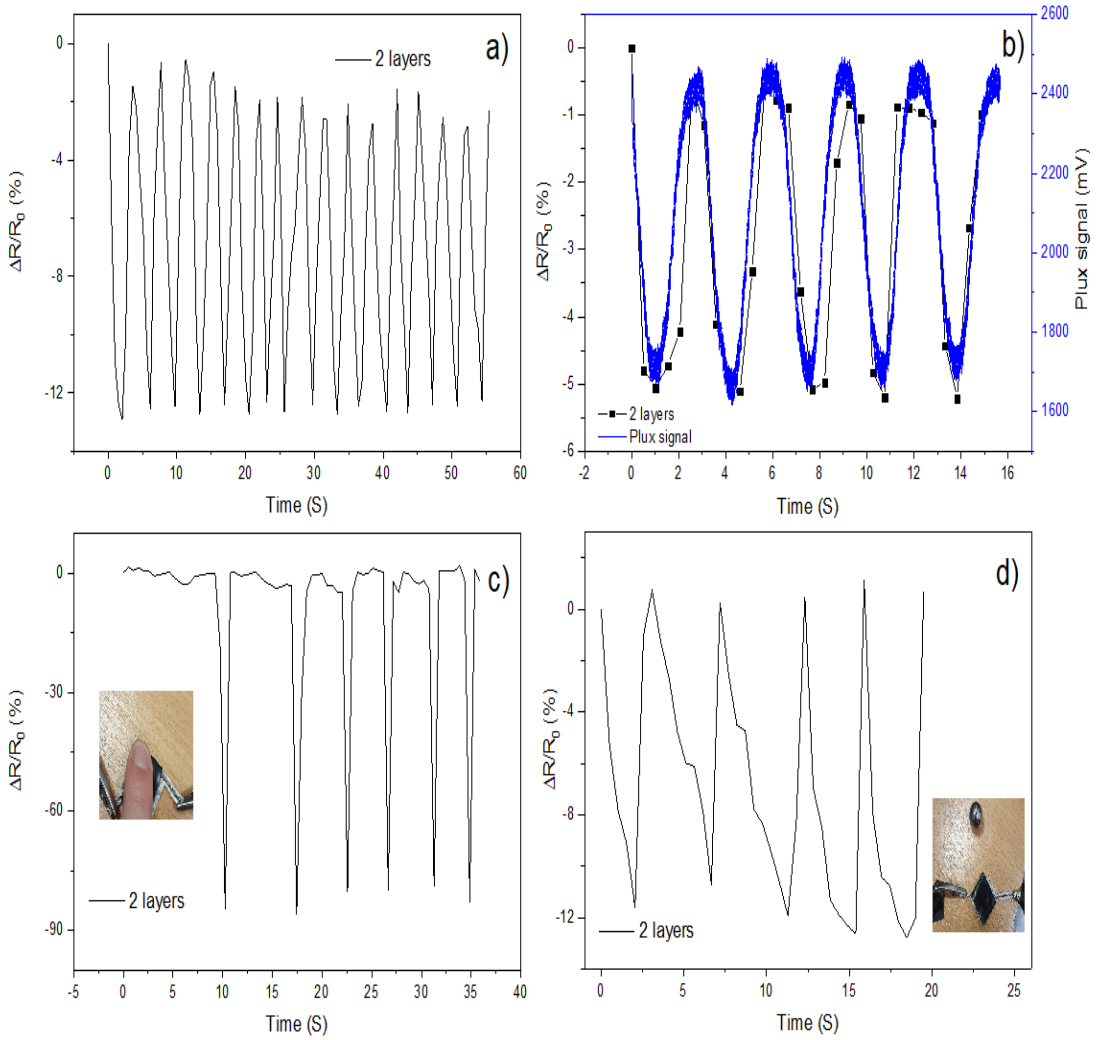

Figure 4-15. a) breathing test, b) breathing test with the Plux signal system, c) finger touch test, d) ball impact test

To investigate the ability of the sensor for bio-signal sensing, the Plux Bio-signal testing system was used as the control group experiment. The 2 layers sensor was placed under the Plux elastic band around the chest location (**Figure 4-16**), and the NI-9219 card was used to record the changes in the resistance during the breathing test. **Figure 4-15b** illustrates the result of the control group experiment. As seen in the **Figure 4-15b**, the 2 layer sensor curve is almost matching the Plux sensor, although sometimes the response speed of the 2 layers sensor is slower than the Plux sensor, the accuracy of the 2 layers sensor is nearly as good as the Plux sensor.

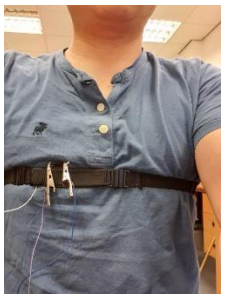

Figure 4-16.Plux bio-signal elastic band and the sensors

Figure 4-15 c-d shows the results of the finger touch and ball impact test respectively. It can be clearly seen that this two-layer piezoresistive sensor has a good response speed and recovery speed which makes it capable of working as a wearable sensor for human movement detection and bio-signal detection.

4.4 Conclusion

This paper has developed several embroidered piezoresistive sensors with different embroidery designs and materials. During the research, it was found that multilayer embroidered designs will improve the conductivity of piezoresistive sensors. The modified two-layer embroidered piezoresistive sensor shows a good sensitivity with high response speed and recovery speed. Although the washability performance of the sample is unsatisfactory, it can be improved by encapsulation using a flexible resin. It can be concluded that this two-layer embroidery design is capable of working as a wearable sensor for capturing human motions and for bio-signal detection.

4.5 Summary

Although electrotextiles are a relatively new area, within a short period of time, it has become a very popular field of study the world over. One of the drawbacks these materials face is that unlike conventional materials used in the construction of sensors,

the properties of e-textiles can easily be influenced by many external factors such as movement, vibration, any mechanical deformation, temperature, humidity and other variables like perspiration when measured on human beings. We designed and manufactured an embroidered piezoresistive sensor with graphene coated (from the National Graphene Institute, University of Manchester), carbon (Carbon Tenax, Tibtech) and silver coated (Silverpam 250, Tibtech) electroconductive sewing yarns. During the embroidery process, the yarn tension, yarn orientation and yarn twist/untwist, level of yarn compression can be easily controlled by the embroidery machine (Brother IS-V5) and embroidery CAD design software (PE-Design). Through the modelling work, an embroidered sensor was manufactured with high flexibility, good sensitivity, fast responsivity and good mechanical stability. Furthermore, the embroidered piezoresistive sensor was used to measure the ECG and BCG signals from the human body. Based on the performance of the embroidered piezoresistive sensor, it has promising applications in wearable technology and bio-signal sensing.

4.6 References

[1] X. Tao, *Wearable electronics and photonics*. 2005. pp. 177–197.

[2] F. Chiarugi *et al.*, “Measurement of heart rate and respiratory rate using a textile-based wearable device in heart failure patients,” in *Computers in Cardiology*, 2008, vol. 35, pp. 901–904.

[3] M. Peltokangas, J. Verho, and A. Vehkaoja, “Night-time EKG and HRV monitoring with bed sheet integrated textile electrodes,” *IEEE Trans. Inf. Technol. Biomed.*, vol. 16, no. 5, pp. 935–942, 2012.

[4] M. Sibinski, M. Jakubowska, and M. Sloma, “Flexible temperature sensors on fibers,” *Sensors*, vol. 10, no. 9, pp. 7934–7946, 2010.

[5] J. Meyer, “Textile pressure sensor: Design, error modeling and evaluation,” *Ph.D. Diss.*, pp. 1–120, 2008.

[6] L. M. Castano and A. B. Flatau, “Smart fabric sensors and e-textile technologies: A review,” *Smart Materials and Structures*, vol. 23, no. 5. 2014.

[7] X. Lin and B. C. Seet, “A Linear Wide-Range Textile Pressure Sensor Integrally Embedded in Regular Fabric,” *IEEE Sens. J.*, vol. 15, no. 10, pp. 5384–5385, 2015.

[8] O. Atalay and W. R. Kennon, “Knitted strain sensors: Impact of design parameters on sensing properties,” *Sensors (Switzerland)*, vol. 14, no. 3, pp. 4712–4730, 2014.

[9] P. Bosowski, M. Hoerr, V. Mecnika, T. Gries, and S. Jockenhövel, “Design and manufacture of textile-based sensors,” in *Electronic Textiles: Smart Fabrics and Wearable Technology*, 2015, pp. 75–107.

[10] A. Bonfiglio and D. De Rossi, *Wearable monitoring systems*. 2011, pp.86-92.

[11] S. Radavičiene and M. Juciene, “Influence of embroidery threads on the accuracy of embroidery pattern dimensions,” *Fibres Text. East. Eur.*, vol. 92,

no. 3, pp. 92–97, 2012.

[12] D. A. Chernenko, “Systematization of Design Parameters for Automated Embroidery and Modelling of Deformation System of ‘Fabric-Embroidery,’” Russia, 2006.

[13] Ž. Juchnevičienė, M. Jucienė, and S. Radavičienė, “The research on the width of the closed-circuit square-shaped embroidery element,” *Medziagotyra*, vol. 23, no. 2, pp. 186–190, 2017.

Chapter 5 - Investigation of graphene based embroidered moisture sensors

5.1 Introduction

Clothing, which is able to maintain a micro-climate around the body is generally designed to make the wearer feel comfortable when worn close to the body [1]. Being the closest layer to the body, textiles provide an ideal platform for integrating sensors and actuators to monitor the body's physiological signals and the environment around them. By using the clothing worn by an individual as the scaffold for integrating various bio-sensors, it may be possible to observe and solve a wide range of behavioural and developmental problems and decreased quality of life using both passive smart material which can only sense the environment and the active smart material that can not only sense the environment but also react to the information.

A large amount of research is available on using the sensing ability of intelligent textile sensing devices to measure physiological data from the human body such as heart rate [2-3], body temperature [4] and external pressure on the body [5]. Even though not as popular as heart rate sensors, passive wearable humidity sensors have a large range of applications such as sports and healthcare due to its ability to monitor the variation of human sweat levels and disabilities of the human body such as urine related incontinence [6]. It is possible to measure human sweat generation rate during physical exercising to monitor the body hydration status and the quantity of liquid needed to be supplied. Similarly, a patient's body bleeding rate can be monitored to understand the severity of the wound suffered and when to replace any wound care material applied over a blood effusion. Again, a wireless humidity sensor can be used to check whether the diaper worn by an infant or an older adult need to be changed

[7-8]. Nowadays, with the advances in the medical treatments and their successes, due to the large number of the elderly population present in many countries, more and more incontinence problems of elders are reported. Not only the older adults but also the infants and some children are affected by nocturnal enuresis [9]. This has the capacity to precipitate a wide range of behavioural and developmental problems and decreased quality of life. Currently, humidity sensors made as rigid sensors on large area flexible substrates [10-11], or directly printed onto the surface of a substrate by screen printing [12] are common. However, the disadvantage of these moisture sensors is their short life span due to the use of corrosive materials, low flexibility, low comfort, poor washability and usually only one-point, faulty and inefficient measurement. To overcome these drawbacks, this research aims to manufacture and investigate an embroidered humidity sensor made using an advanced modern material, namely graphene, and compare its performance against traditional materials such as silver and carbon.

By definition, embroidery is a textile-finishing method that can be used to apply a given yarn material to a textile substrate in a defined geometry [13]. When compared to other textile production technologies, embroidery technique is a convenient alternative because it is a low labour-intensive method during design and production processes. It also allows CAD based sensor geometry design and accurate construction. The manufacturing process of embroidered sensors can be described as a one that can use fine metallic wires, conductive coated or other conductive yarns and attach them to fabrics by stitching techniques to form electrical circuits of defined geometries. Conductive yarn and yarn embroidery can be accomplished on single or multiple layers of fabric or can be applied to various types of textile and apparel products in one step [14]. The advantage of embroidery is that just one manufacturing process can be used when combining the conductive tracks with the supporting electronics in complex and essential geometries. Furthermore, embroidery is a convenient technique that creates electronic

devices, since the conductive paths and electronic devices are connected within the same manufacturing process. Embroidery offers advantages over knitting or weaving and presents a relatively effective process to implement wearable electronics suitable for a wide range of materials (metal yarn, elastomeric yarn) and can be designed into different geometries. Not like the other textile techniques, embroidered structures can be directly made on ready-to-wear clothes and the sensor area can be easily covered by other embroidered decorative patterns to improve its artistic and commercial properties. The decorative embroidered patterns can also be used to protect the embroidered sensors from abrasion during wearing.

Humidity and moisture detection are of vital importance in medical, athletic, industrial and in-home applications. It is essential to monitor the humidity level while producing food, semiconductor, pharmaceutical, and wood [15]. A textile moisture sensor can be built to detect humidity changes in the environment or measure the moisture level on a surface. The working principle of a moisture sensor can be based on the changes in the capacitance (in the condition of changing dielectric constant) or resistance in the material according to changes in the moisture level. Resistive textile humidity sensors can respond to liquid-vapour or moisture because of varying electrical conductivity [16]. Liquid vapour speed is expressed by moisture with specific humidity, while the percentage of vapour contained in the air under a prescribed temperature compared to the vapour contained in the air at a measuring temperature is called relative humidity (RH).

The working principle of a resistive humidity sensor is designed based on monitoring the change of reactive resistance in the hygroscopic medium. In this case, sensing process is started with absorbing liquid and ionic function groups by hygroscopic action where the electrical conductivity will increase accordingly resulting in a resistive signal that is proportional to the actual moisture level [17].

The capacitive humidity sensors are comprised of two electrodes and a dielectric placed between the electrodes. The capacitance change of the dielectric constant will determine the RH values. Therefore, in a capacitive humidity sensor, the dielectric material should be hydrophilic, which guarantees the liquid absorption ability. While the conductive fluid is introduced to the two-electrode sensor system, there should be an electrical connection present between the two electrodes, and thus the humidity signals can be monitored. In this case, the capacitive humidity sensor is a more suitable sensor technology; where the utilisation of electroconductive yarn makes it more precise than a resistive humidity sensor [9].

However, the measurement of resistance is relatively easier compared to capacitance, and due to the high surface-volume ratio of resistance sensors, it can measure humidity changes in the environment up to 90% relative humidity at room temperature. Additionally, high sensitivity of capacitance sensors to dust particles is another reason why a resistive moisture/ humidity sensor is preferred.

5.2 Methodology

5.2.1 Materials

Embroidered electrotextile sensors consist of electroconductive upper sewing yarn, non-electroconductive lower sewing yarn, substrate fabric and the temporary backing material. In this paper, three different conductive sewing yarns were used to manufacture the moisture sensor: silver coated sewing yarn, carbon fibre twisted yarn and graphene coated sewing yarn. Silver coated yarn is a standard yarn and compared to the other conductive yarn, silver coated sewing yarn shows a higher electroconductivity. Generally, there are three types silver yarns used in sensor fabrication: twisted short fibre silver yarn, continuous filament silver yarn and elastic

silver yarn.

Since the mechanical properties of an embroidered pattern are mainly dependent on the yarn and substrate fabric, elastomeric silver sewing yarn (Silverpam 250, Tibtech) was used in the research work carried out for this paper. Silverpam 250 is a grafted antibacterial yarn based on 99% pure silver alloy grafted on a polyamide-based material with a linear resistivity of 198 ohms/m and linear density of 250 dtex. However, it was noted that the resistance of the silver coated yarn is subject to change due to its tendency to oxidise over time.

To observe a moisture sensor that is not subject to oxidisation, carbon (Carbon Tenax, Tibtech) and graphene (from the National Graphene Institute, University of Manchester) were used. The resistance of the Carbon coated sewing yarn was observed to be stable and relatively lower cost while the newly discovered 2D material, graphene has opened up a wide range of flexible electronics applications due to it's outstanding electrical, mechanical, membrane and other performance properties. Carbon Tenax is a high-tech material which shows high strength and durability. Carbon Tenax is a twisted sewing yarn with a resistivity around 218 ohms per meter and has a count of 0.14 grams per meter. It is a yarn with "Z" twist with a break elongation of 1.5%. Carbon fibre is a multifuctional material, with a high range of applications in areas such as golf club shafts, car parts and aircraft wings. Due to those applications, carbon fibre has become more and more important in our daily lives in recent times. The non electroconductive upper sewing yarn is a normal polyester sewing yarn (ISACORD 40). The upper yarn is usually nonconductive to prevent conductive particles from the friction between the upper yarn and the needle hole to be deposited on the fabric.

Non-elastic woven fabrics were used as the substrate fabric in this paper. As for the backing material, three types of backing materials are available to be used in

embroidery: heat removal, liquid soluble and glue type backing material. Heat removable backing material needs to be removed by a hot iron which will have a huge influence on the resistance of the conductive yarn. According to a simple test, the resistance of the silver embroidered sensor will be increased 10%-20% after ironing treatment. Glue type backing material needs to use a glue to attach the nonwoven backing material to the substrate which is normally used for decorative embroidered products. It's generally hard to remove once set which means the residual nonwoven backing material will have an effect on the mechanical properties of the embroidered sensor. The embroidery frame which was used to fix the substrate fabric and backing material is 100 mm X 100 mm.

5.2.2 Device design and fabrication

To produce the embroidered moisture sensor, the sensor was designed on PE-Design embroidery CAD software. Moisture sensor comprises two separate electrodes with a gap between them. When an electroconductive liquid is applied to the sensor area, these two electrodes will be electrically connected with a defined electrical resistance.

5.2.3 Moisture sensing

In order to characterise the moisture sensor, the moisture sensors were placed on a conditioned lab to control the temperature and humidity. A liquid dispenser was used to apply the saline solution on the sensor area at the periphery of the sensor or at the middle of the sensor area. The NI-9219 data acquisition was connected to the sensor during the test to measure the changes in electrical resistance.

5.2.4 Characterisation

A Brother IS-V5 embroidered machine, which is a general-purpose CAD enabled embroidery machine was used to manufacture the moisture sensors described in this paper. The Zwick/Roll computerised tensile testing machine was used to carry out the tensile and bending tests for the sensor samples and a National Instrument data acquisition card (NI-9219) was used to record the changes in the electrical resistance during the tests.

5.3 Results and Discussion

The working principle of the embroidered moisture sensor can be seen in **Figure 5-1**. For the current work, a saline solution was used as the electroconductive moisture. When the saline solution spread through the cotton fabric surface it completes an electrical circuit allowing the circuit resistance to be measured.

Because the electrical property is mainly based on the conductive sewing yarn, several embroidery patterns were designed to find the moisture sensor with the most suitable mechanical properties. For example, the ideal embroidery design should be flexible, relatively higher strength and the changes in resistance it experiences during strains or bending should be low. **Figures 5-2a to c** are the sketches of the embroidered moisture sensors. The first two designs were selected to provide isotropic bending properties for the moisture sensor while the third sensor is a popular moisture sensor design. From previous work (chapter 4) it was established that a 5 mm stitch length is an ideal value for the research conducted in this PhD work. Therefore, for the present moisture sensor, a 5 mm stitch length was used. After the design process, the substrate fabric and the backing material were fixed by a frame, and once the frame has been placed under the

needle, the embroidered piezoresistive sensor was embroidered using the Brother IS-V5 embroidery machine.

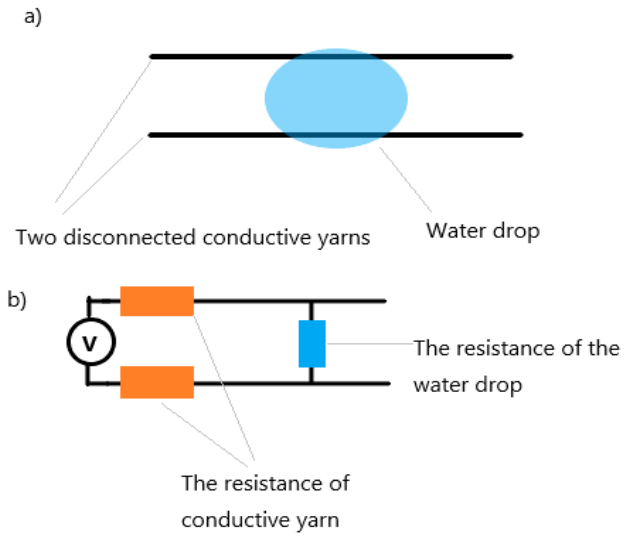

Figure 5-1. The working principle of resistance type moisture sensor

(a) **(b)** **(c)**

Figure 5-2. The three designs of embroidered moisture sensor

Before the moisture test, a FAST (Fabric Assurance by Simple Testing) bending test was done to measure the bending rigidity of the three embroidery designs, where the results are shown in table 4.

Table 4. The results of bending rigidity test of the three designs

Bending rigidity parameters	Average bending length (mm)	Average bending rigidity (uN.m)
Design A	**17.5**	**0.077**
Design B	**20**	**0.11615**

Design C	**29**	**0.2565**

As seen in Table 4, design C shows the highest bending rigidity out of the three while structure A presents the lowest bending rigidity, signifying design A is the most flexible out of the two. However, due to the high flexibility of a garment on which the moisture sensor would be mounted, it should have higher flexibility and enough rigidity to prevent the changes in resistance from bending or stretching.

After the bending rigidity tests, tensile test was carried out on the sensor samples using a Zwick Roell Z50 tensile tester on both vertical and horizontal directions. The changes in resistance of the moisture sensor during the tensile tests are given in Table 5.

Table 5. The results of tensile tests of the three embroidered designs

$\frac{\Delta R}{R_0}$		**Designs**		
		A	**B**	**C**
Direction	**Vertical**	**1.38756**	**1.758796**	**4.58399**
	Horizontal	**2.30716**	**1.577738**	**2.401638**

As seen in Table 5, design B shows the lowest changes in resistance during the tensile test in both directions. Considering the results from Table 4 and 5, design B was selected as the optimum moisture sensor design due to its flexibility, relatively higher strength and the low changes in resistance during strain or bending.

Two parallel conductive sewing lines were tested first to discover the moisture wicking characteristics through the conductive sewing lines and to measure the changes in resistance at the same time. A red food colour gel was mixed with the saline solution

was used to mark its wicking pattern. The difference between pure water and saline solution is that saline solution contains free cations and anions which make saline solution electroconductive. Also, another reason for using the saline solution was to simulate human sweat. **Figures 5-3 a-d** are the images of the two parallel conductive sewing lines after the test, and **Figures 5-4** provides the changes in electrical resistance recorded in each case.

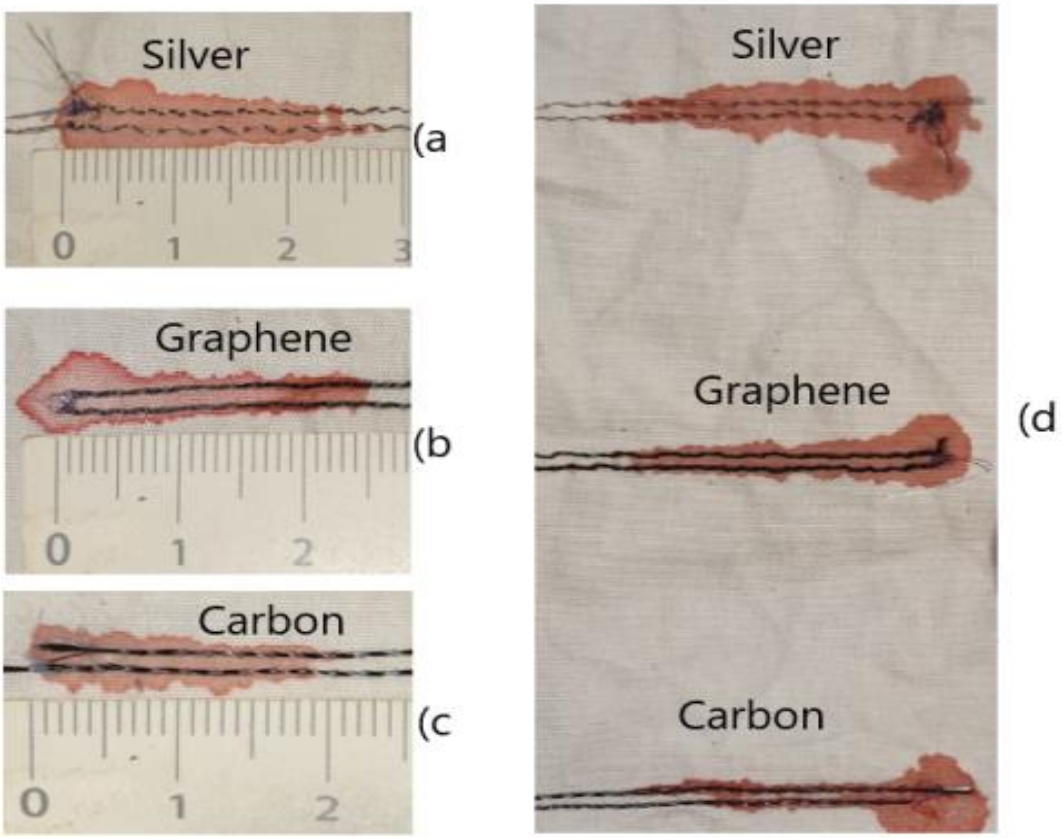

Figure 5-3. a) silver sewing lines after one drop water, b) carbon sewing lines after one drop water, c) graphene sewing lines after one drop water, d) all the three samples after two drops water

Figures above are the images of the samples after the moisture wicking tests. The conductivity of solution is depending on the amount of ion inside the solution, in order to achieve a better result, saltine water was used instead of pure water. As evidenced in the images after the application of one drop and two drops, there is not much of a difference in the moisture wicking performance of the three samples in the direction of

the embroidered lines. Therefore, since the substrate fabric is the same in each case, it can be seen that each of the yarn material did not have a significant difference in the overall wicking performance of the samples. Therefore, in comparing the sensor performance, all the conditions for the sensors are equal, and the sensor sensitivity will purely depend on the material properties of the sensor yarn. These results are given in the figure below.

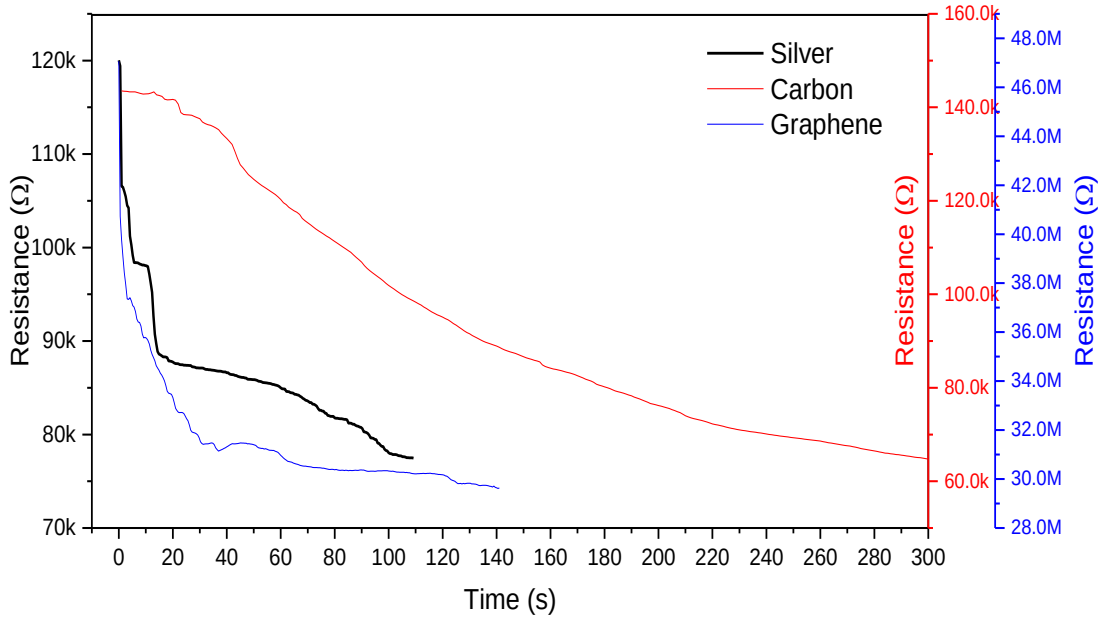

Figure 5-4. Liquid drop test for parallel embroidery lines of silver, carbon and graphene sewing lines

In analysing the moisture detection performance of the silver, carbon and graphene embroidery lines (**Figure 5-4**), the response speed of carbon sewing yarn seems to be the slowest (10 kΩ in 20 s). The reason for this could be the structure of yarns, where the carbon yarn is pure continuous carbon filament while the silver and graphene are polymeric and cotton based that support moisture wicking. As it can be seen**,** after the significant decrease in the electrical resistance, the rate of decrease of electrical resistance of the embroidered silver sample started to slow down (10kΩ in next 80 s) while the electrical resistance of embroidered graphene and carbon samples

experienced much larger changes in the rate of decrease in electrical resistance. Compared to silver and carbon samples, graphene sample shows a relatively faster rate of response. It shows a higher decrease in electrical resistance at the beginning (14000 kΩ in the first 20s), faster speed to achieve a stable situation and stable signal output after the significant drop in the electrical resistance.

Using the knowledge gained in studying the behaviour of parallel embroidered lines, in order to observe the performance of an embroidered sensor design that shows isotropic mechanical behaviour, carbon, silver and graphene conductive sewing yarns were used to manufacture the moisture sensor having the embroidery pattern defined in the design B (**Figure 5-5)**. In the present case, these samples were investigated by depositing liquid droplets at the outer periphery and the centre of the embroidered moisture sensors, as shown in (**Figure 5-5)**. Thereafter the rate of reduction of electrical resistance was observed for the three materials on the deposition of further droplets of the liquid. Since the double Archemedian spiral shapes of the embroidered moisture sensors are in effect double lines of parallel embroidery lines, the test was expected to show similar characteristic behaviour to that seen in **Figure 5-4.** All the tests were carried out in an environment conditioned room (25 centigrade, 65% relative humidity) and the tests were repeated five times.

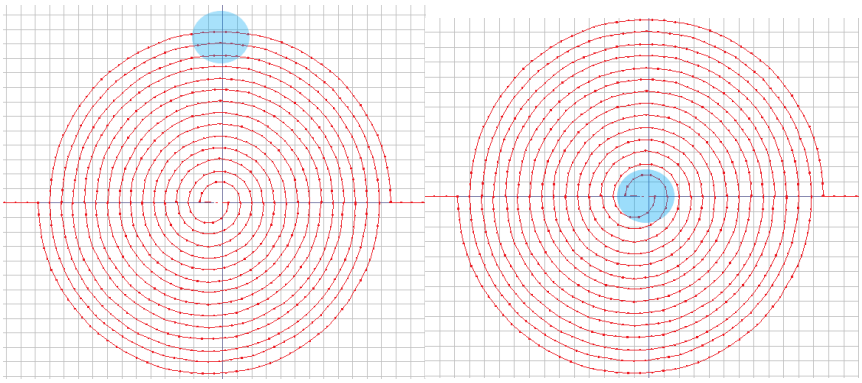

(a) **(b)**

Figure 5-5. Two areas where the liquid drops are applied. (a) the liquid drop applied on the top side of the sensor. (b) the liquid drop applied on the centre of the

sensor.

Figures 5-6 to 5-8 are the results of the liquid droplet tests for the moisture sensors. It can be clearly seen for each material, on the application of an electroconductive liquid, the electrical resistance decreased significantly at the beginning. After that, the electrical resistance of all three sensor types decreased slowley. When liquid wicks through the substrate fabric surface, the conductive liquid and the conductive yarns form an electrical connection and completes a circuit. With the liquid spreading, more embroidery yarns were covered by the liquid and forms a parallel circuit which leads to further decrease of the sensor resistance. If the liquid completely covers the sensor, the resistance will become a very low constant value.

After the liquid drop was applied to the sensor, it starts spreading while at the same time evaporating to the environment. This is apparent by the second half of the resistance vs. time curves where the sensor resistance is seen to increase. This behaviour was seen in the cases of the silver and carbon embroidery sensors. If the sensor is in a closed compartment, when the humidity increases, the resistance of the sensor will decrease. In another scenario, with reference to **Figure 5-5a**, when a drop of liquid was applied on top of the sensor, the liquid could spread out of the sensor which means the amount of the liquid within the sensor in **Figure 5-5a** is less than in **Figure 5-5b**. This also could lead to the resistance of moisture sensor decreasing in **Figure 5-5a** more than in **Figure 5-5b** at the beginning.

In order to visualise the behaviour of the moisture sensor in an environment where the liquid source is uninterrupted during the test, the test was conducted with additional liquid droplets being deposited on the top end and middle part of the sensor. For observing the resulting electrical resistance change and the rate of change, in addition to the test that has only one liquid drop deposited on the sensor, further tests were conducted for two drops and three drops of the liquid being applied on the sensors. The

resulting change in the electrical resistance for each material for the cases of the liquid being dispensed to the top end and the middle of the sensor were recorded and are shown in **Figures 5-6 to 5-8**.

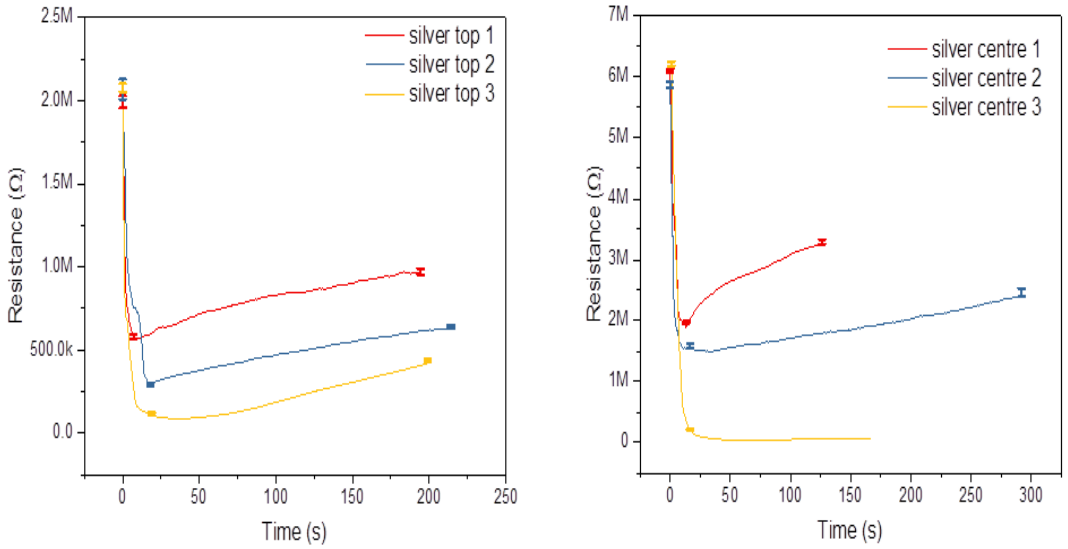

Figure 5-6 (a) Moisture test result of silver moisture sensor (liquid applied on the top side), (b) Moisture test result of silver moisture sensor (liquid applied on the centre of the sensor design)

As it is seen in the graphs, due to the motionlessness of the sensors and the gradual wicking of the liquid in the embroidered sensor, the error bars recorded for each curve is small. The graphs show that the introduction of the liquid droplets has a sudden and significant reduction in electrical resistance. When the liquid droplet source pressure increases, the sudden reduction in the electrical resistance is higher. Also, the increase in the number of droplets can make the changes in electrical resistance more stable after the significant decrease at the beginning. This is understandable since the behaviour is due to the presence of more liquid at the evaporation stage. Again, this behaviour is more pronounced when the drops were deposited in the centre of the sensor.

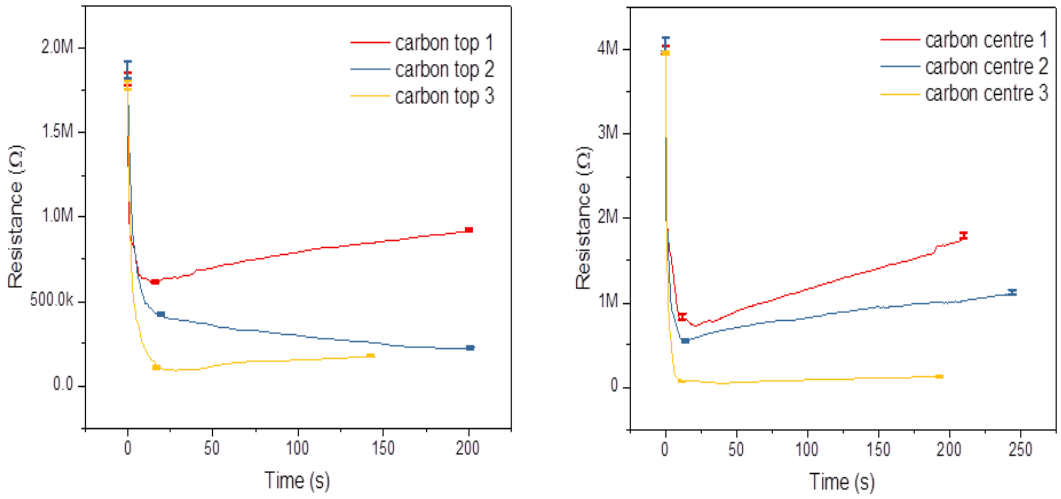

Figure 5-7. (a) Moisture test result of carbon moisture sensor (liquid applied on the top side), (b) Moisture test result of carbon moisture sensor (liquid applied on the centre of the sensor design)

Above characteristics were common to both the carbon and graphene-based sensors. From **Figure 5-6**, it can be seen, for all the moisture sensors, by considering the resistance value, the general location of the introduction of the liquid droplets are identifiable. While the liquid evaporation stage was similar for silver and carbon, for graphene the evaporation stage shows more stable behaviour.

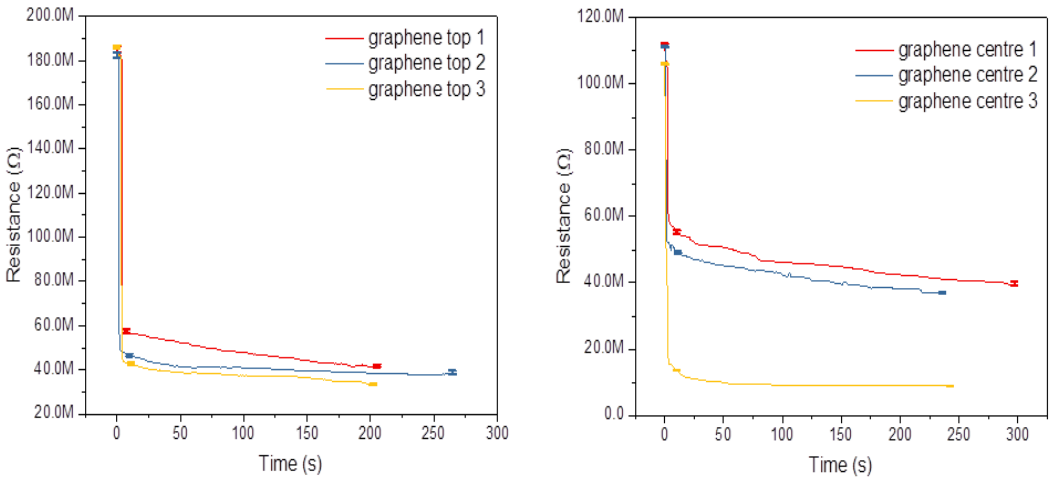

Figure 5-8. (a) Moisture test result of graphene moisture sensor (liquid applied on the top of the sensor design), (b) Moisture test result of carbon moisture sensor (liquid applied on the centre of the sensor design)

Figures 5-6 to 5-8 show that the highest change in resistance of the moisture sensor is about 89.3%, 82.5% and 92% for silver, carbon and graphene moisture sensor respectively. It is possible that this behaviour might be due to the differences between the mechanical properties of the three yarns. The silver and graphene yarns used in this research were coated on polyester and cotton respectively, which have a relatively better liquid-absorption tendency than carbon fibre twisted yarn. Higher liquid-absorption will lead to faster liquid spreading speed and larger spreading area. However the higher sensitivity of the graphene yarn still produces a bigger change in the electrical resistance on the introduction of moisture making the graphene based embroidered sensors to be the easiest to recognise presence of moisture. Compared to **Figure 5-6 and 5-7**, this embroidered moisture sensor achieves a better result when more liquid drops were applied, similar to in an environment of higher humidity.

5.4 Conclusion

During this research, it was found that embroidered resistance type moisture sensors are capable of responding to moisture absorption at very high speeds. The moisture sensors that were embroidered using carbon, silver and graphene sewing yarn showed that all of them are capable of identifying moisture absorption and evaporation. Out of the three sensor types, graphene sewing yarn showed relatively better performance, especially during the moisture absorption stage with quicker response compared to the other two sensor types. The carbon sewing yarn used in this research is a carbon fibre twisted yarn which can not absorb and pass liquid easily like metallic or graphene

coated polyester or cotton yarn. After the liquid drops were applied on the sensors, the resistance of the carbon moisture sensor decreased slower compared to silver and graphene moisture sensors. The results show that the sensors are capable of identifying the location of moisture introduction and also has a different response based on the moisture pressure. The results show that these moisture sensors have applications in areas such as measuring the sweat level of human body, monitoring incontinence in a baby or adult diaper and the moisture of humidity in the environment.

5.5 Summary

Wearable sensors have had a rapid development in the recent times and became an advanced and attractive field of smart sensors and electronic textile technologies. There is a huge demand for developing smart sensors in biological sensing areas, such as long-term health monitoring, physical training, and wound moisture monitoring. Therefore to create comfortable and convenient to wear advanced sensors, electronic textiles have been investigated.

The incorporation of the smart sensors over textiles can be realised by different techniques, such as knitting, weaving, metal coating, stamp transfer, screen printing, embroidery, and electrospinning. Embroidery has been revealed as one of the most effective fabrication methods when incorporating the conductive yarns with the substrate. The repeatability of embroidery patterns, cost estimation, and complexity of the manufacturing process have been presented.

This paper presents research focused on embroidered moisture sensor elements for smart textile applications in incontinence detection, or thermal comfort monitoring use include durability, response speed, non-toxicity and the comfort aspect of clothing. In this work, two specially prepared conductive yarns are used to integrate into woven cotton fabrics with an effective and accurate textile technique – embroidery, to characterize two moisture sensor geometries.

5.6 References

[1] X. Tao, *Wearable electronics and photonics*. 2005,pp.177-197.

[2] F. Chiarugi *et al.*, "Measurement of heart rate and respiratory rate using a textile-based wearable device in heart failure patients," in *Computers in Cardiology*, 2008, vol. 35, pp. 901–904.

[3] M. Peltokangas, J. Verho, and A. Vehkaoja, "Night-time EKG and HRV monitoring with bed sheet integrated textile electrodes," *IEEE Trans. Inf. Technol. Biomed.*, vol. 16, no. 5, pp. 935–942, 2012.

[4] M. Sibinski, M. Jakubowska, and M. Sloma, "Flexible temperature sensors on fibers," *Sensors*, vol. 10, no. 9, pp. 7934–7946, 2010.

[5] J. Meyer, "Textile pressure sensor: Design, error modeling and evaluation," *Ph.D. Diss.*, pp. 1–120, 2008.

[6] P. Salvo, F. Di Francesco, D. Costanzo, C. Ferrari, M. G. Trivella, and D. De Rossi, "A wearable sensor for measuring sweat rate," *IEEE Sens. J.*, vol. 10, no. 10, pp. 1557–1558, 2010.

[7] V. Candas, J. P. Libert, G. Brandenberger, J. C. Sagot, C. Amoros, and J. M. Kahn, "Hydration during exercise - Effects on thermal and cardiovascular adjustments," *Eur. J. Appl. Physiol. Occup. Physiol.*, vol. 55, no. 2, pp. 113–122, 1986.

[8] R. J. Maughan, S. M. Shirreffs, and J. B. Leiper, "Errors in the estimation of hydration status from changes in body mass," *J. Sports Sci.*, vol. 25, no. 7, pp. 797–804, 2007.

[9] I. Parkova, A. Valisevskis, and A. Vilumsone, "Test of Moisture Sensor Activation Speed," *Int. J. Electr. Comput. Electron. Commun. Eng.*, vol. 8, no. 4, pp. 656–660, 2014.

[10] R. B. Katragadda and Y. Xu, "A novel intelligent textile technology based on silicon flexible skins," in *Proceedings of the IEEE International Conference on Micro Electro Mechanical Systems (MEMS)*, 2007, pp. 301–304.

[11] G. López, V. Custodio, and J. I. Moreno, “LOBIN: E-textile and wireless-sensor-network-based platform for healthcare monitoring in future hospital environments,” *IEEE Trans. Inf. Technol. Biomed.*, vol. 14, no. 6, pp. 1446–1458, 2010.

[12] C. Kutzner, R. Lucklum, R. Torah, S. Beeby, and J. Tudor, “Novel screen printed humidity sensor on textiles for smart textile applications,” in *2013 Transducers and Eurosensors XXVII: The 17th International Conference on Solid-State Sensors, Actuators and Microsystems, TRANSDUCERS and EUROSENSORS 2013*, 2013, pp. 282–285.

[13] P. Bosowski, M. Hoerr, V. Mecnika, T. Gries, and S. Jockenhövel, “Design and manufacture of textile-based sensors,” in *Electronic Textiles: Smart Fabrics and Wearable Technology*, 2015, pp. 75–107.

[14] T. Mac, S. Houis, and T. Gries, “Metal fibers,” *Tech. Text.*, vol. 47, pp. 17–32, 2004.

[15] M. D. Husain, R. Kennon, and T. Dias, “Design and fabrication of Temperature Sensing Fabric,” *J. Ind. Text.*, vol. 44, no. 3, pp. 398–417, 2014.

[16] J. Avloni, R. Lau, M. Ouyang, L. Florio, A. R. Henn, and A. Sparavigna, “Polypyrrole-coated nonwovens for electromagnetic shielding,” *J. Ind. Text.*, vol. 38, no. 1, pp. 55–68, 2008.

[17] A. Swaminathan, “Electrical Characterization of a Textile Sensor for Moisture Detection,” University of Borås, pp.201.

Chapter 6 – Investigation of a graphene based flexible embroidered temperature sensor

6.1 Introduction

Smart textiles and specifically textile sensors draw a high level of attention and have become a hot topic over the last few years. Especially, development of wearable sensing technologies to monitor various measurable health indicators of human beings' such as body temperature [1], external pressure on the body [2], and heart rate [3-4], are priorities in the field of smart textiles. Body temperature is an important and basic physiological parameter which can directly reflect health conditions [5-7], provide early warning on possible infections or ailments [8-9]. Nowadays, rigid sensors or externally mountable printed sensors are the main types of temperature sensors used in the medical field. Due to their stable properties and high degree of accuracy, solid sensors are generally more popular in the medical markets. However, the main disadvantages of rigid and externally mounted printed sensors are their relative inflexibility and poor comfort in comparison to textile-based sensors. Additionally, these types of sensors are most suitable for only one-point measurement and are associated with poor washability [10]. To solve these problems, much research is being conducted in the wearable sensing research fields especially for the last five years.

Many authors have investigated different types of technologies for manufacturing textile-based temperature sensors. Several of them have concentrated on thin metal films [11-14] which are manufactured by using metal particles such as nickel, gold or silver on polyamide or polydimethylsiloxane substrates, which show high accuracy, fast response speed and excellent signal resolution. While polymeric yarn used for textile manufacturing requires a certain degree of flexibility, generally metal thin films

that are coated on them are not suitable for long-term contact with the human body and also most of them are not flexible. Temperature sensing fabrics (TSF) that are widely used [15-16], are usually made by inserting a conductive metallic yarn into a knitted structure. It shows a highly flexible, linear relationship between temperature and resistance, and can be used in high humidity environments with a small temperature error (± 0.15°C). Polanský et al. used embroidery to manufacture their temperature sensors, three different designs were described in their research paper [17]. The embroidered temperature sensors show a linear dependence between the electrical resistance and temperature and good long-term stability. They also found that compared to other types of textile temperature sensors, embroidered temperature sensors can achieve a large area measurement, and the embroidered sensors do not need additional encapsulation which will lead to a fast response speed to sudden changes in the temperature. Besides the large measuring area, the embroidered sensors can be easily combined with existing garment or other textile manufacturing processes.

Embroidery is a textile-finishing method that can be used to apply a given yarn material to a textile substrate in a defined geometry [18]. When compared to other textile production technologies, embroidery technique is a convenient alternative because it is a low labour-intensive method utilising a design and production process. It also allows CAD based sensor geometry design and multilayer accurate construction. The manufacturing process of embroidered sensors can be described as using fine metallic wires, electroconductive coated or other conductive yarns attached to the fabrics by stitching techniques to form designed electrical circuits or other designed shapes. Conductive yarn and yarn embroidery can be accomplished on single or multiple layers of fabric or can be applied to various types of textile and apparel products in one step. The advantage of embroidery is that just one manufacturing process will be used when combining the conductive tracks with the supporting electronics in complex and essential geometry [19]. Furthermore, embroidery is convenient to create electronic

devices, since the conductive paths and electronic devices are connected within the same manufacturing process. Embroidery offers advantages over knitting or weaving, embroidery technique presents a relatively more effective process to implement wearable electronics and are suitable for different materials (metal yarn, elastomeric yarn) and can be designed as different geometries. Not like the other textile techniques, embroidered designs can be directly made on ready-to-wear clothes and the sensor area can be easily covered by the other embroidered decoration patterns to improve its artistic and commercial properties, the decorative embroidered patterns can also protect the embroidered sensor from abrasion.

Graphene is the thinnest and strongest materials with an excellent thermal electrical property which made it an ideal material for temperature sensor or heating element construction. The high thermal conductivity made it can sense the changes in temperature and response to it by variation of the electrical resistance.

The working principle of a temperature sensor is based on the resistance of the conductive yarn varies due to the changes in its temperature. The equation (6-1) below showing the relationship between the resistance of the conductive yarn:

$$R_{ref} = \frac{4l\rho_{ref}}{\pi d^2} \quad (6\text{-}1)$$

Where,

R_{ref} is the resistance of the conductive yarn at the reference temperature

P_{ref} is the resistivity of the conductive yarn at the reference temperature

l is the length of the conductive yarn, and

d is the diameter of the conductive yarn

The equation (6-2) below stated the relationship between temperature and the resistance of the conductors:

$$R = R_{ref}[1 + \alpha(T - T_{ref}) \quad (6\text{-}2)$$

where,

R= conductor resistance at temperature "T",

R_{ref}= conductor resistance at reference temperature T_{ref},

α = Temperature coefficient of resistance for conductor material.

6.2 Modelling

In order to understand the electromechanical behaviour of the embroidered stitch lines a line of embroidered stitches was modelled using known electrical theory. In an embroidered stitch line, the binding of the top sewing yarn and the bottom sewing yarn is carried out in the thickness of the fabric. Therefore, in order to carry out binding of the top and the bottom yarns, the stitch line rather than being straight needs to start from the first quadrant of the needle hole to the third quadrant of the next needle hole. As shown in **Figure 6-1**, the centre of the binding loop in the thickness of the fabric, in the upper yarn plane is denoted 'O', the starting point of the upper yarn in the first quadrant of the needle hole and the centre of the upper stitch are 'A' and 'B' respectively. As shown in **Figure 6-2**, for a full stitch, these points are defined by C, D, O, A and B.

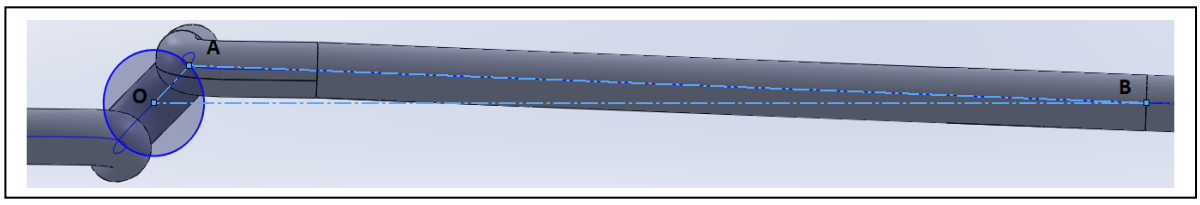

Figure 6-1. Half of the embroidery stitch on top surface

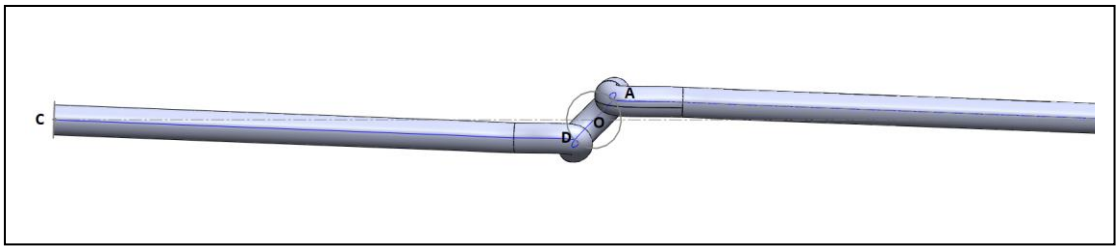

Figure 6-2. Single embroidery stitch on top surface

Embroidery sewing yarn parameters are defined as follows.

$n = number\ of\ stitches$

$l_{st} = length\ between\ two\ needle\ punches$

$r = needle\ hole\ radius$

$d = thread\ diameter$

$t = fabric\ thickness$

In order for the sewing yarn, embroidery fabric and the needle to be compatible and for the sewing yarn to bend without kinking, it requires:

$$t \geq 2d \quad ----------(6-2)$$

$$r \geq 4d \quad ----------(6-3)$$

If O is the origin

$$\text{angle AOB} = \theta \quad ----------(6-4)$$

Coordinates of point A

$$A \equiv (x_A, y_A) \quad ----------(6-5)$$

$$x_A = rsin(\theta) \quad ----------(6-6)$$

θ can be set at different values. In the present case, it can be approximated to a very small angle of;

$$Sin(\theta) = \frac{d}{4r} \quad ----------(6-7)$$

Then the path function for the straight length of the embroidered stich can be given as;

$$y = \frac{-2rsin\theta}{(l_{st} - 2rcos\theta)}x + \frac{l_{st}rsin\theta}{(l_{st} - 2rcos\theta)} \quad ----------(6-8)$$

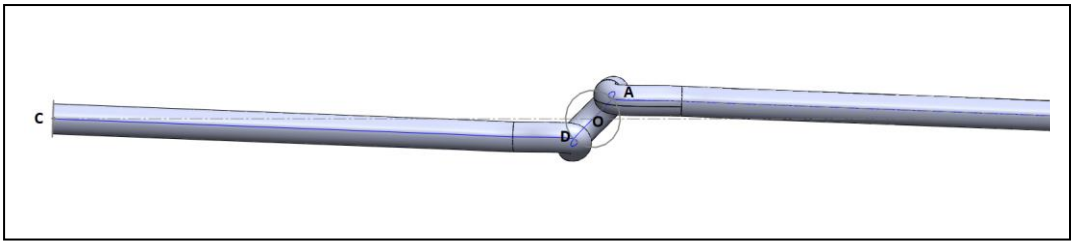

Figure 6-3. Top view of top and bottom embroidery yarns

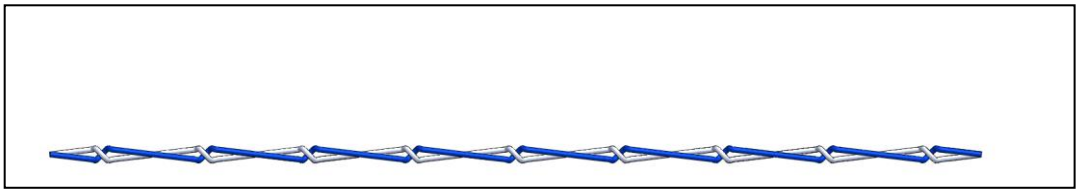

Figure 6-4. Front elevation view of top and bottom embroidery yarns

The upper sewing yarn path is defined by the spline curve through the coordinates C_u, D_u, O_u, A_u and B_u, which constitutes the total upper embroidery yarn length per stitch;

$$C_u \equiv \left[0,0,\left(\frac{t+d}{2}\right)\right] - (6-9)$$

$$D_u \equiv \left[\left(\frac{l_{st}}{2} - rcos\theta\right), -rsin\theta, \left(\frac{t+d}{2}\right)\right] - - - - - - - - - - (6-10)$$

$$O_u \equiv \left[\frac{l_{st}}{2}, 0, -\frac{d}{2}\right] - (6-11)$$

$$A_u \equiv \left[\left(\frac{l_{st}}{2} + rcos\theta\right), rsin\theta, \left(\frac{t+d}{2}\right)\right] - - - - - - - - - - (6-12)$$

$$B_u \equiv \left[l_{st}, 0, \left(\frac{t+d}{2}\right)\right] - (6-13)$$

Similarly, the lower sewing yarn path is defined by the spline curve through the coordinates *C, D, O, A and B*;

$$C \equiv \left[0,0,-\left(\frac{t+d}{2}\right)\right] - (6-14)$$

$$D \equiv \left[\left(\frac{l_{st}}{2} - rcos\theta\right), rsin\theta, -\left(\frac{t+d}{2}\right)\right] - - - - - - - - - - (6-15)$$

$$\mathrm{O} \equiv \left[\frac{l_{st}}{2}, 0, \frac{d}{2}\right] - (6-16)$$

$$\mathrm{A} \equiv \left[\left(\frac{l_{st}}{2} + rcos\theta\right), -rsin\theta, -\left(\frac{t+d}{2}\right)\right] - - - - - - - - - - (6-17)$$

$$B \equiv \left[l_{st}, 0, -\left(\frac{t+d}{2}\right)\right] - (6-18)$$

$\theta = \frac{\pi}{2}$ and considering the triangle CDO

$$Length\ CD = \frac{\frac{r}{\sqrt{2}}}{sin\left[tan - \left(\frac{r\sqrt{2}}{l_{st} - r\sqrt{2}}\right)\right]}$$

Therefore, top surface visible yarn length per stitch = stitch length =

$$\frac{\frac{r}{\sqrt{2}}}{sin\left[tan - \left(\frac{r\sqrt{2}}{l_{st} - r\sqrt{2}}\right)\right]} - - - - - - - - - - - - - - - - - - - (6-19)$$

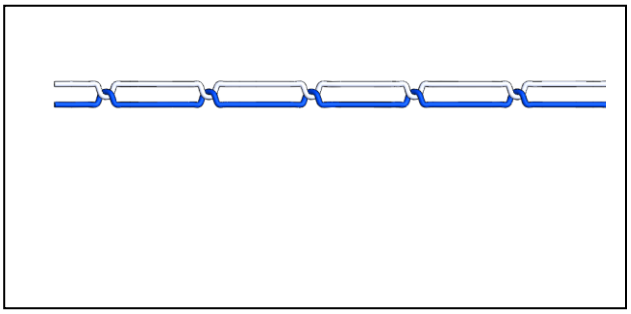

Figure 6-5. Loop length of the top and bottom yarns in the fabric

$$\text{Loop length within the fabric} = t + 2d + r(\pi - 2) - - - - - - - - - - (6-20)$$

Equations (6-19) and (6-20) provides the embroidery stitch length and the loop length within the fabric thickness which is used to determine the electrical resistance in the embroidery stitch and the hidden loop length.

Therefore;

For a single stitch, the original $R_{0,stitch}$ resistance is given by;

$$R_{0,stitch} = \rho\left[\frac{r\sqrt{2}}{sin\left[tan - \left(\frac{r\sqrt{2}}{l_{st} - r\sqrt{2}}\right)\right]}\right] + \frac{\rho_m}{2}\left(\frac{\pi p_f}{w}\right)^{\frac{1}{2}} - - - - - - - - - - (6-21)$$

Where, $\frac{\rho_m}{2}\left(\frac{\pi p_f}{w}\right)^{\frac{1}{2}}$ is the electrical resistance explained by Holm's electrical contact resistance theory [23]. This component can be approximately determined through an experimental data set between the transverse compressive force and the resulting

electrical resistance when an electroconductive sewing yarn is compressed.

In considering the heating effect in the loop length within the fabric, stitch length in the above equation would be replaced by the loop length within the fabric.

For a line of embroidery stitches with *n* stitches, the original series resistance is given by*;*

$$R_0 = n\left[\left[\frac{\rho r\sqrt{2}}{sin\left[tan - \left(\frac{r\sqrt{2}}{l_{st} - r\sqrt{2}}\right)\right]}\right] + \frac{\rho_m}{2}\left(\frac{\pi p_f}{w}\right)^{\frac{1}{2}}\right] - - - - - - - - - - (6-22)$$

Where ρ is the electrical resistivity in ohms per unit length while ρ_m represents the volume resistivity of the material.

For parallel construction with N lines, *the original resistance is given by;*

$$R_0 = \frac{n}{N}\left[\left[\frac{\rho r\sqrt{2}}{sin(\,tan^{-}\left(\frac{r\sqrt{2}}{l_{st} - r\sqrt{2}}\right))}\right] + \frac{\rho_m}{2}\left(\frac{\pi p_f}{W}\right)^{\frac{1}{2}}\right] - - - - - - - - - - - -(6-23)$$

When the fabric carrying the embroidered lines are under tensile forces, due to the elongation of the material, which could be plastic and elastic elongation, the material would experience a change in resistance. Generally, for multi filament short fibre yarn, the displacement of fibres would be a permanent plastic condition, which is unrecoverable. This would cause a permanent electromechanical change in the yarn. However, when the embroidery is carried out on a woven fabric, the degree of forces a wearable sensor or a heating embroidery lines would experience would be small tensile or compressive loads. The bending strain would be high due to draping. However, this again would not cause permanent deformation in the fabric structure. Therefore, it could be considered that during normal use of these wearable sensors and actuators, the

embroidered yarn would be functioning within elastic limits with very small plastic deformation.

When the electroconductive sewing yarn (under yarn) and the top sewing yarn are at high contact stresses, there would be constrictive transverse forces on the electroconductive thin films on the sewing yarn. The resulting hardness in the contact is represented by the parameter ρ_f in the above equation. The Contact force is represented by the parameter W.

During the tensile, compressive and bending strains the fabric would experience, the changes in the contact force would cause fluctuations in the sewing yarn electrical resistance.

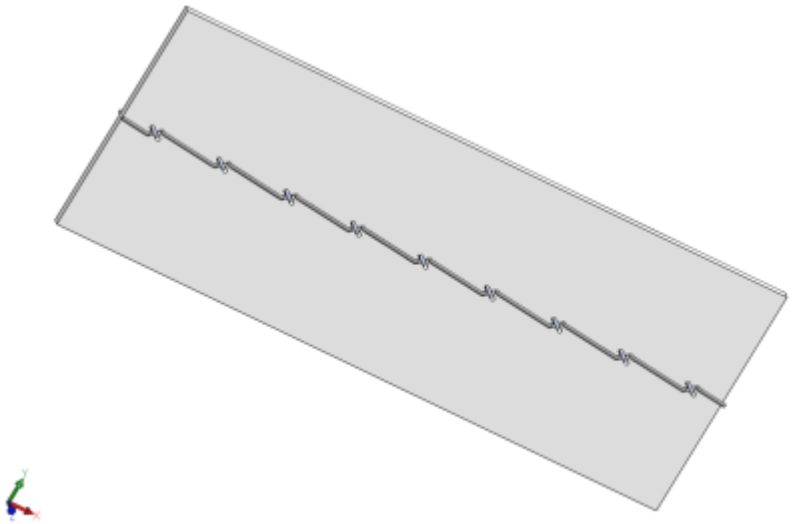

Figure 6-6. Series construction of embroidered stitches

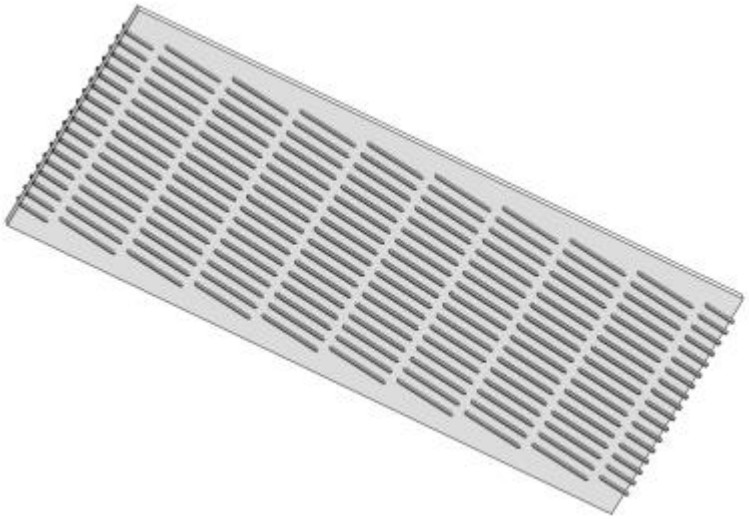

Figure 6-7. Parallel construction of a series of embroidered stitches

Under transverse compressive forces, the resulting original electrical resistance for a series of sewing stitches (**Figure 6-6**) in a line can be given by;

$$R_0 = n\frac{\rho_m}{2}\left(\frac{\pi p_f}{W}\right)^{\frac{1}{2}} + n\left[\frac{\rho r\sqrt{2}}{sin(\,tan^{-}\left(\frac{r\sqrt{2}}{l_{st}-r\sqrt{2}}\right))}\right] - - - - - - - - - - - - (6-24)$$

For a parallel construction of series of embroidery lines, having N parallel embroidered electro conductive lines, the original embroidery parallel construction equivalent electrical resistance could be given using the equation below;

$$R_0 = \frac{n}{N}\left[\frac{\rho_m}{2}\left(\frac{\pi p_f}{W}\right)^{\frac{1}{2}} + n\left[\frac{\rho r\sqrt{2}}{sin(\,tan^{-}\left(\frac{r\sqrt{2}}{l_{st}-r\sqrt{2}}\right))}\right]\right] - - - - - - - - - - - - (6-25)$$

Figure 6-8 shows the experimental results for graphene, silver and carbon sewing yarn.

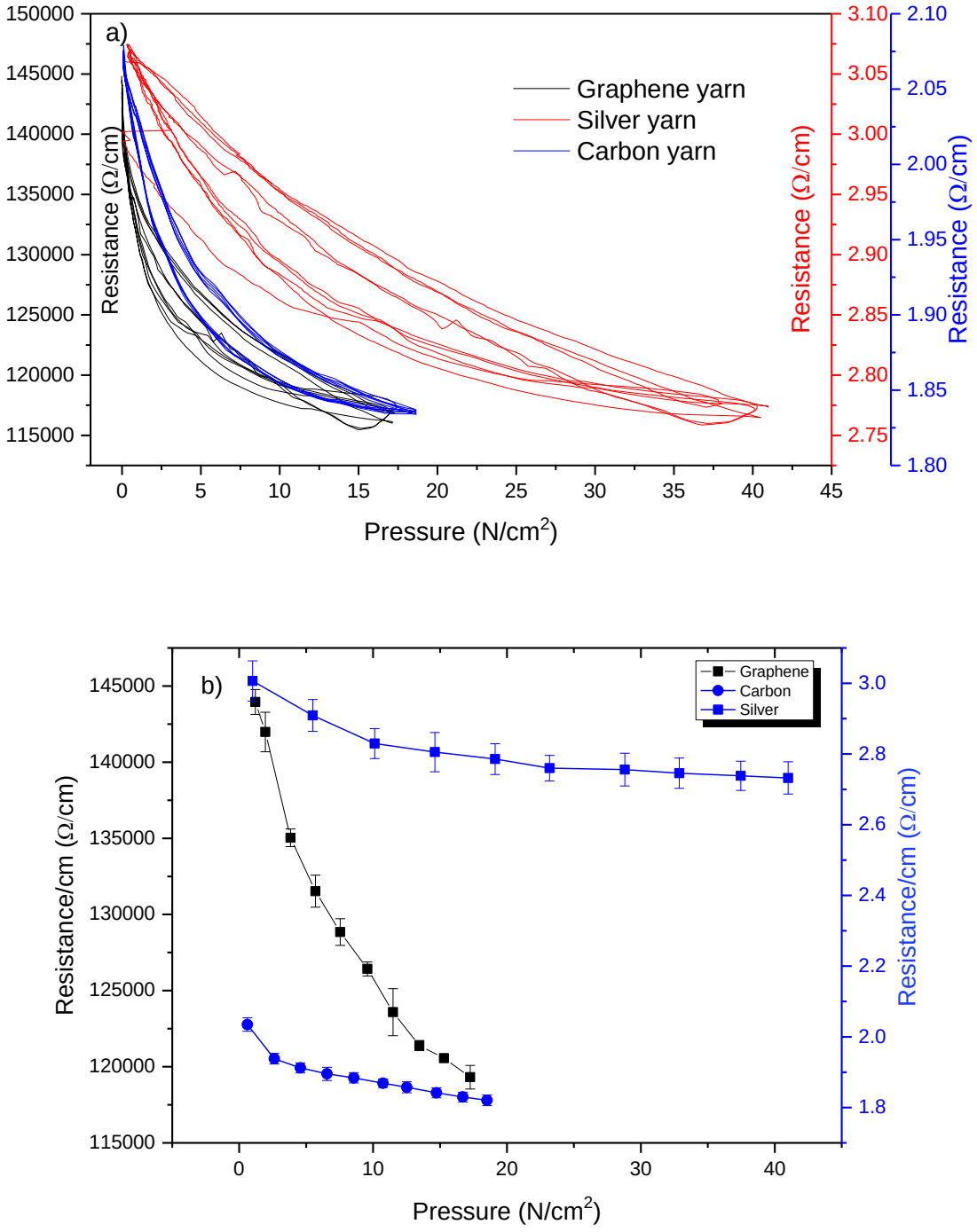

Figure 6-8. (a) Cyclic electrical resistance vs pressure curves for graphene, silver and carbon sewing yarn, (b) Final unloading curve electrical resistance vs pressure for graphene, silver and carbon sewing yarn

Figure 6-8 (a) and **(b)** show the electrical resistance and pressure relationship for graphene, silver and carbon sewing yarn. As it can be seen the relationship is inversely proportional which qualitatively verifies the equations (6-24) and (6-25).

When using embroidery stitches for temperature sensors, the stitch lines are generally not subjected to either tensile or compressive loading. Therefore, in designing the temperature sensors the electrical resistance of the embroidered temperature sensor depends on the electrical resistance of the yarn in the stitches and the electrical resistance of the yarn in the top and bottom binding yarn. However, since the yarn in the binding area is held within the hole made in the fabric by the needle, this yarn is held under tension with top and bottom yarn applying compressive forces against each other. The major consideration for determining the electrical resistance of the electroconductive yarn in this case is the compressive force between the top and bottom yarn. Therefore, experiments were carried out to determine the contribution of the yarn to yarn compressive force to total electrical resistance of the embroidered temperature sensor.

Therefore **Figure 6-8 (a)** and **(b)** shows the increase in the linear electrical resistance of the electroconductive yarn when it is compressed in the thickness direction. To this end, **figure 6-8 (a)** shows the cyclic hysteresis loop for electrical resistance vs. compressive force graph. The figure shows that compared to carbon and silver yarn, graphene coated cotton yarn has a higher change in relative electrical resistance. Also compared to silver and carbon yarn, graphene yarn has a much finer hysteresis loop area signifying that the reliability of the graphene yarn is much higher in transverse compression. This shows that the contribution to the electrical resistance in the embroidery design by the yarn to yarn compressive forces may be much higher than the linear resistance of the yarn in the stitches on the surface of the fabric. **Figure 6-8 (b)** shows that considering the final unloading curve of the cyclic test results, the slope of

the graphene yarn is much steeper and more suitable for the embroidered temperature sensors.

When an electrical current is sent through an embroidered electroconductive line of stitches, the resulting heating effect is given by the following equation (6-26);
Assuming 100% energy conversion to heat, the electrical heating due to the voltage V can be represented by the following equation*;*

$$\frac{V^2}{R_0[1+\alpha(T_t-T_0)]}\Delta t = mc_v(T_t-T_0) - - - - - - - - - - - - - - - (6-26)$$

Where,

Δ t is a small change in time (time increment)

m = mass of the electrically heating material

c_v= heat capacity of electrically heating material

6.3 Methodology

6.3.1 Materials

Silver sewing yarn (silverpam 250) as the standard yarn with high conductivity was used in this paper. However, due to the oxidisation of the silver, the resistance of the yarn is not stable. To avoid the disadvantages in using the silver sewing yarn for manufacturing embroidered sensors, carbon sewing yarn (Carbon Tenax, Tibtech) and graphene coated sewing yarn (from the National Graphene Institute, University of Manchester) were used. Carbon sewing yarn is usually stable and has a relatively lower price while graphene coated sewing yarn has opened up a wide range of flexible electronics applications due to its outstanding electrical, mechanical, membrane and

other performance properties.

Due to the fact that the mechanical properties of an embroidered pattern mainly depend on the yarn and substrate fabric, elastomeric silver sewing yarn (Silverpam 250, Tibtech) was used in this paper. Silverpam 250 is a grafted antibacterial yarn based on 99% pure silver alloy grafted on a polyamide-based material with a linear electrical resistivity of 198 ohms/m and linear density of 250 dtex.

Carbon fibre is a multifuctional material, with unlimited range of applications, such as golf club shafts, car parts an aircraft wings. Due to those applications, carbon fibre has becomes more and more applications in our daily lives in recent times. Carbon Tenax is a high-tech material with high strength, efficency and durability. Carbon Tenax used in this paper is a twisted sewing yarn with a resistivity which can reach up to 218 ohms per meter. It is a "Z" twist yarn with a break elongation of 1.5%.

An embroidered sensor consists of conductive sewing yarn (in the present case the lower yarn), nonconductive sewing yarn (upper yarn), substrate fabric and the backing material. For the research reported in this paper, water soluble backing material was used for embroidery due to convenience in removal. Also investigations have shown that water soluble backing materials cause relatively low changes in resistance before and after the removal of the backing material compared to other backing materials. Also, non-elastic nonwoven fabrics were used as the substrate fabric for the sensor construction.

6.3.2 Device design and fabrication

The pattern of temperature sensors and the machine instructions were created using computer software (PE-Design). A Brother IS-V5 embroidered machine was used to manufacture the sensor patterns. As seen in equation 6-1 and 6-2, the working

performance of the temperature sensor is mainly based on the electrical properties which are determined by the type of electroconductive material of the sewing yarn. Three different embroidered temperature sensor designs were manufactured to find the one with the most suitable mechanical properties, sensor area and stitch density for the temperature sensor being designed. For the final application, these designs should show good flexibility and relatively smaller changes in resistance during tensile or bending tests.

6.3.3 Temperature sensing

In order to characterise the embroidered temperature sensors, they were placed on a heated oven which can provide heat and control the inner temperature. The Zwick-Roell computerised tensile testing machine was used to test the mechanical properties of the temperature sensor. A NI-9219 data acquisition card was used to measure the changes in resistance during the test.

6.4 Result and Discussion

Figures 6-9a - c are the three sketches of the temperature sensors that were embroidered using silver coated sewing yarn (Silverpam 250, Tibtech), carbon sewing yarn (Carbon Tenax, Tibtech) and the graphene coated sewing yarn where they were used as the bottom yarn. The upper yarn is usually a nonconductive yarn to prevent the conductive particles from the friction between the upper yarn and the needle hole. After the design process, the substrate fabric and the backing material (which is used to increase the stiffness of the substrate fabric) were fixed by a frame, and once the frame has been placed under the needle, the embroidered piezoresistive sensor can be manufactured using the embroidery machine.

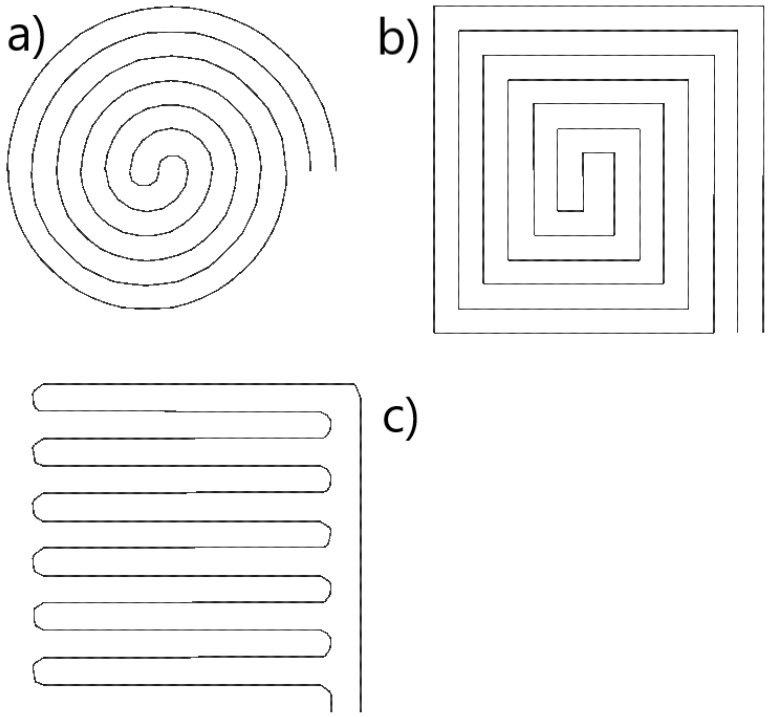

Figure 6-9. Sketches of embroidered temperature sensor. Sensing area 40*40 mm

As stated before, the electrical properties of the embroidered sensor are mainly dependent on the stress strain experienced by the conductive sewing yarn. Embroidery sensor designs A, B and C were designed, using the optimum stitch length determined in the previous chapter, that is 5 mm, to find out the design with the most suitable mechanical behaviour for the best performing temperature sensors and the heat patches. Because the temperature sensor made in this paper is used to monitor the body temperature, the embroidered sensors are designed to be directly embroidered on a close-fitting garment that would present good flexibility and relatively smaller changes in resistance during tensile or bending test. The bending rigidity of the embroidered sensor is a key factor for the sensor performance since lower bending rigidity will lead to less changes in electrical resistance of the sensor due to body movement. Hence, a FAST test for bending rigidity is an essential test for these embroidered designs. **Table 6** describes the bending characteristics of the three designs.

Table 6. The results of bending rigidity test of the three designs

Embroidered designs	Average bending length (mm)	Average bending rigidity (uN.m)
Design A	**17.5**	**0.077**
Design B	**20**	**0.11615**
Design C	**25**	**0.2187**

As seen in table 6, design A shows the lowest bending rigidity while design C is the highest stiffness out of the three designs. This means design C would not be the most suitable embroidered sensor design for a wearable sensor garment compared to design A. However, design B still presents higher flexibility and certainly has the suitable rigidity to prevent the changes in resistance due to bending.

Besides the bending rigidity test, tensile tests were also carried out to test the mechanical behaviour of the three designs. The three embroidered sensors were stretched on both horizontal and vertical directions; meanwhile the changes in resistance (ΔR/Ro) were recorded by using the NI data acquisition card. **Table 7** shows the results of ΔR/Ro when the fabric sensors were under extension on a tensile tester.

Table 7. The results of tensile tests of the three embroidered designs

$\frac{\Delta R}{R_0}$		Designs		
		A	**B**	**C**
Direction	**Vertical**	**3.34625**	**2.77823**	**4.51721**
	Horizontal	**2.52234**	**2.94117**	**3.76293**

In **Table 7**, it can be seen that embroidery design B has relatively lower changes in

resistance during the tensile test on both side ($\Delta R/R_0$ is 2.778% in vertical direction and 2.941% in the horizontal direction). Considering both the bending rigidity and tensile test results, design B was selected as the optimum for further experiments due to its relatively higher flexibility and lower deviation in resistance due to mechanical deformation. **Figure 6-10** shows the tensile cyclic test results of the design B. As it can be seen, the temperature sensor made using design C has excellent mechanical properties, good recovery, a small hysteresis loop and a stable electromechanical response over time.

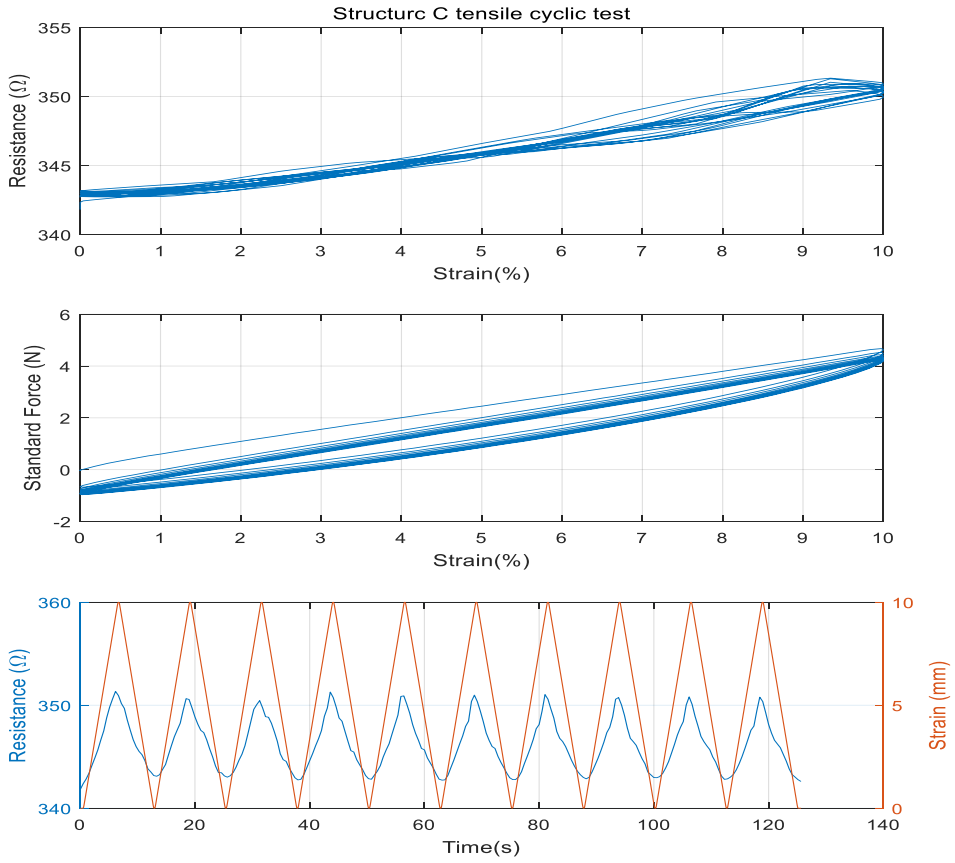

Figure 6-10. Tensile cyclic results of the design B

In order to observe the effect of an increase in the sensing area of the temperature sensor, the size of design B was increased from 40 mm to 60 mm in diameter, namely 2827 mm^2 sensing area (**Figure 6-11** is the updated design B).

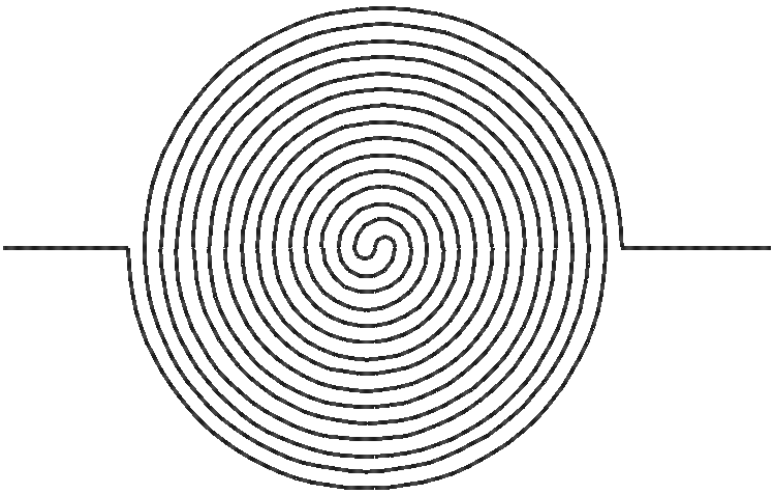

Figure 6-11. Updated temperature sensor design with 2827 mm2 sensing area.

The main working principle of the temperature sensor is the electrical resistance of the conductive yarn that will vary in relation to temperature changes experienced by the embroidered design. In order to characterise the embroidered temperature sensors, they were placed in a heated oven where the temperature was varied under control. In a comfortable environment, the temperature of the skin surface of a healthy adult is generally expected to vary between 36.5 and 37.5 °C [22]. In order to cover this range, the performance of the embroidered temperature sensor was tested between 25 and 45 °C, inside the oven shown in **Figure 6-12**.

Figure 6-12. Heat oven

Figure 6-13 to 6-15 illustrate the relationship between the resistance of the temperature sensors and the heated oven inner temperature from 25 to 45 °C.

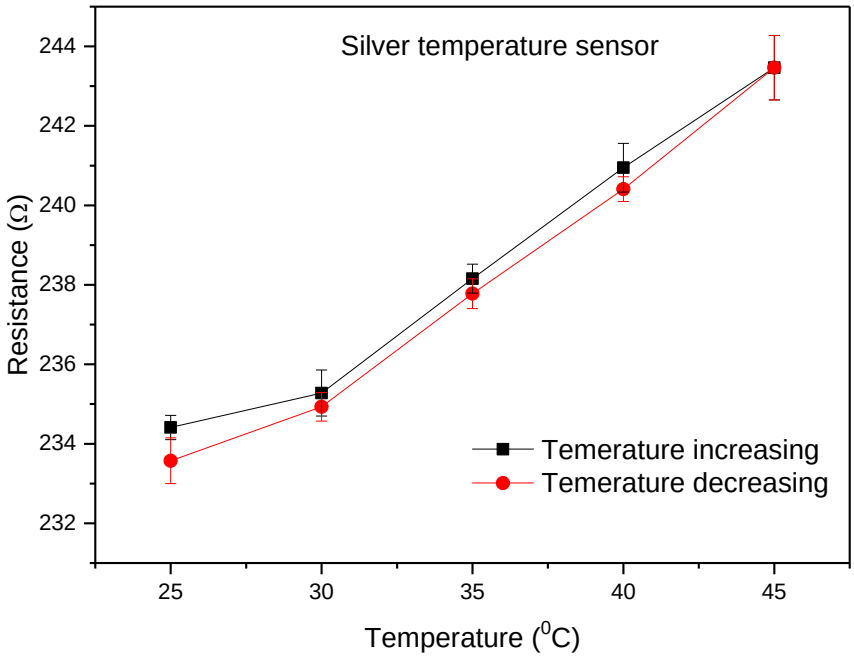

Figure 6-13. Relationship between temperature and resistance of the silver temperature sensor

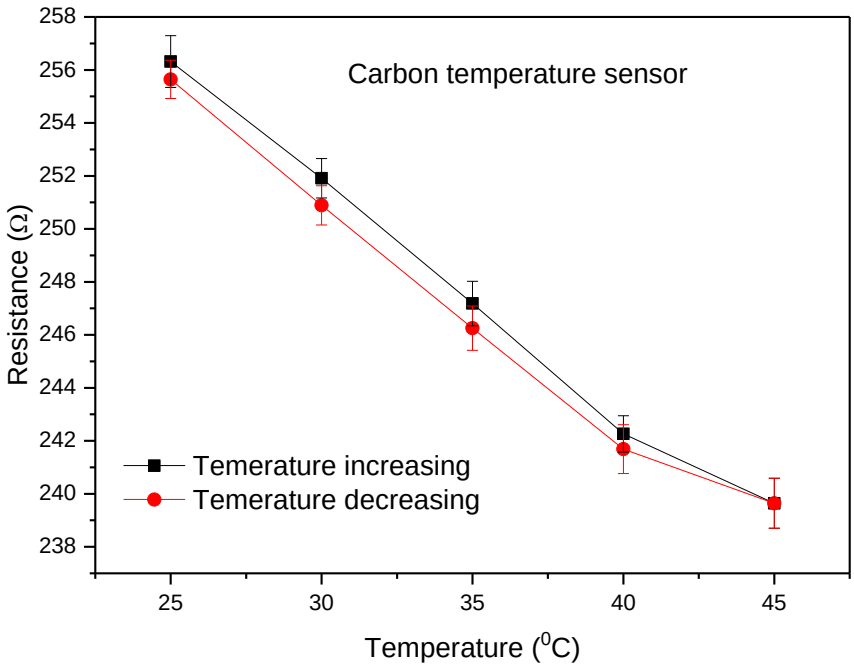

Figure 6-14. Relationship between temperature and resistance of carbon temperature sensor

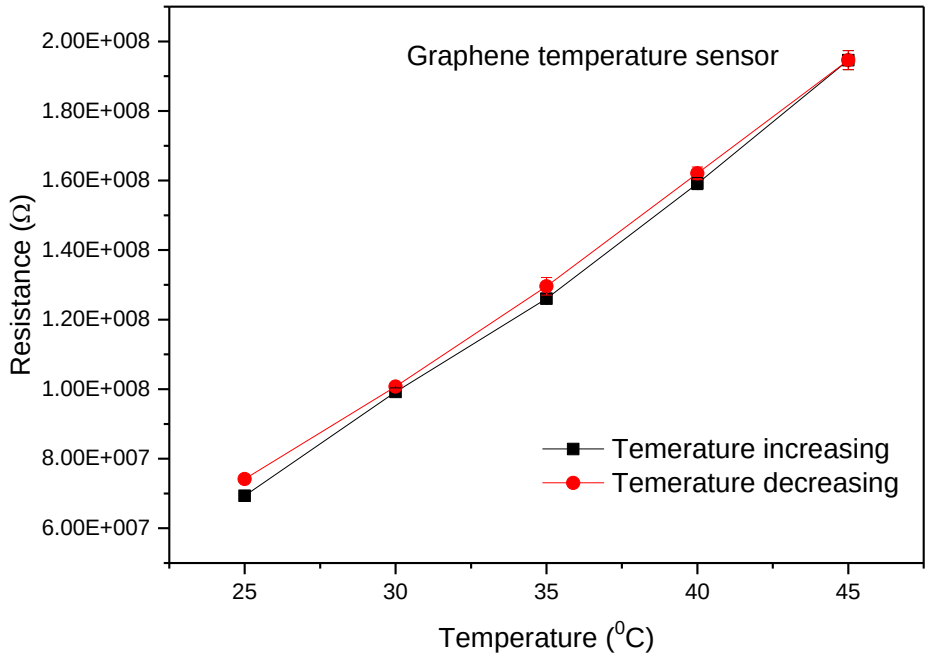

Figure 6-15. relationship between temperature and resistance of graphene temperature sensor

As can be seen from the figures, the temperature gradient of the silver embroidered design is the lowest while the embroidered carbon yarn design shows a temperature gradient approximately twice that of silver temperature sensors. However, the electrical resistance vs. temperature graph of graphene temperature sensors shows a linear relationship with a very high temperature gradient between resistance and temperature at the range of 25 to 45℃. Again, it is noteworthy to show that while silver and graphene temperature sensors show a positive linear relationship between electrical resistance and temperature, carbon embroidered sensor shows a negative linear relationship. In all three sensor materials, the resistance of all the temperature sensors shows a negligible hysteresis during temperature increasing and decreasing.

The stability test is carried out to observe the performance of the temperature sensor

against a stable temperature. The results of the temperature stability test are plotted in **Figures 6-16 to 6-18**, and all of the three temperature sensors show good stability when under stable temperature. After the stability test, the heated oven was turned off and the electrical resistance vs. temperature curve can be seen to drop back to the room temperature. During the cooling process, the electrical resistance of all the three temperature sensors has a linear relationship with temperature, and the heating and cooling gradients of graphene temperature sensor are higher than that of carbon and silver temperature sensors which means the graphene temperature sensor is more suitable for fast temperature responses.

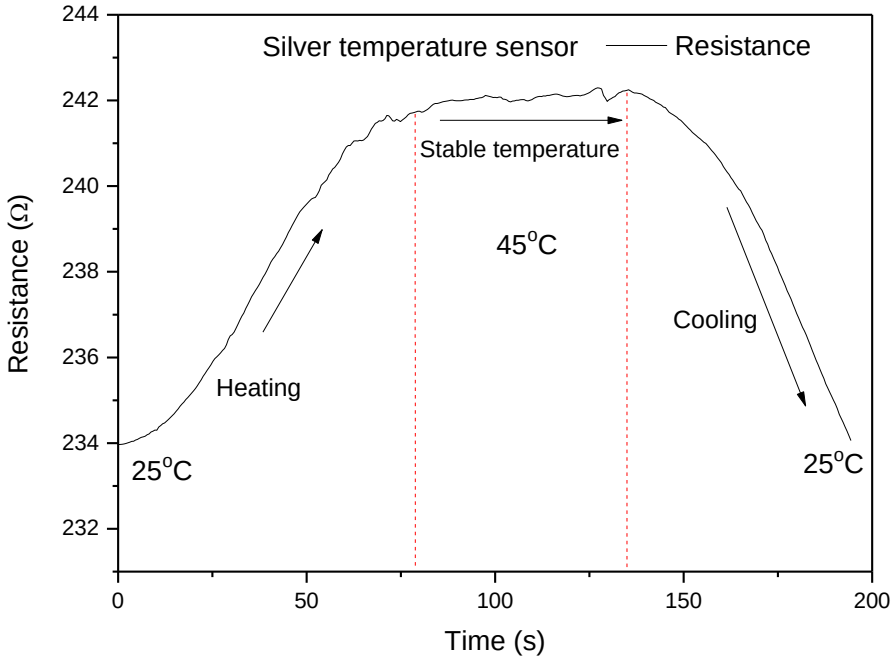

Figure 6-16. Resistance of silver temperature sensor during temperature increasing, keeps stable and decreasing.

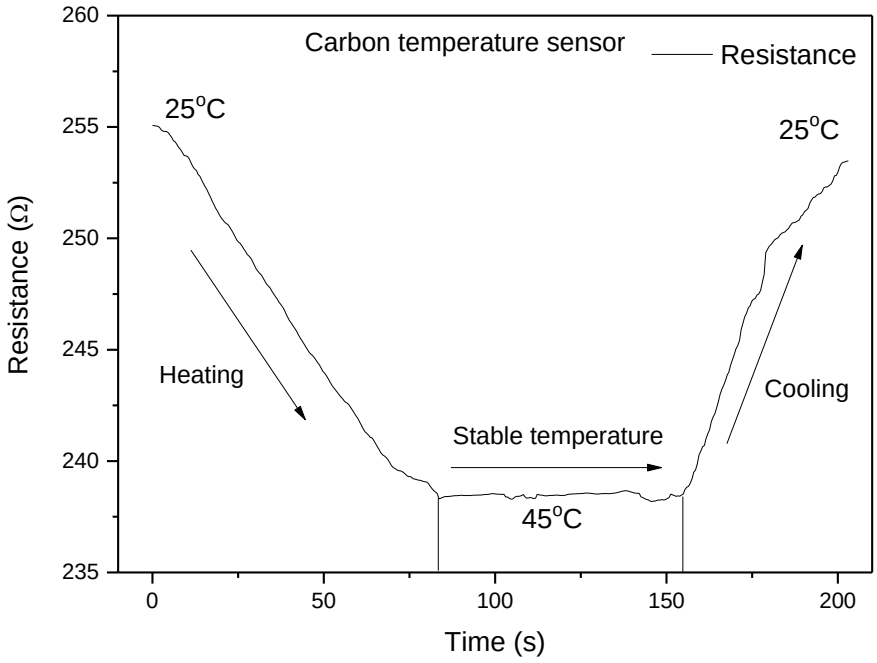

Figure 6-17. Resistance of carbon temperature sensor during temperature increasing, keeps stable and decreasing

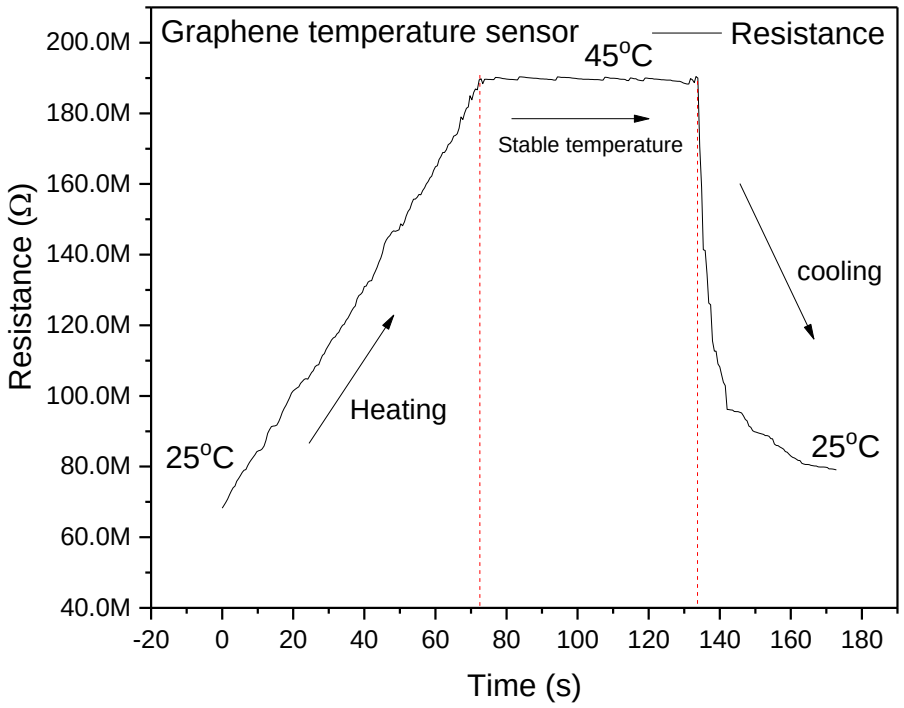

Figure 6-18. Resistance of carbon temperature sensor during temperature

increasing, keeps stable and decreasing.

After the stability test, the carbon and silver temperature sensors were placed in the heated oven at the same time and the temperature was increased from room temperature to 30 °C to test the response speed of these sensors. The results of the response speed test are plotted in **Figures 6-19 to 6-20**. It can be clearly found that the response speed of graphene temperature sensor is very much faster than that of silver and carbon temperature sensors (approximately 10.64s, 11s and 16.5s respectively).

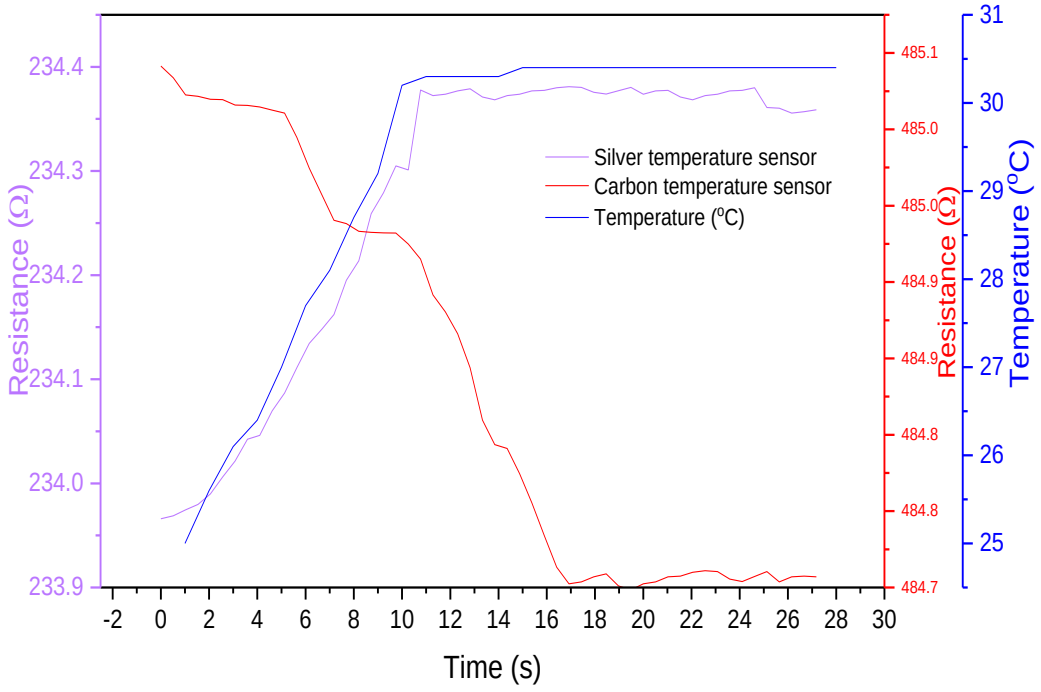

Figure 6-19. Results of response speed tests of silver and carbon temperature sensors

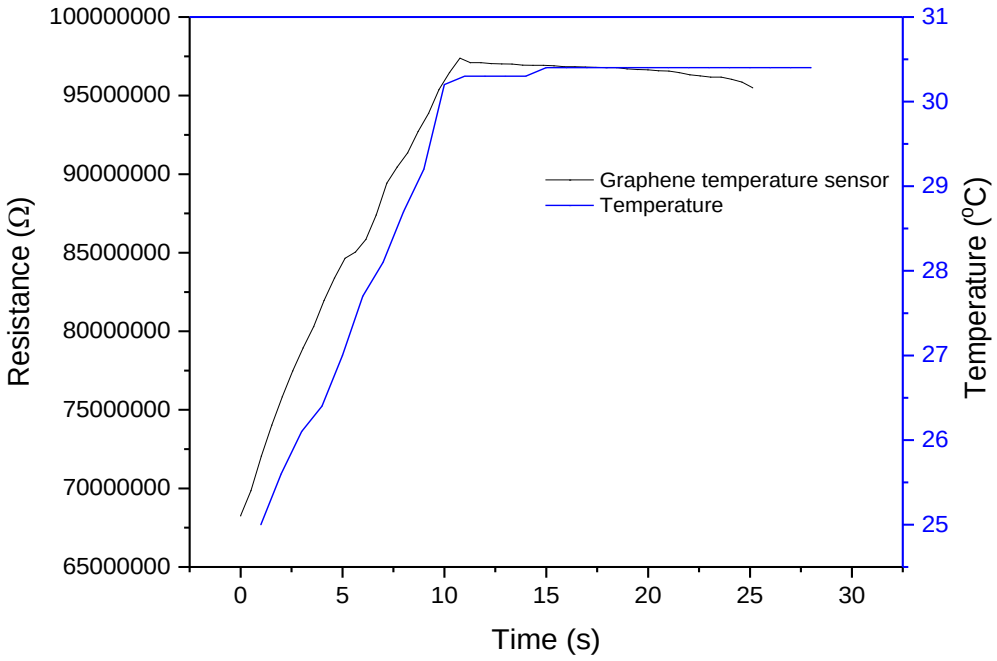

Figure 6-20. Results of response speed tests of graphene temperature sensors

According to the test results above, graphene embroidered temperature sensor manufactured in this study presents relatively better performance than carbon and silver embroidered temperature sensors. It shows good long-term stability, faster response speed and minor hysteresis performance during temperature increasing and decreasing, indicating the superiority of graphene embroidered sensors as temperature sensors. Moreover, when compared to carbon and silver temperature sensor, graphene temperature sensor is more sensitive to temperature changes.

From the above experiments carried out it clearly shows that out of the three sensing materials, graphene outperforms the other two. Therefore, the superior material performance of graphene can be seen to be retained by the graphene coated yarn. However still graphene is characterised by very high resistivity. Therefore, generally graphene is not one of the preferred materials for heating patches. That shows special strategies are required when designing embroidered heating patches out of graphene coated yarn.

In the present case, in order to create graphene-based heating patches, very small graphene widths (Red colour in **Figure 6-21**) between silver bus bars were embroidered with graphene coated yarn placed. Both the top and bottom yarn were electroconductive yarn to reduce the total electrical resistance of the heating element.

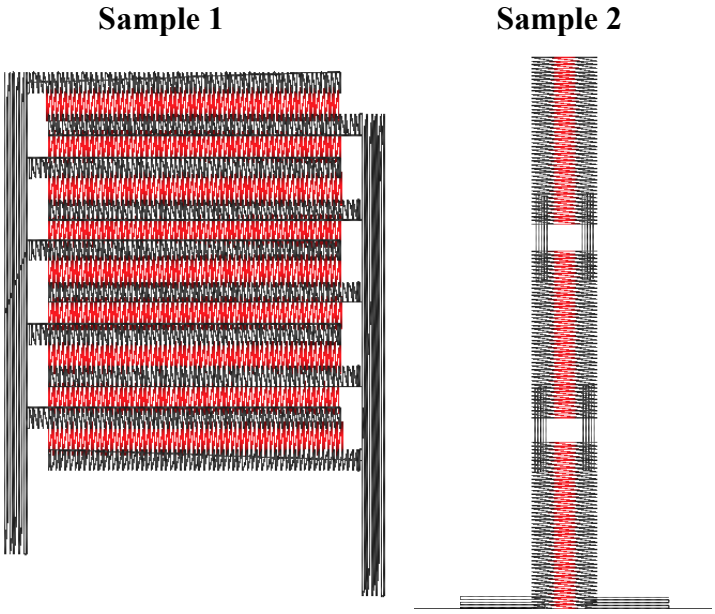

Figure 6-21. The sketch of the heating elements

The temperature sensing performance of the modified sensor was characterised by using the same heating oven with the temperature varying from 25° C to 45 ° C and the changes in resistance during the test can be seen in **Figure 6-22**, where the temperature

sensors show the thermoelectric properties of the graphene yarn.

These samples were heated by applying a dc voltage of 4.5 volts across them and the resulting resistance vs temperature characteristics were recorded. The results are shown in **Figures 6-22 to 6-23**

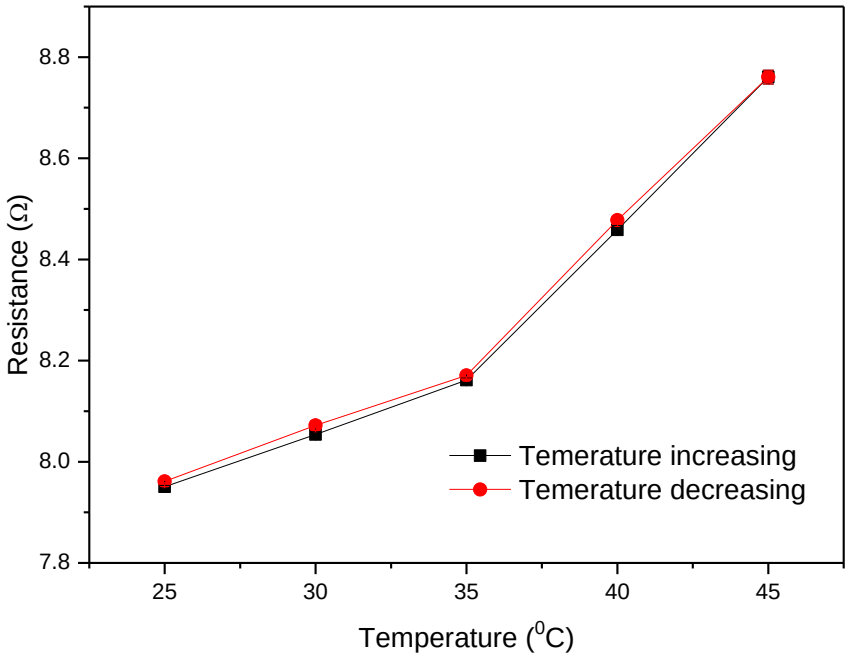

Figure 6-22. The changes in resistance of heating elements while temperature increasing.

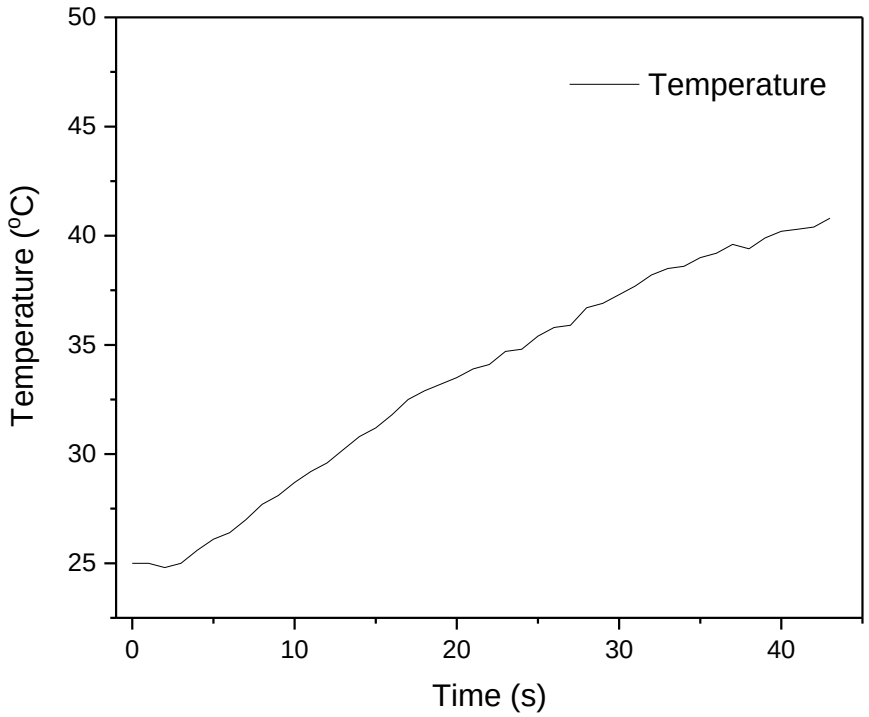

Figure 6-23. The changes in temperature of the surface of temperature sensor while heating.

The electromechanical performance of this heating patch is presented in **figure 6-22 and 6-23**. It can be seen that the electrical resistance of the heating patch decreased immensely compared to mega ohms resistance values generally observed in the case of the graphene yarn. Also **figure 6-23** shows that the heating rate was around one degree centigrade per second, and the temperature of the sensor can be increased from room temperature to more than 40 ° C in a short time (35 s)

Figures 24 and 25 are the thermal scan images of the sample 1 and 2 during the heating process with a dc voltage of 4.5 volts applied.

Sample 1 heating patch

Time 00:18.841

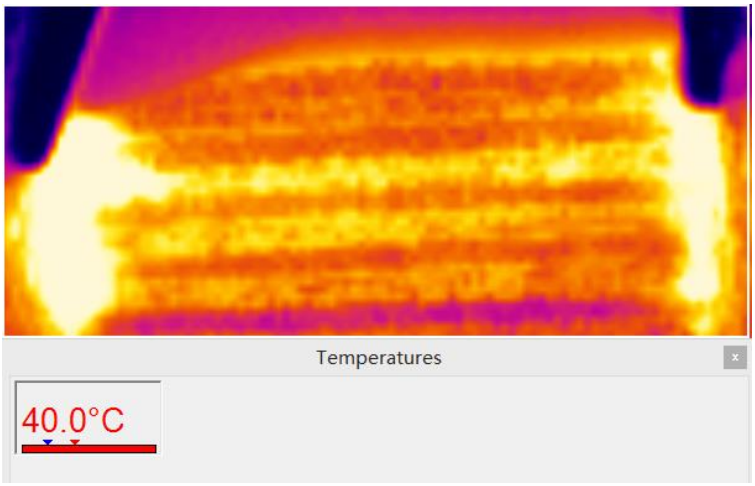

Time: 00:40.028

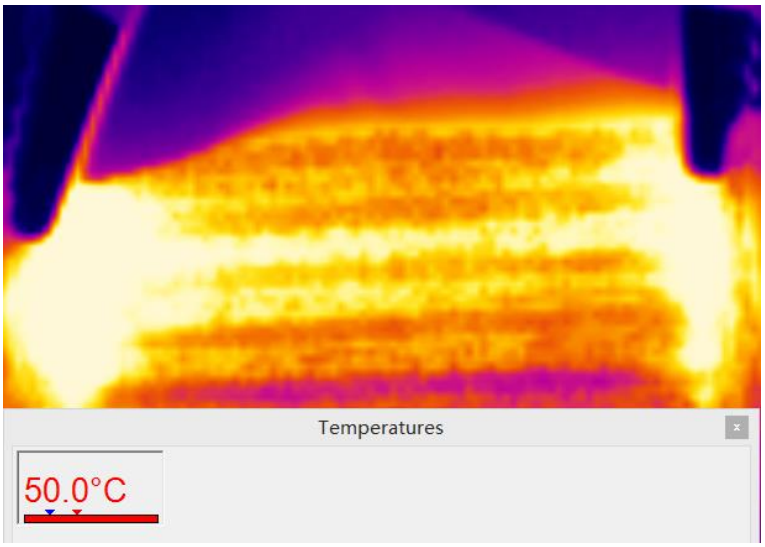

Figure 6-24. The thermal scans for sample 1 heating patch during the heating phase.

Figure 6-24 shows that by having shorter widths of graphene patches between relatively lower resistance silver bus bars the graphene patches can be made to heat up. However due to the resistance in the silver patches and the size of the silver patches they would heat up to a higher level. However, by replacing the silver yarn with fine stranded copper embroidered wire, it would be possible to prevent the high heat in the bus bar area.

Sample 2 heating patch

(a) At the beginning 00:00

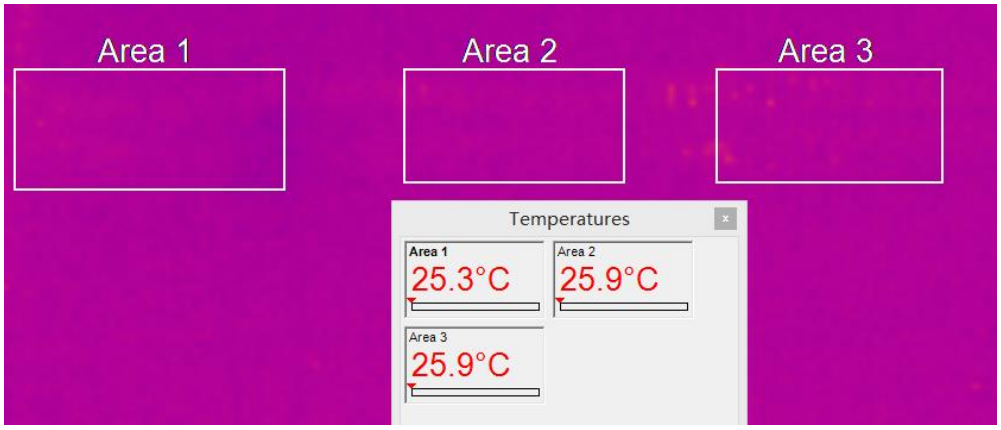

(b) At time interval: 00:17.255

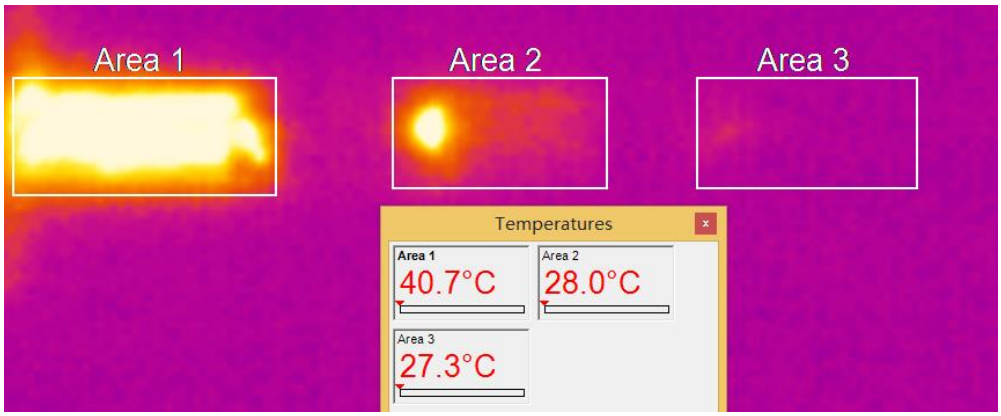

(c) At time interval: 01:53.763

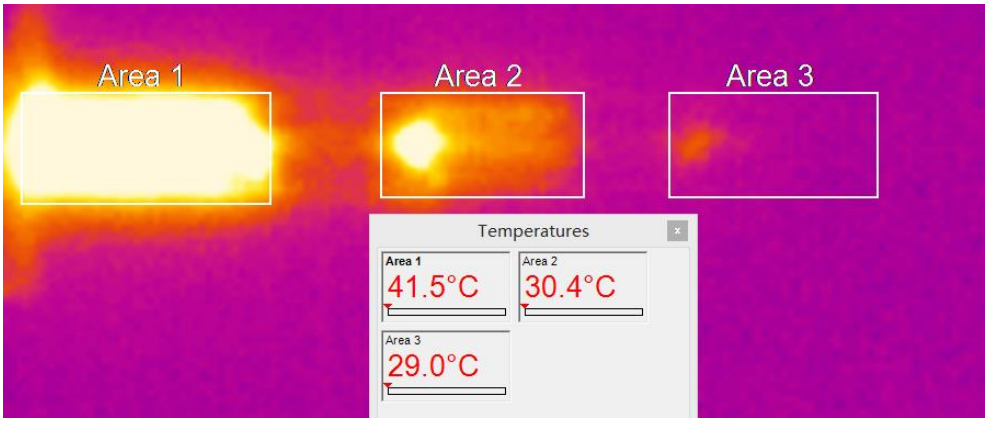

(d) At time interval: 03:22.104

(e) At time interval: 05:20.565

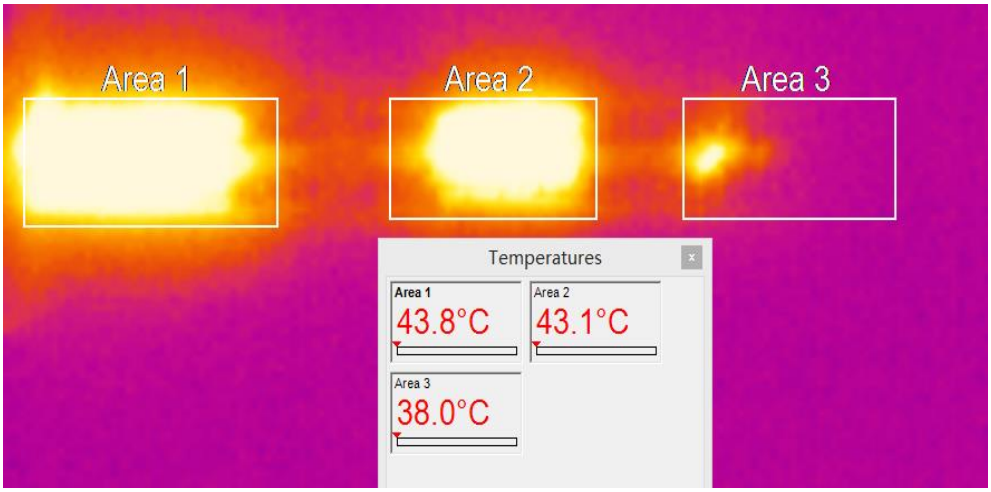

Figure 6-25. The thermal scans for sample 2 heating patch during the heating phase.

Figure 6-25 shows the heating of the embroidered sample 2 having narrow graphene patches powered by electrical power through silver bus bars. Also, due to the lower electrical resistance of silver compared to graphene, the silver area can be seen to heat to a higher level, initially. However, as time goes on, it can be seen that graphene patches too are heating up. More importantly, it should be noted through using stranded copper wire to power the graphene patches, the graphene can be made to heat to a higher level.

6.5 Conclusion

This paper introduced a novel method of creating temperature sensors and heating patches out of an advanced 2D material compared against established thermal materials.

The paper tries to show the flexibility of embroidery method when used to create custom sensor designs, relatively easily on a garment without any other pre or post processes. It also shows that the incorporation of multiple layers too is an easy and less costly process compared to other sensor manufacturing processes such as screen or inkjet printing and knitting.

The heating and cooling performance of the embroidered sensor using graphene coated yarn shows a superior performance and also as a temperature sensor, it is preferable to the traditional silver or much more affordable carbon materials. Also, it shows that graphene coated yarns can obtain excellent electrical properties associated with graphene and keep the mechanical flexibility of the core yarn.

The paper explored the electromechanical theory of operation of the sensors which is in agreement with the experimental observations. Additionally, the results of the embroidered graphene heating patches show that by incorporating multiple layers of graphene yarn, it is possible to overcome the problems of placing graphene multiple layers as experienced in processes such as printing and still achieve a relatively low equivalent electrical resistance across the heating patches. It shows that this method allows graphene heating patches to be distributed across a material and shows methods of incorporating heating patches not only in the wearable sensing field but also in areas such as fibre placement in preform manufacturing in the composites industry.

6.6 Summary

This paper introduces an embroidered temperature sensor made using electroconductive coated yarn and sewing yarns. Three types of electroconductive yarns were used: graphene coated cotton yarn, twisted carbon filament and silver coated sewing yarns. In order to observe the performance of the electroconductive yarn as temperature sensors and as heating patches, three different embroidery designs were manufactured, and through the tensile and bending rigidity test, the sensor designs with most suitable mechanical properties was selected for further experiments. The test temperature was varied from 25 to 45 °C to cover the ranges of healthy human skin temperature (36.5-37.5°C). The experimental results are presented to evaluate and compare the relative response speed, error and long-term stability. The paper further presents a mathematical study of the electromechanical performance of the embroidered designs and verifies this study using experimental results.

6.7 References

[1] M. Sibinski, M. Jakubowska, and M. Sloma, “Flexible temperature sensors on fibers,” *Sensors*, vol. 10, no. 9, pp. 7934–7946, 2010.

[2] J. Meyer, “Textile pressure sensor: Design, error modeling and evaluation,” *Ph.D. Diss.*, pp. 1–120, 2008.

[3] F. Chiarugi *et al.*, “Measurement of heart rate and respiratory rate using a textile-based wearable device in heart failure patients,” in *Computers in Cardiology*, 2008, vol. 35, pp. 901–904.

[4] M. Peltokangas, J. Verho, and A. Vehkaoja, “Night-time EKG and HRV monitoring with bed sheet integrated textile electrodes,” *IEEE Trans. Inf. Technol. Biomed.*, vol. 16, no. 5, pp. 935–942, 2012.

[5] T. Q. Trung and N. E. Lee, “Flexible and Stretchable Physical Sensor Integrated Platforms for Wearable Human-Activity Monitoringand Personal Healthcare,” *Adv. Mater.*, 2016.

[6] M. K. Law, S. Lu, T. Wu, A. Bermak, P. I. Mak, and R. P. Martins, “A 1.1 μW CMOS smart temperature sensor with an inaccuracy of ±0.2 °C (3σ) for clinical temperature monitoring,” *IEEE Sens. J.*, 2016.

[7] F. F. Lee, F. Chen, and J. Liu, “Infrared thermal imaging system on a mobile phone,” *Sensors (Switzerland)*, 2015.

[8] K. K. Sadasivuni, A. Kafy, H. C. Kim, H. U. Ko, S. Mun, and J. Kim, “Reduced graphene oxide filled cellulose films for flexible temperature sensor application,” *Synth. Met.*, 2015.

[9] J. Yang *et al.*, “Wearable temperature sensor based on graphene nanowalls,” *RSC Adv.*, 2015.

[10] R. Soukup, A. Hamacek, L. Mracek, and J. Reboun, “Textile based temperature and humidity sensor elements for healthcare applications,” in *Proceedings of the 2014 37th International Spring Seminar on Electronics Technology, ISSE 2014*, 2014, pp.

407–411.

[11] D. J. Lichtenwalner, A. E. Hydrick, and A. I. Kingon, “Flexible thin film temperature and strain sensor array utilizing a novel sensing concept,” *Sensors Actuators, A Phys.*, 2007.

[12] S. Y. Xiao, L. F. Che, X. X. Li, and Y. L. Wang, “A novel fabrication process of MEMS devices on polyimide flexible substrates,” *Microelectron. Eng.*, 2008.

[13] M. D. Husain and R. Kennon, “Preliminary investigations into the development of textile based temperature sensor for healthcare applications,” *Fibers*, 2013.

[14] M. L. Hammock, A. Chortos, B. C. K. Tee, J. B. H. Tok, and Z. Bao, “25th anniversary article: The evolution of electronic skin (E-Skin): A brief history, design considerations, and recent progress,” *Adv. Mater.*, 2013.

[15] M. D. Husain, R. Kennon, and T. Dias, “Design and fabrication of Temperature Sensing Fabric,” *J. Ind. Text.*, vol. 44, no. 3, pp. 398–417, 2014.

[16] M. D. Husain, O. Atalay, A. Atalay, and R. Kennon, “Uncertainty analysis of the temperature-resistance relationship of temperature sensing fabric,” *Fibers*, 2016.

[17] R. Polanský *et al.*, “A novel large-area embroidered temperature sensor based on an innovative hybrid resistive thread,” *Sensors Actuators, A Phys.*, vol. 265, pp. 111–119, 2017.

[18] P. Bosowski, M. Hoerr, V. Mecnika, T. Gries, and S. Jockenhövel, “Design and manufacture of textile-based sensors,” in *Electronic Textiles: Smart Fabrics and Wearable Technology*, 2015, pp. 75–107.

[19] T. Mac, S. Houis, and T. Gries, “Metal fibers,” *Tech. Text.*, vol. 47, pp. 17–32, 2004.

Chapter 7 – Conclusion and future work

7.1 Conclusion

The main aim of this research was to develop graphene based reliable, comfortable and low flexural rigidity embroidered textile sensors for pressure sensing, moisture sensing and temperature sensing applications and compare their performance to metal coated and carbon based embroidered sensors made for the same purposes. The literature survey has shown the level of embroidered sensor technology investigated and developed by the scientific community up to current times. Guided by literature, it was necessary to develop a piezoresistive sensor with high flexibility, good sensitivity and portability, especially for detecting human movement and other bio-signals. As is the case when using carbon and metallic material based embroidered sensors, the sensor response speed was a main point that this research targeted to improve. In addition to that, high sensitivity, high gauge factor and the ability to have large area sensors were considered as other points of interest. Since washability was another important parameter which is prefered in these type of sensors that too was investigated. However, the washability is associated with the application of electroconductive material on to the fibres/ filaments or yarn. Since rather than the development of the graphene coated yarn, it is the design, construction, modelling and evaluation of the embroidered sensors that was the main aim of the research, washability investigation was limited to evaluation and reporting of the washability outcome of the sensors.

The investigations that were carried out has shown that various designs of the embroidered sensors mainly impact the mechanical properties and moisture wicking in the sensor embroidered fabrics. When it comes to the resistance of the sensor and its sensitivity, gain and speed of response, mainly the material properties, yarn to yarn interaction, stitch size, the number of stitches and the reliability of the sensor yarn are

the main important factors. Although the fastness of the silver coating on the silver yarn is much better than the graphene coating and the use of carbon filaments in the carbon yarn makes it a more stable yarn compared to the graphene coated yarn, due to the properties of the graphene flakes, its coated architecture and the electromechanical properties it shows, graphene coated yarn has proved to be a better sensing material for all three types of sensors. The ability of the graphene coated sensing yarn to show superior relative change in resistance under tension, compression, heating and moisture wicking, when used in embroidery applications, the research has shown how to construct graphene based embroidered sensors, the important parameters to address when constructing them and by comparing with other materials, the research has show by what factor the graphene based sensors are superior to similar sensors made with carbon and silver yarn. Although no theoretical study was conducted to analyse the bending rigidity of different embroidered sensor designs, the research, in this case, was based on tried and tested sensor designs by the research community. The research shows that it is possible to engineer the embroidered patterns using the PE-Design software, in which the stitch density, yarn orientation and stitch size can be adjusted. In addition to this, the yarn tension can also be adjusted to the most suitable value on the embroidery machine. The research shows how the sensor design process can be carried out to produce highly sensitive embroidered pressure, temperature and moisture sensors.

The experiments carried out have shown that stitch length and the density of stitch lines are important parameters that determine the bending rigidity of the sensor fabric, which determines the drapability of the sensor fabrics, Experiments were carried out to determine the optimum stitch density and size for embroidered samples of silver, carbon and graphene. During the experiments, when the stitch density was increased, the sensor became stiffer, mainly due to the increase of the number of stitches. The same pressure was applied on the sensor, in which the deformation nominal to the stiffer sensor is relatively lower due to the flexibility. Therefore, the changes in the resistance of the

stiffer sensor are not as notable as the flexible sensor. However, by increasing the stitch size and density at the same time, it was possible to overcome this problem. The optimum stitch line separation was found to be 2 mm while the stitch size was found as 5 mm, while the sensors with larger stitch size show higher flexibility.

It was also found that even though having multiple layers of embroidery yarn may make the sensors more rigid, the piezoresistive sensors with multiple layers can achieve good electroconductivity as well. The results also showed that piezoresistive sensors with sandwich structure have a high sensitivity and a good stability, as compared to the single layer structures. During the piezoresistive sensor tests, the graphene sewing yarn was able to achieve a better sensitivity with both single and multiple layer structures. Sensors, with the graphene sewing yarns, present a higher sensitivity, good electrical response to changes in pressure and good stability during the cyclic test and the long-term stability test. Although the washability test results were somewhat unsatisfactory, it can be further improved with encapsulation, by using a flexible encapsulation material (e.g. ecoflex), which will not affect the original mechanical behaviour of the sample.

As for the moisture sensors, experimenting with several different structures have shown that the sensor design with the Archimedean spiral shape was the most suitable design. The result shows that the sensor with graphene sewing yarn achieves better performance, due to the properties of graphene. In this process, the embroidered moisture sensor made by graphene coated yarn presents a higher response speed (generally in few second, the resistance will achieve a stable level), good stability and relatively higher sensitivity.

Temperature sensors made to detect and monitor the temperature of the human skin showed that the temperature sensors made with graphene sewing yarn shows a better

performance. It achieves a relatively higher response speed, good stability during the constant temperature test and the highest sensitivity out of the three materials for changes in the temperature. It was found, the resistance of the temperature sensors was too high to be used for heating elements. Therefore, a modified temperature sensor was made by using silver and graphene yarn in multiple layers. Experiments on this type of heating fabric showed that it has lower electrical resistance (around 10 ohms) and it can be heated up to around 40℃ within 40s. It also shows a good temperature sensing ability with a high response speed and stable result.

7.2 Future works

1. The metallic coated yarn was chosen in this research due to its high conductivity and flexibility. However, the silver coated yarn used in this project is not an optimised yarn because of its tendency to corrode and oxidise in the environment. Other metallic coated yarns, like stainless steel, copper and even pure metallic yarn could be further investigated to manufacture the embroidered sensors. However, their sensitivity properties are not expected to surpass graphene based sensors.
2. Graphene coated cotton yarn used in this research has a good thermal & electrical property and good reaction to changes in the compression and moisture. However, the strength of this yarn is too weak. Graphene coated polyester yarn could be further improved to get better stretchability, flexibility and washability.
3. Embroidered sensors with elastomeric conductive yarn are still not optimised for embroidery fabrication methods. At the beginning of this research, an elastomeric silver wrapped Lycra yarn was tested for embroidered strain sensor. However, due to the high elasticity of the yarn, the sample was not neat and clean, and thus, the performance was poor. But further research can be carried out in the direction of

using electroconductive elastomeric yarn, in order to produce embroidery samples, by using the standard embroidery or tailored fibre placement technologies.

4. The yarn used in this research was electroconductive coated yarn. Therefore, the washability of the sample is not satisfactory. In future research, encapsulation can be used to protect the sensor structure with some flexible resin, like Evo 50.
5. Embroidery machine consists of two sets of sewing yarn; where the top yarn is generally non-conductive due to the friction between the needle hole and the yarn will produce many conductive powders over the substrate fabric. With only one side conductive, the resistance of the sensors can be relatively higher than where both the top and bottom yarn are electroconductive. Further work can be considered, in order to use fine and soft metallic yarn or conductive yarn, with an insulation layer as the top yarn.
6. In order to make the samples neat, clean and tight, the yarn tension should be adjusted to meet the different density, stitch size and the diameter of the yarn. In order to model the optimum yarn tension for stitch density, yarn diameter and stitch length, further modelling should be carried out.
7. In this research, only standard embroidery lock stitch was investigated. In further research, textile electrodes made by chain-stitch embroidery technique and textile sensors made with pure metallic yarn or higher diameter conductive yarn using tailored fibre placement techniques can be considered.
8. Improvements in the accuracy and reliability of the embroidery temperature, moisture and piezoresistive sensors are needed. And the direction of further research can be focused on response speed and the noise level of the sensor.
9. The multifilament sewing yarns investigated in this research prevents very close stitch densities being tested. In order to overcome this, monofilament sewing yarn could also be investigated in further research.

Appendix

Appendix A

Cyclic results of embroidered piezoresistive sensor with different densities, stitch sizes and sensor sizes.

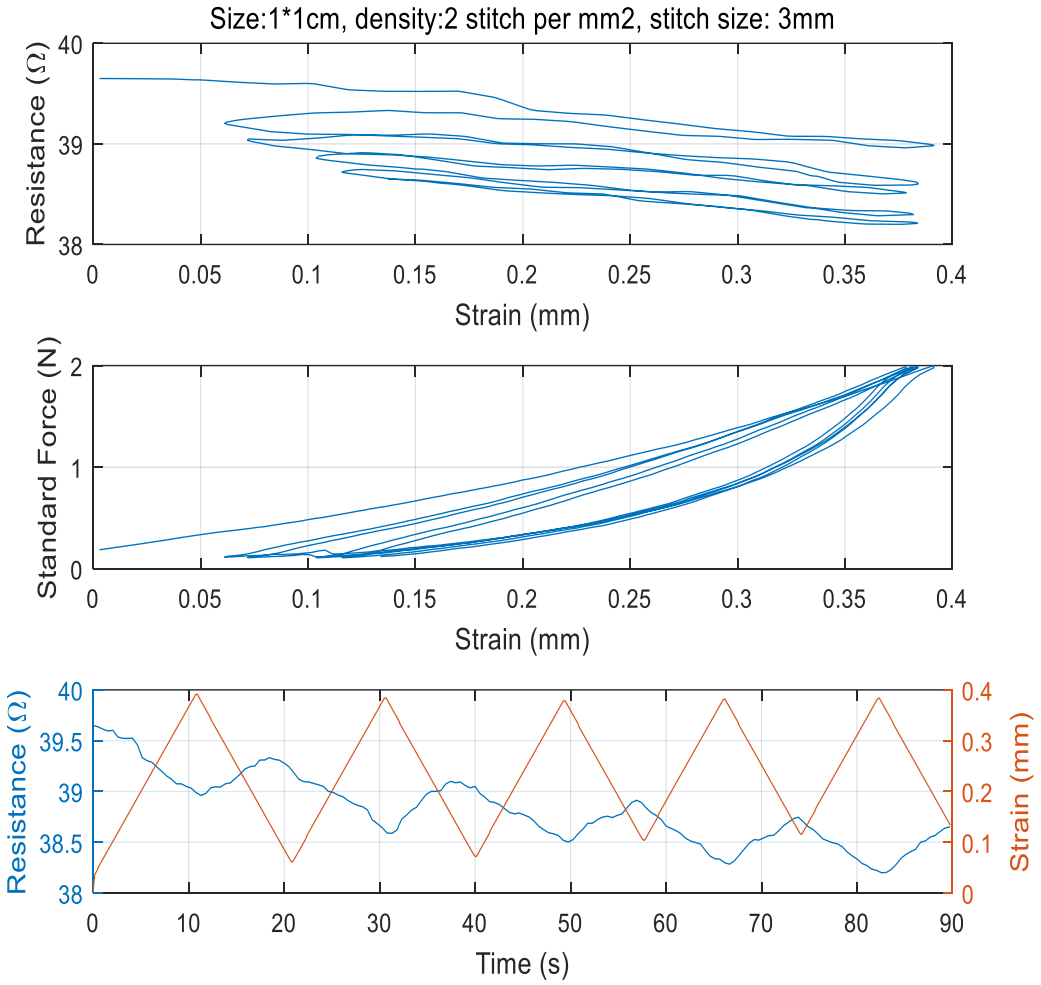

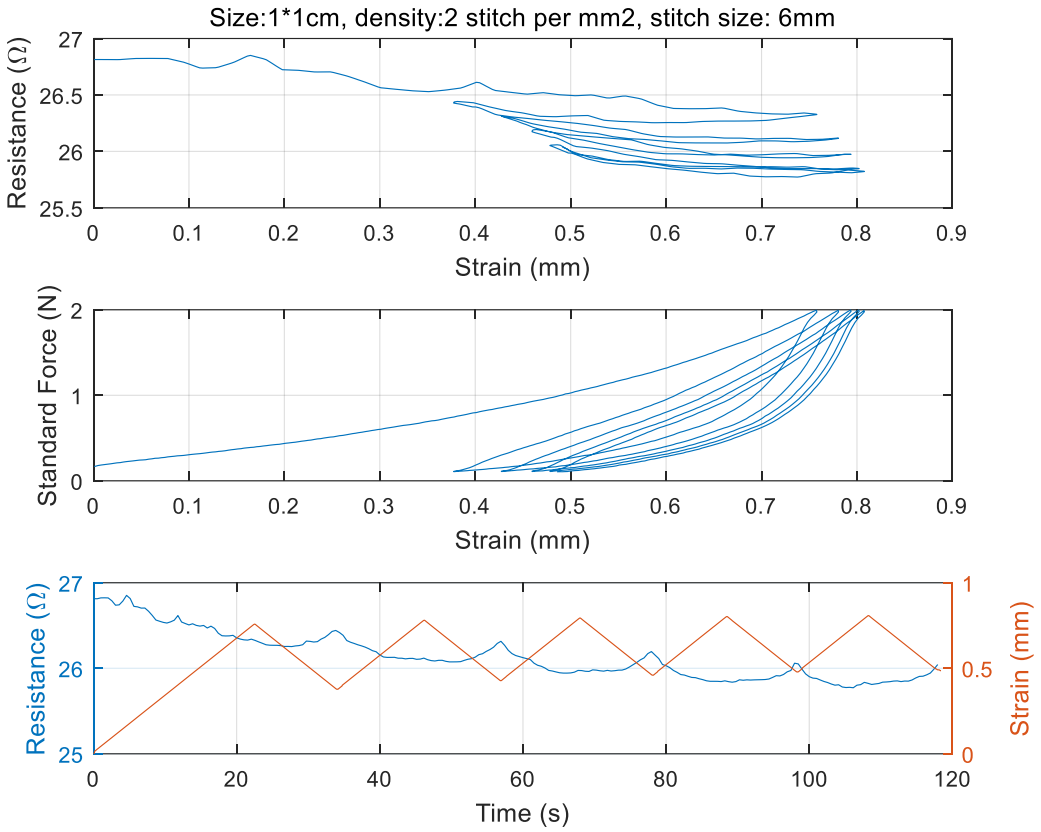
Size:1*1cm, density:2 stitch per mm2, stitch size: 6mm
Resistance (Ω)
Strain (mm)
Standard Force (N)
Strain (mm)
Resistance (Ω)
Strain (mm)
Time (s)

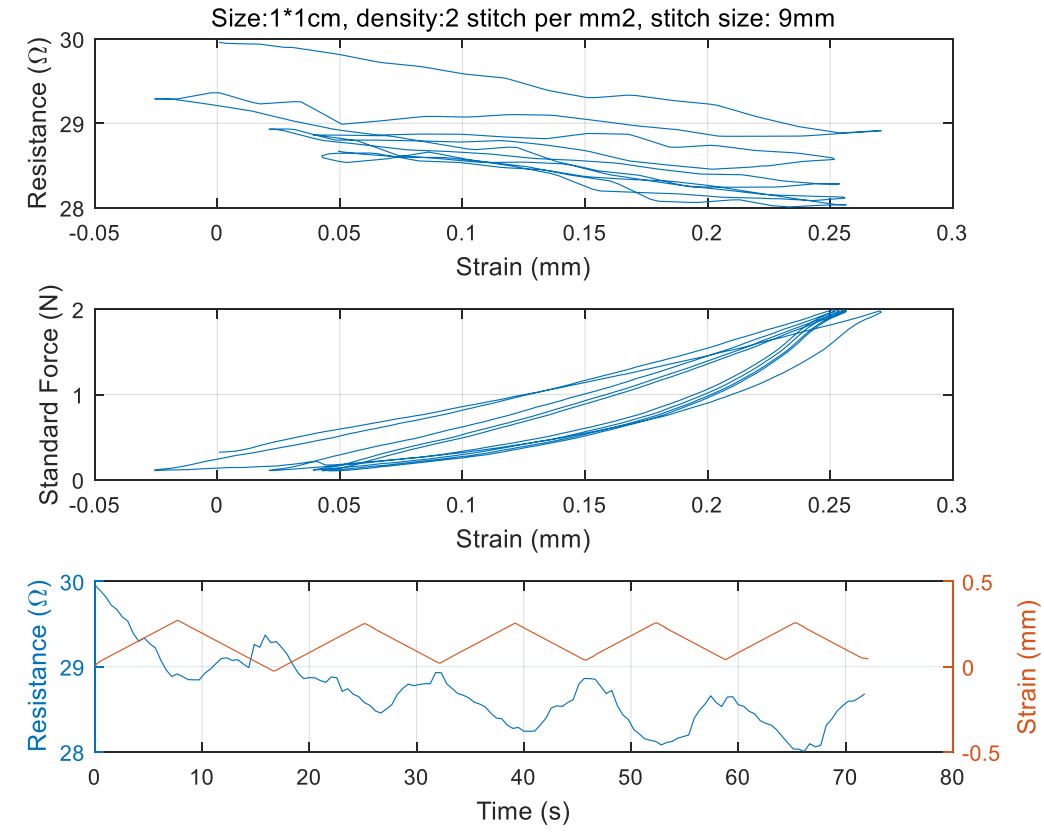
Size:1*1cm, density:2 stitch per mm2, stitch size: 9mm
Resistance (Ω)
Strain (mm)
Standard Force (N)
Strain (mm)
Resistance (Ω)
Strain (mm)
Time (s)

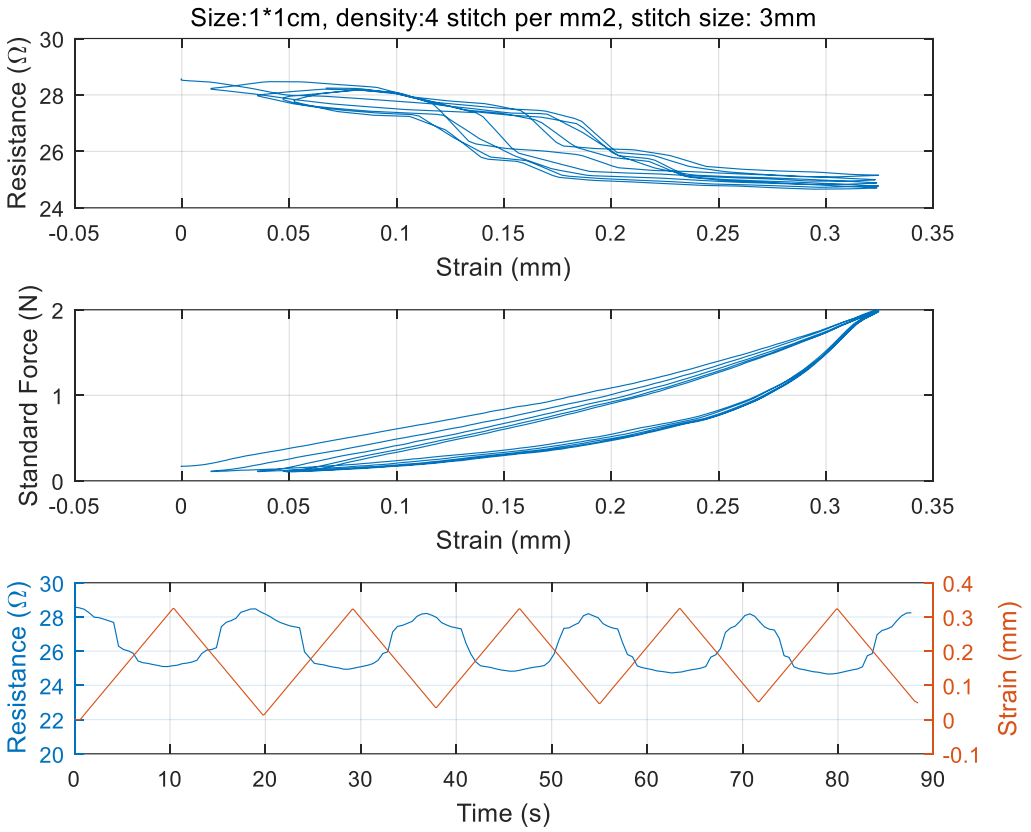
Size:1*1cm, density:4 stitch per mm2, stitch size: 3mm
Resistance (Ω)
Strain (mm)
Standard Force (N)
Strain (mm)
Resistance (Ω)
Strain (mm)
Time (s)

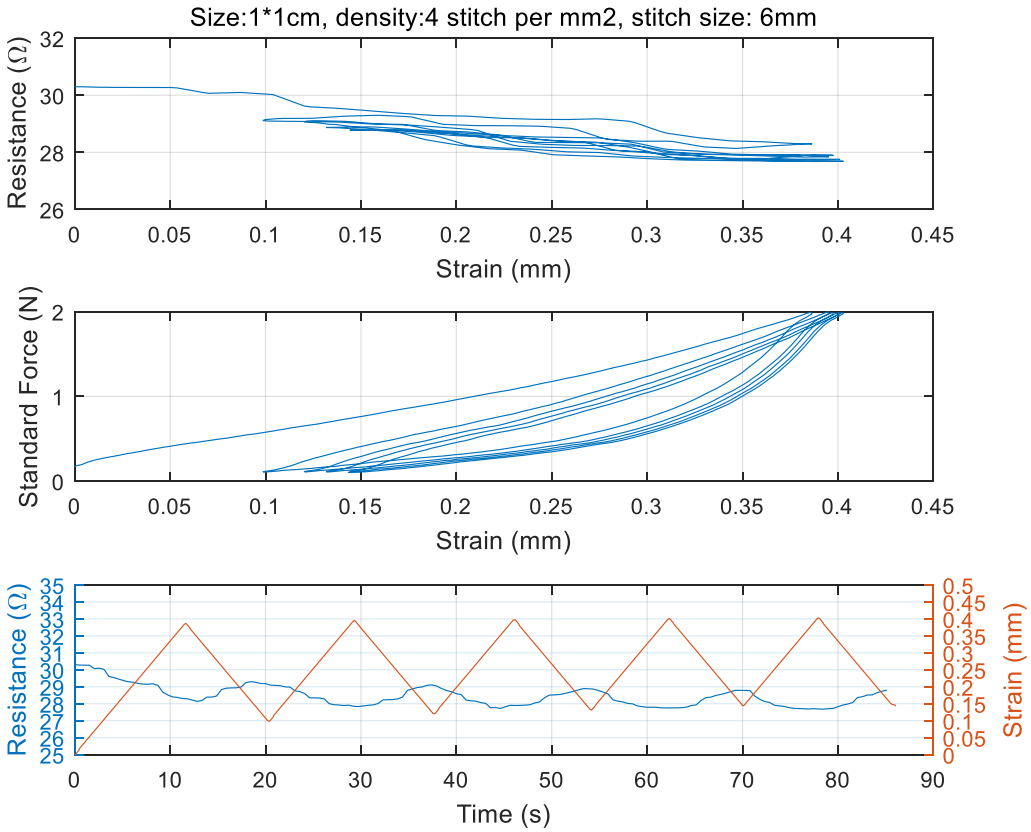
Size:1*1cm, density:4 stitch per mm2, stitch size: 6mm
Resistance (Ω)
Strain (mm)
Standard Force (N)
Strain (mm)
Resistance (Ω)
Strain (mm)
Time (s)

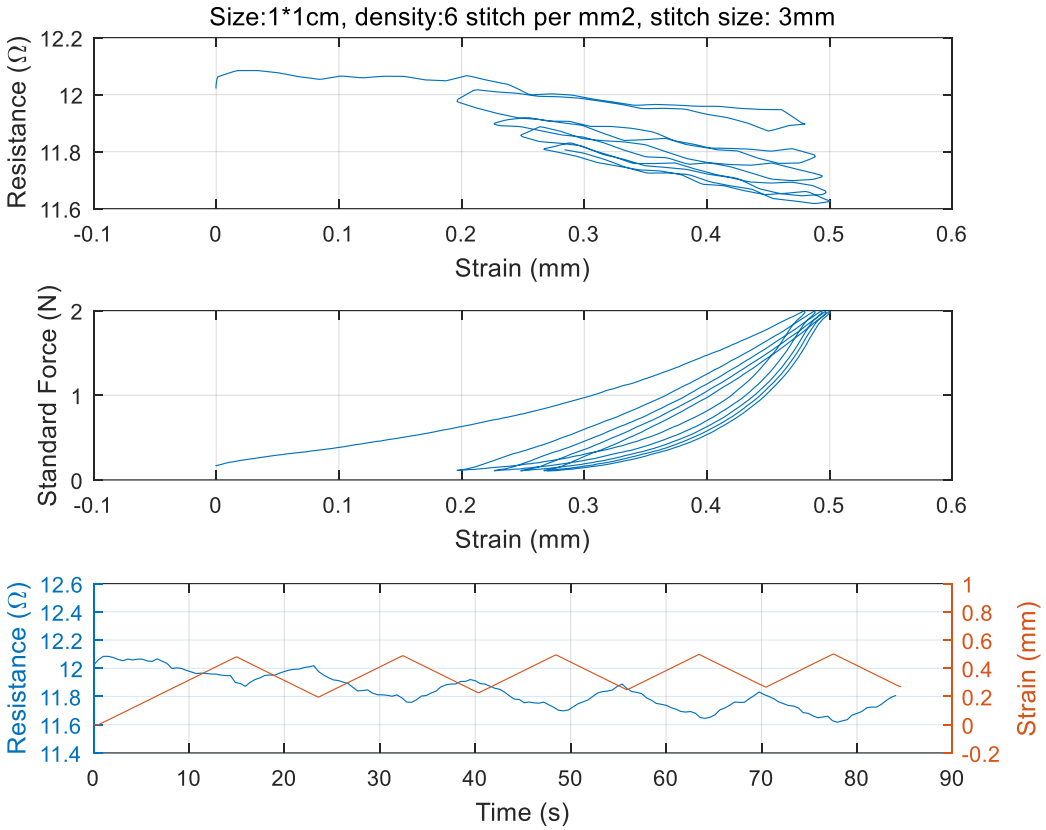
Size:1*1cm, density:6 stitch per mm2, stitch size: 3mm
Resistance (Ω)
12.2
12
11.8
11.6
-0.1
0
0.1
0.2
0.3
0.4
0.5
0.6
Strain (mm)
Standard Force (N)
2
1
0
-0.1
0
0.1
0.2
0.3
0.4
0.5
0.6
Strain (mm)
Resistance (Ω)
12.6
12.4
12.2
12
11.8
11.6
11.4
Strain (mm)
1
0.8
0.6
0.4
0.2
0
-0.2
0
10
20
30
40
50
60
70
80
90
Time (s)

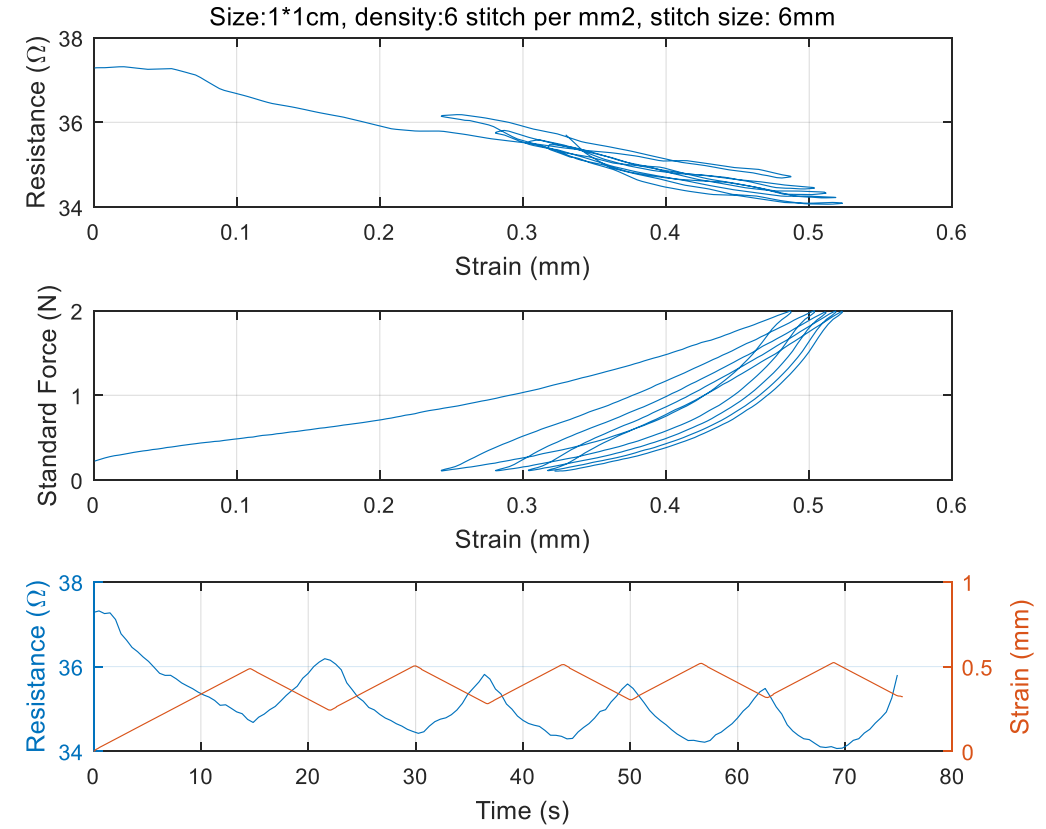
Size:1*1cm, density:6 stitch per mm2, stitch size: 6mm
Resistance (Ω)
38
36
34
0
0.1
0.2
0.3
0.4
0.5
0.6
Strain (mm)
Standard Force (N)
2
1
0
0
0.1
0.2
0.3
0.4
0.5
0.6
Strain (mm)
Resistance (Ω)
38
36
34
Strain (mm)
1
0.5
0
0
10
20
30
40
50
60
70
80
Time (s)

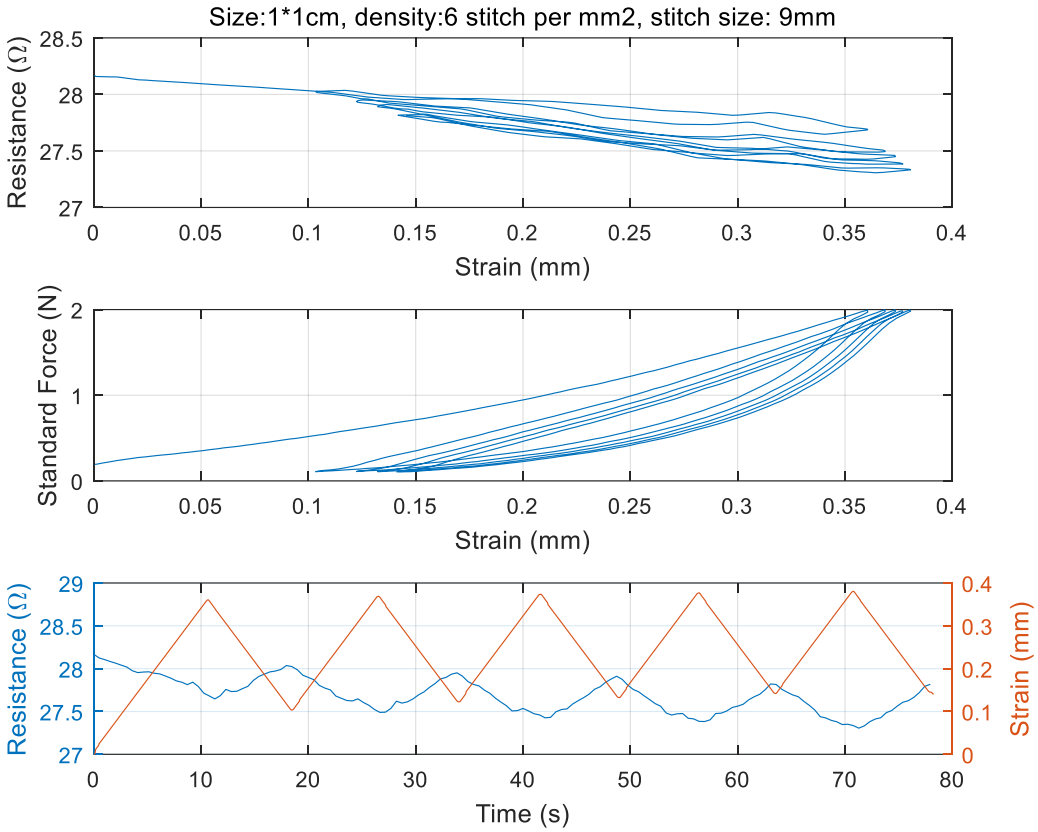
Size:1*1cm, density:6 stitch per mm2, stitch size: 9mm
Resistance (Ω)
Strain (mm)
Standard Force (N)
Strain (mm)
Resistance (Ω)
Strain (mm)
Time (s)

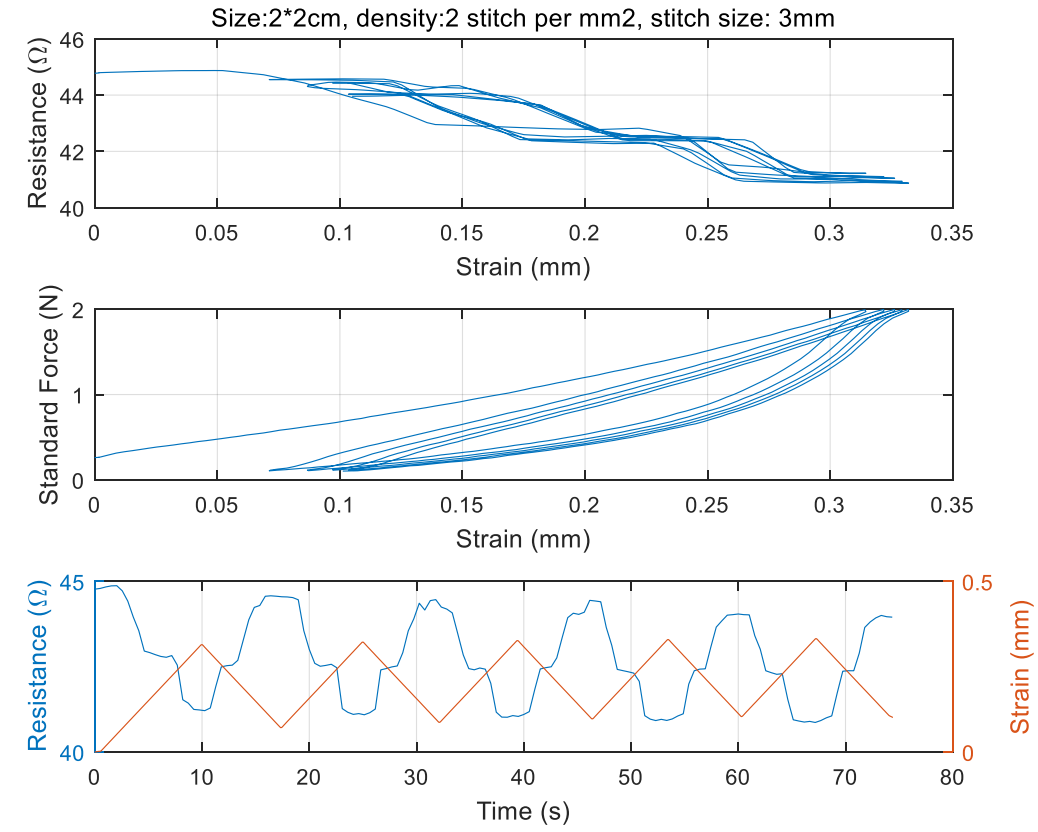
Size:2*2cm, density:2 stitch per mm2, stitch size: 3mm
Resistance (Ω)
Strain (mm)
Standard Force (N)
Strain (mm)
Resistance (Ω)
Strain (mm)
Time (s)

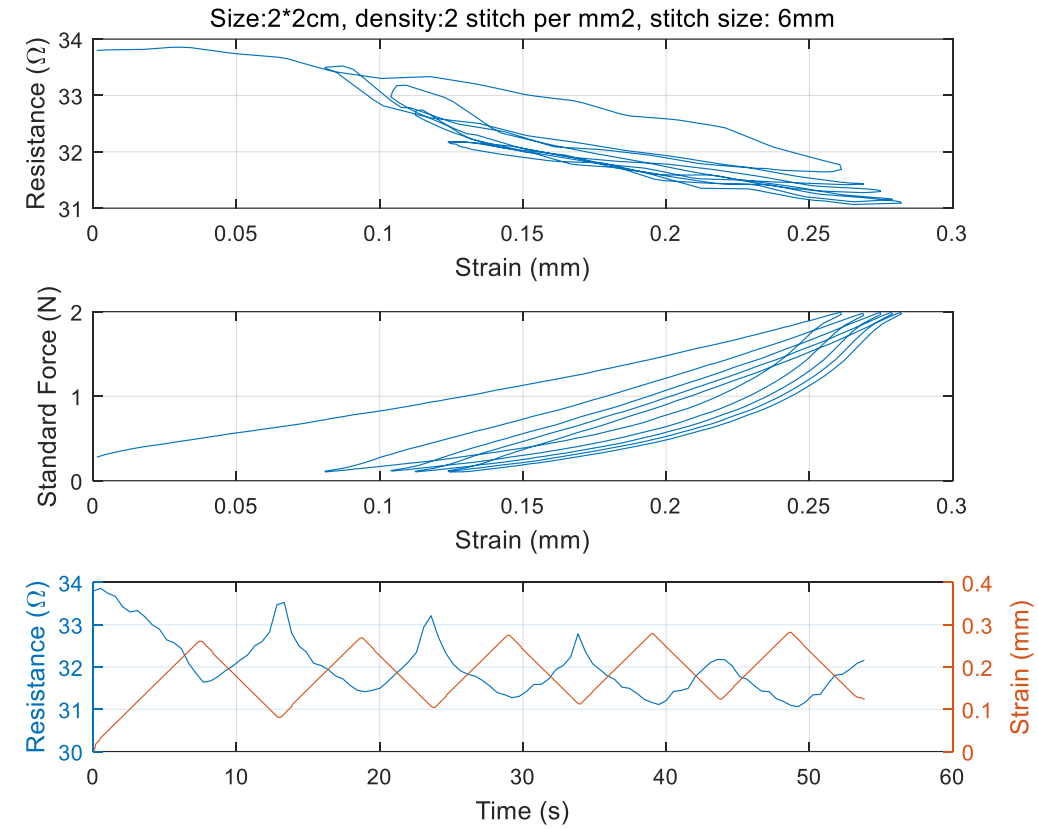
Size:2*2cm, density:2 stitch per mm2, stitch size: 6mm
Resistance (Ω)
Strain (mm)
Standard Force (N)
Strain (mm)
Resistance (Ω)
Strain (mm)
Time (s)

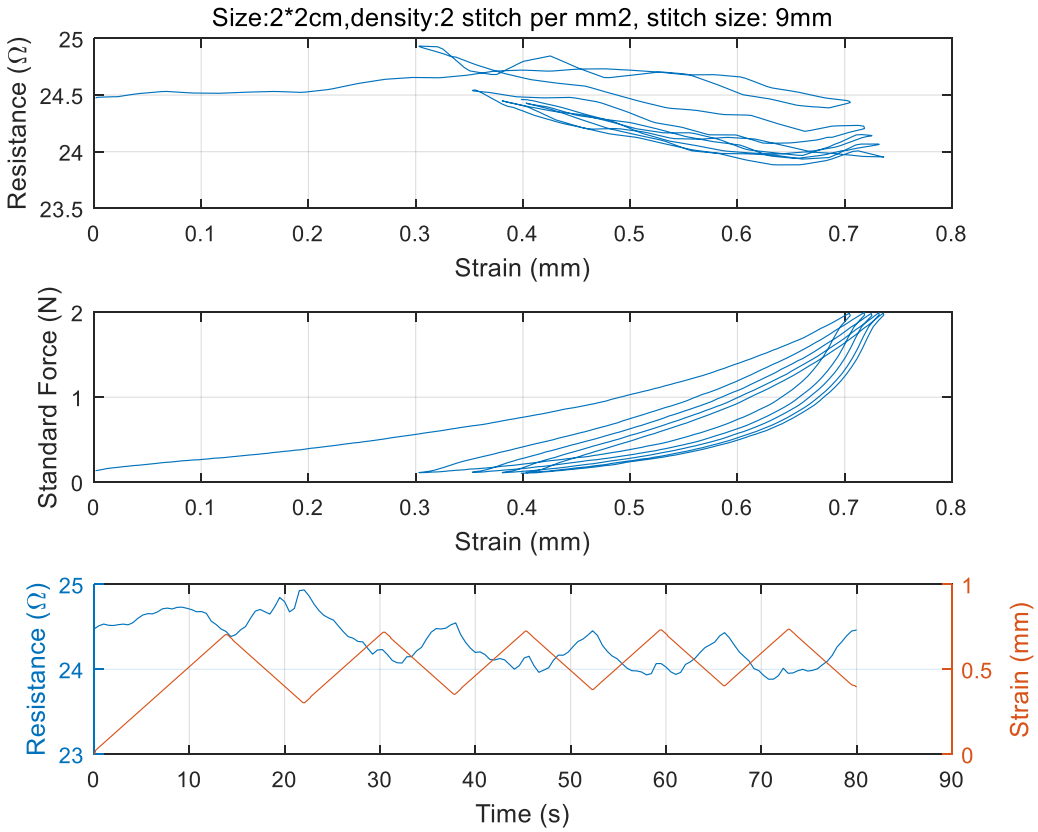
Size:2*2cm,density:2 stitch per mm2, stitch size: 9mm
Resistance (Ω)
Strain (mm)
Standard Force (N)
Strain (mm)
Resistance (Ω)
Strain (mm)
Time (s)

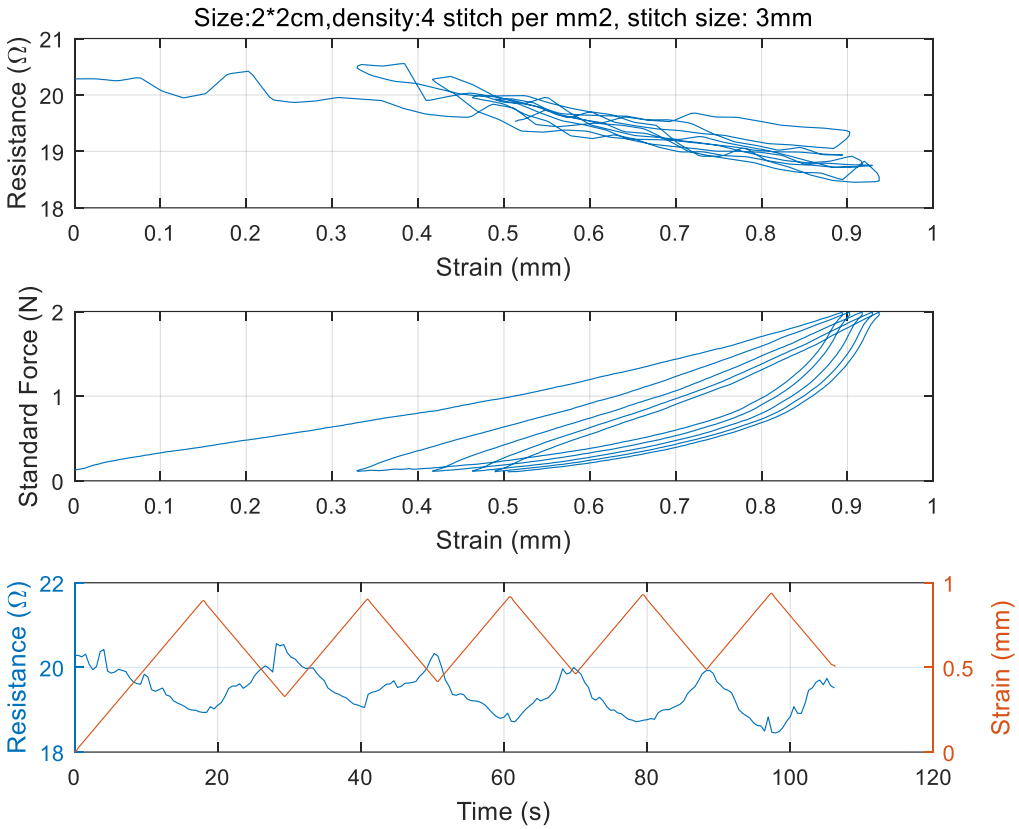
Size:2*2cm,density:4 stitch per mm2, stitch size: 3mm
Resistance (Ω)
Strain (mm)
Standard Force (N)
Strain (mm)
Resistance (Ω)
Strain (mm)
Time (s)

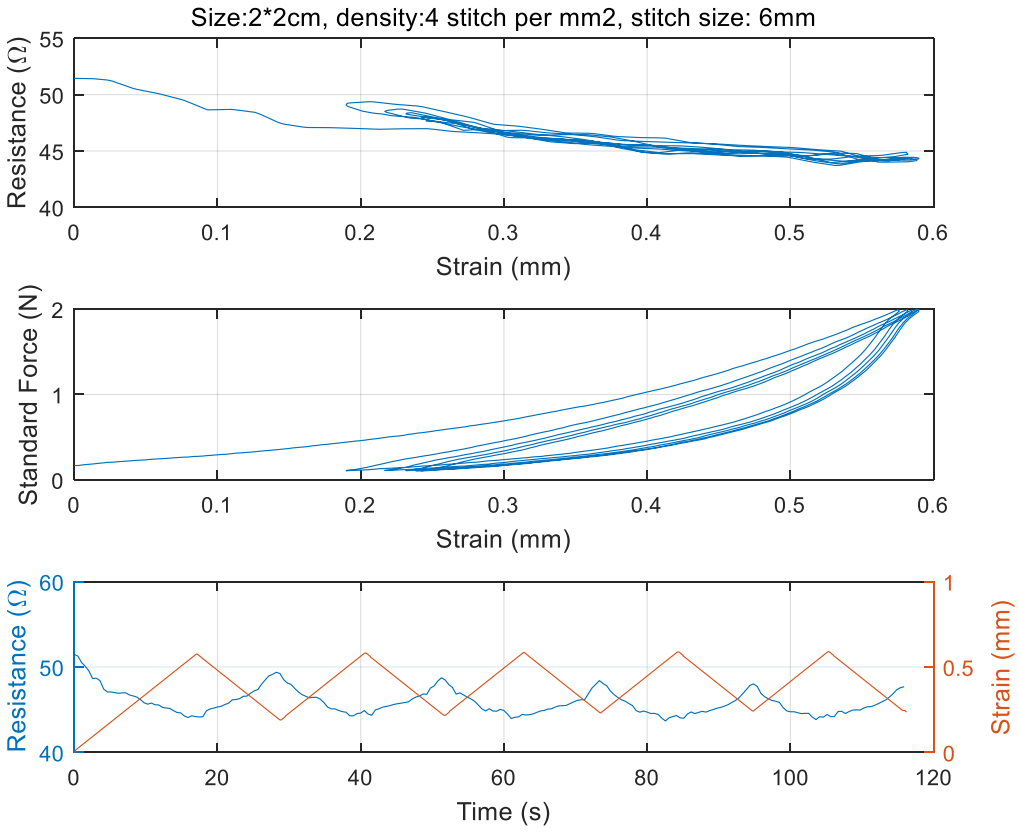
Size:2*2cm, density:4 stitch per mm2, stitch size: 6mm
Resistance (Ω)
Strain (mm)
Standard Force (N)
Strain (mm)
Resistance (Ω)
Strain (mm)
Time (s)

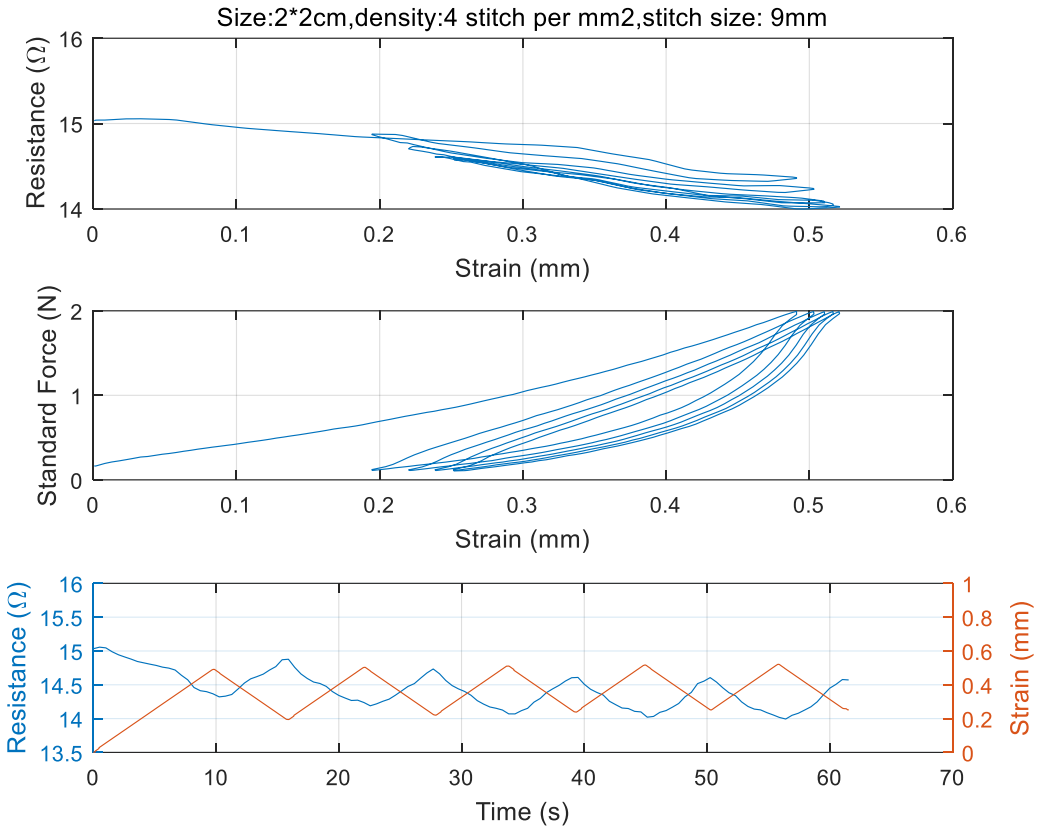
Size:2*2cm,density:4 stitch per mm2,stitch size: 9mm
Resistance (Ω)
Strain (mm)
Standard Force (N)
Strain (mm)
Resistance (Ω)
Strain (mm)
Time (s)

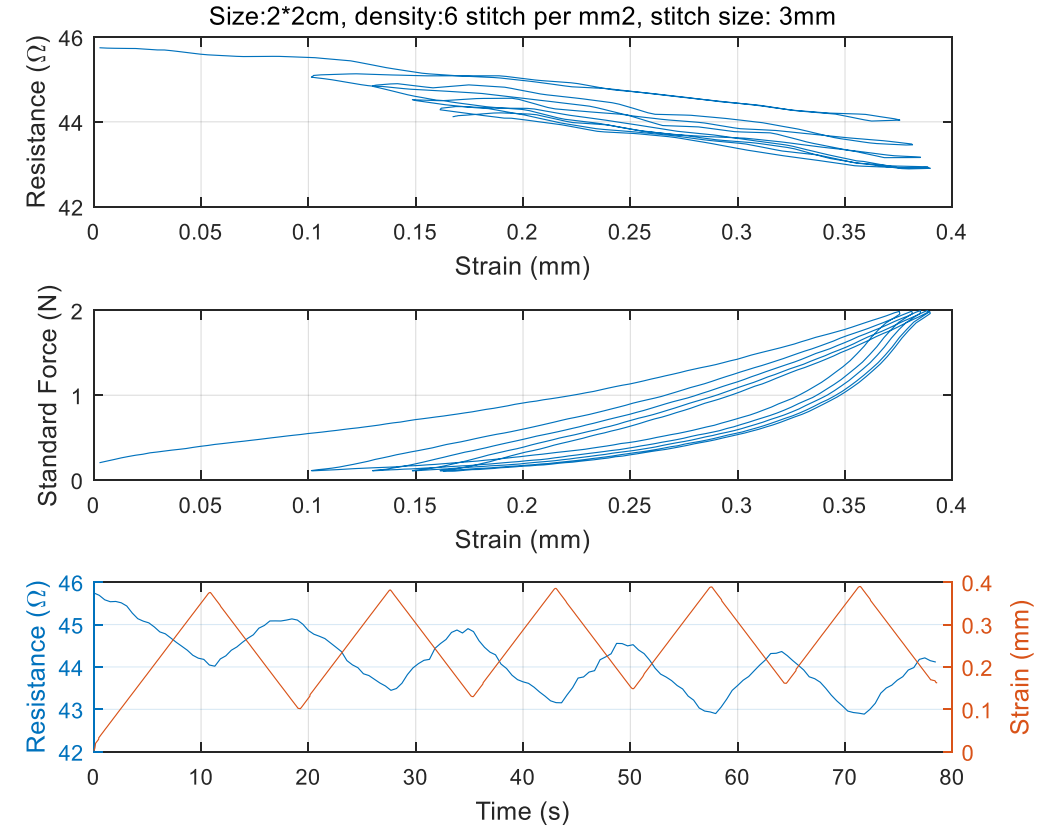
Size:2*2cm, density:6 stitch per mm2, stitch size: 3mm
Resistance (Ω)
Strain (mm)
Standard Force (N)
Strain (mm)
Resistance (Ω)
Strain (mm)
Time (s)

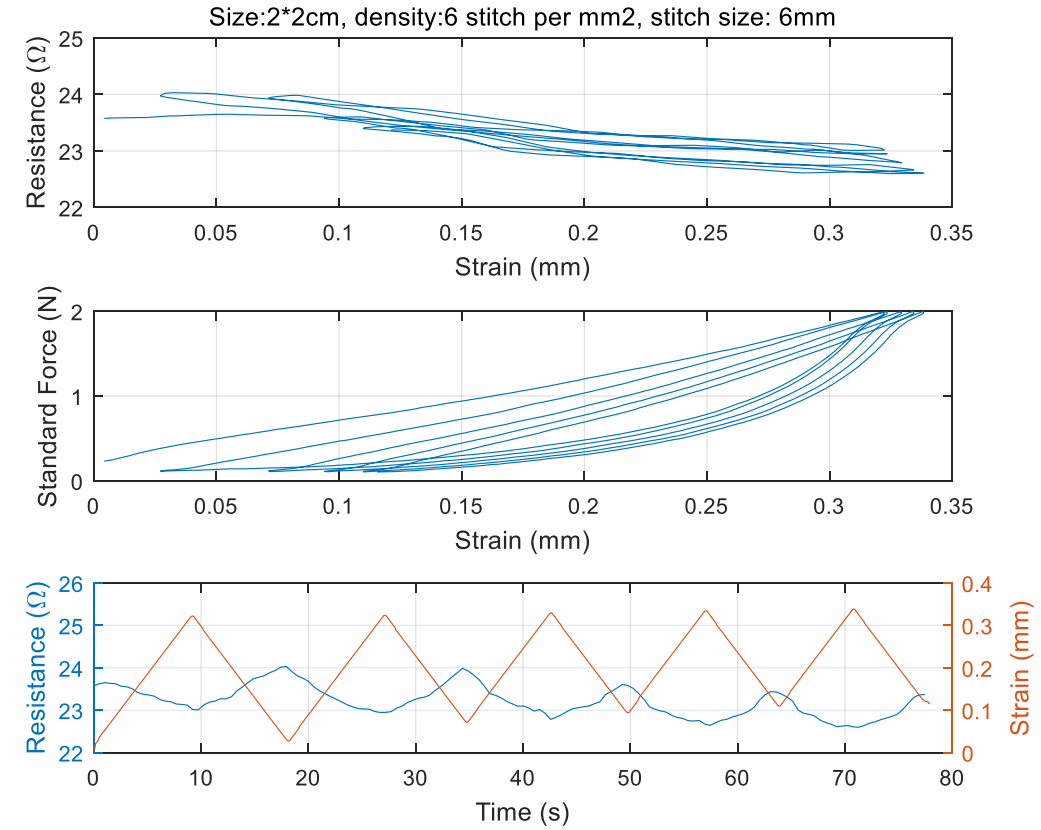
Size:2*2cm, density:6 stitch per mm2, stitch size: 6mm
Resistance (Ω)
Strain (mm)
Standard Force (N)
Strain (mm)
Resistance (Ω)
Strain (mm)
Time (s)

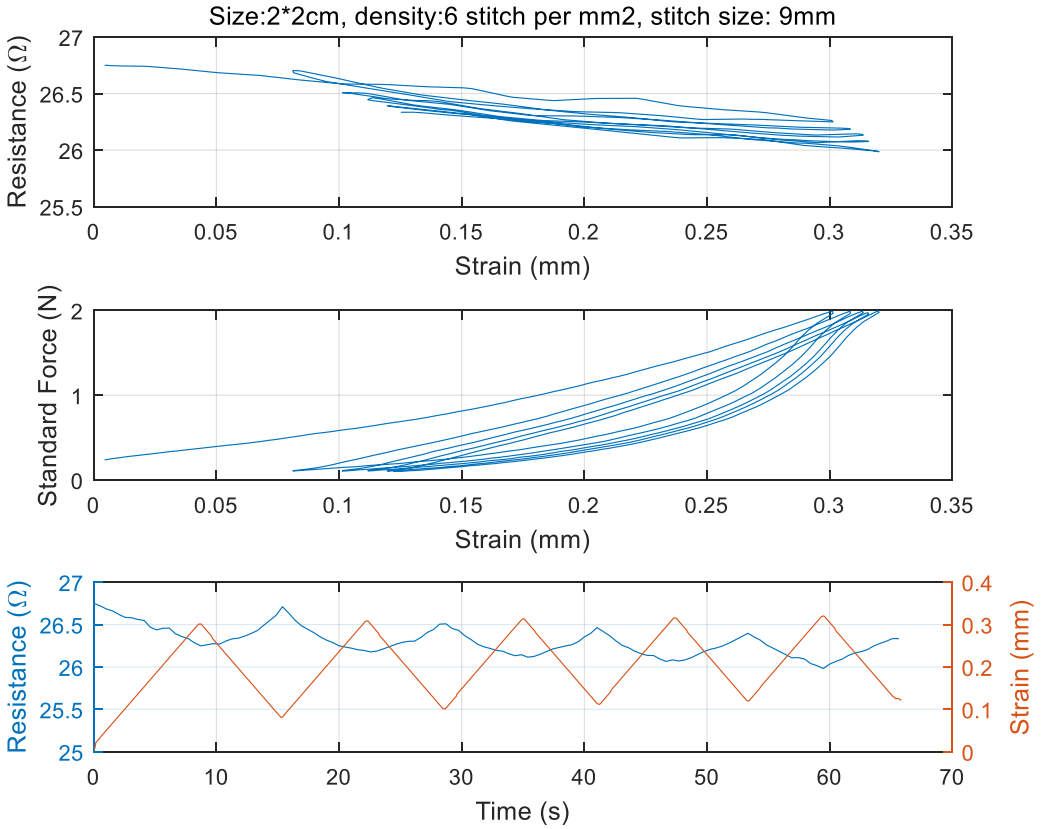
Size:2*2cm, density:6 stitch per mm2, stitch size: 9mm
Resistance (Ω)
Strain (mm)
Standard Force (N)
Strain (mm)
Resistance (Ω)
Strain (mm)
Time (s)

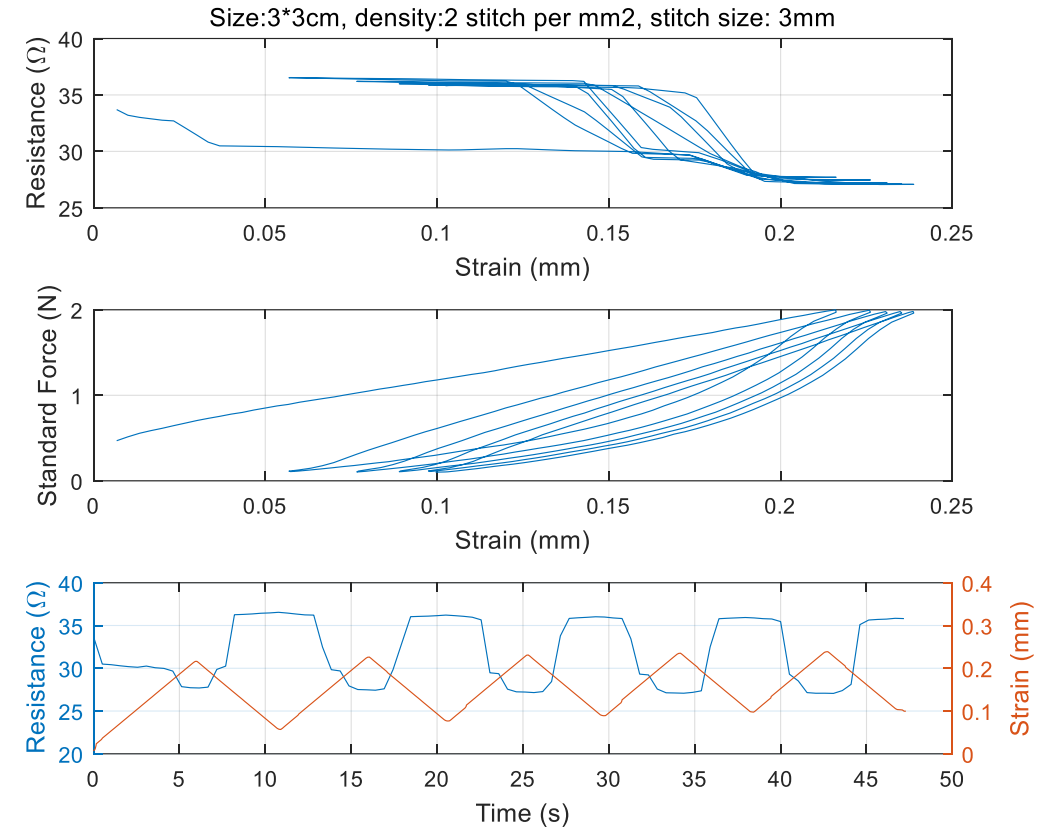
Size:3*3cm, density:2 stitch per mm2, stitch size: 3mm
Resistance (Ω)
Strain (mm)
Standard Force (N)
Strain (mm)
Resistance (Ω)
Strain (mm)
Time (s)

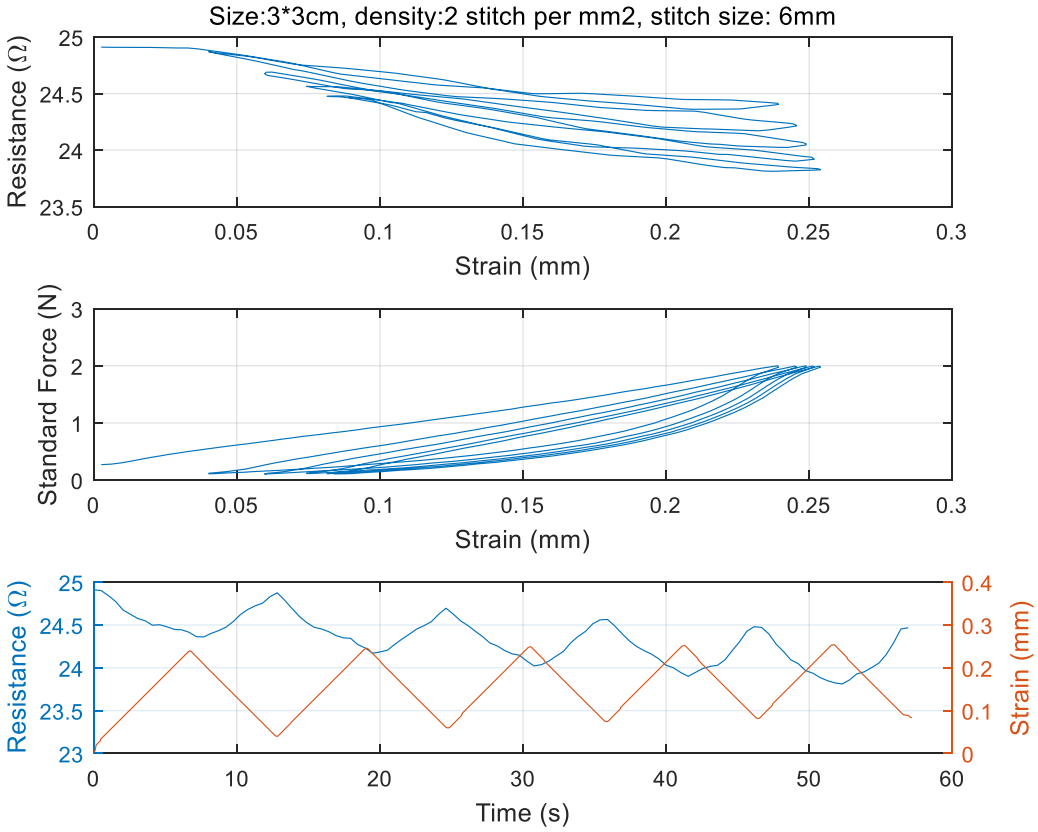
Size:3*3cm, density:2 stitch per mm2, stitch size: 6mm
Resistance (Ω)
Strain (mm)
Standard Force (N)
Strain (mm)
Resistance (Ω)
Strain (mm)
Time (s)

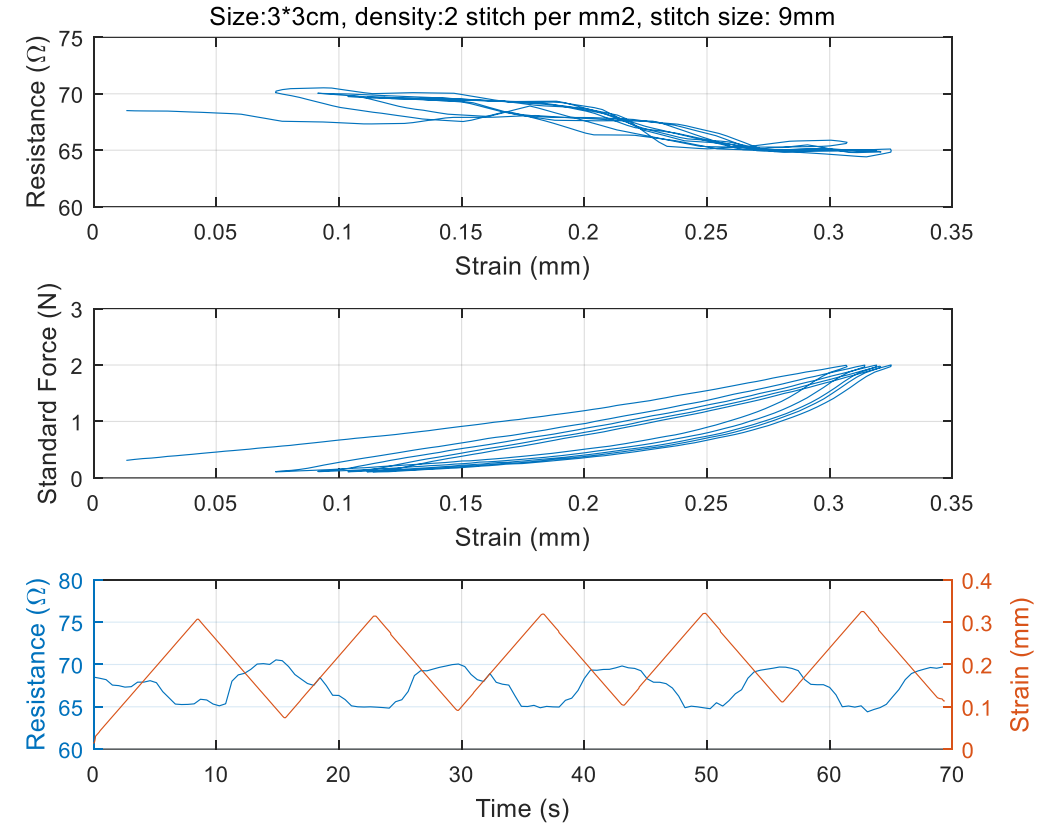
Size:3*3cm, density:2 stitch per mm2, stitch size: 9mm
Resistance (Ω)
Strain (mm)
Standard Force (N)
Strain (mm)
Resistance (Ω)
Strain (mm)
Time (s)

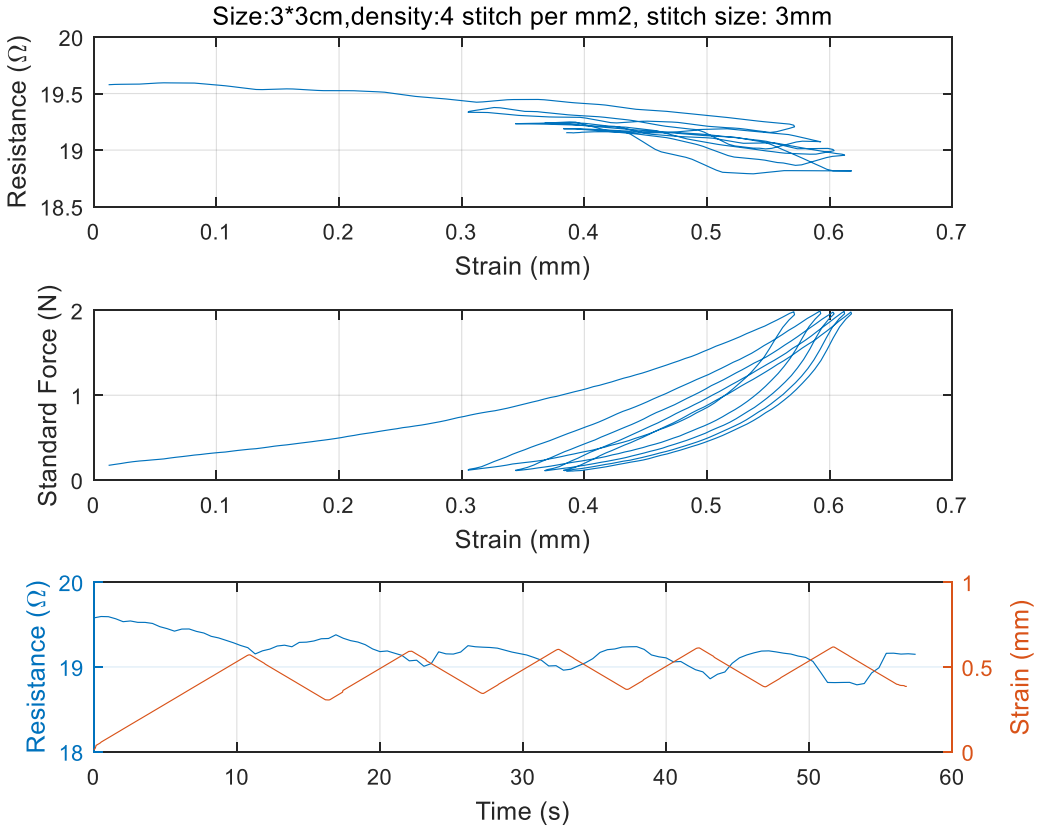
Size:3*3cm,density:4 stitch per mm2, stitch size: 3mm
Resistance (Ω)
Strain (mm)
Standard Force (N)
Strain (mm)
Resistance (Ω)
Strain (mm)
Time (s)

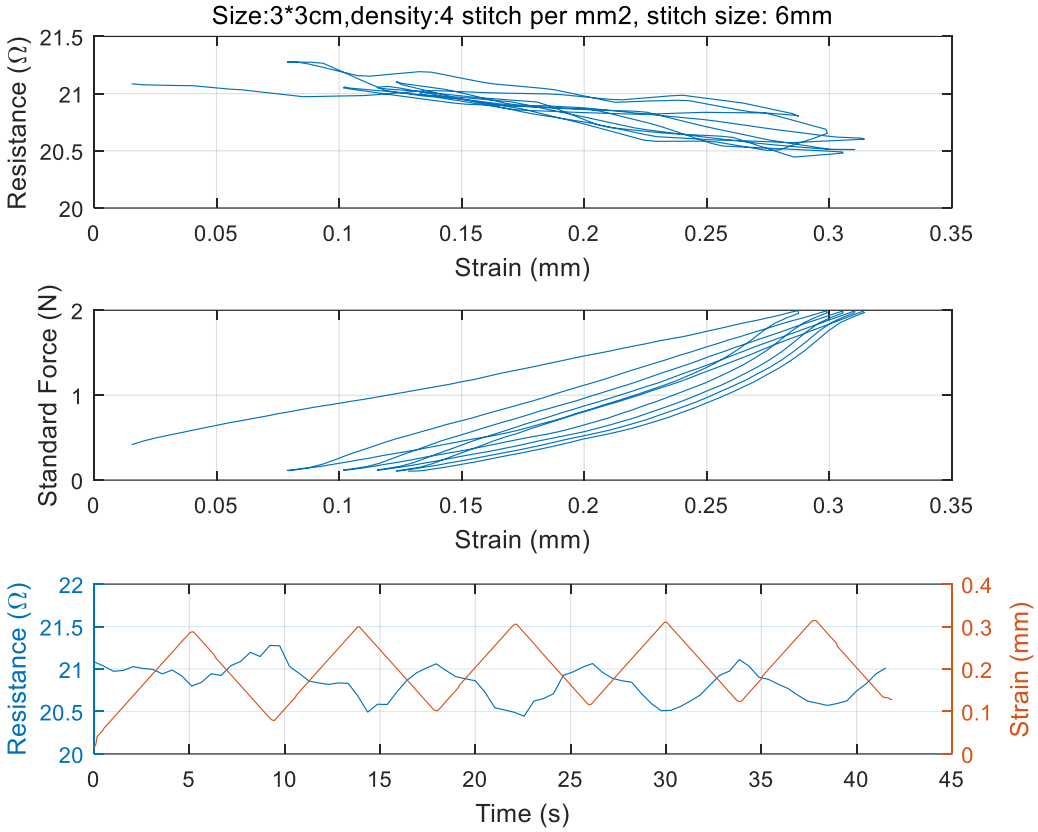
Size:3*3cm,density:4 stitch per mm2, stitch size: 6mm
Resistance (Ω)
Strain (mm)
Standard Force (N)
Strain (mm)
Resistance (Ω)
Strain (mm)
Time (s)

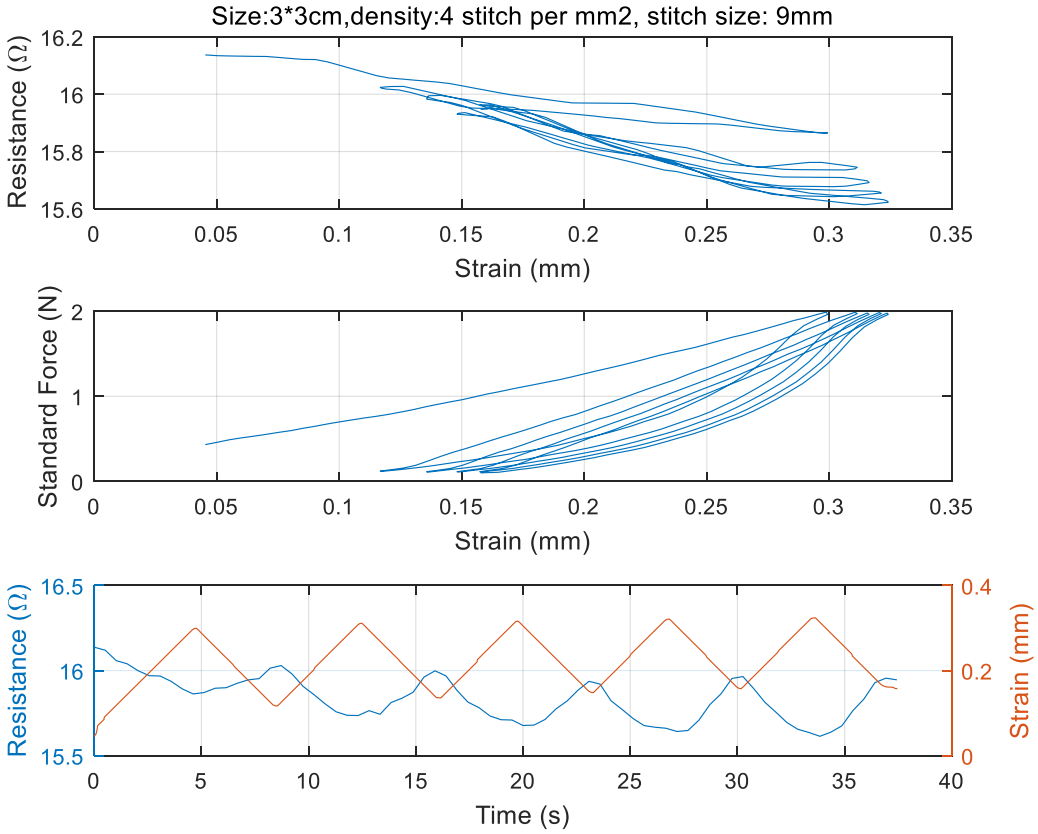
Size:3*3cm,density:4 stitch per mm2, stitch size: 9mm
Resistance (Ω)
Strain (mm)
Standard Force (N)
Strain (mm)
Resistance (Ω)
Strain (mm)
Time (s)

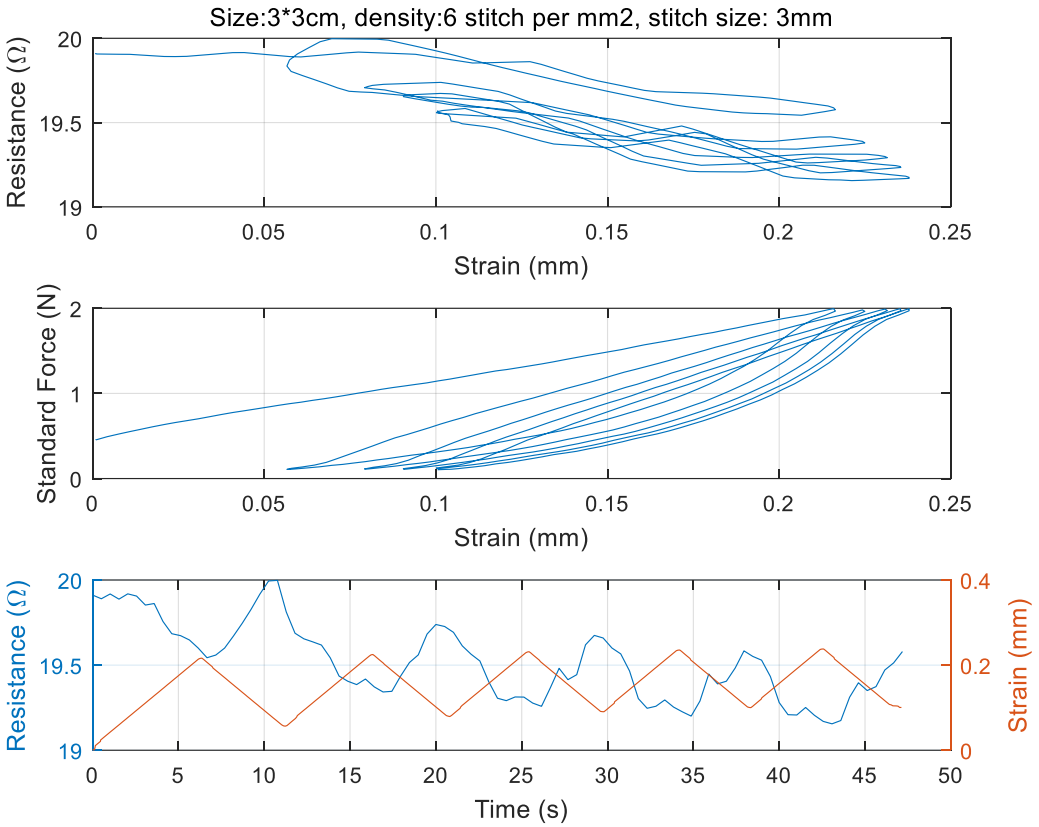
Size:3*3cm, density:6 stitch per mm2, stitch size: 3mm
Resistance (Ω)
Strain (mm)
Standard Force (N)
Strain (mm)
Resistance (Ω)
Strain (mm)
Time (s)

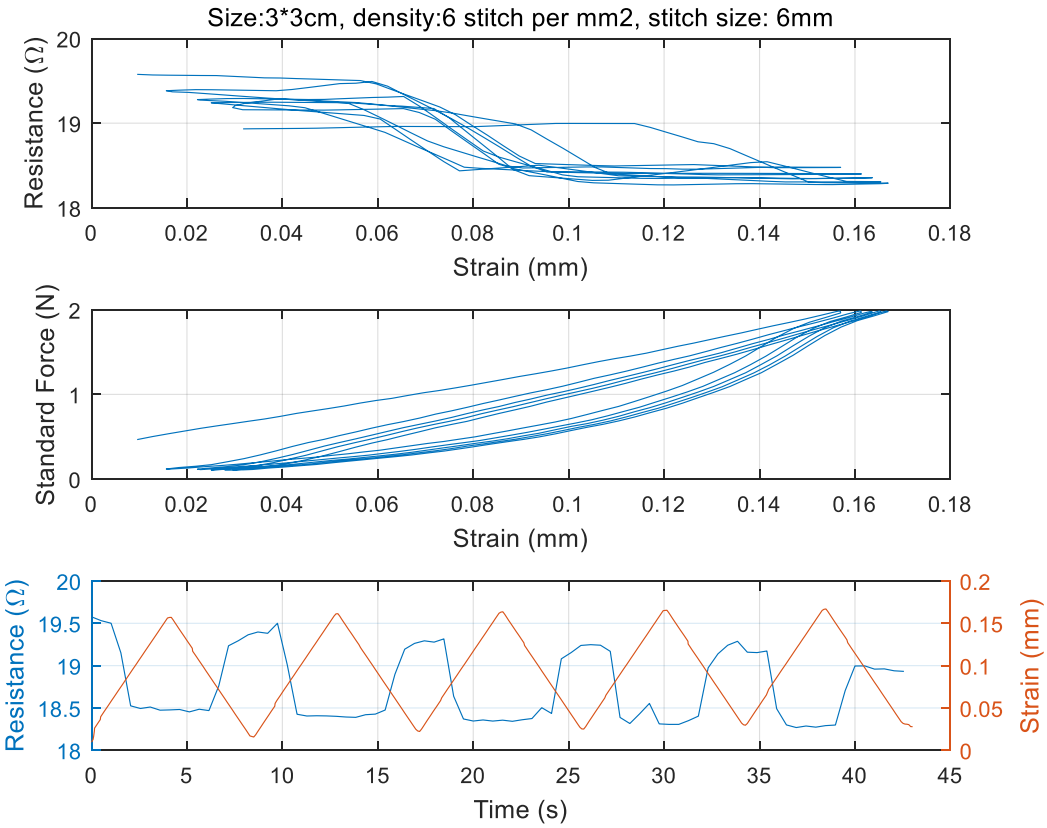
Size:3*3cm, density:6 stitch per mm2, stitch size: 6mm
Resistance (Ω)
Strain (mm)
Standard Force (N)
Strain (mm)
Resistance (Ω)
Strain (mm)
Time (s)

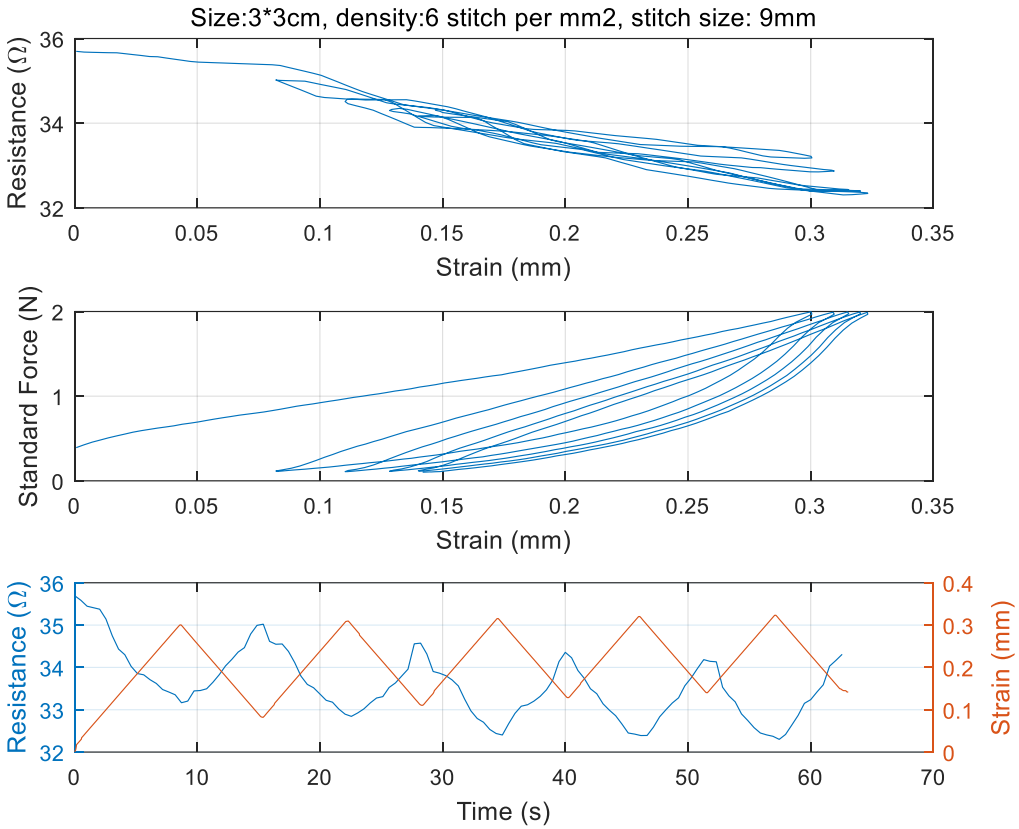
Size:3*3cm, density:6 stitch per mm2, stitch size: 9mm
Resistance (Ω)
Strain (mm)
Standard Force (N)
Strain (mm)
Resistance (Ω)
Strain (mm)
Time (s)

Appendix B

Compression test results of embroidered piezoresistive sensors with different stitch sizes and stitch densities. (Chapter 5 is mainly focused on 0.5 and 1 stitch density; the figures below are samples with other density values)

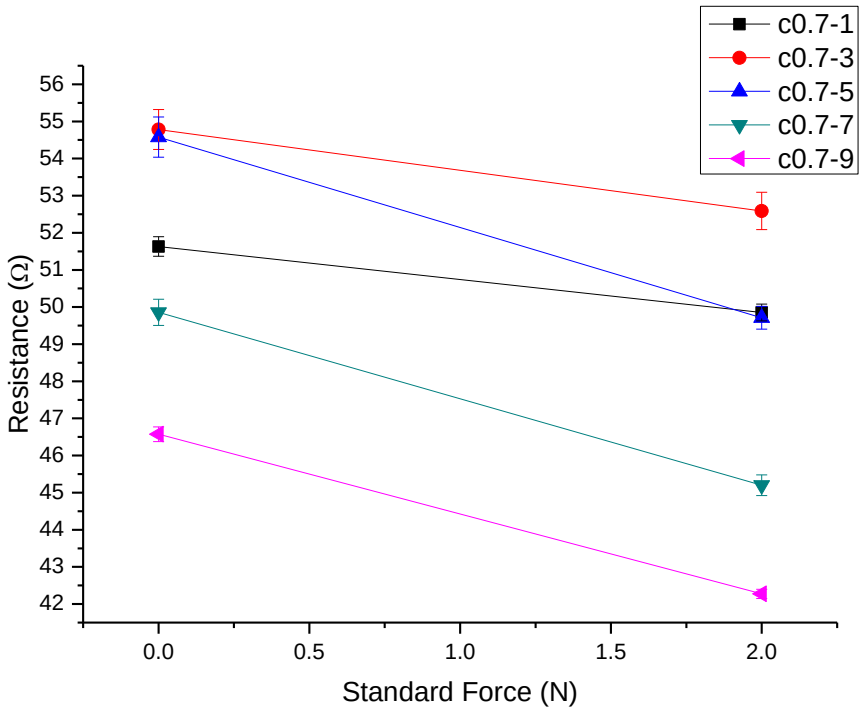

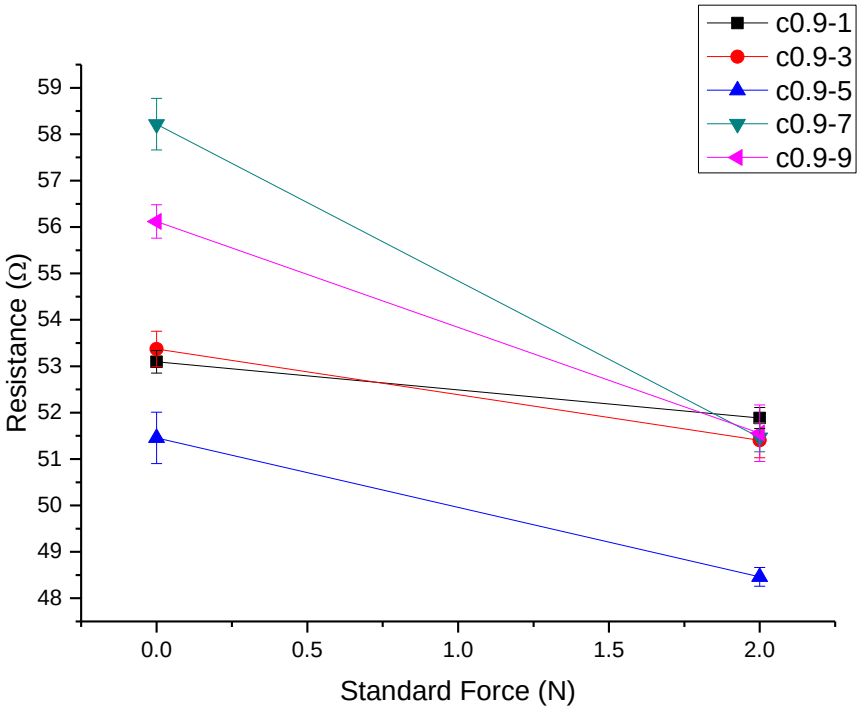
c0.9-1
c0.9-3
c0.9-5
c0.9-7
c0.9-9
Resistance (Ω)
59
58
57
56
55
54
53
52
51
50
49
48
0.0
0.5
1.0
1.5
2.0
Standard Force (N)

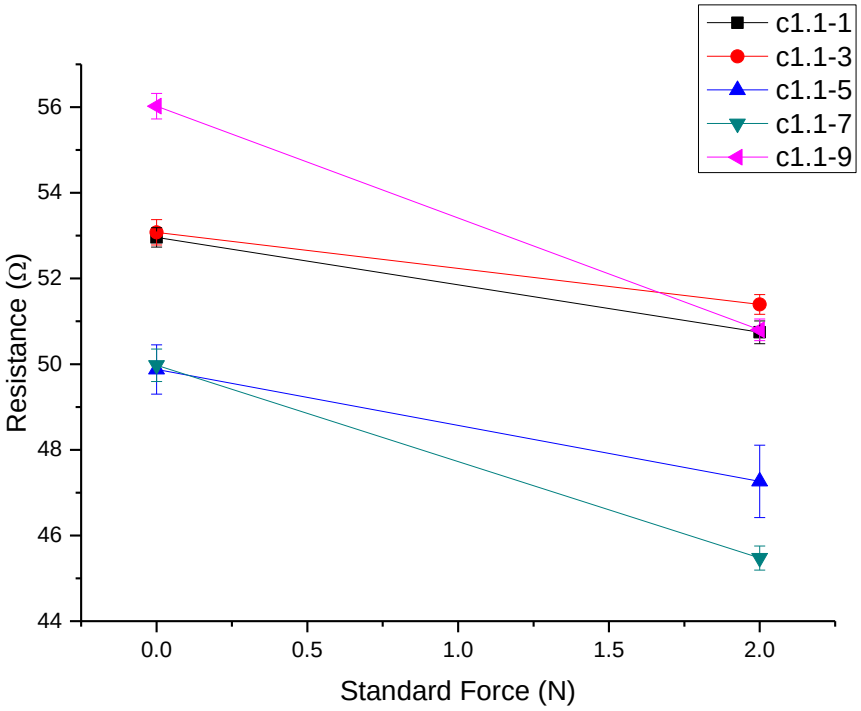
c1.1-1
c1.1-3
c1.1-5
c1.1-7
c1.1-9
Resistance (Ω)
56
54
52
50
48
46
44
0.0
0.5
1.0
1.5
2.0
Standard Force (N)

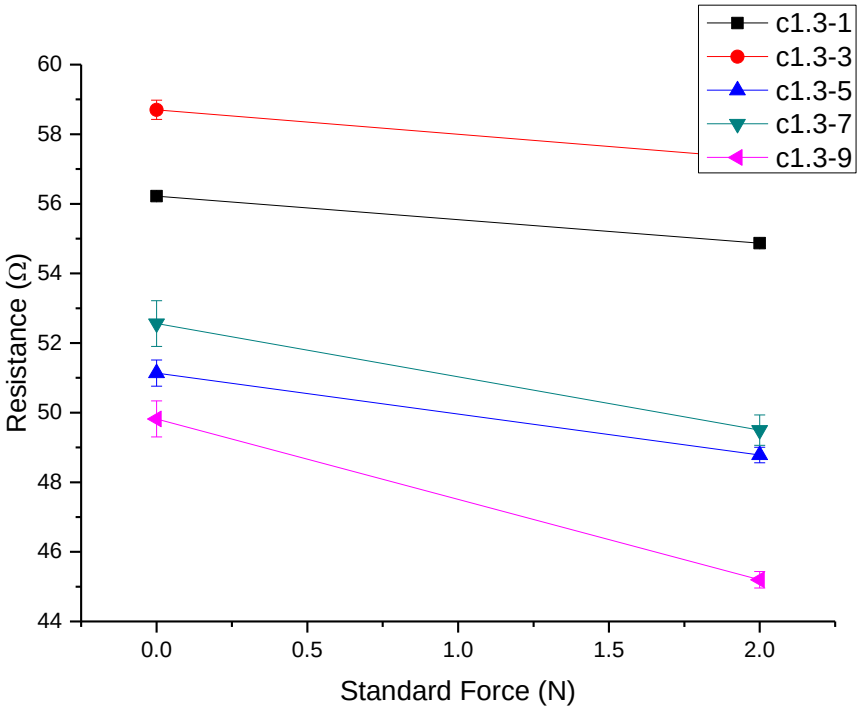
c1.3-1
c1.3-3
c1.3-5
c1.3-7
c1.3-9
Resistance (Ω)
60
58
56
54
52
50
48
46
44
0.0
0.5
1.0
1.5
2.0
Standard Force (N)

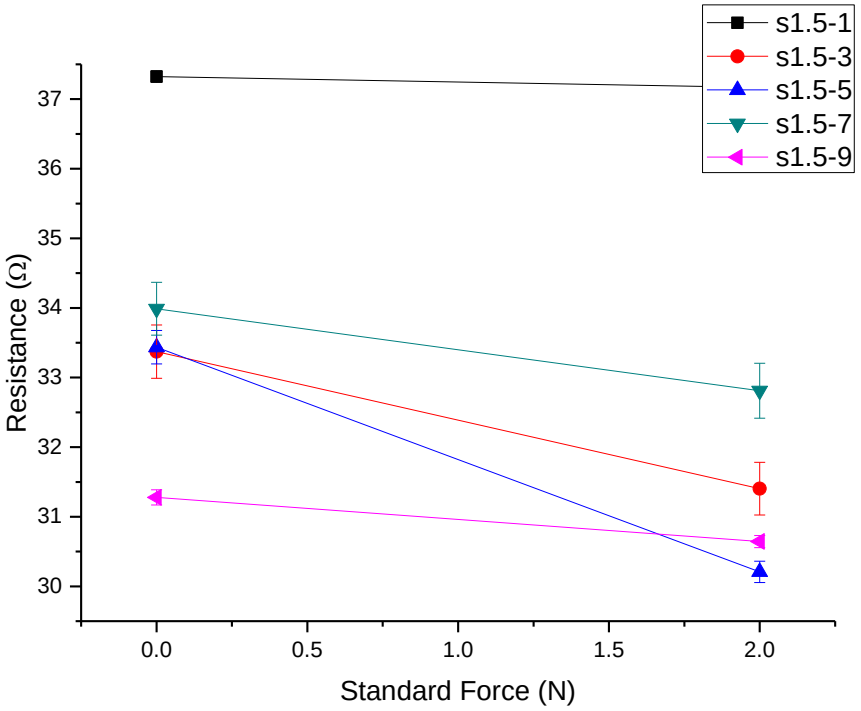
s1.5-1
s1.5-3
s1.5-5
s1.5-7
s1.5-9
Resistance (Ω)
37
36
35
34
33
32
31
30
0.0
0.5
1.0
1.5
2.0
Standard Force (N)

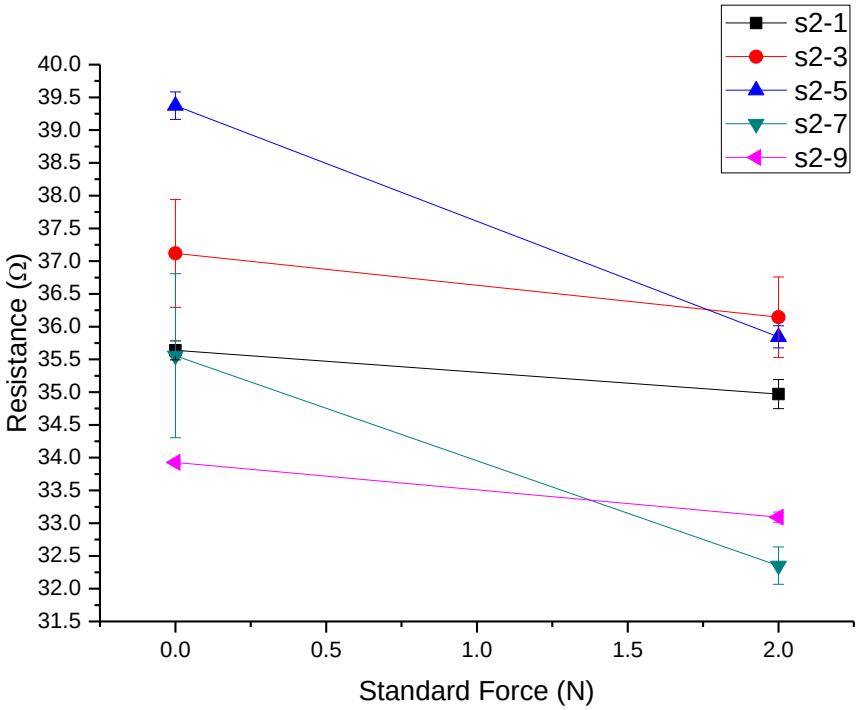
s2-1
s2-3
s2-5
s2-7
s2-9
Resistance (Ω)
Standard Force (N)
40.0
39.5
39.0
38.5
38.0
37.5
37.0
36.5
36.0
35.5
35.0
34.5
34.0
33.5
33.0
32.5
32.0
31.5
0.0
0.5
1.0
1.5
2.0

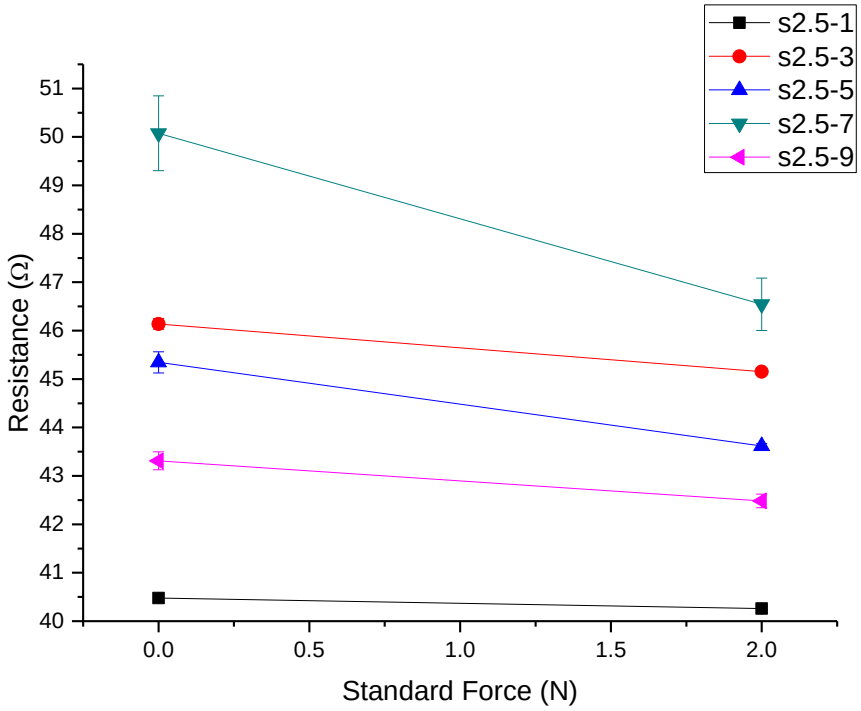
s2.5-1
s2.5-3
s2.5-5
s2.5-7
s2.5-9
Resistance (Ω)
Standard Force (N)
51
50
49
48
47
46
45
44
43
42
41
40
0.0
0.5
1.0
1.5
2.0

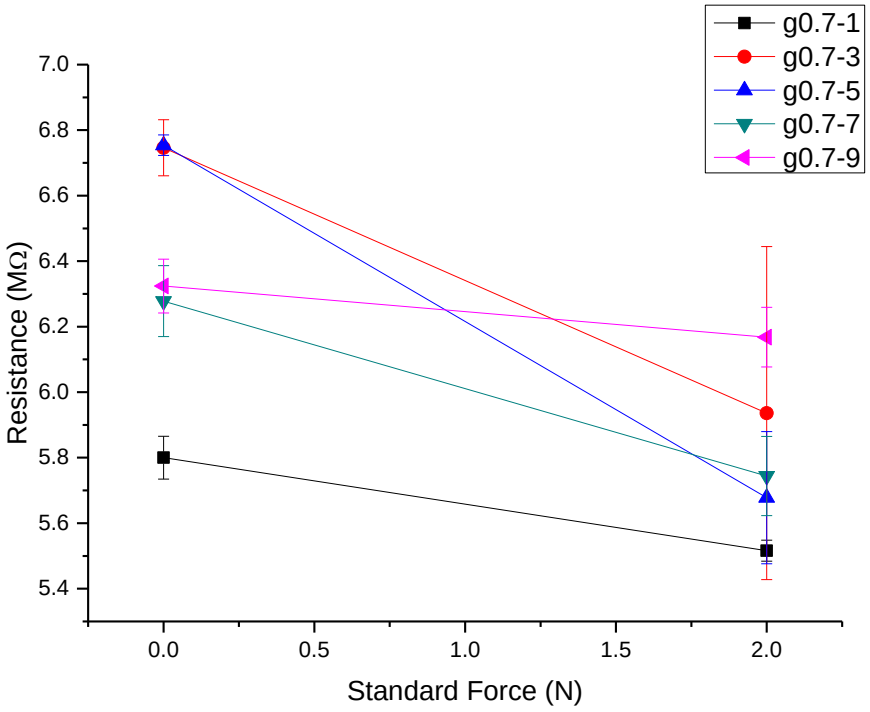
g0.7-1
g0.7-3
g0.7-5
g0.7-7
g0.7-9
Resistance (MΩ)
Standard Force (N)
7.0
6.8
6.6
6.4
6.2
6.0
5.8
5.6
5.4
0.0
0.5
1.0
1.5
2.0

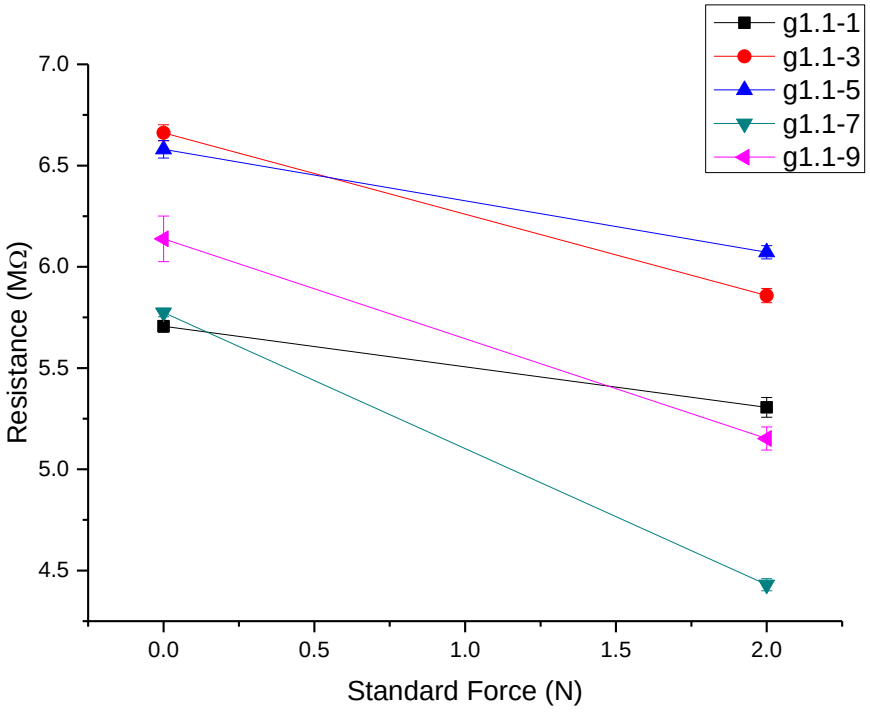
g1.1-1
g1.1-3
g1.1-5
g1.1-7
g1.1-9
Resistance (MΩ)
Standard Force (N)
7.0
6.5
6.0
5.5
5.0
4.5
0.0
0.5
1.0
1.5
2.0

Appendix C

The tensile cyclic test results of the three temperature structures

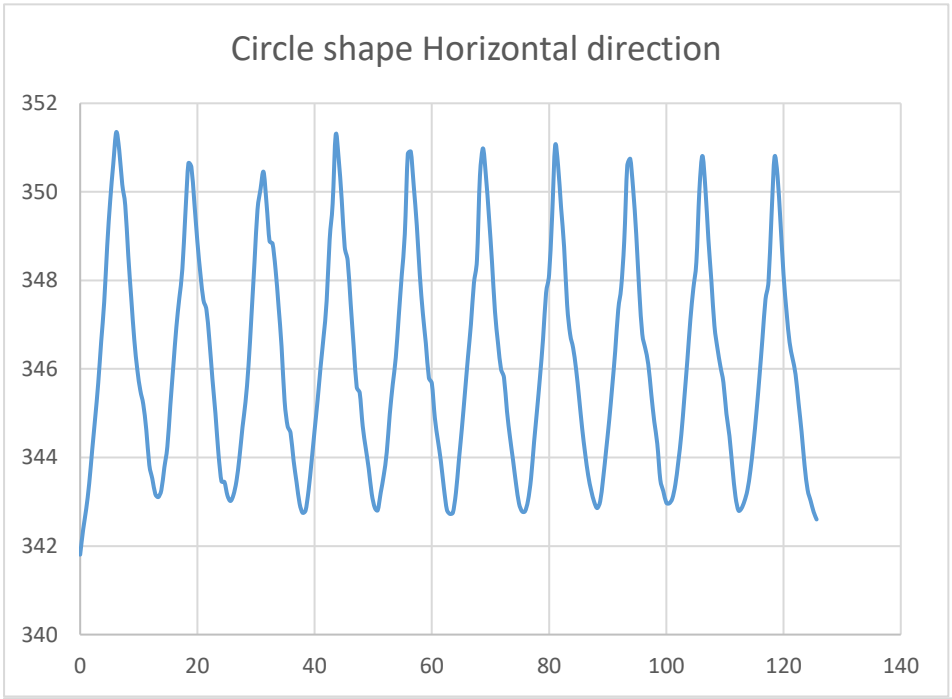

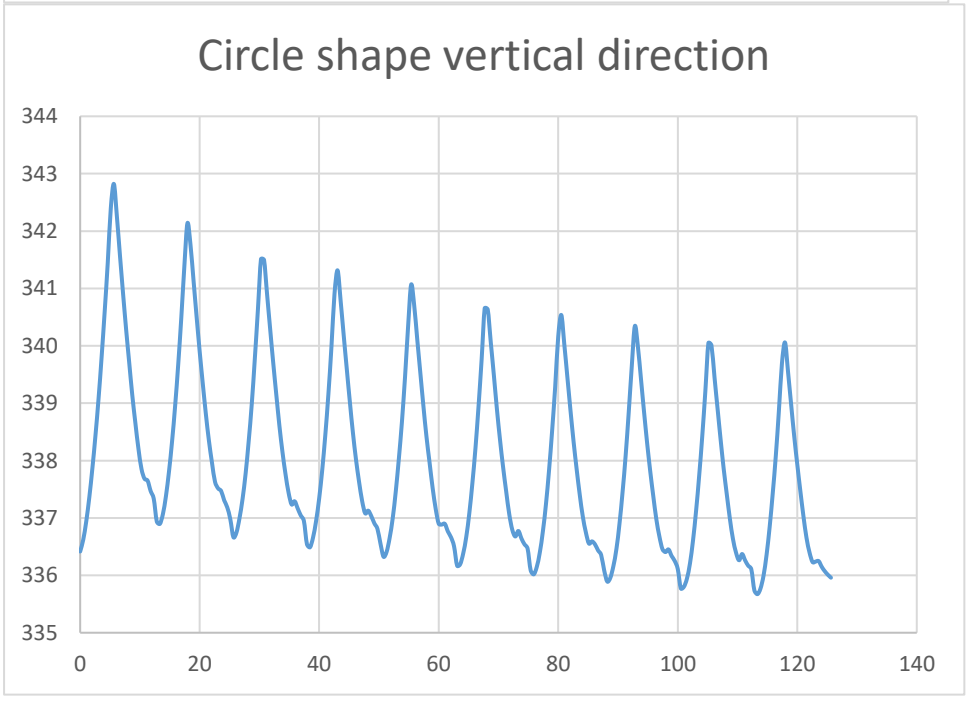

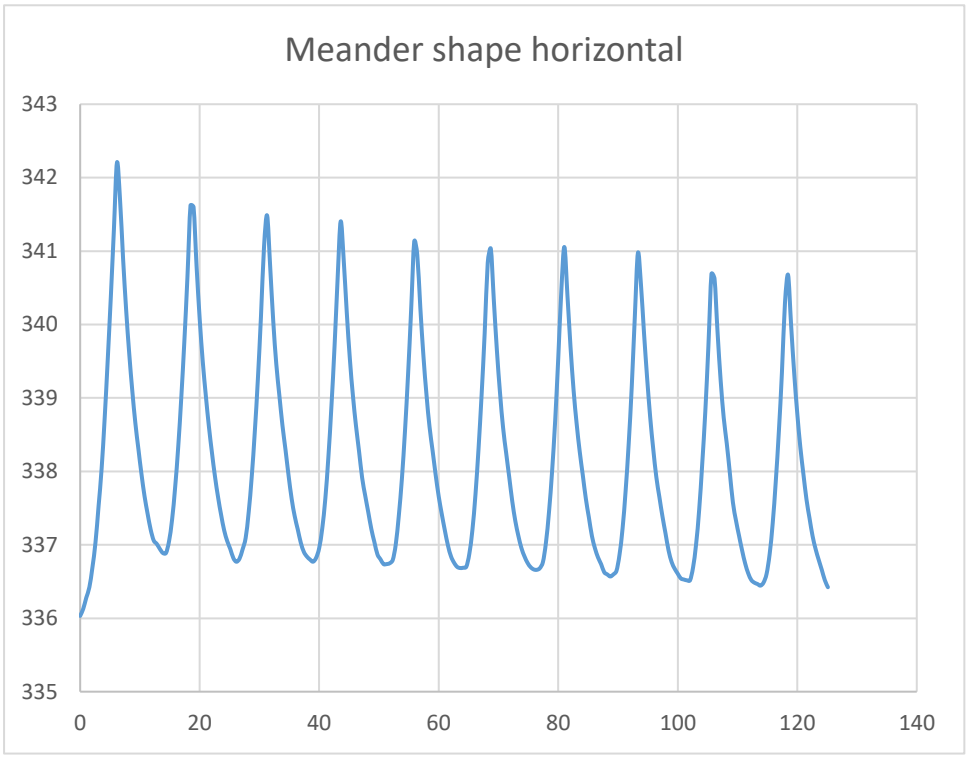
Meander shape horizontal
343
342
341
340
339
338
337
336
335
0
20
40
60
80
100
120
140

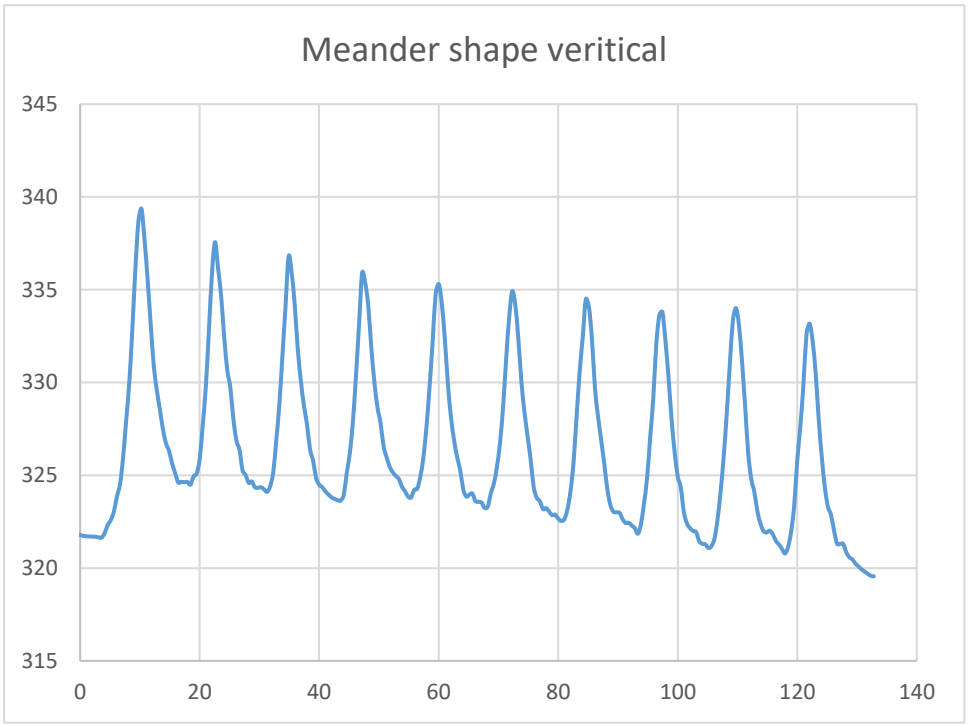
Meander shape veritical
345
340
335
330
325
320
315
0
20
40
60
80
100
120
140

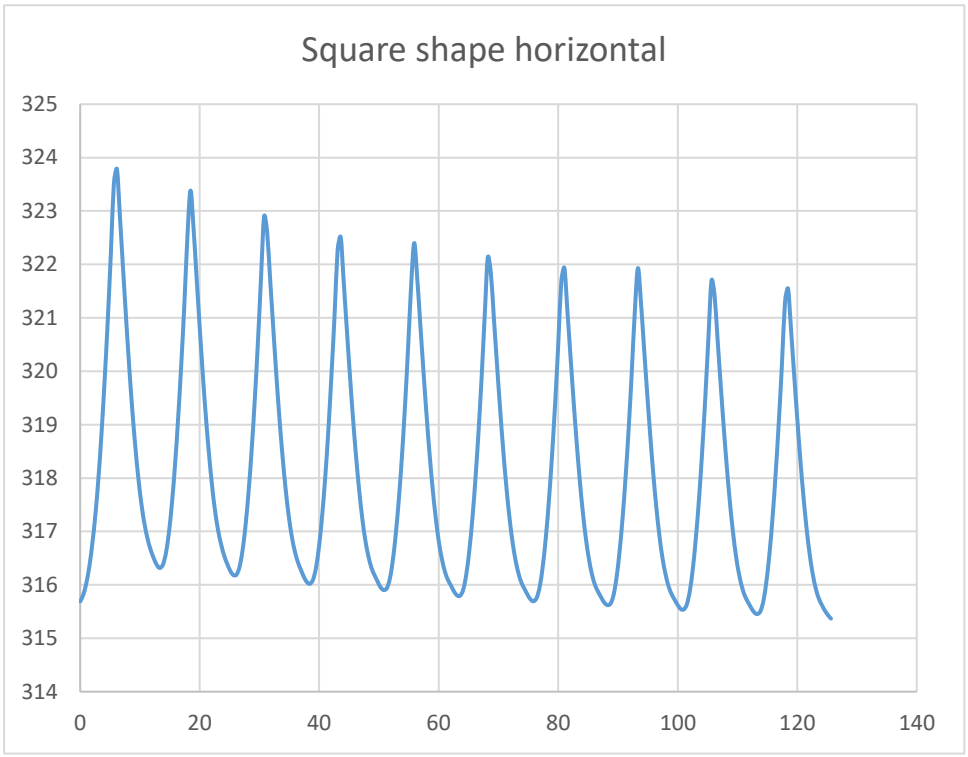
Square shape horizontal
325
324
323
322
321
320
319
318
317
316
315
314
0
20
40
60
80
100
120
140

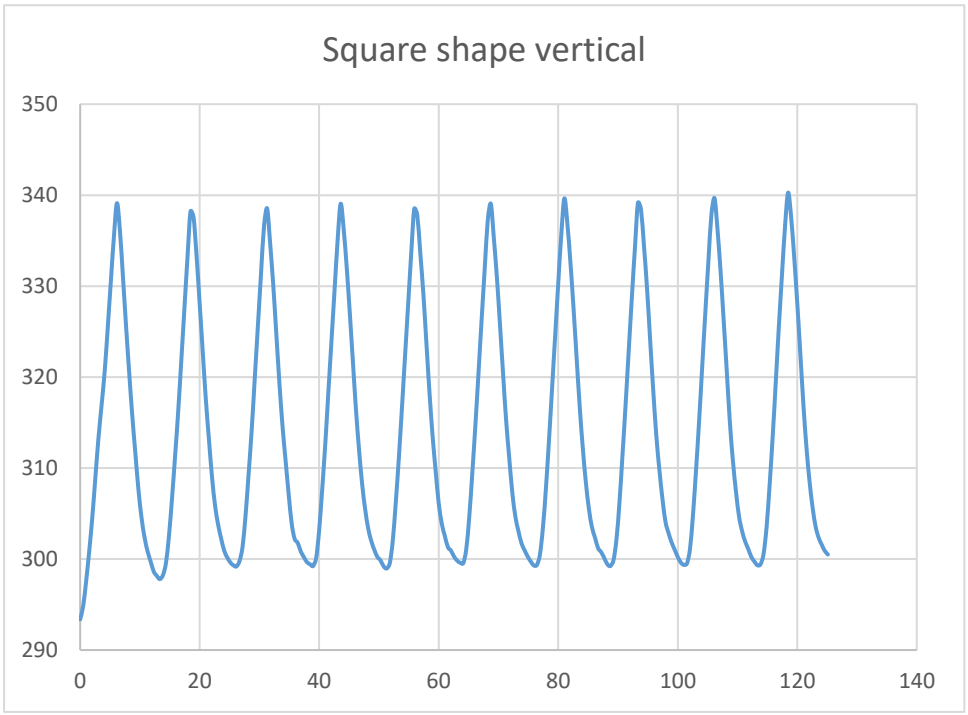
Square shape vertical
350
340
330
320
310
300
290
0
20
40
60
80
100
120
140

Appendix D

Yarn compression and cyclic test results

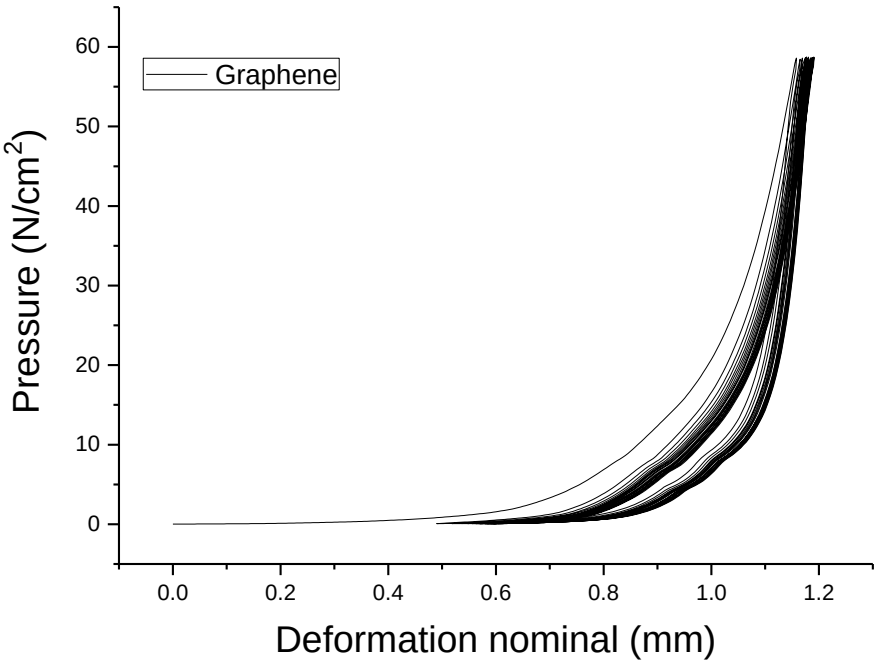

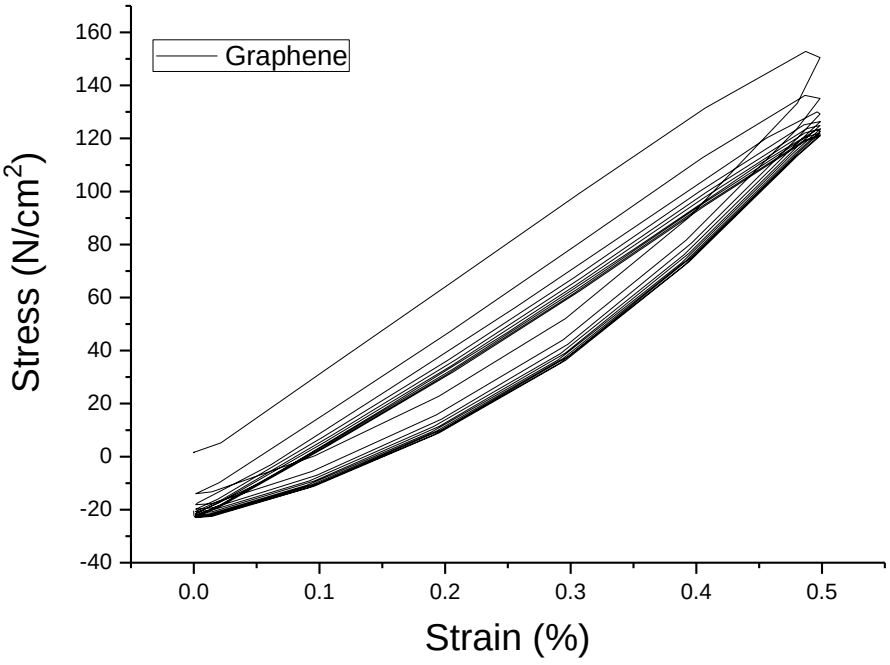

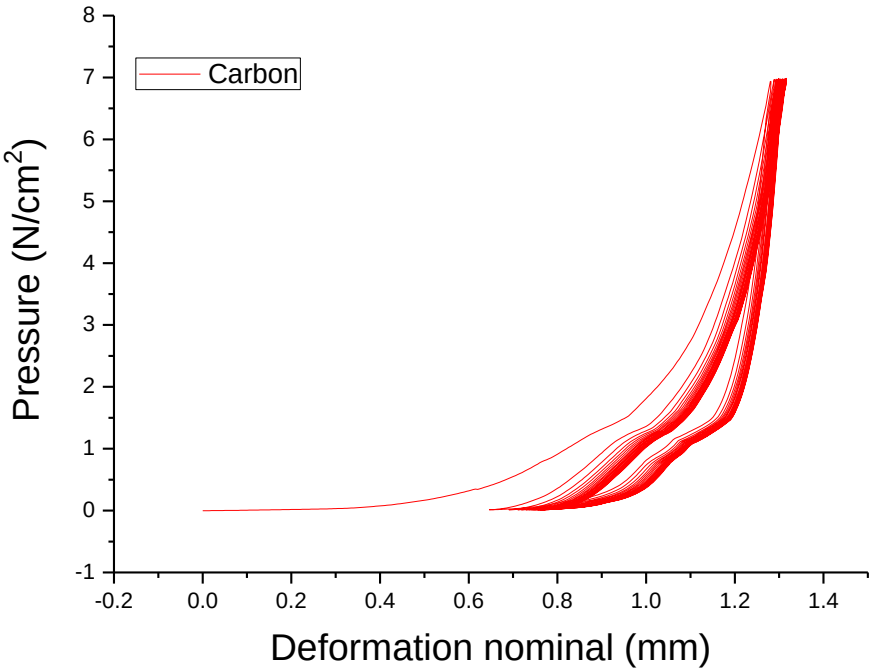
Carbon
Pressure (N/cm2)
Deformation nominal (mm)
8
7
6
5
4
3
2
1
0
-1
-0.2
0.0
0.2
0.4
0.6
0.8
1.0
1.2
1.4

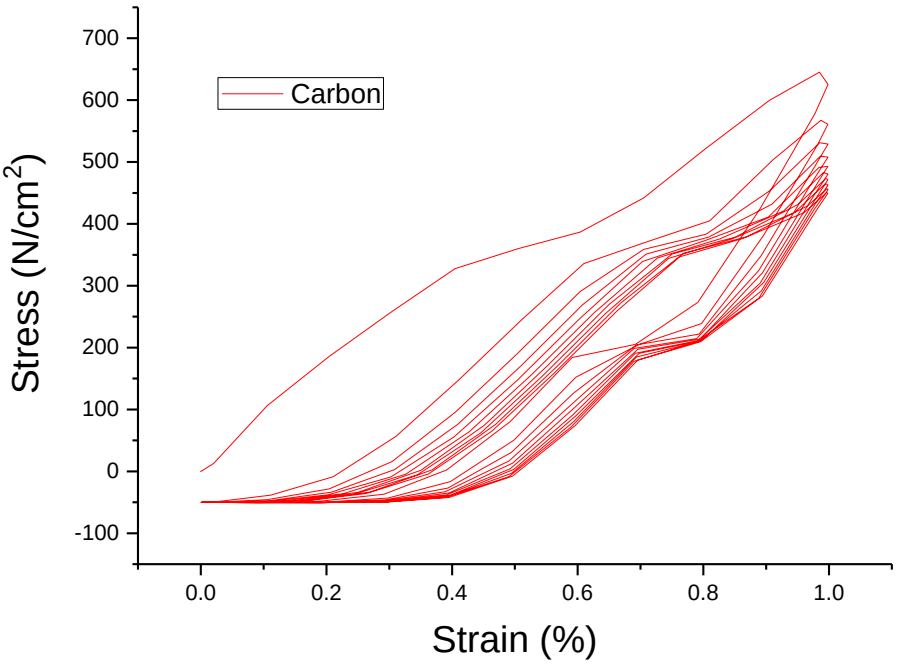
Carbon
Stress (N/cm2)
Strain (%)
700
600
500
400
300
200
100
0
-100
0.0
0.2
0.4
0.6
0.8
1.0

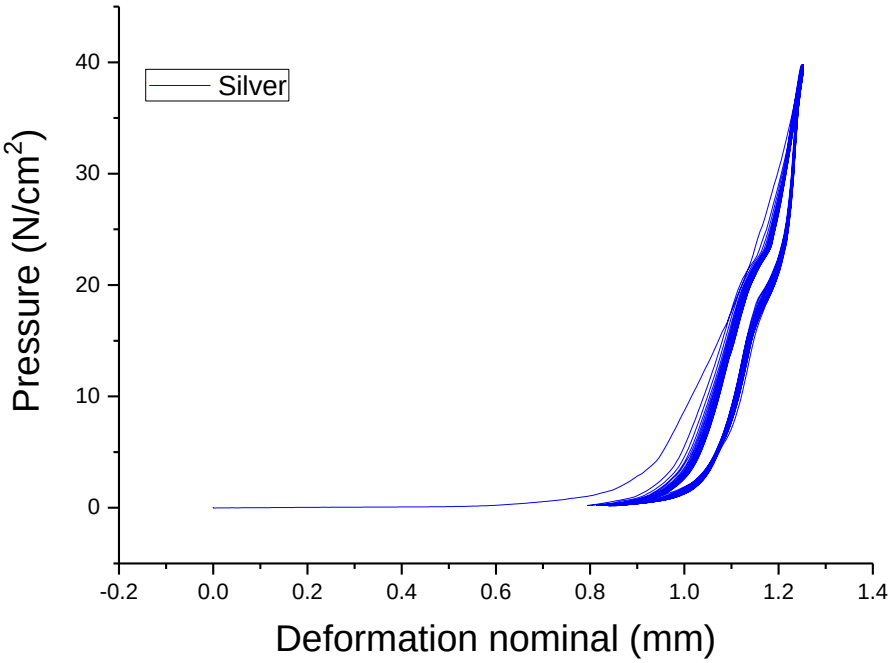
Silver
Pressure (N/cm2)
Deformation nominal (mm)
40
30
20
10
0
-0.2
0.0
0.2
0.4
0.6
0.8
1.0
1.2
1.4

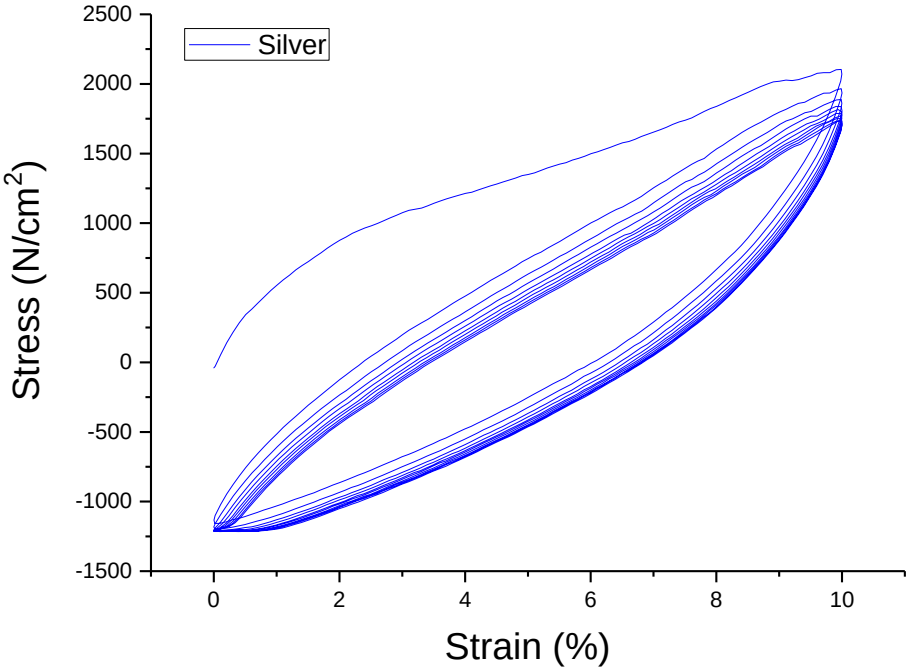
Silver
Stress (N/cm2)
Strain (%)
2500
2000
1500
1000
500
0
-500
-1000
-1500
0
2
4
6
8
10

Appendix E

The influence of the sewing yarn orientation

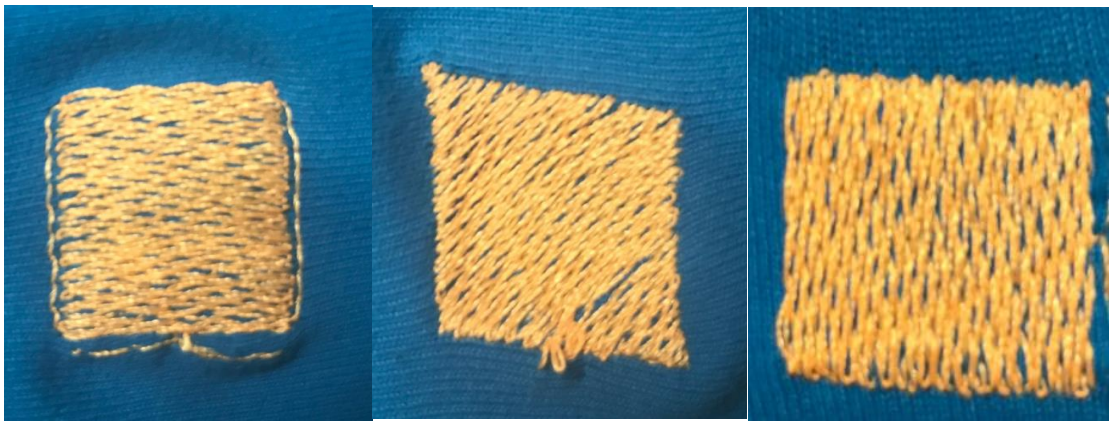

left)0°, middle) 45°, right) 90°

The designed structure is 20*20 mm. However, the size of sample with 0° is 18*20 mm, sample with 45° becomes a diaper shape, and the size of the sample with 90° is 19*20 mm.

Hence, the yarn orientation used in this research is 0°, and the area difference is eliminated by modifying the digital area after compared to the embroidered pattern.